University of Strathclyde
Department of Naval Architecture, Ocean and Marine Engineering

Multi-Objective Robust Early Stage Ship Design Optimisation under Uncertainty

By
Alexandros Priftis

A thesis presented in fulfilment of the requirements for the degree of Doctor of Philosophy

2019

This thesis is the result of the author's original research. It has been composed by the author and has not been previously submitted for examination which has led to the award of a degree.

Signed: Alexandros Priftis
Date: 10/10/2019

Abstract

Shipping industry has become very competitive, while a lot of research is carried out in the shipbuilding world to investigate possible ways to improve ship design and create efficient and economical ships. Technological improvements allow the detailed exploration of design space and assist the theory of optimisation in becoming a vital part of ship design. Advanced software tools are available to designers and researchers to expand their design optimisation methodologies and introduce not only more efficient techniques, but also more robust approaches to ship design.

The topic of ship design optimisation has been investigated by numerous researchers, who have established structured methodologies which can be applied to real case studies and produce efficient solutions to the ship design problem. However, the definition of the ship design problem changes often due to the introduction of new ship types, international regulations and technological improvements.

This thesis contributes to the aforementioned developments with regard to the ship design optimisation problem. The mission is to develop a methodology for a multi-objective robust early stage ship design optimisation under uncertainty. Several aspects of ship design are incorporated, taking into account the holistic ship design model. Various performance indicators are used as measures of merit to evaluate the response of possible solutions to the problem. New regulations are incorporated to the optimisation problem, investigating their impact on its solution. In addition, uncertainty quantification is applied throughout the proposed methodology, while its effect on the ship design optimisation problem is examined.

Acknowledgements

I would like to express my sincere gratitude to Dr. Evangelos Boulougouris for supervising and funding this PhD study. He provided me with useful guidelines and support throughout my postgraduate studies to complete my research work.

Special thanks must be directed to the HOLISHIP H2020 EU project, TRAM H2020 EU project and ETP Knowledge Exchange PJ149-M project for supporting this study financially.

My sincere thanks also go to my second supervisor, Prof. Osman Turan, who provided useful feedback to improve the quality of my work.

I would also like to thank Prof. Apostolos Papanikolaou, who helped me set the basis for this PhD study by supervising my undergraduate Diploma thesis and teaching me the fundamentals of Naval Architecture.

I would like to express my gratitude to my family, Nikos, Mary and Fay for their constant support and encouragement throughout my studies. I could not have completed this work without their support.

Finally, I would like to thank all my friends and colleagues who encouraged me throughout my studies going through the same struggles in our academic life, Christos Gkerekos, Sofia Koukoura, Beatriz Navas de Maya, Sotiris Chouliaras and Konstantinos Dikis.

Research output

The following research output has been published as part of this research work:

- Journal articles:

Priftis, A., Boulougouris, E. & Turan, O. 2019. Multi-objective robust early stage ship design optimisation under uncertainty utilising surrogate models. *Ocean Engineering*. *(Submitted – under review)*

Priftis, A., Boulougouris, E., Turan, O. & Papanikolaou, A. 2018. Parametric Design and Multi-Objective Optimisation of Containerships. *Ocean Engineering*, 156, 347-357.

Priftis, A., Papanikolaou, A. & Plessas, T. 2016. Parametric Design and Multiobjective Optimization of Containerships. *Journal of Ship Production and Design*, 32, 1-14.

- Conference papers:

Priftis, A., Boulougouris, E. & Turan, O. 2018. Parametric Design and Holistic Optimisation of Post-Panamax Containerships. *13th International Marine Design Conference*. Finland.

Priftis, A., Boulougouris, E. & Turan, O. 2018. Parametric Design and Holistic Optimisation of Post-Panamax Containerships. *7th Transport Research Arena*. Austria.

Priftis, A., Boulougouris, E., Turan, O. & Papanikolaou, A. 2017. Parametric Design and Multi-Objective Optimisation of Containerships. *International Conference in Shipbuilding and Offshore Engineering*. India.

Priftis, A., Boulougouris, E., Turan, O. & Papanikolaou, A. 2016. Parametric Design and Multi-Objective Optimisation of Containerships. *International Conference on Maritime Safety and Operations*. United Kingdom.

In addition, the author has contributed to research work related to the following projects:

- TRAM (2018-2022) H2020 EU project:

Deliverable 3.1: Restrictions for parametric ship modules

- HOLISHIP (2016-2020) H2020 EU project:

Deliverable 3.1: Requirements and standards
Deliverable 3.2: Stability and hydrodynamic tools (concept design)
Deliverable 3.3: Stability and hydrodynamic tools (contract design)

- ETP Knowledge Exchange PJ149-M "Assessment of seakeeping characteristics of windfarm vessels" project:

Final report: Assessment of seakeeping characteristics of vessels "MCS Sirocco", "MCS Typhoon" & "MCS Zephyr"

Contents

Abstract 3

Acknowledgements 4

Research output 5

Contents 7

Abbreviations 11

Nomenclature 13

1 Introduction 16

1.1 Introduction 16

1.2 Problem definition 18

1.3 Thesis objectives 19

1.4 Contribution to the research field 20

1.5 Thesis structure 21

2 Critical review 23

2.1 Introduction 23

2.2 Ship design 23

2.2.1 Traditional approaches 23

2.2.2 New methods 25

2.2.3 Summary 26

2.3 Optimisation in ship design 26

2.3.1 Single-objective optimisation 28

2.3.2 Multi-objective optimisation 30

2.3.3 Ship design optimisation under uncertainty 40

2.3.4 Summary 44

2.4 Identification of research gap 45

3 Theoretical background 47
3.1 Introduction 47
3.2 Parametric modelling 47
3.3 Ship design optimisation problem 49
3.4 Optimisation algorithms 52
3.5 Surrogate models 56
3.6 Multi-criteria decision analysis 59
3.7 Uncertainty quantification 61
3.8 Summary 65
4 Proposed methodology 67
4.1 Introduction 67
4.2 Parametric hull model 69
4.3 Ship model 72
4.3.1 Surface and room definitions 72
4.3.2 Resistance estimation 74
4.3.3 Lightweight estimation 77
4.3.4 Deadweight breakdown 78
4.3.5 Loading conditions 79
4.4 Objective functions and constraints 80
4.4.1 Container capacity ratio 81
4.4.2 EEDI 81
4.4.3 RFR 83
4.4.4 Container stowage ratio 84
4.4.5 Calm water resistance CFD calculations 85
4.4.6 IMO second generation intact stability criteria 88
4.4.7 Midship section structural analysis 89

4.5 Design of experiment 90
4.6 Surrogate models 91
4.6.1 Calm water resistance CFD calculations 92
4.6.2 IMO second generation intact stability criteria 93
4.6.3 Uncertainty quantification 93
4.7 Multi-objective optimisation 96
4.8 Multi-criteria decision analysis 98
4.9 Summary 99
5 Case studies 101
5.1 Introduction 101
5.2 Containership case study 101
5.2.1 Challenges associated with containership design 101
5.2.2 Optimisation problem setup 103
5.3 Ro-Pax vessel case study 118
5.3.1 Challenges associated with Ro-Pax vessel design 118
5.3.2 Optimisation problem setup 119
5.4 Summary 135
6 Results 137
6.1 Introduction 137
6.2 Containership case study 137
6.2.1 Baseline model 137
6.2.2 Surrogate models 138
6.2.3 Multi-objective optimisation 146
6.2.4 Multi-criteria decision analysis 152
6.3 Ro-Pax vessel case study 162
6.3.1 Baseline model 162

6.3.2 Surrogate models 162
6.3.3 Multi-objective optimisation 170
6.3.4 Multi-criteria decision analysis 175
6.4 Summary 184
7 Discussion and conclusions 188
7.1 Introduction 188
7.2 Thesis review 188
7.3 Novelty elements 191
7.4 Accomplishment of thesis objectives 193
7.5 Future work 194
7.6 Summary 196
References 197
A Calculation of excessive acceleration stability criterion 205
B Calculation of parametric roll stability criterion 208
C Calculation of pure loss of stability criterion 213

Abbreviations

AP	Aft perpendicular
c_M	Midship section coefficient
c_P	Prismatic coefficient
c_W	Waterplane area coefficient
CAD	Computer aided design
CAE	Computer aided engineering
CFD	Computational fluid dynamics
CPC	Centre plane curve
DWL	Design waterline
DWT	Deadweight
EEDI	Energy efficiency design index, a MARPOL measure of CO_2 emission per unit of transport in [gr CO_2/(ton mile)]
FEM	Finite element method
FOB	Flat of bottom
FOS	Flat of side
FP	Forward perpendicular
GM	Metacentric height
HPC	High performance computer
IFO	Intermediate fuel oil
IGES	Initial graphics exchange specification (file format)
IMO	International maritime organisation
L_{BP}	Length between perpendicular
L_{WL}	Length waterline
LCB	Longitudinal centre of buoyancy
MARPOL	International convention for the prevention of marine pollution from ships (IMO)
MDO	Marine diesel oil
NPV	Net present value
NSGA 2	Non-dominated sorting genetic algorithm 2

OOI	Oil outflow index
RANS	Reynolds-averaged Navier-Stokes
Ro-Pax	Roll-on/roll-off passenger (ship type)
RFR	Required freight rate
SAC	Sectional area curve
SFOC	Specific fuel oil consumption
SGIS	Second generation intact stability criteria (IMO)
SOLAS	International convention for the safety of life at sea (IMO)
TEU	Twenty feet equivalent unit (standardised container size)
USD	United States dollar
VCG	Vertical centre of gravity

Nomenclature

$f(\boldsymbol{x},\boldsymbol{y})$	Objective function (measure of merit)
$g(\boldsymbol{x},\boldsymbol{y})$	Set of inequality constraints
$h(\boldsymbol{x},\boldsymbol{y})$	Set of equality constraints
$\boldsymbol{x}$	Vector of the design variables
$\boldsymbol{y}$	Vector of the parameters independent of the designer choice
a_k	Step size
$\boldsymbol{d}_k$	Direction vector
$\boldsymbol{g}(x)^T\boldsymbol{\beta}$	Trend function
$\varepsilon(\boldsymbol{x})$	Gaussian Process error model
$u(F(\boldsymbol{x}))$	Utility function
w_i	Weighting factor
$\boldsymbol{\xi}$	Error or tolerance related to design variable vector
$\boldsymbol{\varphi}$	Stochastic error related to objective function vector
R_{Total}	Total resistance
R_F	Frictional resistance
k_1	Form factor describing the viscous resistance of the hull form in relation to the frictional resistance
R_{APP}	Resistance of the appendages
R_W	Wave braking resistance
R_B	Pressure resistance introduced by the bulbous bow
R_{TR}	Pressure resistance introduced by immersed transom
R_A	Model-ship correlation resistance
ρ	Sea water density
g	Gravitational acceleration
$H_{W,1/3}$	Significant wave height
B	Ship’s breadth
L_{BWL}	Length of the bow on the waterline to 95% of the maximum breadth

V_{10}	Wind speed at ten metres above the sea surface
C_{AA}	Wind resistance coefficient
ρ_{air}	Density of air
V	Ship's speed
V_{Wind}	Wind speed
A_F	Frontal projected area of the ship above the sea level
P_B	Installed power
η_S	Shaft efficiency
P_D	Delivered power
η_D	Propulsive efficiency
LS	Lightship
W_{ST}	Steel weight
W_{OT}	Outfit weight
W_M	Machinery weight
W_F	Fuel, diesel and lubrication weight
W_{FW}	Fresh water weight
W_{PR}	Provisions weight
W_{CR}	Crew weight
W_S	Stores weight
B	Water ballast
$\boldsymbol{v}$	Fluid velocity
U_r	Artificial force that compresses the region under consideration
k	Turbulence kinetic energy
ε	Rate of dissipation of turbulence energy
G_k	Generation of turbulence kinetic energy due to the mean velocity gradients
G_b	Generation of turbulence kinetic energy due to buoyancy
Y_M	Contribution of the fluctuating dilatation in compressible turbulence to the overall dissipation rate
σ_k	Turbulent Prandtl number for k
σ_ε	Turbulent Prandtl number for ε

μ_t	Turbulent –or eddy– viscosity
$\rho_{X,Y}$	Pearson correlation coefficient between X and Y

1 Introduction

1.1 Introduction

International shipping is the backbone of global trade. Reports suggest that seaborne trade is constantly growing, having expanded at 4% in 2017. More than ten billion tons of goods were transported by ships that year (UNCTAD, 2018). Global containerised trade increased by 7.5% in 2018 (UNCTAD, 2018). As far as passenger transport is concerned, the total number of passengers embarking and disembarking in European Union ports saw a slight increase of 0.4% in 2016, despite the overall decrease of 11% over the period of 2011-2016 (Figure 1) (Eurostat, 2018). Nevertheless, the global ferry market seems to start improving its shape again (Baird, 2017).

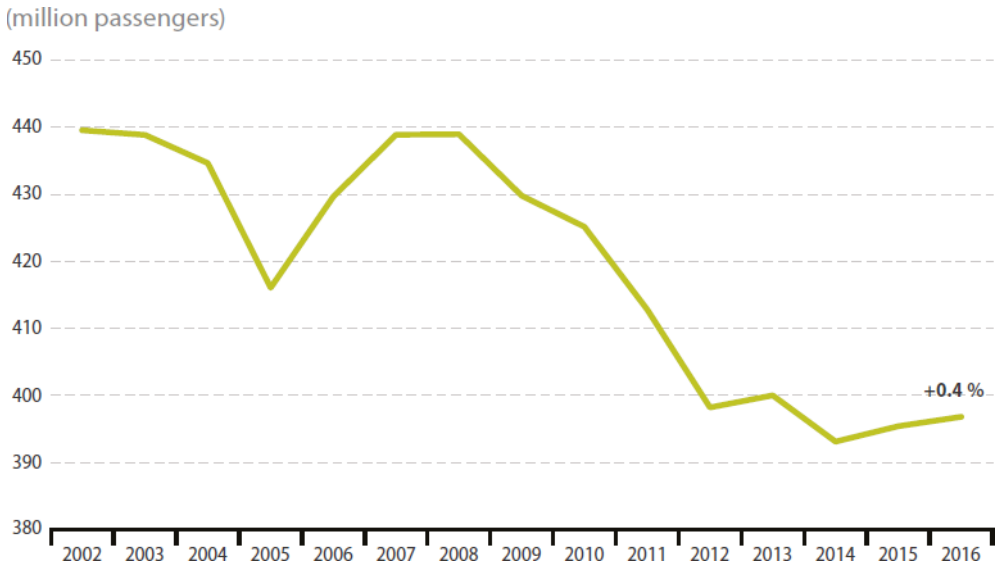

Figure 1: Number of seaborne passengers embarked and disembarked in all ports of the European Union (Eurostat, 2018)

An increased seaborne trade has led to a global fleet growth. The deadweight tonnage of the commercial shipping fleet grew 3.3% between 2017 and 2018

(UNCTAD, 2018). A positive outlook can be observed for the passenger ships as well, with many of the vessels of the global fleet currently being up to their second refurbishments. Considering that nowadays it is more economical to replace a ferry than to refurbish it, many ship owners opt for a fleet replacement (Baird, 2017).

As prominent as the future of maritime industry might be, there are several uncertainties which can affect the former. World economy growth is fragile and has considerable impact on oil prices and freight rates. In addition, the constant effort put by international organisations to achieve a safer and more environmentally friendly shipping industry, often results in the introduction of new rules or amendments on existing ones, which greatly affect the ship design process.

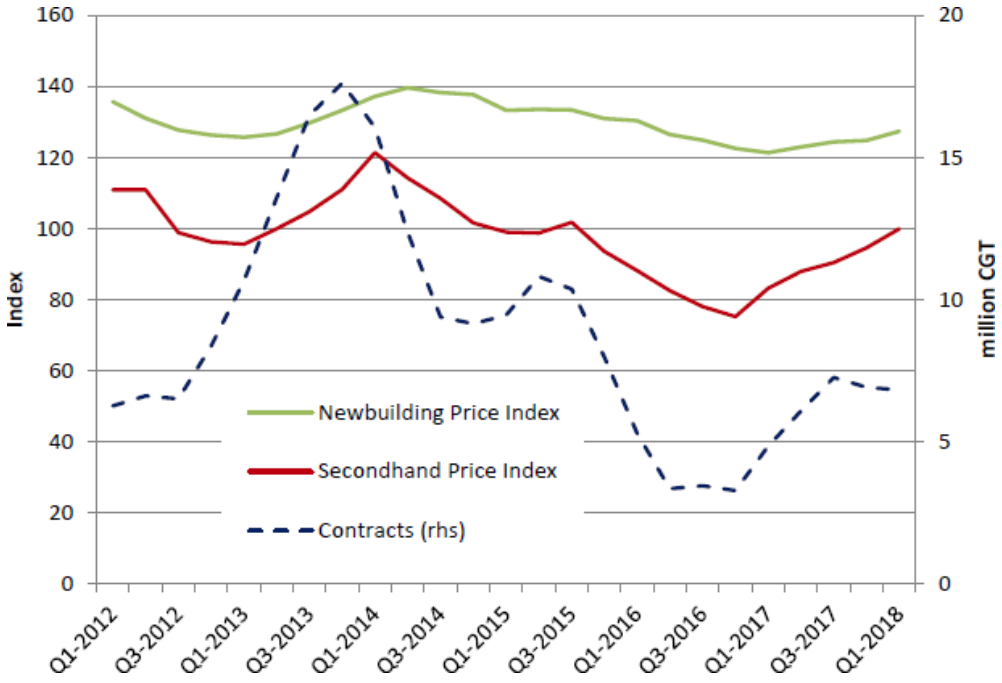

Figure 2: Price indices and shipbuilding contracts (OECD, 2018)

Besides uncertainty, the constant endeavour of shipping companies for economic growth constantly urges the shipbuilding industry to introduce new and cost-efficient designs of various ship types. These designs have to comply with international standards in terms of passenger safety and protection of the environment. In addition, the recent developments and technological improvements in the systems and energy sources used on board need to be taken into account. Figure 2 shows the recent

trends with regard to the newbuilding and second-hand price indices compared with the shipbuilding contracts. Newbuilding price index (expressed as USD per DWT values) continues its upward movement started back in 2017. Similar trend is observed for the second-hand price index. Both price indices seem to be affected by the number of shipbuilding contracts, which has been recovering since end of 2016, after a major downward trend between 2013 and 2016.

The increasing number of constraints in the design process adds to the complexity of the ship design problem. The need for design space exploration is greater than ever and the recent advancements in CAD allow naval architects to perform detailed optimisation on ship design. Such practice can lead to optimised, efficient and novel ship designs, which satisfy all the criteria set by international organisations.

1.2 Problem definition

As technology progresses, access to powerful tools which can assist naval architects in the ship design process becomes wider. The practice of an iterative procedure involving complex calculations leading to a final design does not benefit from the availability of modern CAD tools available nowadays. Hence, a new design approach needs to be introduced which takes advantage of the available computational power, producing results that reflect the overall performance of the design in short lead times.

On the other hand, the ever-increasing constraints in the ship design problem call for a detailed exploration of the design space. It then becomes clear that although modern software tools can decrease the computational time when a single design is required, naval architects have to find new ways and apply novel methods when numerous design variants need to be examined. A combined use of low- and high-fidelity tools can produce satisfactory results, depending on the required level of detail.

In addition, an increased complexity in the design process affects the level of uncertainty associated with the results. The reliability of a design created in the initial steps, where the design space exploration is sensible, is questionable when there is shortage in available data. Increasing the robustness of a design methodology by taking into account the effects of uncertainty, leads to more confident decisions on which variant to select among the designs produced in an optimisation process.

1.3 Thesis objectives

Definition of the problem in Section 1.2 gives the detailed description of the research problem which needs to be solved in this thesis. The ultimate goal of this work is to contribute to the holistic methodology for ship design in its conceptual phase.

The methodology shall be able to produce a design based on the selection of values for key design variables and should include the generation of the vessel's external and internal geometry, along with all the computations which are essentially required for the completion of the conceptual ship design phase. In addition, the produced design should be checked to identify whether regulation compliance is met or not.

Furthermore, an optimised final design shall be identified from a thorough optimisation procedure incorporated in the methodology, which takes into account the uncertainties arising in the various steps of the design process. The required computational time is kept to the minimum by use of surrogate models in lieu of computationally heavy processes.

The concept design phase is selected for the implementation of the optimisation study, since major decisions are taken during this step regarding the design of the ship. The expected level of detail in the calculations taking place during the concept design phase is not as great as in the steps closer to the construction phase, allowing the integration of numerous computations in a design optimisation loop without requiring a prohibitive amount of time to obtain results.

The research outcome of this study ought to satisfy the following objectives:

- Development of a parametric design for the vessel's external and internal geometry
- Expansion and improvement of the current methodologies for the multi-objective optimisation of ship design
- Incorporation of elements related to holistic approach to design methodology
- Investigation of the effect of the newly introduced second generation intact stability criteria on the design elements of various ship types
- Improvement of the robustness of the optimisation process via consideration of uncertainty
- Improvement of the speed of the optimisation process via use of surrogate models
- Evaluation of the proposed methodology on case studies involving different ship types

1.4 Contribution to the research field

As mentioned in Paragraph 1.3, this work aims to contribute to the holistic methodology for ship design in its conceptual phase. Taking into account the recent developments with regard to the integration of uncertainty in ship design, this thesis focuses on the effects of the former on the ship design methodology. Uncertainty quantification is investigated in various ways demonstrated through two case studies presented in Chapter 5. Uncertainty quantification becomes a key part of both the main optimisation phase and the decision making phase. This work illustrates the differences of the impact of each approach in an optimisation study. Ultimately, the robustness of the optimisation results is enhanced through the application of the proposed methodology.

In addition, the effect of newly introduced objectives and constraints in ship design optimisation is examined. New environmental and stability regulations introduced or

currently under development by the IMO are taken into consideration in the optimisation procedure. Passenger vessels are optimised taking into account the newly developed IMO second generation intact stability criteria for the first time. The impact of the latter on the design variants production during a multi-objective optimisation run is investigated to understand how they affect the feasible design space and the identification of the optimal solution.

1.5 Thesis structure

The thesis consists of 7 Chapters. The content of each Chapter is described below.

In Chapter 1 a brief introduction to the topic of ship design is provided and the problem addressed in this research is defined. The aim and main objectives of the thesis are laid out and its structure is presented.

Chapter 2 presents a critical review of ship design methods, ship design optimisation and optimisation under uncertainty. The review focuses on both theory and application, along with discussion on the relevant work. The research gap addressed in this study is identified.

In Chapter 3 the theoretical background of multi-objective robust early stage ship design optimisation under uncertainty is presented. The basic principles of ship design methodologies, parametric ship design, multi-objective optimisation, surrogate models, decision making and uncertainty quantification are introduced.

Chapter 4 presents the proposed methodology to the ship design optimisation problem. The research workflow is analysed and explained in detail.

In Chapter 5 two case studies are employed to evaluate the proposed methodology. The first case study describes the multi-objective optimisation of a containership design, incorporating aspects of economics, intact stability, ship resistance and structural integrity. On the other hand, the second case study illustrates the multi-

objective optimisation of a Ro-Pax ferry design with regard to building cost, economics, intact stability and ship resistance.

Chapter 6 contains the analysis of the results of the two case studies. Detailed graphs and tables illustrate the outcome of the application of the proposed methodology while the results are evaluated and discussed.

In Chapter 7 the whole research presented in this thesis is reviewed and its contributions and achievements are presented. The discussions are outlined and further considerations are suggested for future work on the basis of experience gained during this study. Final conclusions emerging from this study are presented.

Finally, a few Appendices are included in the end containing explanatory notes regarding the IMO second generation intact stability criteria taken into consideration in this study.

2 Critical review

2.1 Introduction

This Chapter focuses on the critical review of existing approaches and methods related to ship design, spanning a period of around fifty years. Ship design has evolved dramatically through the years, as it is influenced not only by technology, but also by historical events, economy and people's mentality.

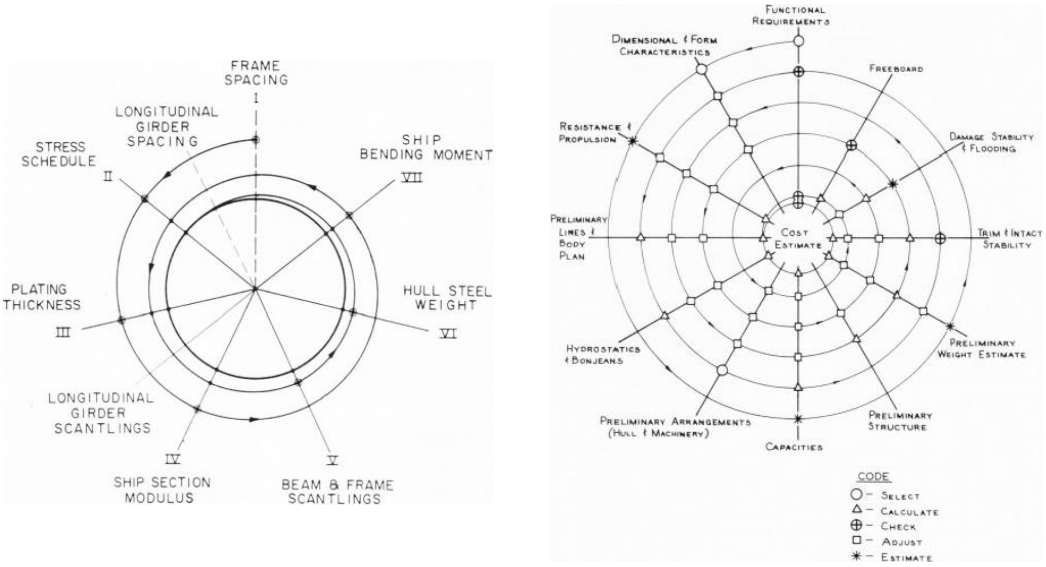

Figure 3: Design spiral according to Evans (1958) (left) and Murphy et al. (1963) (right)

2.2 Ship design

2.2.1 Traditional approaches

The first attempt to define a methodology for ship design was made by Evans (1958), who introduced the design spiral in order to describe the ship design process (Figure

3). In this method, ship design is viewed as a sequential iterative process. The design starts with the interpretation of the requirements by the ship owner and their translation to a conceptual design. Every aspect of naval architecture is examined sequentially until a complete cycle of calculations is completed. At the end of each cycle, the produced design is evaluated and the process is repeated until the objectives are met and no constraints are violated. In each repetition, the complexity of the design increases, moving from the conceptual phase to the detailed design. A single final design is produced, whose midship section structural weight is kept to a minimum.

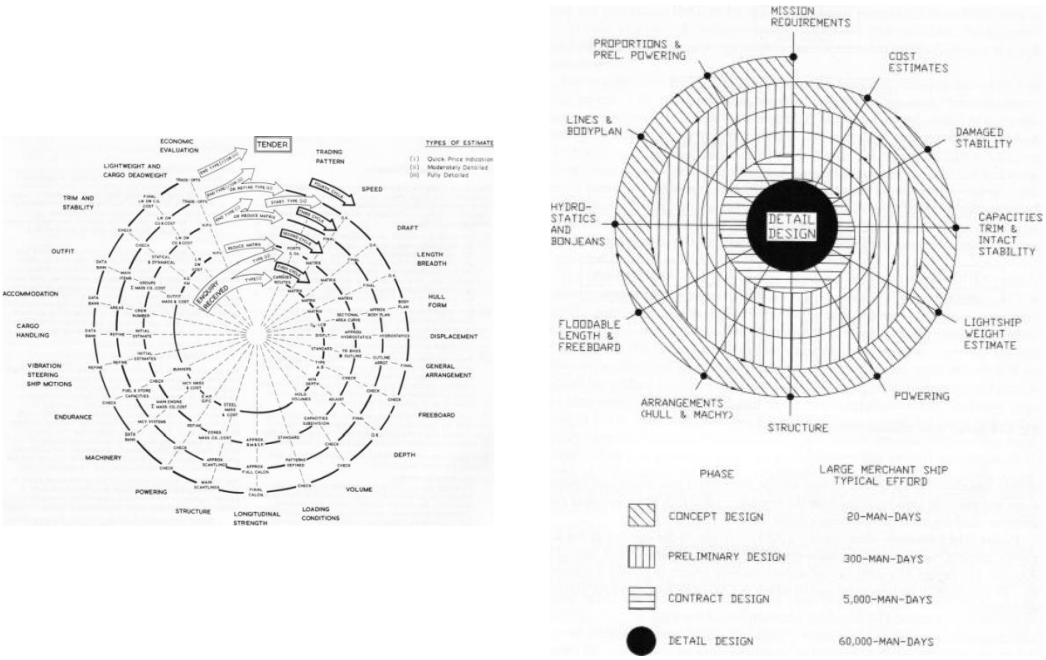

Figure 4: Design spiral according to Hurst (1971) and Buxton (1976) (left) and Kiss (1980) (right)

Based on the original design spiral, several representations of its initial form were introduced in the following years. Murphy et al. (1963) focused on the minimisation of the building and fuel cost (Figure 3). Hurst (1971) and Buxton (1976) modified the form of the design spiral, aiming at economically reliable shipyard tenders (Figure 4). Kiss (1980) and Gale (2003) set the minimisation of cost as the objective of the design spiral process (Figure 4).

2.2.2 New methods

Following the improvements in technology, further research was conducted to optimise the ship design process. In that respect, new methods were introduced. Decision-based design was proposed, according to which, the principal role of the designer is to make decisions. The latter influence the progression of the design and differentiate the proposed method from the traditional approaches mentioned in Paragraph 2.2.1 in a way that they can happen both concurrently and sequentially. In addition, the capabilities of computers are taken seriously into account and their contribution to the design stages becomes apparent (Mistree et al., 1990).

Table 1: Ship design methods

Method	Author	Date	Description
Design spiral (weight)	Evans	1958	Sequential, iterative process aiming at the lightest structure
Design spiral (cost)	Murphy et al.	1963	Objective changes to minimisation of cost
Design spiral (tenders)	Hurst, Buxton	1971, 1976	Shipyard tenders become the main objective
Design spiral (cost)	Kiss, Gale	1980, 2003	Ship design based on minimisation of cost
Decision-based	Mistree et al.	1990	Introduction of decision making in the design process
Set-based	Parsons and Singer	1999	Modular approach with application in naval ship design
Risk-based	Papanikolaou, Vassalos	2009	Rule-based design with safety as the main objective
Holistic	Papanikolaou	2010	Life cycle approach

Based on the automotive industry, set-based design approach was introduced a few years later (Parsons and Singer, 1999). According to this method, the first step is to define several sets of design parameters that lead to various designs being created concurrently. Exchange of information takes place in order to discard the dominated designs, until a more globally optimum solution is found. The level of detail in the design process rises gradually as the sets of design parameters are narrowed down.

Risk-based design approach was introduced later by Papanikolaou and Vassalos. According to this approach, safety plays an important role in ship design, which is based on probabilistic concepts. Intact and damage stability are considered as the main objectives and probability and risk theories are applied to create a design that meets all the safety-related criteria (Papanikolaou, 2009).

By all means, the space of the feasible solutions in the design process is massive. This, in correlation with the complexity of the design constraints and the importance of the decisions made by naval architects call for more sophisticated approaches in ship design. According to Papanikolaou, a systemic approach considers the ship as a complex system integrating a variety of subsystems and their components. The latter can be described by ship functions. Adding the life cycle in the design process renders the task even more convoluted, however this leads to a comprehensive, holistic approach (Papanikolaou, 2010a).

2.2.3 Summary

All in all, the established ship design methodologies have evolved significantly throughout the fifty years examined in this review, ranging from sequential and rather time-consuming processes to more sophisticated approaches, while from 2010 onwards the holistic approach seems to be the most reliable method which produces comprehensive results (Table 1). The benefits of this procedure are apparent after the construction of the vessel. By considering the life cycle of a ship in the design phase, a robust design is produced, for which the designer can feel confident about its economic feasibility until the end of its life.

2.3 Optimisation in ship design

As the ship design methods have evolved through the time, the concept of optimisation has become a vital part of them. Depending on the area and the level of optimisation, several categories of tasks can be identified in that respect; basic ship

design, ship compartmentation, hull shape design and powering, ship structural design and process design (Nowacki, 2003). Researchers once focused on single-objective optimisation problems; however the trend nowadays is the solution of complex, multi-objective optimisation ones.

In order to solve an optimisation problem, designers and researchers may apply various methods, each associated with advantages and disadvantages. Bertram (2003) has reviewed relevant developments regarding the available optimisation techniques. Genetic algorithms have been widely used as they have been found to be quite robust and efficient for problems involving many integer variables. These algorithms generally avoid getting stuck to local optima by evaluating various points in the design space. However, it remains unknown whether genetic algorithms can be successfully used in any optimisation problem (Bertram, 2003).

Another approach to the solution of an optimisation problem is the utilisation of concept exploration models. It resembles the principles of an exhaustive search simulation, as essentially a large set of design variants is generated by varying design variables. Each of these variants is evaluated and the best solution is identified. Hence, the efficiency of this method quickly decreases as the number of design variables rises. There have been attempts to overcome this problem, either by applying constraints and rejecting design variants which violate them (Georgescu and Verbaasm, 1990), or by reducing the number of design variables (Erikstad, 1994). Applications of concept exploration models in ship design include the optimisation of small warship design (Eames and Drummond, 1977); SWATH design (Nethercote et al., 1981) and cargo ship design (Georgescu and Verbaasm, 1990, Winjnolst and Waals, 1995).

Attempts to increase the efficiency of solving complicate ship design optimisation problems have led to the development of algorithms tailored to individual problems. Examples of such algorithms include CHWARISMI (Söding, 1977) and DELPHI (Bertram, 1998, Bertram and Isensee, 1998, Gudenschwager, 1988). Such algorithms generally accept as input all relevant knowledge to the problem in form of relations,

check whether the problem can be solved or not and then numerical computations are performed to provide the solution. Schneekluth and Bertram (1998) developed such an algorithm to optimise containership design. Drawbacks of this approach may include the error occurrence due to problem misformulation or unclear definition, while the developed algorithms generally lack user-friendliness.

Knowledge-based systems were introduced to increase the user-friendliness of the aforementioned approach. Based on artificial intelligence, knowledge-based systems include a general database where all the basic functions are stored and engineers can then contribute by adding more functions and rules to develop a specific system. The advantage is that in theory the order of the knowledge is not important. Knowledge-based systems have been used in ship and propeller design optimisation, yielding results in short lead times (Dai and Hambric, 1995, Dai et al., 1995).

2.3.1 Single-objective optimisation

Even if at first it seems that optimising a design in the maritime industry is prohibitive, given the complexity of ships as systems, significant research has been conducted since the 1960s. In this Paragraph, a review of the work carried out with regard to the solution of single-optimisation problems in ship design is presented.

At the early design stages, the principal dimensions of the vessel are set, based on the owner's requirements. An optimisation based on the main dimensions can have a great impact in the ship's economic potential. The objectives can be based on the building cost or the life cycle cost and the revenue. In general, the amount of design variables is limited to the main dimensions and their ratios, while the constraints related to the problem are mostly physical bounds, regulations and safety requirements. There has been a considerable amount of research on this topic, mostly dealing with merchant vessels, such as bulk carriers and general cargo ships. Mandel and Leopold (1966), Gilfillan (1969), Nowacki et al. (1970) and Fisher (1972) focused on the optimisation of the required freight rate using several methods, ranging from exponential random search to parametric studies and non-linear

programming. On the other hand, Puchstein (1969) and Kupras (1976) optimised cargo ships based on their building cost using similar methods.

Instead of focusing on the exterior shape of the hull, other researchers tried to optimise the internal compartmentation of ships. This problem involves numerous constraints in terms of available space and the ultimate purpose is to find the best arrangement which meets the requirements for capacity, access, safety, comfort and cost. Methodologies have been developed to solve the optimisation problem of internal compartmentation (Figure 5) (Kanerva, 2002, Nehrling, 1976).

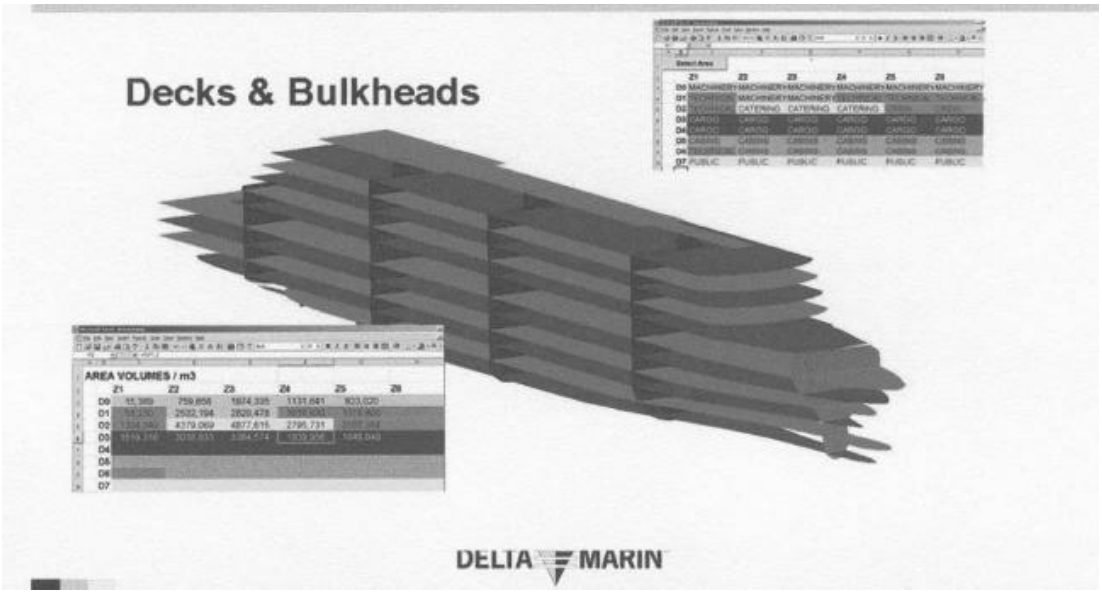

Figure 5: Compartmentation for parametric simulation-based design (Kanerva, 2002)

Apart from the basic ship design, research has been carried out in terms of the overall hull shape and its hydrodynamic performance. The main objective in this case is the minimisation of the wave resistance. In order to achieve this, a set of free form parameters controlling the shape of the hull is used as design variables. Potential constraints for this problem include hull geometry limitations or hydrodynamic performance, such as motions and manoeuvring. Significant work undertaken in that respect includes Michell (1898), Wigley (1935) and Weinblum (1932), who applied linearised wave resistance theory.

The introduction of the computational fluid dynamics in ship design optimisation was followed by further research, as the accuracy of the results became higher and the optimised designs more credible than before. Duy and Hino (2015) focused on the hydrodynamic shape optimisation of a containership transom. Zhao et al. (2015) proposed the optimisation of the ship hull surface with regard to the wave resistance using the wavelet method. Zakerdoost et al. (2013), Han et al. (2012) and Peri et al. (2001) employed computational fluid dynamics methods to minimise the total resistance.

Another area that has attracted research in the field of ship design optimisation is the structural design. The aim is to optimise the ship in terms of weight and cost. The design variables in this case involve size and type of scantling members as well as configuration variables, such as coordinates of nodes. The feasibility of the design is mostly affected by relevant regulations. Examples of relevant research include the work of Evans and Khoushy (1963) and Buxton (1966), who developed the design spiral aiming at a minimum midship section weight. Liu et al. (1981) and Hughes (1983) expanded the optimisation problem by including all major substructures in their application and employing sequential linear programming to minimise the cost and weight of the structure.

The research mentioned above has contributed significantly to the field of ship design optimisation by introducing new methods and approaches in various aspects of ship design. However one major downside of solving a single-objective optimisation problem is the lack of an all-around solution. Focusing on one objective, such as the minimisation of the midship section weight or the minimisation of the overall resistance may lead to solutions that are incompetent in other aspects.

2.3.2 Multi-objective optimisation

Optimisation problems based on a single objective can be formulated in a straightforward manner. On the other hand, the addition of objectives requires careful handling of the problem. Essentially, an optimisation problem based on many

objectives –most commonly referred to in the literature as "multi-objective optimisation problem"– needs to be transformed to a single-objective optimisation one. There are several options to select from, including keeping one criterion as objective and formulating the rest as constraints, or apply decision making procedures to identify the optimal design (Sen and Yang, 1998).

The result of a multi-objective optimisation problem is a set of solutions which perform the best in each discipline. This set lies on the so-called Pareto front, named after Vilfredo Pareto, an Italian engineer and economist, who used the concept in his studies of economic efficiency and income distribution.

The advancements in computer hardware and software tools have made the solution of multi-objective ship design optimisation problems nowadays possible. Addressing and optimising several aspects and elements of a ship's life has become the norm in the recent years. Starting from the stages of design and moving to the construction and operation phases, effort is made to define a holistic ship design optimisation methodology.

Most of the work mentioned in Sections 2.2 and 2.3 can be considered as the first steps towards this attempt, since many of them follow the principle of transforming a multi-objective optimisation problem to a single-objective by focusing on one objective and translating the rest to constraints. Nowacki (2018) refers to these studies as the baseline to multi-objective ship design optimisation; however, they are confined in specific features of ship design. He underlines the importance of consideration of the whole life cycle of a ship in order to perform a thorough economic analysis of a design. Through a holistic, multi-attribute optimisation, all stakeholders involved in the life of a ship, such as the builders, operators, suppliers and customers are taken into account, while compliance to international regulations is investigated and emphasis is put on producing environmentally friendly and safe designs. In Table 2 some of the most important studies on multi-objective ship design optimisation, organised by the design model they are based on are mentioned.

- Synthesis model:

The synthesis model is considered as the first generation of design models. According to this, a single objective is assumed during the optimisation process and the rest of the design requirements are treated as constraints. The aim is to identify the best design based on the single objective, which does not violate any of the constraints. The examples of research studies presented in Table 2 for the synthesis model date back to the 1960s up to the 1990s, when the constraints to be considered were a fraction of what should be included in an optimisation study today due to the low complexity of the design applications during that time period.

Table 2: Ship design optimisation models

Model	Approach	Measure of merit	References
Synthesis	Penalty factors, gradient methods, direct search	Life cycle cost, required freight rate, net present value, capital recovery factor	(Kuniyasu, 1968, Mandel and Leopold, 1966, Murphy et al., 1963, Nowacki et al., 1970, Nowacki et al., 1990, Söding and Poulsen, 1974)
Multi-objective	Pareto optimisation, utility functions, graphical visualisation	Economics, safety, environment, etc.	(Papanikolaou, 2010b, Papanikolaou et al., 2011)
Risk-based design	Pareto optimisation, utility functions, graphical visualisation	Economics, safety, naval criteria, environment, etc.	(Boulougouris et al., 2004, Papanikolaou, 2009)
Holistic design	Pareto optimisation, utility functions, graphical visualisation	Economics, safety, naval criteria, environment, etc.	(Boulougouris et al., 2011, Köpke et al., 2014, Papanikolaou, 2010a, 2011)

- Multi-objective model:

The development of multi-objective models began a few years later, with most studies undertaken in the 2000s and 2010s. The multi-objective model is based on the principle that ships have more than one purpose in their lifetime. Hence, design development should address all of the potential roles in the life of a ship while

considering the rules and regulations applied to the specific ship type. These purposes introduce more objectives in the design process.

Nowacki (2018) classifies the reasons why multiple purposes may occur. A ship might be built to perform varying tasks (e.g. multi-purpose offshore vessels, ore/bulk/oil carriers). In addition, multiple parties are involved in a design project; not only the directly related, such as the designer and the owner, but also classification societies, legal authorities and insurance companies. It is inevitable that these stakeholders are having conflicting interests during the ship's lifetime, which should be addressed in the design process. Moreover, the interests related to the operation of a ship are usually used as objectives when trying to optimise a design. The number of these interests is usually more than one, with three basic categories being pinpointed by Nowacki (2018); finance, safety and environment. These interests cannot be combined to form a single objective; hence, a multi-attribute optimisation problem inevitably arises. These interests are usually expressed by standardised measures, such as required freight rate, probability of compliance with SOLAS safety rules and energy efficiency design index. Finally, history has a significant impact in the formulation of the objectives of a ship design optimisation problem. Maritime accidents throughout the history have triggered changes in the international regulations regarding ship construction and operation, thus affecting the ship design process. The complexity of most regulations nowadays has increased compared to the past and it is more sensible to incorporate them as objectives rather than constraints in an optimisation problem.

Examples of research work implemented based on the multi-objective model are presented below.

Ehlers et al. (2015) performed a multi-objective optimisation study focusing on the structural design of chemical product tankers. Objectives include the production cost, weight and fatigue life. The latter is examined based on guidelines specified in classification society rules. Hence, the objectives are related to the relevant elements of ship design, namely economics, safety and environment. A decision support

algorithm involving the stakeholder preferences obtained through a semi-structured interview combined with a formal assessment of stakeholder utility functions is used to identify the optimal design. The results of this study indicate the trade-offs between the examined criteria, while the applied methodology regarding the decision making process illustrates the possibilities of including the stakeholder preferences as early as in the concept design stage.

Zaraphonitis et al. (2003) developed a formalised multi-objective optimisation procedure for the internal compartmentation of a Ro-Pax ship. The financial and safety aspects of the design are examined by considering the ship's survivability after damage and the transport capacity and building cost as the main objectives of the study. The results illustrate the importance of using such a design tool in the preliminary design stage for the assessment of numerous designs with regard to their internal compartmentation which affects its survivability based on SOLAS regulations. Similar studies were performed by the same authors for cruise ships, taking into account the probabilistic concept introduced by SOLAS 2009 regulations (Figure 6) (Zaraphonitis et al., 2013).

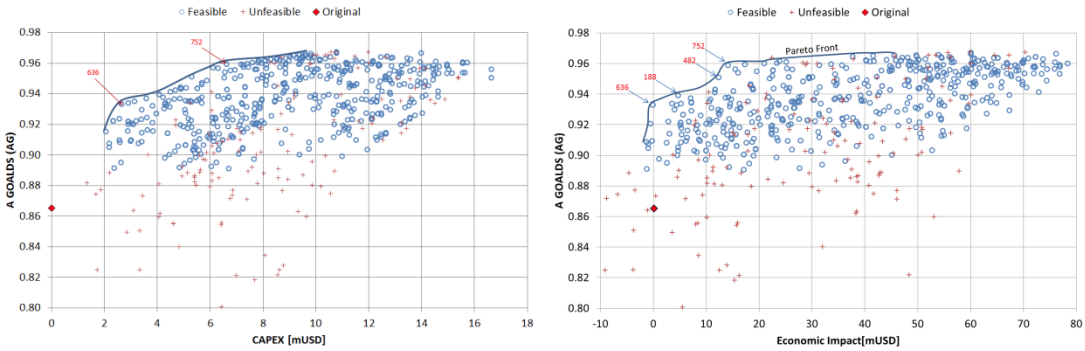

Figure 6: Optimisation study results on survivability of cruise ships based on SOLAS 2009 probabilistic concept (Zaraphonitis et al., 2013)

Papanikolaou et al. (2011) proposed a methodology for an integrated design and multi-objective optimisation approach to ship design. The objectives of this optimisation study include the RFR, EEDI and OOI (Figure 7). Hence, finance and environment are taken into account, while safety is implied by the consideration of

MARPOL rules as constraints. A parametric model of an Aframax tanker is used for demonstration purposes. The integrated design approach connects several software systems for analysis and simulations. The authors stress the importance of robust parametric models for various ship types to allow highly automated optimisation process by adjusting the values of the design variables associated with the parametric model (Figure 8).

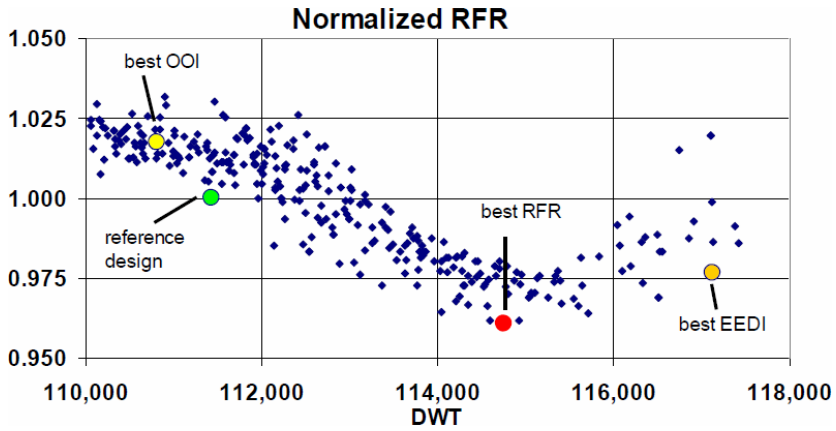

Figure 7: Designs established by means of integrated CAE approach (Papanikolaou et al., 2011)

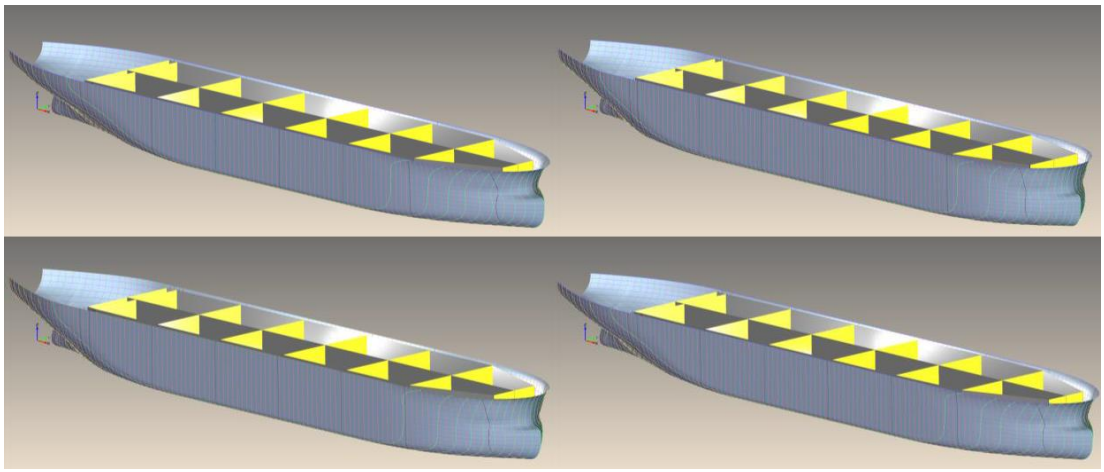

Figure 8: Parametrically generated hull forms (Papanikolaou et al., 2011)

- Risk-based model:

The risk-based model is based on the assumption that complex systems which operate under hazardous conditions are prone to extensive damage and complete

failure. Therefore, prevention of such conditions should become a priority in the design process. Basic concepts of hazard investigation rely on deterministic theory. Risk-based models look into safety in more detail by applying probabilistic theory.

Such design models apply the risk theory in all elements associated with a ship's life cycle. Designers look at all possible operational scenarios which affect a ship's performance with regard to safety and economics and try to predict the probability of occurrence of events that impact the ship's life negatively, using risk theory. Adhering to the principles of multi-objective and holistic models, all damages affecting any of the stakeholders of a ship are included in the analysis.

Nowacki (2018) observes the effects of the utilisation of risk theory in the analysis. In particular, the design process moves away from the rule-based principles. Even though safety is regarded as a constraint in the optimisation problem, in risk-based models it is treated as an objective instead.

One could say risk-based models introduce the effect of uncertainty in ship design, a topic investigated in more detail in Paragraph 2.3.3. Nowacki (2018) suggests that uncertain hazards are quantified as probabilistic risks. These risks then become measures of merit in the optimisation process. The result of such practice is the identification of a more robust all-around solution which is not affected by external hazards (e.g. adverse weather conditions, crew competency, fuel or material price).

Examples of research work based on the risk-based model are presented below.

Typical example of the application of risk-based model in ship design optimisation is the study performed by Papanikolaou (2010b) on an Aframax tanker. The internal arrangement of the cargo space varies throughout the optimisation, considering several configuration setups with differences spotted in the number of cargo tanks in both longitudinal and transverse direction and the type of bulkheads. The main objective of the study is to reduce the accidental oil outflow, while minimising the steel weight and maximising the cargo capacity. The assessment is based on

probabilistic methods. Interesting results, showing the effect of the configuration setup on the oil outflow, were produced in this study (Figure 9).

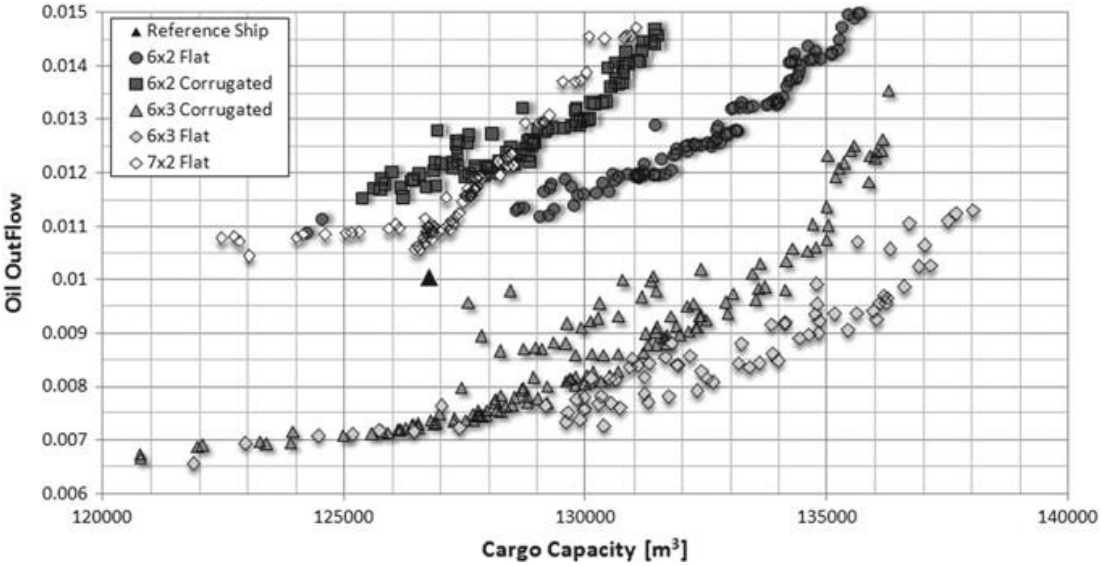

Figure 9: Oil outflow vs. cargo capacity for various internal setup configurations (Papanikolaou, 2010b)

Risk-based models focusing on safety of passengers can be applied in cases where passenger vessels are being optimised. European Union funded project SAFEDOR (2005-2009) contributed to the development of methodologies related to risk assessment during the life cycle of a ship. In design phase hazards such as collision, grounding, flooding, fire and explosion are evaluated to investigate the survivability of a ship. In operation phase, the management of the residual risk every design possess over the lifetime of a ship is evaluated, focusing on the monitoring and maintenance of on-board safety systems and sensors. The project produced several publications describing methodologies and applications on risk-based ship design optimisation (Breinholt et al., 2012, Papanikolaou, 2009).

- Holistic model:

The fourth model presented in Table 2 is the holistic model. The term holistic derives from the Greek word ὅλος (hólos), meaning “whole”, “entire”, “complete”. The purpose of such a design model, as mentioned in Paragraph 2.2.2, is to investigate all

aspects of a ship simultaneously, through separate measures of merit. The difference from the multi-objective model lies in the extent of the life of a ship taken into consideration during the optimisation process. In addition, the number of indices selected to represent each influence is different. In a holistic model, the performance of a ship regarding a specific purpose (e.g. economics) is measured by more than one indicator. For instance, the required freight rate in connection with the energy efficiency design index can be used to estimate the economic performance of an oil tanker. Such practice eventually leads to a comprehensive, holistic appreciation of a ship design.

According to Nowacki (2018), a holistic model, by definition, would require all influences to be considered in the design process. However, he prefers to confine the investigation to all influences that are actually relevant to the issue examined in each case. In fact, this approach seems more feasible than incorporating every element affecting the life of a ship in a single study. Not only over-constraining of the optimisation problem is avoided, but also more sensible solutions are obtained. Nevertheless, in order to classify a problem as a holistic design optimisation, the presence of economics, safety and environment in the problem definition is required.

Papanikolaou (2018) suggests that a recent trend of introducing scientific disciplines in the general ship design problem –design for safety (Breinholt et al., 2012, Papanikolaou, 2008, 2009, Vassalos, 2007) design for efficiency (Boulougouris and Papanikolaou, 2009), design for production (Okumoto et al., 2009, Simpson et al., 2014, Singer et al., 2009), design for arctic operation (Riska, 2009) and design for X (Andrews and Erikstad, 2015, Andrews et al., 2018, Papanikolaou et al., 2009)– indicate the need for new approaches and the availability of methods and software tools to successfully address the ship design optimisation problem in a holistic way.

A selection of research studies which treat the ship design optimisation problem from a holistic point of view is presented below.

Köpke et al. (2014) performed a holistic optimisation of a high efficiency and low emission containership, as part of the joint industry project CONTIOPT (2012-2013). Taking into account the latest safety and environmental international regulations, they used genetic algorithms to optimise a parametric containership model with regard to the RFR, EEDI, carried water ballast, container capacity and port efficiency. This example satisfies the criteria to classify it as a holistic optimisation study, as the aspects examined –financial competence and environment– are measured using multiple efficiency indicators. The RFR, amount of water ballast carried on-board, container capacity and port efficiency indicate whether the design is competitive in the containership market, while the consideration of rules regarding water ballast management and greenhouse gas emissions illustrate the levels of environmental friendliness of the design.

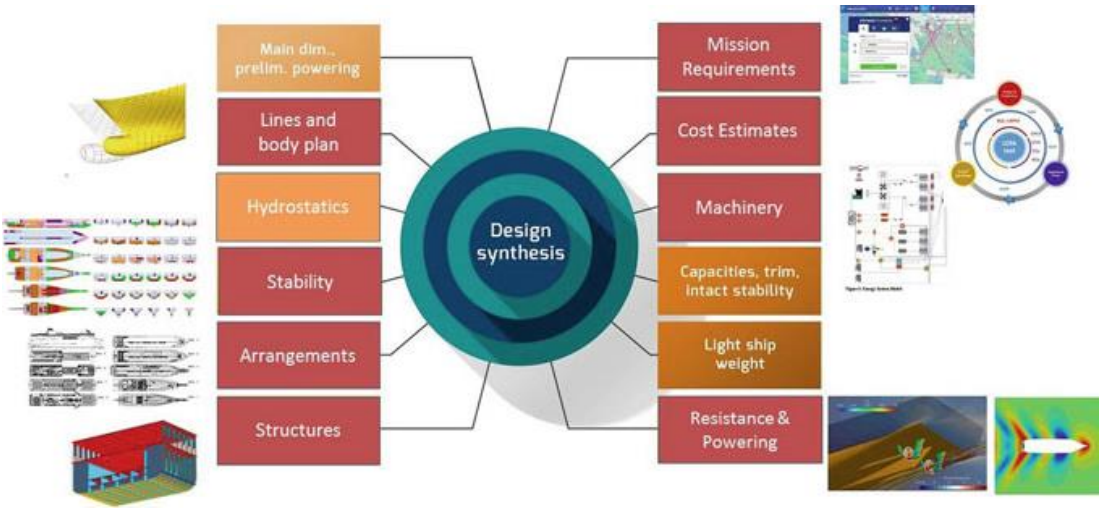

Figure 10: HOLISHIP approach (HOLISHIP, 2016-2020)

HOLISHIP (2016-2020) project is a joint effort of forty European Union stakeholders to provide solutions for ship design in a holistic way. The main aim is to create a new synthesis concept, according to which information from one design discipline can be instantly provided to the rest and changes can be propagated directly from one system to the other (Figure 10). Numerous publications have been produced based on the ongoing research on the project. These include the application of compliance matrix models based on ship operational needs during the early ship design stage (Guegan et al., 2018), development of life cycle ship performance

assessment tools considering both costs and environmental aspects (Gualeni and Maggioncalda, 2018) and integration of software tools for a holistic design optimisation of offshore support vessels (De Jongh et al., 2018).

The overall progress of the project is presented in the publication of Marzi et al. (2018). The coupling of the developed tools within the project and the use of surrogate models is demonstrated through an application case and their contribution to an efficient holistic optimisation study becomes evident. Computational time is controlled via the utilisation of surrogate models, while the variety of software tools allow the exploration of several ship design disciplines at once.

The holistic model is applied not only on merchant vessels but also on naval ships (Boulougouris and Papanikolaou, 2013). The owner's requirements for the merchant vessel are substituted by the navy's mission requirements. Yet, the holistic design concept remains the same. Aspects such as the internal compartmentation and structural arrangement affect performance indicators such as compliance to international regulations, combat strength and survivability.

2.3.3 Ship design optimisation under uncertainty

In most engineering problems, the design parameters are known to a certain extent. For many years, research on ship design had been overlooking the impact of uncertainty on optimisation and had been focusing on deterministic solutions to the problems investigated. However, lately, as mentioned in Paragraph 2.3.2, researchers have been evaluating the significance of uncertainty and its effects. This trend has introduced one more term associated with optimisation studies; robustness.

An optimal design can be characterised as robust when its quality does not deviate much from optimality when small changes occur in the problem (Branke et al., 2008). Traditional optimisation methodologies that overlook uncertainty tend to produce non-robust, over-optimised designs that do not correspond to reality. On the contrary, robust optimisation methods take input uncertainties in the design

variables, as well as uncertainties within the system or model into account and try to find optimal solutions in a noisy, uncertain environment. The results of a robust optimisation end up being insensitive to variations occurring in their operating environment (Steponavice and Miettinen, 2012). Contrary to single-objective optimisation problems, robustness in multi-objective optimisation is complicated, as it has to be defined for all Pareto solutions. The number of objectives is inevitable increased should the designer decide to incorporate uncertainty in the problem. Consequently the decision making process becomes convoluted.

Table 3: Robustness models in multi-objective optimisation

Author	Date	Approach
De Groot	1970	Minimisation of the expectation of the general loss in the performance of the solution
Taguchi and Phadke	1986	Minimisation of the variance of the objective values
Tu et al.	1999	Probabilistic constraints' assessment model
Trosset et al.	2003	"Minmax" approach
Deb and Gupta	2006	Minimisation of the mean effective and worst value of the objective function
Barrico and Antunes	2006	Degree of robustness concept
Hassan and Clack	2008	Degree of insensitivity to changes in the environment
Erfani and Utyuzhnikov	2011	Tuneable robust function

One of the most common approaches to incorporate the effects of uncertainty in a problem is the assignment of probability functions to the design parameter, instead of using single values. Brefort and Singer (2018) characterise this as epistemic uncertainty that stems from many sources, including the limited information of a vessel model, the difficulty identifying precise design performance targets and the difficulty to identify the precise bounds on the validity of the analysis tools. Therefore, it becomes clear that a level of uncertainty is introduced from the process itself in the solution of the design problem. Nikolopoulos and Boulougouris (2018)

have investigated three categories of uncertainty, coming from the environment, the market and the method. The impact of uncertainty is significant, as many design characteristics are not properly defined and the response of the model is ambiguous. If these uncertainties and their effects are captured properly and early enough, the error margin arising along the design process can be minimised.

There have been several studies, which investigate the effect of uncertainty on design optimisation through various approaches (Table 3). One option is to minimise the expectation of the general loss in the performance of the solution (De Groot, 1970). Taguchi and Phadke (1989) tackled uncertainty by minimising the variance of the objective values, which leads to a robust design in a strict sense. Others have incorporated uncertainty in the form of probabilistic constraints' assessment in the minimisation of the objective function (Agarwal, 2004, Agarwal and Renaud, 2004, Du and Chen, 2000, Sues et al., 2001, Tu et al., 1999). Trosset et al. (2003) used the most conservative approach in robust optimisation, the "minmax" approach, which is the minimisation of the worst possible case for the objective function.

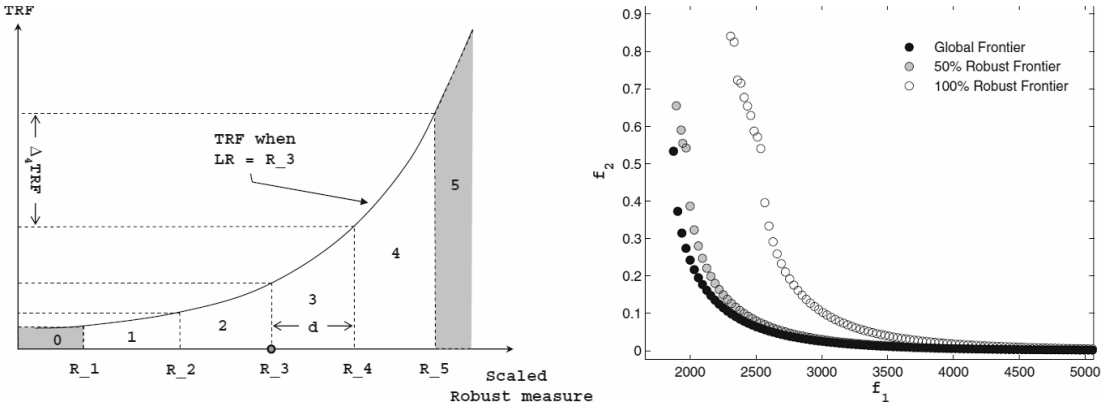

Figure 11: Tuneable robust function (left) and its effect in the definition of the Pareto front (right) (Erfani and Utyuzhnikov, 2011)

In multi-objective optimisation problems, Deb and Gupta (2006) introduced two types of robust solutions involving the mean effective and the worst values of the objective function among a chosen number of solutions in an attempt to gain direct control over the extent of the robustness of the solution . However, depending on the

number of solutions under consideration, the method can be computationally expensive.

Barrico and Antunes (2006) approached the problem by introducing a degree of robustness in the optimisation process. The aim is to determine a set of areas around a solution, so that images of solutions within these areas still belong to a pre-specified area around the objective function. The degree of robustness depends on the size of the areas around the solution and the percentage of the neighbouring points, whose objective function values belong to the pre-specified area around the objective function.

Hassan and Clack (2008) interpreted the robustness of a solution qualitatively as a degree of its insensitivity to changes in the environment. However, this approach may lead to wrong decisions since the objective vectors do not necessarily keep their utility properties.

Erfani and Utyuzhnikov (2011) used a tuneable robust function as an objective in the optimisation problem, which enables the control of the robustness extent by designer preferences (Figure 11).

As far as ship design is concerned, Erikstad and Rehn (2015) have performed a thorough review on uncertainty handling in marine systems design. Uncertainty in the field of maritime research was first introduced utilising approaches, such as real options analysis, found in the financial sector. For instance, Dixit (1989) focused on shipping applications, where several decisions related to the shipping market were evaluated. Other applications involve the analysis of available options in shipbuilding contracts (Hoegh, 1998) and in naval ship design (Gregor, 2003).

Another way to solve the optimisation problem under uncertainty is through the utilisation of probabilities. Stochastic optimisation introduces the probability distributions of design parameters, extending the deterministic optimisation problem to improve the robustness of the solutions. Applications in the marine industry

include vehicle routing problems (Fagerholt et al., 2010), simulation-driven optimisation of bulk carrier design (Nikolopoulos and Boulougouris, 2018), optimisation of ship design for life cycle operation (Plessas et al., 2018) and mission-based ship design under arctic sea ice conditions (Choi et al., 2015).

2.3.4 Summary

Optimisation in ship design has evolved significantly in the past fifty years, starting from simple applications involving single-objective studies and trivial methods. Technological advancements allowed more complex calculations to be incorporated in the optimisation procedure, increasing the number of objectives and elements considered in relevant studies, while the accuracy levels of the results were improved.

Although initial research focused on ship economics, historical events involving catastrophic ship accidents which affected the environment and led to loss of human lives, shifted attention to safety and environment. The introduction of new regulations regarding ship design and operation rendered the design problem more convoluted than in the past, thus calling for a multi-objective optimisation of the design process. At the same time, maritime transport and world economy have been facing significant changes and researchers have been attempting to analyse their effects on a ship's life cycle. Uncertainties were introduced to the ship design optimisation problem and the proposed solutions present robust designs, uninfluenced by external factors.

Despite the significant progress in the field of ship design optimisation, Bertram (2003) advises that a critical review on the results of optimisation studies is recommended. Such studies have a supportive role in the solution of ship design problem and the naval architect continues to be responsible for the final decision.

2.4 Identification of research gap

In this Chapter a review on ship design approaches and design optimisation methodologies is presented. All in all, the field of ship design has evolved significantly, transitioning from conservative approaches to a holistic point of view. Optimisation has become a vital part of the process, focusing on a single objective when it was first introduced, yet investigating the whole life cycle of a ship and every design discipline nowadays. Moving away from deterministic solutions to the ship design problem, researchers are currently attempting to incorporate design uncertainty in a holistic way.

Many ship design optimisation methodologies have been developed in the past fifty years and each one is analysed in this Chapter. Through this review, the research gaps in this scientific field are identified and become the research objectives of this thesis.

Multi-objective optimisation allows the consideration of numerous objectives in each ship design study. Introduction of new regulations become the base for conception of such objectives and research is conducted to identify the feasibility of new designs based on constraints and measures of merit not examined previously. For instance, the development of the second generation intact stability criteria by the IMO adds to the complexity involved regarding the intact stability of ships, especially containerships and passenger vessels, as described later in Chapter 4. New regulations regarding water ballast management extend the design space for cost-efficient merchant vessels. On the other hand, the introduction of the EEDI and the increasing restrictions it introduces in the operation of ships call for more thorough investigation of the ship design problem.

The perpetual incorporation of optimisation objectives could lead to an over-constrained problem with infeasible solutions. The purpose of this thesis is to explore the relation of newly introduced design objectives and their effect on the emerging solutions.

In addition, uncertainty definitely plays an important role the ship design process, according to the review of the research studies mentioned in Paragraph 2.3.3. However, its effect has not been adequately explored in detail in the optimisation process as far as ship design is concerned. The work presented in this thesis incorporates the uncertainty quantification process in various steps throughout the optimisation process and the results are compared and evaluated to identify the impact of uncertainty quantification in the selection of the optimal solution.

3 Theoretical background

3.1 Introduction

In this Chapter an analysis of the principles applied in this study is made. An overview of the parameter-based geometric modelling theory is presented. Furthermore, the generic ship design optimisation problem is defined, while a review of the optimisation methods used to solve the aforementioned problem is made. Finally, a reference to the surrogate models, decision making techniques and uncertainty quantification methods follows. More detailed information regarding the techniques and methods applied in this thesis is provided in each Section of this Chapter.

3.2 Parametric modelling

A requirement for a ship design optimisation problem is the definition of a parametric ship model. Depending on the objective functions of the problem, the model is defined in a parametric fashion, controlled by a set of descriptors (parameters). The designer selects which of these parameters are controlled by the user –determining the set of the design variables of the optimisation problem– and which are dependent on these design variables. According to Harries et al. (2015), two types of parametric modelling are identified, namely the fully-parametric modelling and the partially-parametric modelling. The trade-offs of the various levels of parameterisation are illustrated in Figure 12.

The most traditional path offers great flexibility when someone needs to create a single geometry, involving the manual control of point sets to achieve the desired shape. However, should many variants of a baseline geometry need to be

investigated, a partially- or a fully-parametric model offers the required level of efficiency. In partially-parametric modelling, an existing shape is used as baseline geometry and specific elements are defined by parameters which affect the overall shape. For instance, shift transformation (point movements by a specified amount in the principle directions of a chosen coordinate system) or morphing (interpolation between two or more baseline geometries) techniques can be applied to an initial design, resulting in small changes which reflect the requirements set by the designer regarding the final shape.

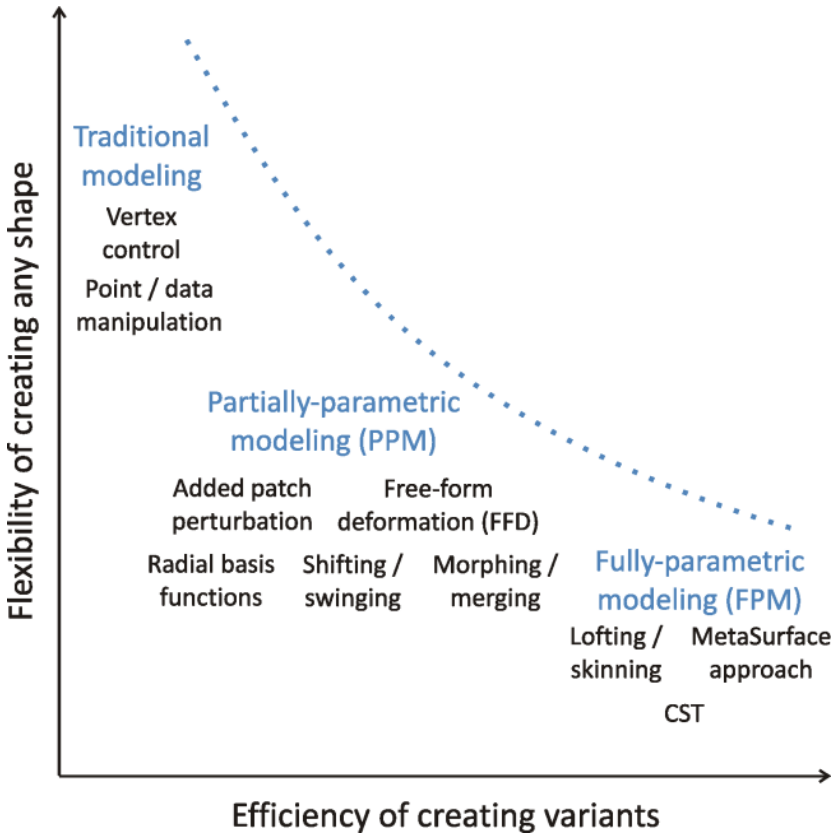

Figure 12: Efficiency vs. flexibility in geometric modelling (Harries et al., 2015)

In a fully-parametric design, the entire geometry is determined by parameters. Essentially, a parametric model can be regarded as a system which takes as input a set of parameters and produces a specific shape. Design cases which involve flow-related objects, such as ship hulls or propellers, contain information that can be described in two distinct directions. In one direction, the design morphology changes

quite slowly, while in the other direction –usually almost orthogonal to the first– there is a building pattern that remains topologically constant (Harries et al., 2015).

A powerful approach is to define the geometry parametrically in both directions, namely the building pattern (curve definition) and the distribution of the inputs to this pattern in the other direction. The result is a mathematically closed definition, the meta-surface (Friendship Systems, 2018).

3.3 Ship design optimisation problem

Ship design can be modelled as a decision process in mathematical terms. Definitions describing this problem are available in literature (Nowacki, 2003, 2018, Papanikolaou, 2010a, 2014). Within a holistic ship design optimisation, we can distinguish several elements constituting the generic problem including the input and output data, the design variables and parameters, the measure of merit functions and the constraints (Figure 13). Each of these elements is described in detail below.

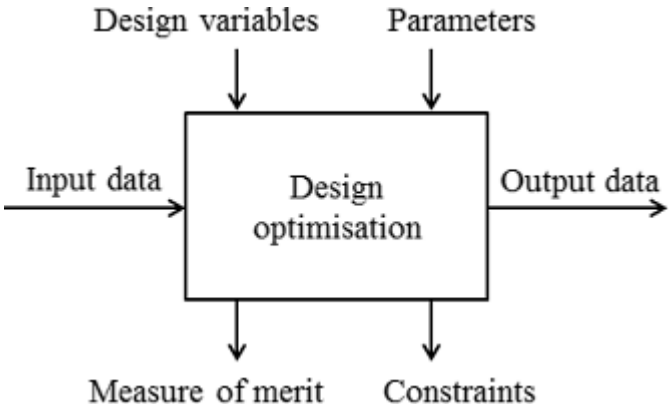

Figure 13: Ship design optimisation problem

- Input data:

The input data include the owner's requirements and the given bounds of the design variables of the optimisation problem. The former can be the required transport capacity expressed by deadweight or payload values, service speed and range. These

specifications can be accompanied by secondary data such as interest rates, steel and fuel price and drawings of ship's general arrangement.

- Output data:

The output data include the set of design variables for which the examined measure of merit functions obtain the mathematically extreme values. If a multi-objective optimisation problem is studied, the optimal solutions are located on the Pareto front and a decision making phase follows to select a design on the basis of trade-offs.

- Design variables:

The design variables refer to a number of parameters influencing directly the design under optimisation. Most commonly, these parameters vary in a continuous way; however they can also be discrete or mixed. These parameters may include the ship's main dimensions, internal space arrangement and structural elements.

- Parameters:

The parameters are closely related to the design variables described above. They usually affect the same ship design elements as the design variables; however they are a function of the free variables and cannot be controlled by the designer. Depending on the optimisation problem, the parameters can become independent and be included to the set of the design variables. They may be known with certainty in advance (deterministic case) or may be uncertain with known probabilities (stochastic case) or with complete uncertainty.

- Measure of merit functions:

The measure of merit functions are the optimisation criteria of the problem. These criteria are in general complex, non-linear functions of the design parameters which refer to the mathematically defined performance and efficiency indicators used to

evaluate each design variant. Most commonly, these performance indicators are reduced to an economic criterion, but there are cases where the objective is focused on a specific ship function, such as the hydrodynamic or seakeeping performance. Moreover, an optimisation problem can be formulated as a single- or multi-stage one, affecting which design variables influence which stage and how each stage contributes to the overall measure of merit (Figure 14). The advantage of multi-stage setups lies in the elimination of irrelevant design variables in each stage, resulting in well-defined, less convoluted optimisation problems.

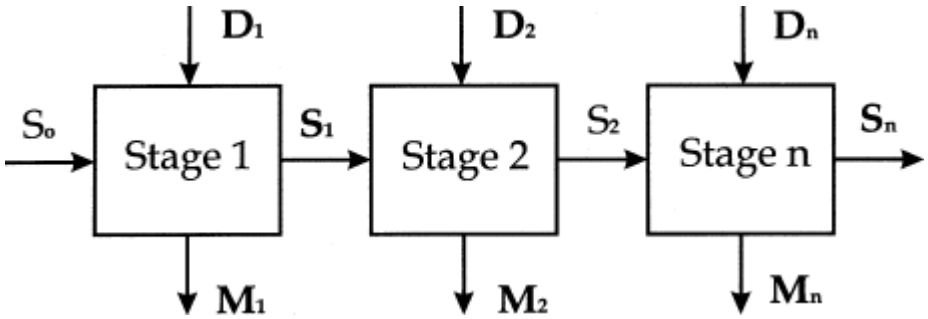

Figure 14: Multi-stage system (Nowacki, 2003)

- Constraints:

The constraints of the optimisation problem involve a set of mathematically defined criteria in the form of inequalities and/or equalities which determine the feasibility of each design variant. The constraints usually result from rules and regulations applied to the design and operation of ships, such as the MARPOL and SOLAS regulations. In addition, constraints may be related to the uncertainty of certain values used as input to the problem, such as the cost of materials or fuel.

The formulation of the multi-objective optimisation task, based on the properties mentioned above is presented in (1):

$$\begin{aligned} &\min\left(f_1(\boldsymbol{x},\boldsymbol{y}), f_2(\boldsymbol{x},\boldsymbol{y}), \dots, f_n(\boldsymbol{x},\boldsymbol{y})\right) \\ &\text{subject to} \\ &g(\boldsymbol{x},\boldsymbol{y}) \leq 0 \text{ and } h(\boldsymbol{x},\boldsymbol{y}) = 0 \text{ and } \boldsymbol{x} \in \boldsymbol{X} \text{ and } \boldsymbol{y} \in \boldsymbol{Y} \end{aligned} \quad (1)$$

f_i, i=1,…,n is the i-th objective function (measure of merit), g and h are a set of inequality and equality constraints respectively, $\boldsymbol{x}$ is the vector of the design variables and $\boldsymbol{y}$ is the vector of the parameters independent of the designer choice. The solution to this problem is a set of Pareto solutions. Geoffrion (1968) defines Pareto optimality mathematically as:

A decision vector $\boldsymbol{x'} \in S$ is properly Pareto optimal if it is Pareto optimal and if there is some real number M such that for each f_i and each $\boldsymbol{x} \in \boldsymbol{X}$ satisfying $f_i(\boldsymbol{x}) < f_i(\boldsymbol{x'})$ there exists at least one f_j such that $f_j(\boldsymbol{x'}) < f_j(\boldsymbol{x})$ and (2) is true.

$$\frac{\mathrm{f_i}(\boldsymbol{x}') - \mathrm{f_i}(\boldsymbol{x})}{\mathrm{f_j}(\boldsymbol{x}) - \mathrm{f_j}(\boldsymbol{x}')} \leq \mathrm{M} \tag{2}$$

An objective vector is properly Pareto optimal if the corresponding decision vector is properly Pareto optimal. A solution is properly Pareto optimal if there is at least one pair of objectives for which a finite decrement in one objective is possible only at the expense of some reasonable increment in the other objective (Figure 15).

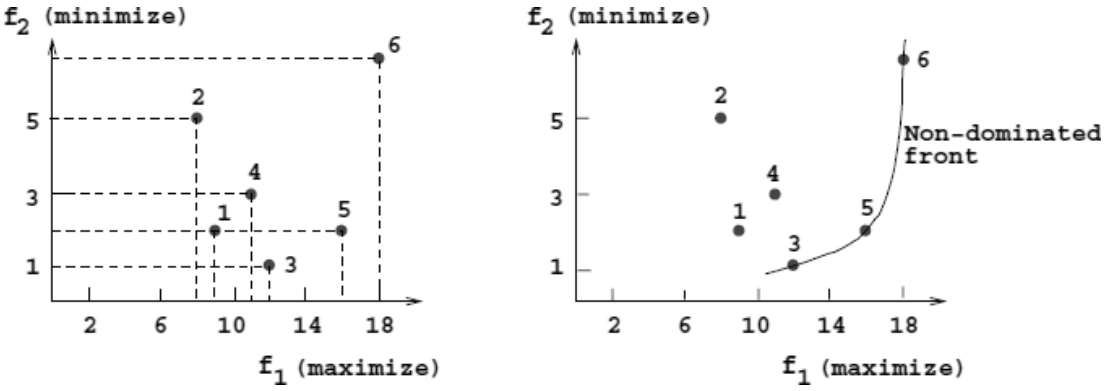

Figure 15: Pareto front (Branke et al., 2008)

3.4 Optimisation algorithms

A common practice before the actual solution of the problem (1) is to explore the design space in order to define the limits of $\boldsymbol{X}$. Running a design of experiment allows the designer to investigate the global response trends and identify the most

significant parameters. In some cases, this is proved rather beneficial to the optimisation process as the number of design variables can be reduced, decreasing the overall computational time. In addition, design of experiments can be used to produce surrogate models, described in Section 3.5. Examples of design of experiment methods can be found in Table 4, depending on their application.

Table 4: Design of experiment methods

Application	Method
Statistical analysis	Factorial, ULH, Latin Square
Surrogate model training	Space filler (ULH, Latin Square)
Optimisation	Space filler (ULH, Random, Sobol)
Design robustness and reliability analysis	Latin Hypercube Sampling, Monte Carlo, Taguchi Orthogonal Arrays

The solution of the problem (1) starts with a design which represents an initial solution described by a set of design variables $\boldsymbol{x}$. The aim is to create a series of design variable vectors $\boldsymbol{x}$ which makes the objective functions smaller step by step, as shown in (3):

$$\mathrm{f}(\boldsymbol{x}_{k+1}) < \mathrm{f}(\boldsymbol{x}_k)$$
where (3)
$$\boldsymbol{x}_{k+1} = \boldsymbol{x}_k + \mathrm{a_k}\boldsymbol{d}_k$$

The parameter a_k represents the step size and $\boldsymbol{d}_k$ is a direction vector. Birk (2003) declares the optimisation algorithms differ by the methods used to select the step size and direction and groups them into two categories; the deterministic and the stochastic algorithms. The former use an analytic scheme to move from one iteration $\boldsymbol{x}_k$ to the next $\boldsymbol{x}_{k+1}$, while the latter apply random numbers at one or more stages of the process, resulting in an unpredictable movement pattern. Birk (2003) suggests that in the majority of maritime applications stochastic algorithms are applied.

Birk (2003) classifies the available optimisation methods in three categories (Table 5). Search methods do not evaluate gradient and curvature information and are mostly suitable for expensive and noisy objective functions where an approximation of the gradient is costly or inaccurate. On the other hand, gradient methods select the search direction $\boldsymbol{d}$ based on information on the gradient ∇f of the objective function. The latter requires the objective functions to be twice continuously differentiable. An example of gradient methods is the sequential quadratic programming algorithms, which, according to Birk (2003), are highly efficient solvers for engineering optimisation problems.

Global optimisation methods aim at finding the global optimum, namely the best design in the feasible design space. Some of the available global optimisation methods are mentioned in Table 5. Branch-and-bound methods divide the feasible region in smaller ones and calculate the lower and upper bounds of the objective functions defined in them. Simulated annealing method resembles the natural process of the recrystallisation of a liquid metal during annealing. In metallurgy, this technique involves heating and controlled cooling of a material to increase the size of its crystals and reduce their defects. The notion of cooling implemented in the simulated annealing algorithm is interpreted as a slow decrease in the probability of accepting worse solutions as the design space is explored, leading to a set of optimal ones.

Table 5: Optimisation algorithms (Birk, 2003)

Category	Method
Search methods	Pattern search, simplex, conjugate directions
Gradient methods	Sequential quadratic programming
Global optimisation algorithms	Branch-and-bound, genetic algorithms, simulated annealing

Genetic algorithms are inspired by the process of natural selection, relying on bio-inspired operators, such as mutation, crossover and selection (Goldberg, 1989,

Holland, 1975). A genetic algorithm produces an improved set of solutions based on information received from previous sets (generations). The best solution of one generation is used to define the next generation, combining the characteristics of the parent solutions. A solution to a problem is represented as a chromosome, which is an array of genes. A typical structure of a genetic algorithm is presented below (Bertram, 2003):

1. Translate the problem into a form that can be used by the genetic algorithm (e.g. binary)
2. Derive a cost or evaluation function to evaluate each solution (chromosome)
3. Generate an initial random population of chromosomes
4. Evaluate each chromosome using the cost function
5. Determine the fitness of each chromosome by comparing its cost with the rest of the population
6. Generate a subset of the current population by selecting the fitter of the population
7. Remove the unfit chromosomes
8. Randomly select pairs of chromosomes in the subset population
9. Create new (child) chromosomes by allowing the pairs to breed using an appropriate cross-over technique
10. Implement a mutation technique to prevent gene stagnation
11. If an optimal solution is found then quit, otherwise go bat to step 4 and repeat

The fitness or objective function is used to map the chromosome's array of genes into a positive number, called individual's fitness. This process can be divided into two distinct phases, namely the decoding –translation of the array of genes (genotype) to the actual performance of the solution (phenotype)– and the actual calculation of the fitness, based on the rest of the population.

The population size, selection, cross-over and mutation attributes affect the robustness of the genetic algorithms. In general, there is no rule of thumb applicable

to any optimisation problem and each of these properties has variable effects on different problems.

The population size affects the chances of finding a global optimal. One may decide to increase the size for better results; however a population size too large will have a negative impact on the computational time. The extent of the genetic material of the individuals in a population transferred to the next is controlled by the selection attribute. The fitness ranking of the individuals influences this process. Solutions with greater fitness are most likely to be used for breeding. In general, genetic algorithm selection techniques reward fitter individuals by letting them reproduce more.

The reproduction process is controlled by the cross-over and mutation properties as well (Figure 16). A cross-over operator creates a new solution by combining information contained in the two parent solutions. The cross-over rate affects the number of random chromosomes chosen to be paired off randomly. Mutation is used to prevent stagnation of genes, thus enabling the genetic algorithm to find an optimal solution. The mutation rate determines the alteration frequency of a value of a particular gene, which results in the introduction of new information to the existing population. Hence, the possibility of getting stuck to a local optimum is reduced.

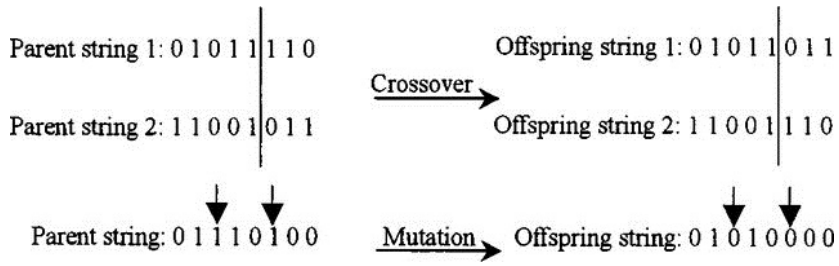

Figure 16: Demonstration of cross-over and mutation functions (Yang et al., 2004)

3.5 Surrogate models

Modern optimisation algorithms avoid employing time-consuming trial and error techniques by applying design space exploration approaches to find the best solution.

Despite the reduced amount of computational time required by the latter, modern optimisation problems involve complex calculations, such as CFD or FEM, which require different approaches to maintain the overall computational time low. Optimisation based on surrogate models is a strategy which allows designers to obtain the same results by substituting expensive simulation software runs with approximation models.

Surrogate models are statistical and numerical models which approximate the input and output behaviour of the system under investigation. Input includes the design variables which affect the response of the system and the output is the actual performance of the system. Although the whole process leads to an approximation of the final result, surrogate models are used to estimate the set of design variables which produce an optimal response. Hence, the result of such an optimisation approach is a predicted optimum, representing an estimation of the true optimum. The main advantage of this approach is the major reduction of the computational time needed to find the optimal solution to the problem. The surrogate model is an analytical function which can be evaluated quickly without running heavy simulations.

The accuracy of the surrogate models depends on the type of algorithm used to produce the model, the number of training points and the complexity of the variations of the solution. It is important to evaluate the accuracy levels before using the surrogate model in the optimisation process, so that further training takes place.

Surrogate models can be categorised into three types; data fits, multi-fidelity and reduced order model, multi-fidelity and data fit surrogates. Reduced order models derive from a high-fidelity model. By computing a set of basic functions that capture the principal dynamics of a system, the high-order system can be projected to a smaller one. Multi-fidelity models involve the use of low-fidelity physics-based model as a substitute for the original high-fidelity one. The low-fidelity model is a separate model not requiring data from the high-fidelity model and involves looser convergence tolerances or omitted physics. The high-fidelity model is needed only

for the definition of the correction functions that are applied to the low-fidelity results.

Data fitting methods involve construction of an approximation of a surrogate model using data generated from the original model. Depending on the number of points used to generate the data fit, three techniques can be identified, namely the local, multi-point and global approximation methods. Global methods are often referred to as response surface methods and involve many points spread over the parameter ranges of interest. Usually designs of experiment are used to obtain the training points used to define the surrogate model. Global methods include polynomial regression, Kriging interpolation (Gaussian Process) and artificial neural networks.

The set of interpolation techniques known as Kriging or Gaussian Processes were initially developed for geostatistics and spatial statistics studies to produce maps of underground geologic deposits based on a set of widely and irregularly spaced borehole sites (Cressie, 1990). In order to properly define a Kriging model, three steps need to be performed; (a) select the trend function, (b) select the correlation function and (c) estimate the correlation parameters. A Kriging emulator $\hat{f}(\boldsymbol{x})$ consists of a trend function (usually a least squares fit to the data $\boldsymbol{g}(\boldsymbol{x})^T\boldsymbol{\beta}$) plus a Gaussian Process error model $\varepsilon(\boldsymbol{x})$, used to correct the trend function (4).

$$\hat{f}(\boldsymbol{x}) = \boldsymbol{g}(\boldsymbol{x})^T\boldsymbol{\beta} + \varepsilon(\boldsymbol{x}) \tag{4}$$

This emulator represents an estimated distribution for the unknown true surface $f(\boldsymbol{x})$. The error model $\varepsilon(\boldsymbol{x})$ makes an adjustment to the trend function so that the emulator will interpolate and have zero uncertainty at the data points it was built from. Ill-conditioning due to poorly spaced sample design can be handled by discarding points that contribute the least unique information to the correlation matrix. Therefore, the points that are discarded are the ones that are the easiest to predict. The resulting surface exactly interpolates the data values at the retained points but the interpolation of the discarded points is not guaranteed.

3.6 Multi-criteria decision analysis

Decision making refers to the selection of one or more alternatives from a list of options. Multi-objective optimisation problems provide a set of optimal solutions which lie on the Pareto front, contrary to single-objective optimisation problems which converge to a single solution. Therefore, a special process has to follow during which a decision is made regarding the selection of the final solution, subject to the method utilised for this purpose.

Multi-criteria decision making can be divided into two categories, the multi-attribute and the multi-objective decision making. The former involves the selection of an alternative from a list based on prioritised attributes of the alternatives. On the other hand, the latter involves a synthesis of an alternative or alternatives on the basis of prioritised objectives.

A convenient way to select an alternative from a list is to use static or moving weights to represent the contribution of each attribute among the alternatives. Particularly, a common practice is to compare the alternatives on the basis of weighted sum of normalised attributes. Normalisation is important for comparability reasons, as the examined attributes are often disproportional. Utility functions utilise moving weights so that the relative contributions made by different attributes to the ranking of the alternatives change with the attribute values themselves (Sen and Yang, 1998).

An ordinary decision making problem with n alternatives a_i, i=1,…,n and k attributes y_j, j=1,…,k is demonstrated in (5). Each pair of alternatives a_i, a_l, l=1,…,n, $i \neq l$, is compared with regard to every attribute. m_{il} represents the relative importance of a_i over a_l with regard to y_j and a pairwise comparison matrix for all the n alternatives in terms of the attribute y_j is formulated (5). The problem is then represented by k pairwise comparison matrices for the k attributes.

$$M = \{m_{il}\}_{n\times n} = \begin{bmatrix} 1 & \cdots & m_{1n} \\ \vdots & \ddots & \vdots \\ m_{n1} & \cdots & 1 \end{bmatrix}$$

where

$$m_{il} = \frac{1}{m_{li}} \; \forall \, i, l = 1, \dots, n \tag{5}$$

The use of utility functions within a multi-objective optimisation problem can provide the best compromise solution during the decision making process. The decision maker's preferences are modelled by a utility function *u(F(**x**))* which combines all the objective functions *f* (as defined in (1)) to one criterion (6).

$$u\big(F(\boldsymbol{x})\big) = u\big(f_1(\boldsymbol{x}), \dots, f_n(\boldsymbol{x})\big) \tag{6}$$

x is the vector of the design variables, as defined in (1). The additive weighting is one of the most common techniques used in conjunction with the utility function approach to identify the best compromise solution. A weight vector is set used to represent the decision maker's preferences. The utility function is then defined as the weighted sum of the objective functions. A scalar objective function is defined (7).

$$\min \; u = W^T F(\boldsymbol{x})$$

where

$$W = [w_1, \dots, w_n]^T \tag{7}$$

w_i is the weighting factor of objective *i*. The utility function may be linear when any objective can be evaluated independently of the rest and bad values of some objectives can be directly offset without limit by good values of other objectives. However when such an assumption is not valid, the utility function can be non-linear. In case of a linear utility function, the change for each unit change of an objective is constant regardless of the base values of the objective.

An example illustrating the difference between a linear and a non-linear utility function is can be found in Figure 17. In one case, an increase of 1000 units in the objective function representing the salary of a person is considered equally preferable

regardless of the initial salary (before the pay rise), while on the other case, the preference changes as the initial salary increases.

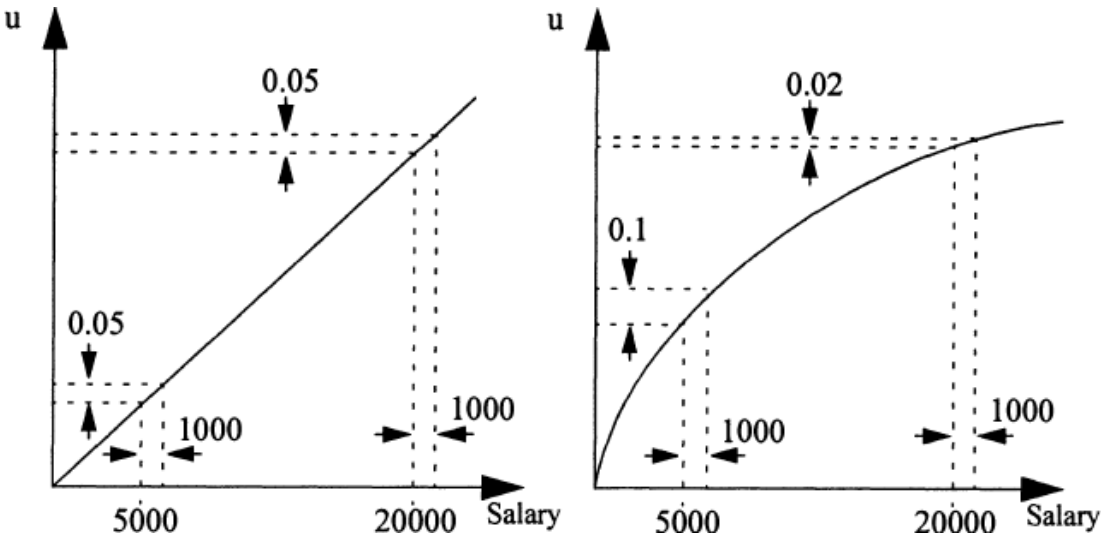

Figure 17: Demonstration of the difference between a linear (left) and a non-linear (right) utility function (Sen and Yang, 1998)

3.7 Uncertainty quantification

Uncertainty quantification or non-deterministic analysis is the process of characterising input uncertainties, forward propagating them through a computational model and performing statistical or interval assessments on the resulting responses. This process determines the effect of uncertainties and assumptions on model output.

Uncertainty quantification aims at gaining an understanding of how variations in parameters affect the response functions of the engineering design problem. In most cases the parameter vector is considered to be uncertain as specified by particular probability distributions. The assignment of a specific distributional structure to the inputs, distributional structure for the outputs can be inferred. This leads to an analysis which is more qualitative than quantitative.

Consideration of uncertainty in an optimisation problem affects the definition of the latter. Based on the formulation of the problem in (1), Diez and Peri (2010) suggest the following alternatives may be true:

- Uncertain design variable vector $\boldsymbol{x}$:

Design variables may be affected by uncertainty due to manufacturing tolerances. Such uncertainties can be classified as external when associated to the analysis models input (Du and Chen, 2000). For a specific design variable vector $\boldsymbol{x'}$, an error or tolerance related to this vector $\boldsymbol{\xi \in \Xi}$ can be defined. $\boldsymbol{\xi}$ can be a stochastic process with a probability density function $p(\boldsymbol{\xi})$. By definition, the expected value of $\boldsymbol{x'}$ is shown in (8).

$$\bar{\boldsymbol{x}}' := \mu(\boldsymbol{x}' + \boldsymbol{\xi}) = \int_{\Xi} (\boldsymbol{x}' + \boldsymbol{\xi}) p(\boldsymbol{\xi}) d\boldsymbol{\xi}$$

where (8)

$$\int_{\Xi} p(\boldsymbol{\xi}) d\boldsymbol{\xi} = 1$$

If the stochastic process $\boldsymbol{\xi}$ has zero expectation (9), then $\bar{\boldsymbol{x}}' = \boldsymbol{x}'$. In general, the probability density function $p(\boldsymbol{\xi})$ depends on the specific design variable vector $\boldsymbol{x'}$.

$$\bar{\boldsymbol{\xi}} := \mu(\boldsymbol{\xi}) = \int_{\Xi} \boldsymbol{\xi} p(\boldsymbol{\xi}) d\boldsymbol{\xi} = 0 \quad (9)$$

- Uncertain environmental and usage conditions (parameter vector $\boldsymbol{y}$):

Many optimisation problems involve parameters addressing environmental and operating conditions which in real life are uncertain. The parameters vector $\boldsymbol{y}$ may be assumed as a stochastic process with a probability density function $p(\boldsymbol{y})$ and expected value as shown in (10).

$$\bar{\boldsymbol{y}} := \mu(\boldsymbol{y}) = \int_{\boldsymbol{Y}} \boldsymbol{y} p(\boldsymbol{y}) d\boldsymbol{y} \tag{10}$$

In this case, no error is defined, since the environmental and operating conditions are treated as stochastic processes in the whole domain of $\boldsymbol{Y}$.

- Uncertain evaluation of the objective function *f*:

The evaluation of an objective function f_i can be affected by uncertainty due to inaccuracy in modelling or computing (Du and Chen, 2000). The assessment of vector $\boldsymbol{f} := [\boldsymbol{f},\boldsymbol{g},\boldsymbol{h}]^T$ containing the objective function, inequality and equality constraints, for a specific, deterministic design point $\boldsymbol{f'} := \boldsymbol{f(x',y)}$ is affected by a stochastic error $\boldsymbol{\varphi} \in \boldsymbol{\Phi}$. Then the expected value of $\boldsymbol{f'}$ is the one shown in (11).

$$\bar{\boldsymbol{f}}' := \mu(\boldsymbol{f}' + \boldsymbol{\varphi}) = \int_{\boldsymbol{\Phi}} (\boldsymbol{f}' + \boldsymbol{\varphi}) p(\boldsymbol{\varphi}) d\boldsymbol{\varphi} \tag{11}$$

The probability density function of $\boldsymbol{\varphi}$, $p(\boldsymbol{\varphi})$ depends on $\boldsymbol{f'}$ and therefore on the design point $\boldsymbol{(x',y)}$. Combining the above uncertainties, the expected value of $\boldsymbol{f}$ is shown in (12).

$$\bar{\boldsymbol{f}} := \mu(\boldsymbol{f}) = \int_{\boldsymbol{\Xi}} \int_{\boldsymbol{Y}} \int_{\boldsymbol{\Phi}} (\boldsymbol{f}(\boldsymbol{x}' + \boldsymbol{\xi}, \boldsymbol{y}) + \boldsymbol{\varphi}) p(\boldsymbol{\xi}, \boldsymbol{y}, \boldsymbol{\varphi}) d\boldsymbol{\xi} d\boldsymbol{y} d\boldsymbol{\varphi} \tag{12}$$

$p(\boldsymbol{\xi},\boldsymbol{y},\boldsymbol{\varphi})$ is the joint probability density function associated to $\boldsymbol{\xi}$, $\boldsymbol{y}$ and $\boldsymbol{\varphi}$. Hence, the expected value of $\boldsymbol{f}$ is a function of the designer choice. The variance of $\boldsymbol{f}$ with respect to the variation of $\boldsymbol{\xi}$, $\boldsymbol{y}$ and $\boldsymbol{\varphi}$ is shown in (13).

$$V(\boldsymbol{f}) := \sigma^2(\boldsymbol{f}) = \int_{\boldsymbol{\Xi}} \int_{\boldsymbol{Y}} \int_{\boldsymbol{\Phi}} \left((\boldsymbol{f}(\boldsymbol{x}' + \boldsymbol{\xi}, \boldsymbol{y}) + \boldsymbol{\varphi}) - \bar{\boldsymbol{f}}(\boldsymbol{x}') \right)^2 p(\boldsymbol{\xi}, \boldsymbol{y}, \boldsymbol{\varphi}) d\boldsymbol{\xi} d\boldsymbol{y} d\boldsymbol{\varphi} \tag{13}$$

Uncertainties in an optimisation problem may be addressed in various ways, such as the minimisation of the variance of *f*, minimisation of the expectation of *f*, minimisation of *f* in the worst possible case or by assessing probabilistic constraints

in the minimisation of *f*. An optimisation process focusing on the uncertainty in the evaluation of the objective function is known as robust design optimisation, while the one focusing on the constraints of the design, treating them as probabilistic inequalities, is known as reliability-based design optimisation.

Uncertainty is classified into two main categories; the aleatory and the epistemic uncertainty. The former are irreducible variabilities inherent in nature while the latter are reducible uncertainties resulting from a lack of knowledge. For the aleatory uncertainties, usually there is sufficient data and probabilistic methods are commonly used for computing response distribution statistics based on input probability distribution specifications. On the other hand, for epistemic uncertainties, any use of probabilistic distributions is based on subjective knowledge. Methods used to quantify these two types of uncertainty can be found in Table 6.

Table 6: Uncertainty quantification methods

Type of uncertainty	Method
Aleatory	Sampling-based (Monte Carlo, Latin Hypercube Sampling), local and global reliability methods, stochastic expansion (polynomial chaos expansion, stochastic collocation)
Epistemic	Local and global interval analysis, Dempster-Shafer evidence theory

Reliability methods used to investigate aleatory uncertainties create approximations based on Gaussian Process models and accurately resolve a particular contour of a response function estimating probabilities using multi-modal adaptive importance sampling. Stochastic expansion methods form an approximation to the functional relation between response functions and their random input.

As far as epistemic uncertainties are concerned, in interval analysis one assumes that nothing is known about an epistemic uncertain variable except that its value lies somewhere within an interval. However, in this case the value is not assumed to have a uniform probability of occurring within the interval. Therefore, the result one gets

using this method is the bounds on the output (defining the output interval) given the interval bounds on the input. Dempster-Shafer theory of evidence models the uncertain input variables as sets of intervals. A basic probability assignment is assigned to each interval, indicating how likely it is that the uncertain input falls within the interval. These intervals may be overlapping, contiguous or have gaps. The intervals and their associated basic probability assignments are propagated through the simulation to obtain cumulative distribution functions on belief and plausibility. Belief is the lower bound on a probability estimate that is consistent with the evidence, while plausibility is the upper bound on a probability estimate that is consistent with the evidence.

Sampling techniques generate sets of samples according to the probability distributions of the uncertain variables and map them into corresponding sets of response functions. Means, standard deviations, coefficients of variation and 95% confidence intervals can be computed for the response functions. Two common sampling methods are the Monte Carlo and Latin Hypercube Sampling. In the former the samples are selected randomly according to the probability distributions, while in the latter a stratified sampling technique is applied for which the range of each uncertain variable is divided into N_s segments of equal probability, where N_s is the number of samples requested. The relative lengths of the segments depend on the nature of the specified probability distribution. For instance, uniform distribution creates segments of equal length, whereas normal distribution creates small segments near the mean and larger ones in the tails. In general, Latin Hypercube Sampling techniques require fewer samples than the traditional Monte Carlo method for the same accuracy in statistics (Aistleitner et al., 2012).

3.8 Summary

In this Chapter an overview of the theoretical background of applications and techniques employed in this thesis is made. The difference between traditional and parametric design approaches is presented in Section 3.2. The generic ship design optimisation problem is presented and each component is analysed in Section 3.3.

In order to solve the optimisation problem, several methods are available to choose from. Genetic algorithms have been used in this thesis and additional information regarding their application is given. In addition, the role of surrogate models in optimisation studies is analysed, while the available types and techniques one can use to define them are presented.

In Section 3.6 the theory of multi-criteria decision making is presented, focusing on the utility function methods, which are applied in the work presented in this thesis. Finally, an overview of uncertainty in optimisation is made, with the most common methods utilised to quantify it being presented in Section 3.7.

4 Proposed methodology

4.1 Introduction

The description of the methodology adopted in this thesis regarding the holistic ship design optimisation under uncertainty is presented in this Chapter (Figure 18). The process begins with the definition of the parametric design and continues with the construction of the ship model. The setup for surrogate models is implemented afterwards. Throughout this process the design variables, objective functions and constraints of the problem are determined. The multi-objective optimisation setup follows, for which genetic algorithms are utilised. The setup is run and the results are analysed in the multi-criteria decision making process.

Based on the most recent developments in the holistic ship design optimisation theory, most of the attributes shown in Figure 10 are investigated to some extent in the proposed methodology; main dimensions and preliminary powering, lines and body plan, hydrostatics, stability, arrangements, structures, mission requirements, cost estimates, capacities, trim and intact stability, lightship weight and resistance.

A novel approach for the quantification of uncertainty in early stage ship design is proposed, while the consideration of recently developed international regulations provides an insight on how the latter affect the optimal design selection.

The general procedure described in this Chapter can be applied to different ship types, provided that the hull geometry and ship model are defined accordingly. In this thesis, the methodology is applied to two different ship types, namely a containership and a Ro-Pax vessel. The case studies are presented in Chapter 5.

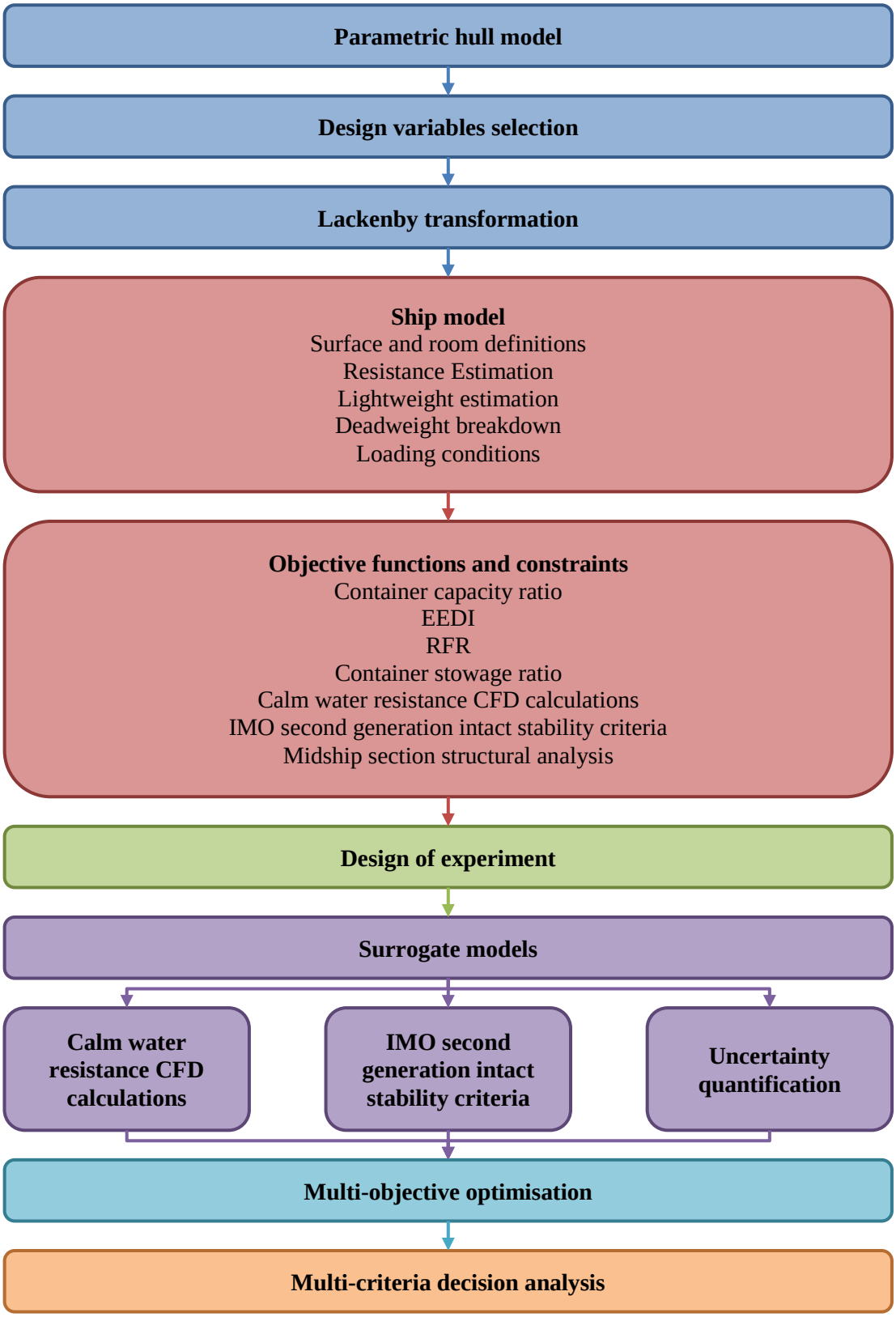

Figure 18: Proposed methodology

4.2 Parametric hull model

The geometric hull model is produced in CAE software CAESES® (Friendship Systems, 2018). It consists of four main parts, namely the aft body, main frame, fore body and main deck.

The use of meta-surfaces in CAESES®, mentioned in Section 3.2, allows the detailed definition of each part, introducing parameters which control the shape of the hull (Figure 19 and Figure 20). The parameters affect the curvature and shape of main curves, such as the deck, flat of bottom, flat of side or stem (Figure 21). They are also responsible for the shape of specific parts of the hull, such as the skeg in the aft section or the bulbous bow (Figure 22 and Figure 23).

The widespread presence of parameters in the hull form definition allows the designer to select which of the available parameters controlling the hull form become the design variables of the problem. These parameters can be controlled by the user directly and change during the optimisation process. The remaining can either be assigned specific values that remain constant throughout the solution of the problem or depend on the values of the design variables. Hence, the versatility of the problem definition is amplified; the user is able to perform an optimisation study focusing on the main dimensions of the vessel or focus e.g. on the bulbous bow shape for a local hull form optimisation.

Once the initial hull is defined, a Lackenby transformation takes place (Lackenby, 1950). This transformation allows the shift of transverse sections along the length of the hull, by adjusting the c_P and position of the LCB (Abt and Harries, 2007). A hydrostatic and a sectional area curve calculation need to be performed on the initial hull and the results are used as input in the Lackenby transformation. The final hull form is produced following the Lackenby transformation. Then it is exported to an IGES file and the process continues with the definition of the ship model.

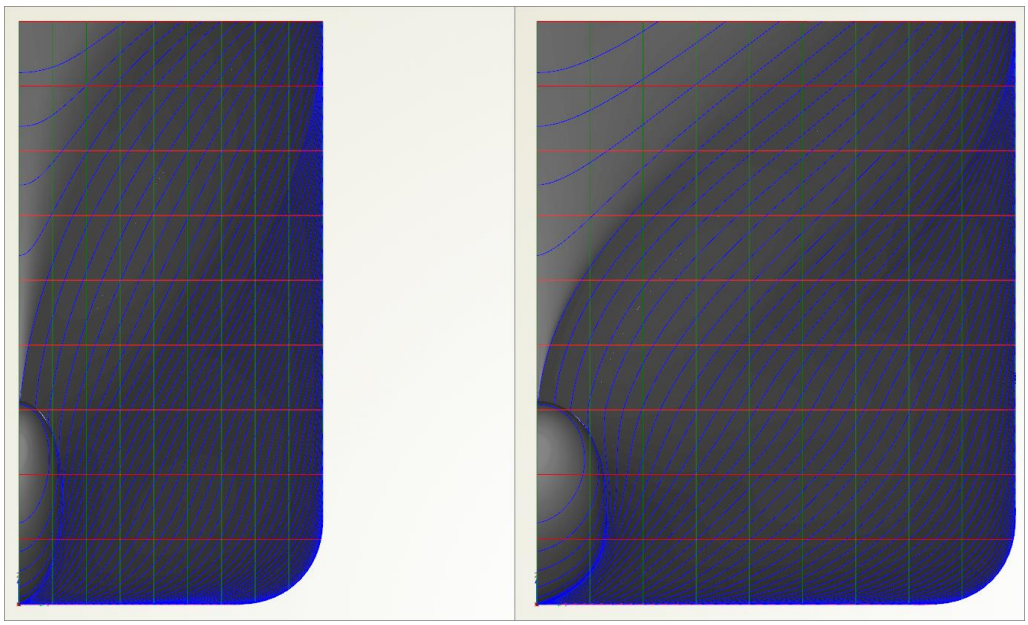

Figure 19: Hull form variation with regard to the breadth

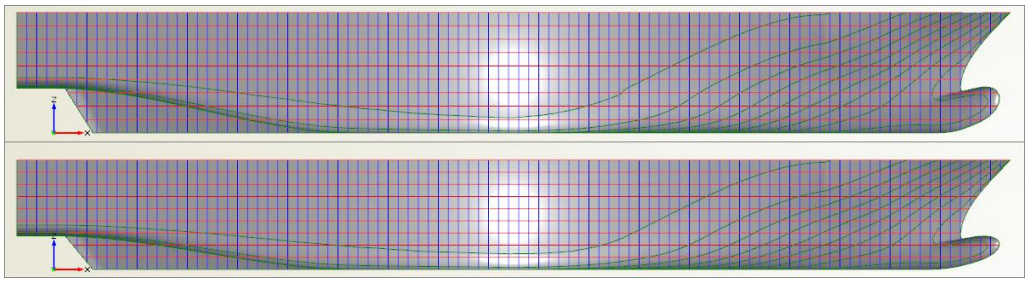

Figure 20: Hull form variation with regard to the draught

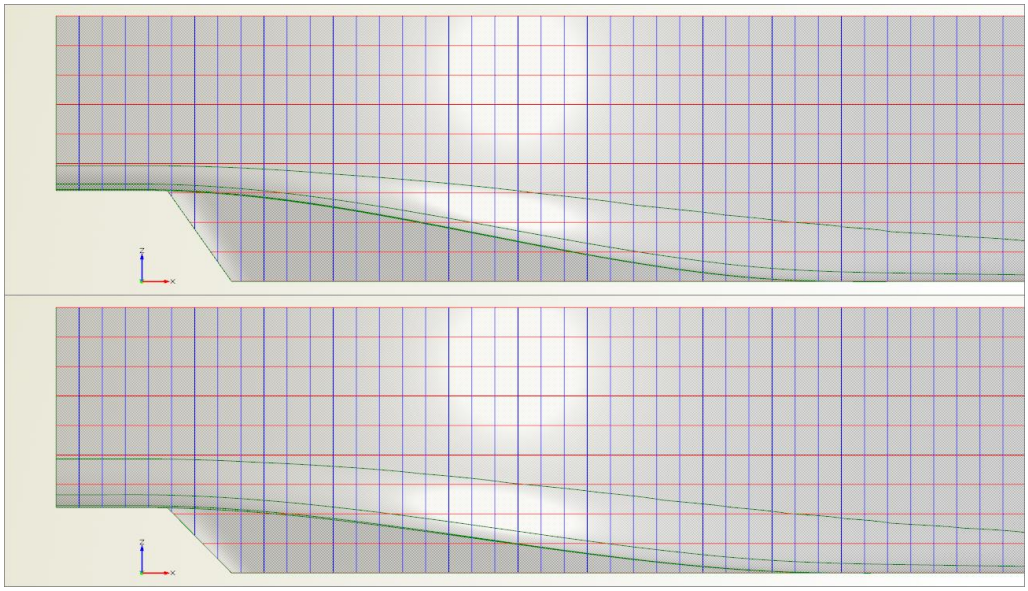

Figure 21: Hull form variation with regard to transom vertical position

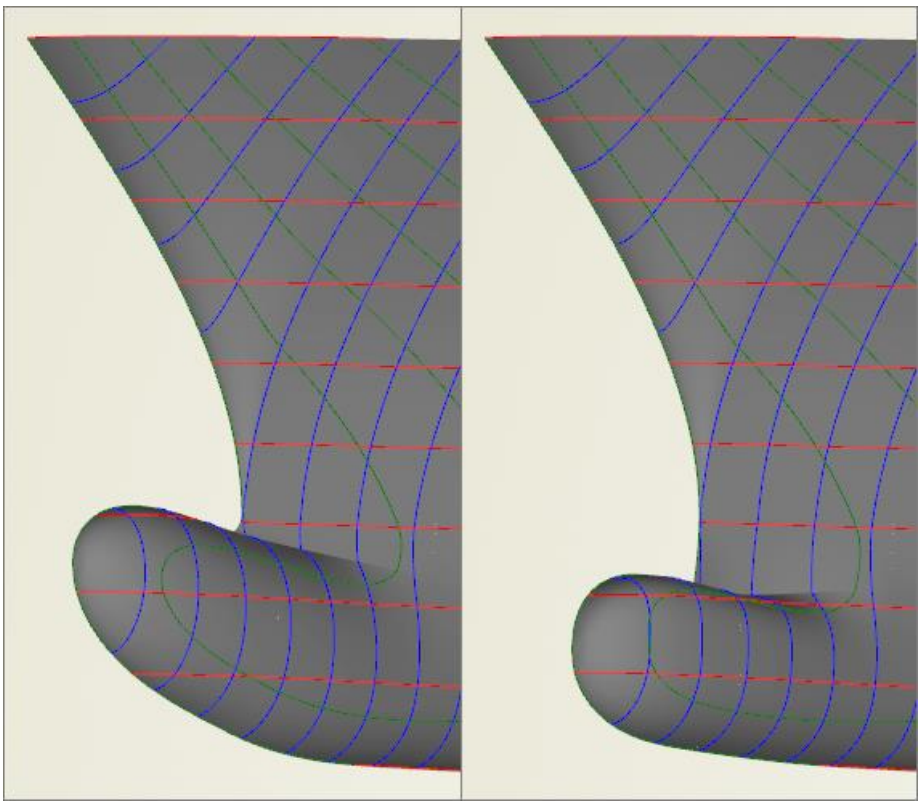

Figure 22: Local hull form variation (bulbous bow)

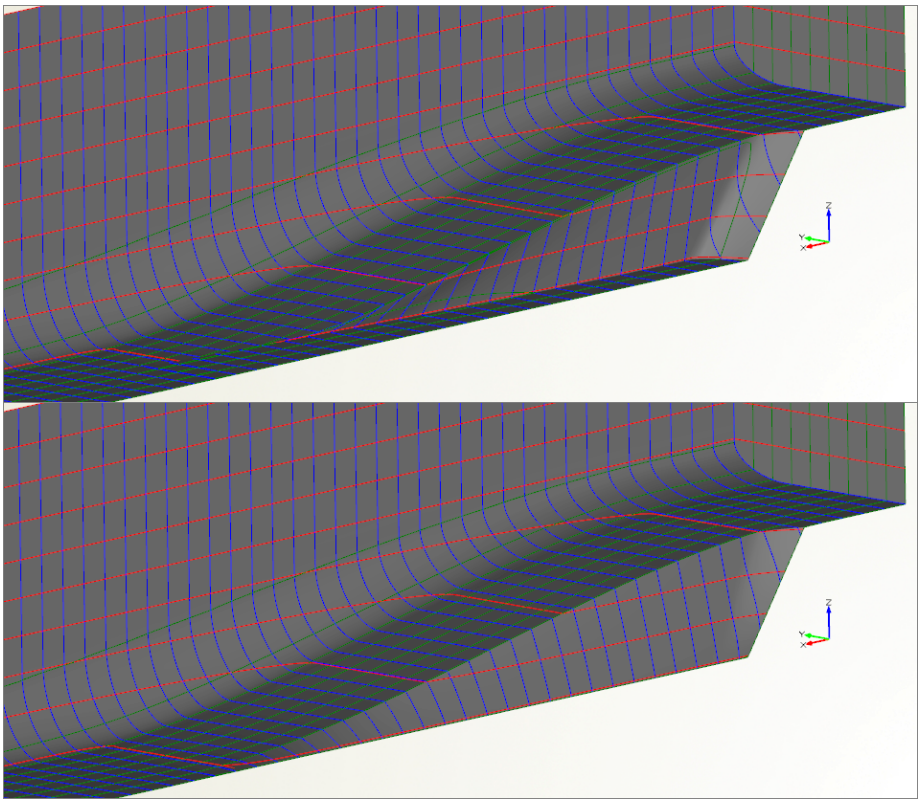

Figure 23: Local hull form variation (aft skeg)

4.3 Ship model

The construction of the ship model involves multiple calculations and definitions such as the internal subdivision of the hull, lightweight estimation and deadweight breakdown. NAPA® is a powerful software tool which allows detailed definition of compartments forming a complete ship model that can be used to define loading conditions (NAPA, 2018). The processes involved in this step need to be parametrically defined and have to be able to accept as input the hull form created in CAESES®. This is implemented through macros defined for this purpose. Hence, the first step is to read the relevant input which involves the IGES file containing the information regarding the hull geometry and the parameters used for the hull definition. Then, the necessary calculations take place locally in NAPA®.

4.3.1 Surface and room definitions

The first step towards the creation of the ship model is the definition of a set of surfaces which are used as limits for the room definition. These surfaces are mostly planes along the longitudinal, transverse or vertical direction, representing bulkheads and decks (Figure 24).

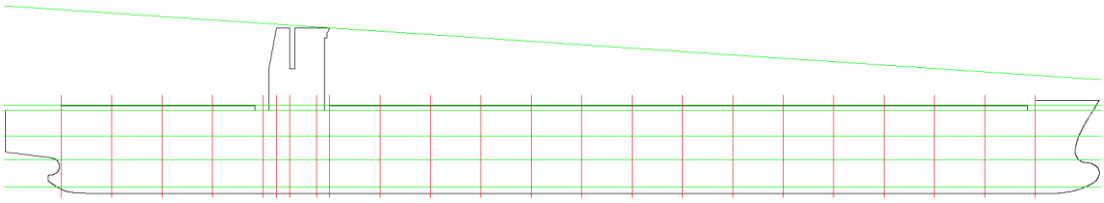

Figure 24: Examples of developed planes in NAPA®

More complex surfaces are created for superstructure and specific rooms, for which straight planes cannot capture sufficiently the geometry. One of the case studies examined in this thesis, namely the containership demonstration case, involves such kind of surfaces for the definition of the cargo space (Figure 25). Containers have specific dimensions which influence the shape of the cargo holds; the inner hull shell defining the double hull setup in particular. In order to maximise the transport

capacity of such kind of vessels, each surface defining one bay (a space along the length of the ship that can hold containers) needs to be designed taking into account the hull shape and the clearance (distance of the double side) for each tier (a space along the vertical direction of the ship that can hold containers). This process is particularly significant for the areas near the stern and bow, where the hull geometry changes rapidly along the longitudinal direction.

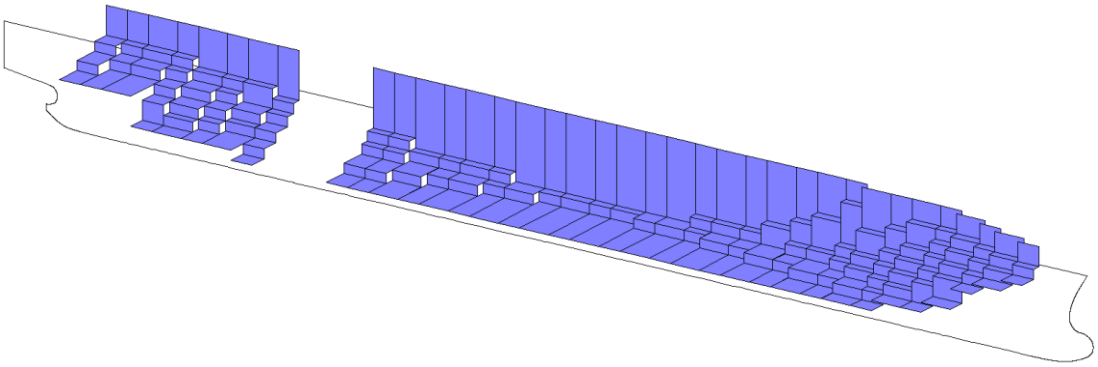

Figure 25: Surfaces developed in NAPA®, used to define cargo holds in the containership case study

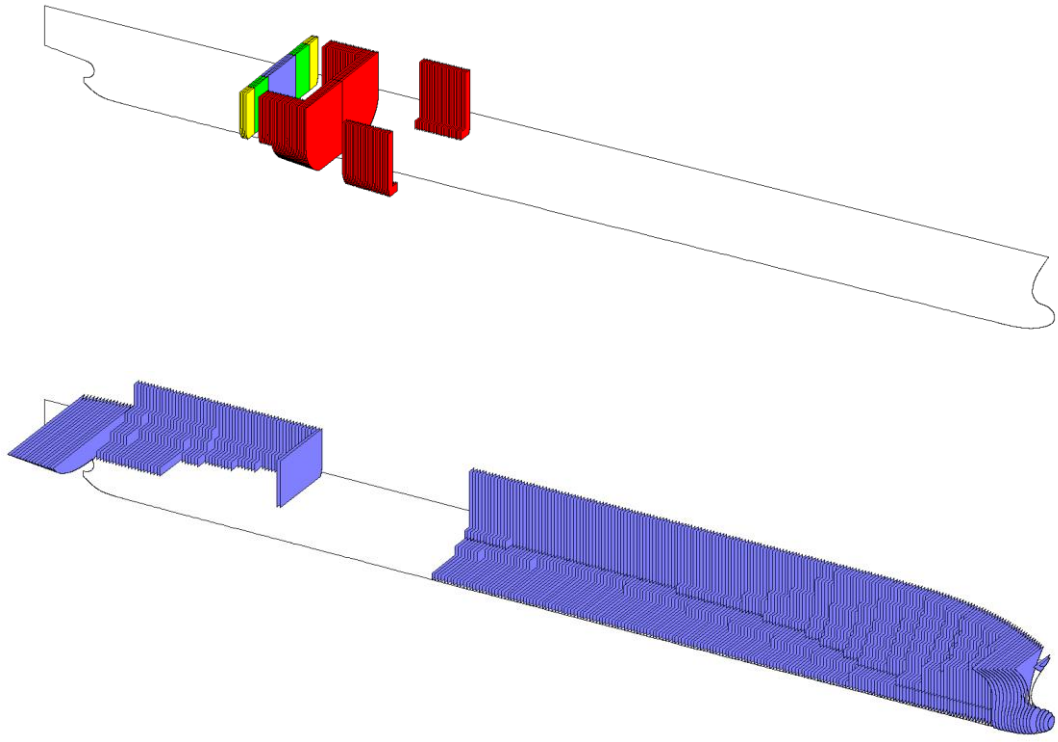

Figure 26: Examples of rooms developed in NAPA®

After the definition of the necessary surfaces, the creation of the rooms takes place (Figure 26). The surfaces are used as limits for the construction of the spaces needed to define a loading case or for which specific information (e.g. area, volume) is required for calculations taking place at a later stage (e.g. lightweight estimation). These include the consumables tanks (fuel oil, diesel oil, lubrication oil, fresh water), water ballast tanks, cargo space, engine room and accommodation space.

The definition of the necessary surfaces and rooms allows further preparations to be carried out. Depending on the ship type being optimised, the container blocks are defined, or the lane metres of the car decks are calculated. Both operations depend on the limits of the relevant rooms (i.e. cargo holds, car decks), specific curves of the parametric hull model (e.g. main deck line), as well as the parameters related to the TEU and standard vehicle dimensions.

The process described above is designed to be performed in a parametric way. Depending on the design variables, the number of the defined surfaces and rooms is adjusted accordingly. For instance, the number of the surfaces forming the inner hull shell depends on the parameter representing the number of bays for a specific design. Likewise, the number of cargo holds and water ballast tanks is adjusted based on the same principle. Another example is the number and height of superstructure decks, both defined by parameters controlled by the designer.

4.3.2 Resistance estimation

Total resistance can be divided into three categories, namely calm water, added wave and wind resistance. These three components are estimated using fast approximation methods. Holtrop and Mennen (1978) method is utilised for the calculation of the first component. Calm water resistance is subdivided into frictional R_F, wave making and wave braking resistance R_W, the additional pressure resistance introduced by the bulbous bow R_B and the immersed transom R_{TR}, the resistance of the appendages R_{APP} and the model-ship correlation resistance R_A (14).

$$R_{Total} = R_F(1 + k_1) + R_{APP} + R_W + R_B + R_{TR} + R_A \quad (14)$$

k_1 is the form factor describing the viscous resistance of the hull form in relation to the frictional resistance. The method conveniently requires as input values which are readily available in the early stages of ship design and provides accurate results, considering the level of detail applied in the calculations. Input values include the main particulars (L_{BP}, L_{WL}, breadth, draught on AP and FP), form coefficients (c_M, c_W) and values related to appendages and specific areas of the hull (transverse bulb area, transom area, wetted area of appendages). The values are either part of the design variables set of the problem (e.g. L_{BP}, draught) or calculated based on the generated hull form (e.g. c_M, transverse bulb area). Dimensions of appendages not known at the early design stage are approximated using formulas based on the ship's main particulars. For instance, the area of bilge keels is based on the ship's length and breadth.

Added wave resistance is calculated using the STAWAVE-1 method (Boom et al., 2013). The STAWAVE-1 method is based on the fact that for today's large ships the head waves encountered in trial conditions are normally short compared to ship length and speed. The added resistance due to the reflection of these short head waves is primarily dependent on the shape of the waterline in the bow region. Similar to the method used for the calm water resistance calculation, STAWAVE-1 provides results instantly requiring a limited amount of input (15).

$$R_{AWL} = 1000\frac{1}{16}\rho g {H_{W,1/3}}^2 B\sqrt{\frac{B}{L_{BWL}}} \quad (15)$$

ρ is the sea water density, g is the gravitational acceleration, $H_{W,1/3}$ is the significant wave height, B is the ship's breadth and L_{BWL} is the length of the bow on the waterline to 95% of the maximum breadth. The calculation of the significant wave height is shown in (16).

$$H_{W,1/3} = 0.21\frac{(1.026V_{10})^2}{g} \tag{16}$$

Weather data based on the operational profile of the ship (i.e. on which region the ship operates) are used to identify the wind speed at ten metres above the sea surface V_{10}.

The wind resistance is calculated according to Jensen (1994). Wind resistance is important for ships with large lateral areas above the waterline, such as containerships or passenger ships. The method requires the ship's V and wind V_{Wind} speed values, along with the frontal projected area of the ship above the sea level A_F (17). The latter can be obtained by the arrangement created in NAPA®, following the definition of the rooms related to the superstructure

$$R_{AA} = C_{AA}\frac{\rho_{air}}{2}(V + V_{Wind})^2 A_F \tag{17}$$

C_{AA} is a coefficient ranging between 0.8 and 1.0, while ρ_{air} is the density of air.

The sum of the three resistance components mentioned above provides the total resistance R_T, which is used to estimate the effective and installed power P_B (18). The latter is computed by applying the propulsive η_D and shaft η_S efficiency. Due to lack of propeller data at this design phase, estimation for the efficiency factors are used, proposed by Schneekluth and Bertram (1998).

$$P_B = \eta_S P_D$$
where
$$P_D = \frac{R_T V}{\eta_D} \tag{18}$$

The process described above is undertaken for various conditions. Calm water resistance and wind resistance are calculated for the design draught at the design speed, as well as at two additional speed values which are set as fractions of the design speed, represented by parameters that can be controlled by the user. These

speed values represent the operating speed in various conditions, i.e. manoeuvring at port or sailing under adverse weather conditions. In addition, the two aforementioned resistance components are estimated for the examined loading conditions, where trim and draught might differ.

4.3.3 Lightweight estimation

Lightweight is estimated using empirical methods. The overall weight is divided into three distinct groups, namely the steel W_{ST}, outfit W_{OT} and machinery W_M weights (19). Despite the concept design stage, there are a few methods which are able to provide accurate estimations for both the weight and the centre of gravity for each weight group. These methods take advantage of the parametric setup, requiring information which either derives from the parameters of the optimisation problem or depends on parametric entities defined at previous stages (e.g. surfaces, rooms).

$$LS = W_{ST} + W_{OT} + W_{M} \tag{19}$$

The steel weight includes the weight of the hull, superstructures and some heavy steel fittings depending on the ship type, such as the container cells. The hull weight is calculated using the Schneekluth method (Papanikolaou, 2014). The method was originally designed for dry-cargo ships; however it is possible to apply it to other ship types, such as passenger vessels or containerships. A standard formula is used to calculate the steel weight of the hull, requiring as input the ship's main particulars, form coefficients and sheer and camber heights. An amendment of this formula is available for the calculation of the hull steel weight of containerships; however the input data remain the same.

Superstructure weight is calculated using the Müller-Köster method (Papanikolaou, 2014). This weight is calculated as a function of the enclosed volume of the superstructure and depends on the location of its structural elements. Input data include the area and height of each superstructure deck, which is obtained from the parametrically defined rooms.

The weight of heavy steel fittings, including the container cells, is calculated using simple formulas taking into account the weight of each part, multiplied by the total number which depends on the generated ship model.

The outfit weight can be estimated using approximation formulas available in Papanikolaou (2014). Taking into account the ship's main particulars (L_{BP}, breadth), as well as a coefficient which depends on the size and type of the ship being optimised, the overall outfit weight is estimated.

Finally, the machinery weight primarily depends on the installed main engine's power. Watson & Gilfillan provide an approximation formula for the calculation of this weight group, taking into account the type of the engine, apart from the installed power (Papanikolaou, 2014).

The centre of gravity for each of the above weight groups is estimated through empirical formulas, deriving from regression analyses on similar ships (Papanikolaou, 2014). Taking the rooms defined at previous stages, as well as the ship's main particulars into account, the centre of gravity is computed to be used in the loading conditions setup.

4.3.4 Deadweight breakdown

Deadweight analysis is a requirement for the definition of the loading conditions and provides values for the payload and weight of consumables (W_F, W_{FW}, W_{PR}), crew W_{CR}, stores W_S and water ballast B (20).

$$\mathrm{DWT} = \mathrm{Payload} + \mathrm{W_F} + \mathrm{W_{FW}} + \mathrm{W_{PR}} + \mathrm{W_{CR}} + \mathrm{W_S} + \mathrm{B} \tag{20}$$

Consumables include the fuel, diesel, lubrication oil W_F, as well as the fresh water W_{FW} and provisions W_{PR} weights. The former group depends on the power of the main and auxiliary engines, time of a round trip, SFOC of the main and auxiliary engines, as well as the efficiency of the auxiliary engines. On the other hand, fresh

water and provision weights depend on the number of people on board and the time of a round trip. Typical values are used for required amount of fresh water and provisions for every person per day. Likewise, crew weight is calculated based on typical values for every person on board. Stores weight depends on the size of the ship, based on similar ship deadweight breakdown data.

Depending on the ship type under consideration, payload is calculated either at this stage or during the loading conditions definition. For instance, a Ro-Pax vessel would normally be required to transport a specific amount of vehicles and passengers. Typical values are used for the weight of each of these elements and depending on the available space (i.e. lane metres, area of passenger spaces) determined by the rooms defined at an earlier stage, as well as typical values for dimensions of vehicles and number of passengers per square metre of passenger spaces (Levander, 2012), the total payload is determined. On the other hand, containerships have a maximum container capacity; however, a typical loading condition involves a homogeneous container stowage, whose number depends on intact stability criteria. Hence, the amount of containers loaded –and consequently the payload value– is defined during the definition of the loading conditions.

4.3.5 Loading conditions

Following the estimation of the lightweight and the deadweight analysis, the loading conditions are defined. In particular, the full load departure condition is examined, where the consumable tanks are fully loaded and the maximum payload is taken into account.

Depending on the ship type, the definition of the loading condition may involve an internal optimisation regarding the payload or not. As mentioned in Paragraph 4.3.4, in containership demonstration case, the amount of containers loaded depend on intact stability criteria. The ship needs to comply with certain rules which are affected by the loading condition's resulting centre of gravity. For this reason, a homogeneous weight for each TEU is assumed –controlled by a parameter– and

containers are loaded in such way to maximise the total amount of containers loaded below and above the main deck, minimising the required amount of water ballast at the same time. The latter is loaded in the AP and FP ballast tanks in order to control the final trim corresponding to the defined loading condition. No water ballast is used for stability reasons.

The process described above is related to the recent developments in international regulations applied to merchant ships regarding the control and management of ship's water ballast and sediments (IMO, 2004). The convention entered into force on September 2017 and requires all ships to implement a water ballast management plan. All ships have to carry a water ballast record book and are required to carry out water ballast management procedures to a given standard in a way to prevent the transfer of invasive marine species and protect the marine environment.

Although various systems and technologies aiming at the minimisation of the transfer of organisms through water ballast to different ecosystems are currently available, their installation on-board ships increases their capital and operating costs. Therefore, research has been focusing lately at solutions to reduce the amount of required water ballast. This problem is more severe for containerships, which inherently carry more water ballast, even at the design load condition. Thus, design solutions for containerships that consider zero or minimal water ballast capacities are very appealing to the ship owners.

4.4 Objective functions and constraints

The definition of the loading conditions concludes the essential computations required to set up the ship model. The next step involves the determination of the performance indicators which are used to evaluate the initial design and its variants during the optimisation process. These performance indicators, forming the objective functions and constraints of the optimisation problem are defined taking advantage of the integration capabilities of CAESES®. A selection of software tools is utilised to define the objective functions and the necessary constraints described below.

4.4.1 Container capacity ratio

This particular performance indicator represents one of the objective functions that can be applied to the containership demonstration case. It is used as an objective function and is an outcome of the loading condition definition process described in Paragraph 4.3.5. The ratio is calculated in NAPA® and is defined as the number of TEUs loaded in the examined load case divided by the maximum TEU capacity of the vessel (Figure 27). The higher the ratio, the larger the amount of containers carried on-board. Therefore, the efficiency of the containership is increased. In terms of the optimisation process, maximisation of the value is desired.

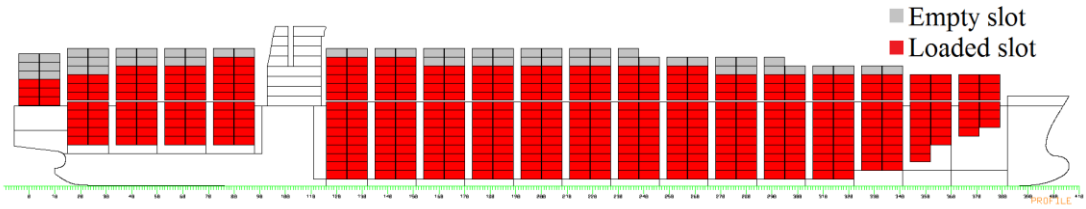

Figure 27: Definition of the container capacity ratio

4.4.2 EEDI

EEDI is a performance indicator that can be used either as an objective function or as a constraint. It can be applied to both cases examined in this thesis, as the relevant IMO regulations refer to various ship types, containerships and Ro-Pax vessels included. EEDI is calculated in NAPA® according to the guidelines set by the IMO. Two values must be calculated; (a) the required EEDI, referring to the regulatory limit of the ship's EEDI and (b) the attained EEDI, referring to the actual EEDI of the ship (IMO, 2012a, b, c).

The required EEDI value is calculated using reference lines developed by the IMO using and analysing data from a large number of existing ships. In (21), *a*, *b* and *c* are parameters depending on the ship type and a result of the regression analysis of the aforementioned data (Table 7). On the other hand, *x* is the EEDI reduction factor which depends on the implementation phase and the year the ship is built (Table 8).

$$\mathrm{EEDI_{Required}} = \left(1 - \frac{\mathrm{x}}{100}\right) \mathrm{ab^{-c}} \quad (21)$$

Table 7: Required EEDI formula parameters (IMO, 2012a, b, c)

Ship type	*a*	*b*	*c*
Containership	174.22	DWT	0.201
Ro-Pax vessel	752.16	DWT	0.381

The attained EEDI value is calculated taking the CO_2 emissions and transport work of the ship into account (22). The emissions are calculated based on the ship's on-board technologies influencing the EEDI levels; the main engine, auxiliary engines, innovative power generation devices and innovative technologies providing mechanical power for the ship propulsion. The transport work is computed by multiplying the ship's capacity in deadweight or gross tonnage at summer load line draught by the reference ship speed, attained at propulsion power specified by the regulations and under calm sea and deep water operation at summer load line draught.

$$\mathrm{EEDI_{Attained}} = \frac{\mathrm{CO_2\ emission}}{\mathrm{Transport\ work}} \quad (22)$$

Table 8: EEDI implementation phases (IMO, 2012a, b, c)

Phase	Year	*x*	
		Containership	Ro-Pax vessel
0	2013-2015	0	N/A
1	2015-2020	10	5
2	2020-2025	20	20
3	2025–	30	30

The rules require the attained EEDI to be less or equal to the required value (23) (IMO, 2012a, b, c).

$$\mathrm{EEDI}_{\mathrm{Attained}} \leq \mathrm{EEDI}_{\mathrm{Required}} \tag{23}$$

Within the concept of holistic ship design optimisation, the EEDI serves as an indicator of efficiency in terms of both economics and environmental friendliness. Since the transport work is inversely proportional to the attained EEDI value, a higher capacity results in a lower EEDI. Low values are desired for the latter to meet the constraint set in (23). Therefore, by minimising the attained EEDI value, not only are the regulations met, but also the ship becomes more economically efficient. As mentioned earlier, the designer may include the minimisation of the attained EEDI value in the objective functions of the optimisation problem, or consider (23) in the constraints of the problem.

4.4.3 RFR

The RFR value indicates the minimum rate that evens the properly discounted ship's expenses. It is a major financial performance indicator taking into consideration both the expenses and earnings of a vessel throughout its lifetime. Its minimisation is desired during the solution of the optimisation problem. Models which are based on the principal ship characteristics known from the early design stages are programmed in NAPA® macros to calculate the RFR (Levander, 2012, SAFEDOR, 2005-2009). In general, the definition of RFR is shown in (24).

$$\mathrm{RFR} = \sum_{\mathrm{i}}^{\mathrm{N}} \frac{\mathrm{PW}_{\mathrm{Operation}} + \mathrm{PW}_{\mathrm{Ship\ acquisition}}}{\mathrm{Cargo\ tonnage}} \tag{24}$$

PW states for the present worth of the cost. Operational costs include fuel, insurance, maintenance and manning expenses, while the ship acquisition costs consist of design, steel, outfit, machinery and overhead expenses. Detailed breakdown depending on the application case is available in Chapter 5. Several parameters

affecting the aforementioned costs, such as crew wage, steel price, labour rates or fuel price are controlled by the user. In addition, the applied discount rate in order to identify the NPV of the costs is defined as a parameter to the problem.

In the Ro-Pax vessel demonstration case, the parametric definition of the RFR calculation process is more complicated than in the containership case, as the earnings refer to more than one element. For instance, passenger tickets include economy class, first class or cabin. Moreover, the price for the transported vehicle can vary between cars and busses or lorries. Hence, relations can be developed between the different rates in form of parameters controlled by the user in order to simplify the computation. The same principle can be applied to the different time periods of operation (i.e. high and low season), during which the prices can fluctuate, providing a more accurate value for the RFR.

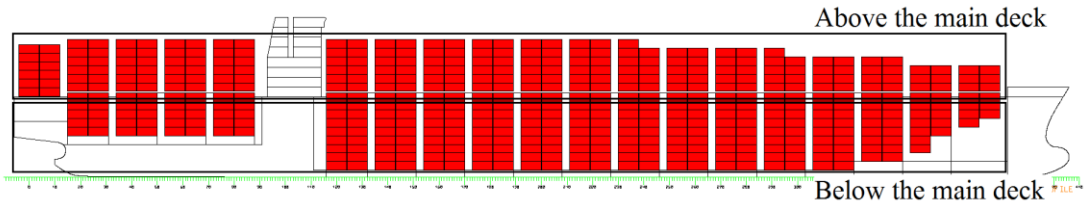

Figure 28: Definition of the container stowage ratio

4.4.4 Container stowage ratio

Container stowage ratio is a performance indicator applied to the containership demonstration case and refers to the ratio of the TEUs stored above the main deck to the ones below the main deck (Figure 28). It is calculated in NAPA® taking as input values produced during the definition of the ship model. The ratio is related to the cargo loading/unloading efficiency of containerships. It is a simplified approach to evaluate the performance of the design during the concept design stage, without requiring complex calculations involving the container stowage plan depending on the route the ship follows.

The maximisation of the ratio is desired within the optimisation problem. The greater the number of containers above the main deck can be translated to shorter loading and unloading times at port, increasing the available voyage time. The latter results in lower mean service speed and consequently lower fuel consumption.

4.4.5 Calm water resistance CFD calculations

One of the objectives of this thesis is to utilise multi-fidelity methods to evaluate each design produced during the optimisation process. The values resulting from each method is compared and differences in the relevant performance indicators can be identified. The accuracy and validity of the results produced by the utilised methods reveal the robustness of both the optimisation method and the design. A design characterised by the same or similar performance regardless of the method applied to obtain the relevant values is robust and reliable.

The principle described above is applied to the calm water resistance estimation. Calm water resistance is calculated in NAPA® using empirical methods, providing a quick alternative to evaluate the hydrodynamic performance of the design. However, in this methodology an additional evaluation is performed for the same objective, using higher fidelity, CFD methods. The parametric hull form is used as input and imported to CFD software Star-CCM+® (Siemens, 2017). The calculations take place in Star-CCM+®, benefiting from the integration capabilities of the presented setup and the software tools used in this process.

The parametric hull is translated to model scale to reduce the required computational time and the required numerical input for the Star-CCM+® model setup is provided by a CAESES® feature. For instance, the model's properties (mass, centre of gravity, moment of inertia, wetted surface), solver parameters, stopping criteria and coordinates of the volumetric mesh refinements mentioned below are calculated based on the parameters of the problem and provided as output by the developed CAESES® feature.

Within Star-CCM+®, macros are used, responsible for the various actions required to define the computational setup. The process starts with the mesh generation, including the definition and formation of the necessary volumetric mesh refinements on areas close to the hull surface to refine the free water surface area (Figure 29). The latter is performed parametrically, depending on the parameters affecting the hull shape. Afterwards, the physical and numerical setup is defined. The method utilised is the Volume of Fluid in conjunction with the k-ε turbulence model to simulate the flow characteristics.

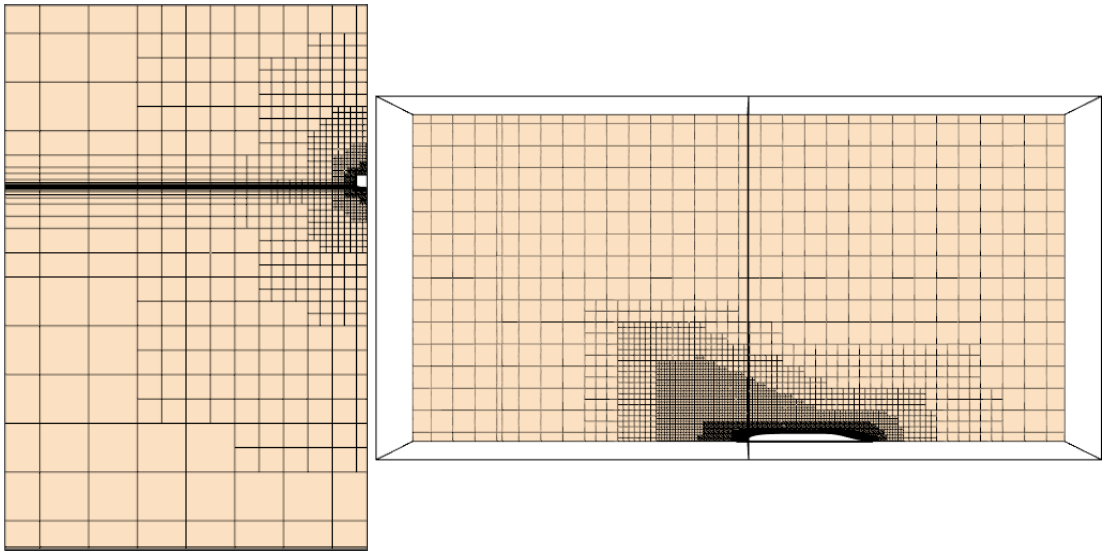

Figure 29: Mesh generation in Star-CCM+®

Volume of Fluid method is a numerical Euler method of free surface approximation. Euler methods are generally described by a grid which can be either stationary or non-stationary. In case of the latter, the grid motion is determined by the change of the surface shape. The Volume of Fluid method allows following the shape and position of the surface. The flux motion is described by Navier-Stokes equations, solved separately using RANS equations, such as the k-ε model described below.

The method is based on the use of a fractional function *C*, which is determined as an integral of the fluid's characteristic functions in a grid cell. *C* is a continuous function, with $0 \leq C \leq 1$. If the cell is empty (i.e. there is no fluid), $C=0$. If the cell is full, $C=1$. Derivative of the fractional function must be equal to zero (25).

$$\frac{\partial \mathrm{C}}{\partial \mathrm{t}} + \boldsymbol{v}\nabla \mathrm{C} + \nabla[\mathrm{C}(1-\mathrm{C})\mathrm{U_r}] = 0 \tag{25}$$

where $\boldsymbol{v}$ is the fluid velocity and U_r is an artificial force that compresses the region under consideration.

The k-ε model was first proposed by Jones and Launder (1972) and is considered the standard turbulence model for engineering simulation of flows. It is a two equation model describing the turbulence by means of two transport equations. The first transported variable is the turbulence kinetic energy k, while the second transported variable is the rate of dissipation of turbulence energy ε.

The two transport equations for the standard k-ε model are shown in (26) and (27).

$$\frac{\partial}{\partial \mathrm{t}}(\rho \mathrm{k}) + \frac{\partial}{\partial \mathrm{x_i}}(\rho \mathrm{k u_i}) = \frac{\partial}{\partial \mathrm{x_j}}\left[\left(\mu + \frac{\mu_\mathrm{t}}{\sigma_\mathrm{k}}\right)\frac{\partial \mathrm{k}}{\partial \mathrm{x_j}}\right] + \mathrm{G_k} + \mathrm{G_b} - \rho\varepsilon - \mathrm{Y_M} + \mathrm{S_k} \tag{26}$$

$$\frac{\partial}{\partial \mathrm{t}}(\rho \varepsilon) + \frac{\partial}{\partial \mathrm{x_i}}(\rho \varepsilon \mathrm{u_i}) = \frac{\partial}{\partial \mathrm{x_j}}\left[\left(\mu + \frac{\mu_\mathrm{t}}{\sigma_\varepsilon}\right)\frac{\partial \varepsilon}{\partial \mathrm{x_j}}\right] + \mathrm{C_{1\varepsilon}}\frac{\varepsilon}{\mathrm{k}}(\mathrm{G_k} + \mathrm{C_{3\varepsilon}G_b}) - \mathrm{C_{2\varepsilon}}\rho\frac{\varepsilon^2}{\mathrm{k}} + \mathrm{S_\varepsilon} \tag{27}$$

where G_k represents the generation of turbulence kinetic energy due to the mean velocity gradients, G_b represents the generation of turbulence kinetic energy due to buoyancy, Y_M represents the contribution of the fluctuating dilatation in compressible turbulence to the overall dissipation rate and $C_{1\varepsilon}$, $C_{2\varepsilon}$, and $C_{3\varepsilon}$ are constants. σ_k and σ_ε are turbulent Prandtl numbers for k and ε respectively. S_k and S_ε are user-defined source terms. μ_t is the turbulent –or eddy– viscosity, computed by combining k and ε as shown in (28).

$$\mu_\mathrm{t} = \rho \mathrm{C_\mu}\frac{\mathrm{k}^2}{\varepsilon} \tag{28}$$

where C_μ is a constant.

The simulation results are obtained after setting the solver parameters and stopping criteria –controlled by parameters accessible to the user.

During the post-processing phase, the results corresponding to the model are converted to full-scale to obtain the calm water resistance for the design to be optimised.

As mentioned in the beginning of the Paragraph, the output of this operation is used to compare the results obtained through two different methods (detailed but time-consuming CFD calculation and fast but approximating method proposed by Holtrop and Mennen (1978)). In the optimisation phase, the difference between the values for the calm water resistance obtained through the aforementioned methods is used as an objective function, for which minimisation is desired –the lower is the difference, the more robust is the response of the design.

4.4.6 IMO second generation intact stability criteria

A recent development regarding the safety regulations applied to merchant vessels is the introduction of the second generation intact stability criteria. These criteria are being developed by the IMO (2018). The introduction of ships with newly developed design characteristics and operation modes has challenged the assumption that the current intact stability criteria are sufficient to prove their stability. Hence, the new criteria are performance-based and address five modes of stability failure; excessive acceleration, parametric roll, pure loss of stability, stability under dead ship condition and surf-riding/broaching.

As far as ships with slender hull forms (e.g. containerships, Ro-Pax vessels) are concerned, parametric roll is considered one of the most important modes of stability failure (Peters et al., 2011). Pure loss of stability failure mode should also be investigated, as the considerable flare found in the aft and fore parts of a slender hull results in significant changes in the waterplane area when the ship sails through waves. These changes may result in a large roll angle or even capsize (Peters et al.,

2011). Likewise, excessive acceleration failure mode should be checked in these ship types, due to high superstructures found in such kind of ships. Therefore, the draft criteria of level 1 and 2 for excessive acceleration, parametric roll and pure loss of stability failure modes according to SDC 6/5 are included in this methodology (IMO, 2018). Further information on the background of each examined criterion can be found in Appendices A, B and C.

These checks are performed using macros (referred to as "features" in CAESES®), taking as input the hull geometry and the output of the computations performed during the definition of the ship model. Level 1 checks are meant to be simple and conservative, in order to quickly detect any vulnerability to each of the three failure modes. Level 2 checks are more complex, thus less conservative, taking into account more design- and operation-related aspects in order to determine whether the ship is vulnerable to either of the examined failure modes. For each failure mode, several features are developed within CAESES®, connecting various external software tools to evaluate certain parameters required to perform these computations. Maxsurf® Stability (Bentley Systems, 2014) and Matlab® (Mathworks, 2014) are integrated in the procedure to perform the required calculations and solve complex equations defined in the regulations.

4.4.7 Midship section structural analysis

In accordance with the principles set by the holistic design approach, several aspects of naval architecture are incorporated and evaluated in this methodology. Structural integrity is important for assessing the ship's safety and compliance with regulations regarding structural strength. Containership sizes have been increasing lately, with several designs able to transport up to 21000 TEUs being already in operation. The structure of such ships requires attention in design due to their internal arrangement to avoid structural failure.

The midship section design is analysed to check its structural strength according to Lloyd's Register rules (Lloyd's Register, 2014) using CAESES® features. Based on

the generated internal geometry, a setup of the midship section is created. The strakes and longitudinal stiffeners are taken into account. The minimum required section modulus, moment of inertia and the permissible bending and shear stress are calculated according to the relevant rules. In addition the minimum required plate thickness and stiffener section modulus for each midship section panel are computed and considered as a starting point to check whether the setup passes the criteria. In case the latter is not achieved, an internal optimisation takes place using the Tangent Search method. The plate thicknesses and the stiffener profile types constitute the design variables set, while the minimum required section modulus, moment of inertia and permissible bending and shear stress are set as the constraints of the problem. The process identifies the combination of plate thicknesses and stiffener profiles that satisfies the limits set by the regulations.

4.5 Design of experiment

Once the preparatory steps for the setup of the ship design optimisation problem are completed, designs of experiment take place. The benefits of this step are outlined in Section 3.4. In addition, designs of experiments are required for the next step, which is the definition of the surrogate models. These runs allow the determination of the effect of each design variable on specific evaluations and consequently reduce the complexity of the production process of the surrogate models.

The Sobol algorithm is utilised at this step. Sobol algorithm is a quasi-random sequence, in which test points are scattered in a purely random manner (Azmin and Stobart, 2015). The number of design variants is selected, the design variables and constraints are set and each design is evaluated according to the setup applied, depending on the required output. For instance, the design of experiment for the definition of the surrogate model responsible for the calm water resistance CFD calculations does not evaluate the ship model and objectives and constraints described in Sections 4.3 and 4.4, since they are redundant to the calculations performed to obtain the desired output. On the contrary, the parametric hull model is

generated and the relevant CFD software tool is utilised, as described in Paragraph 4.6.1.

The results of the design of experiments are analysed. Either the limits or the amount of the design variables are modified based on their effect on the design at the optimisation phase or the output is used to construct the surrogate model at the next step.

4.6 Surrogate models

Following the setup of the objective functions and constraints calculation and the relevant design of experiment runs, an evaluation is performed to decide which computations would be eligible to be substituted by surrogate models. The criteria taken into consideration are the following:

- Computational setup; requirement to use specific operating system prohibits utilisation of software tools designed to operate on other operating systems
- Computational time per design variant; computations requiring significant amount of time per design variant prolongs the duration of the optimisation phase
- Number of design variables per computation; the higher the number of design variables, the greater the amount of evaluations required to produce an accurate surrogate model
- Variance of output; inconsistency in results impedes the definition of an accurate surrogate model, as a high number of evaluations is required to achieve the latter

Based on the aforementioned criteria, three computation setups are selected to be substituted by surrogate models in the optimisation phase; (a) the calm water resistance CFD calculations setup, (b) the IMO second generation intact stability criteria setup and (c) the uncertainty quantification setup.

The process followed to define the surrogate models is divided into three phases; (a) the preparation phase, in which designs of experiment are run to create a pool of design variants, (b) the generation phase, in which the surrogate model is defined using the Kriging method and the pool as input and (c) the evaluation phase, in which the surrogate model is tested for its accuracy by obtaining the results of both the actual simulation and the surrogate model for a specified number of newly defined design variants. The consistent, high accuracy of the Kriging method in the definition of the surrogate models, in conjunction with the fast evaluation times (both illustrated in Chapter 6), proves the suitability of this response surface method in the presented methodology.

4.6.1 Calm water resistance CFD calculations

The calm water resistance CFD calculations mentioned in Paragraph 4.4.5 require utilisation of HPC facilities in order to be able to obtain results in a sensible period of time. The setup may be required to be defined in specific operating system, depending on the HPC facilities, conflicting with the compatibility of other software tools used in the proposed methodology.

In addition, CFD calculations –even if run on a HPC– demand substantial computational time per evaluation, making their integration to a typical optimisation process often inconvenient. For instance, a typical computation for a containership or Ro-Pax vessel used in the case studies of this thesis requires around thirty minutes to run on one node (40 cores), 2 x Intel Xeon Gold 6138 20 core 2.0 GHz CPU with 192 GB RAM per node. Yet, depending on the set of design variables used, the results are generally consistent.

Therefore, the calm water resistance CFD calculations setup can be conveniently used to create a surrogate model which provides valid results and be used in the optimisation phase.

4.6.2 IMO second generation intact stability criteria

Computations needed to be performed for the evaluation of the IMO second generation intact stability criteria –mentioned in Paragraph 4.4.6– can be run locally on a personal computer. Nevertheless, the setup requires various software tools to be run simultaneously, due to the complexity and variance of the calculations (e.g. hydrostatic, numerical) required to be run. Therefore, a substantial amount of computational time in needed for each design variant –around fifteen minutes on an Intel Core i7-4790 3.6 GHz CPU with 8 GB RAM.

Each of the criteria takes a considerable amount of data as input to be able to predict the variance of the results, however, the results described in Chapter 6 shows consistency without requiring prohibitive amount of design variants in the preparation phase.

4.6.3 Uncertainty quantification

Uncertainty quantification setup is a set of computations required to be run for the uncertainty analysis of the problem. Essentially, the setup is identical to the procedure described in Sections 4.3 and 4.4. The difference lies on the values assigned to specific design variables. Various methods –mentioned in Chapters 2 and 3– have been applied to quantify the uncertainty in an optimisation problem. In addition, the higher is the complexity of the problem, the stronger is the presence of uncertainty along the process.

In the proposed methodology, uncertainty is taken into account and investigated throughout the design and optimisation processes in key areas. Normally, design variables and parameters of the problem are assigned specific values and the solution of the problem returns a single result. In the uncertainty quantification setup, the objective is the evaluation of the variance in the results, affected by the values assigned to the identified parameters. Hence, the first step is the determination of the uncertain parameters specific to the problem under investigation. Their uncertainty

arises either from external factors or from lack of knowledge due to the early stage of ship design investigated in this methodology. For instance, fuel price is identified as uncertain due to its daily fluctuation, affected by the global market. The fuel price directly affects the RFR value. On the other hand, the propulsive and shaft efficiency are considered uncertain because of the lack of detailed propulsion calculations due to insufficient input during the concept ship design stage. These efficiency factors affect the main engine power, which in turn influences the fuel consumption, required amount of fuel oil carried on-board, loading condition and RFR value. The latter demonstrates not only the interrelation of the numerous computations performed to produce a ship design, but also the transfer of uncertainty along the design process.

The former category of uncertain design variables are assigned a probability distribution based on known, historical data. Analysis of the data provides the required input to produce the probability distributions. For example, calculation of the mean and standard deviation of a dataset allows the definition of a normal probability distribution assigned to an uncertain parameter. On the other hand, uncertain parameters for which data are not available due to the investigated design stage are assigned a variance factor produced by a normal probability function, whose limits are determined by the user. The mean value used in this case is equal to the value used in the normal calculations setup, where uncertainty is not taken into account.

Following the identification of the uncertain design variables and parameters of the problem, the ship model definition presented in Section 4.3 is amended to quantify the uncertainty involved in the results of the following calculations:

- Calm water, added wave and wind resistance
- Lightweight estimation
- Deadweight analysis
- RFR

The aforementioned computations are directly affected by the uncertain design variables due to the latter being the input to the former. However, as mentioned earlier, calculations influenced by the uncertainty effects are not limited to the list above. For instance, objectives' values, such as the container capacity ratio, change depending on the values of the uncertain parameters.

Overall, the aim of the process is to identify the variance of the results which are used as objective functions or constraints in the solution of the optimisation problem. This is achieved by investigating several scenarios for each design variant during the optimisation phase, during which the uncertain parameters are assigned random values based on their probability distribution (Figure 30). These scenarios are created using the Latin Hypercube Sampling method, mentioned in Section 3.7. Optimisation software tool Dakota® (Sandia, 2018) is connected to CAESES® during the optimisation run and produces a number of scenarios set by the user by employing the Latin Hypercube Sampling technique. The standard deviation of the results is computed and used as an optimisation objective, for which minimisation is desired.

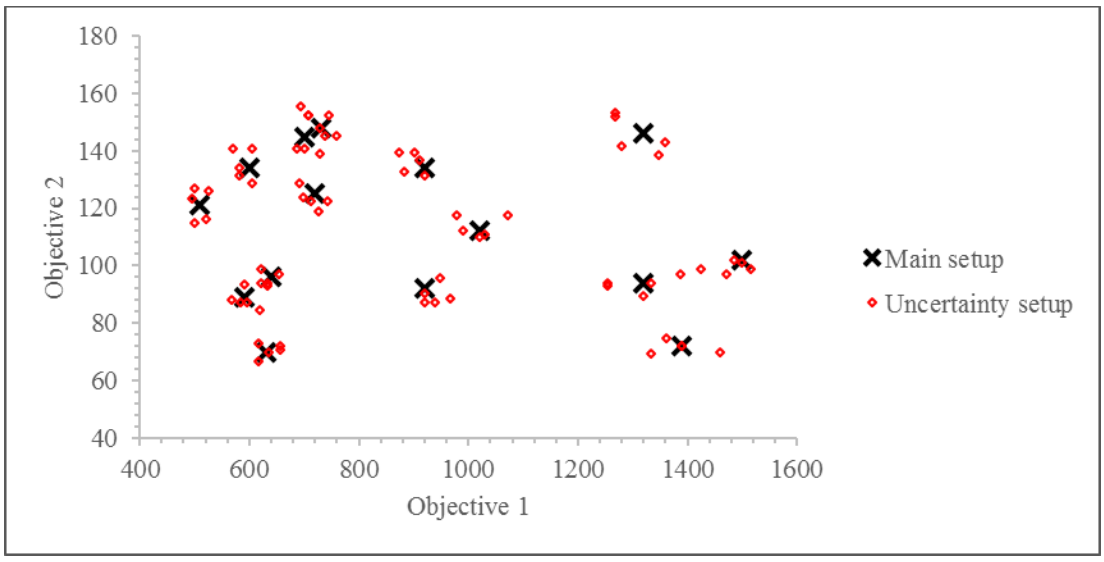

Figure 30: Uncertainty quantification setup

The scenarios investigation takes place for each design variant during the optimisation phase. Although the duration of the computations required to investigate a single scenario does not exceed the amount of a few minutes, running the

simulations numerous times for each design would lead to excessive computational time. Therefore, surrogate models are utilised to substitute the actual simulations with approximation models. A design of experiment is run during which both the absolute and uncertain design variables change to provide results for the objective functions and constraints affected by the uncertain parameters.

4.7 Multi-objective optimisation

The final preparatory step of the optimisation setup is the selection of the method used to perform the multi-objective optimisation. The NSGA 2 method is utilised in this methodology (Deb et al., 2002).

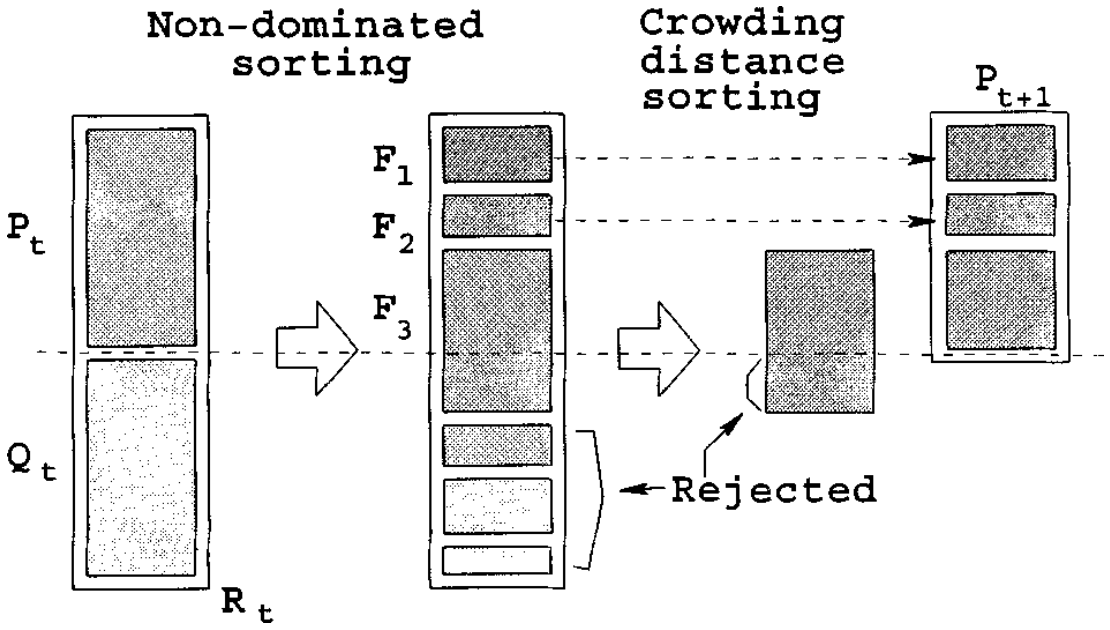

Figure 31: NSGA 2 procedure (Deb et al., 2002)

NSGA 2 is a genetic algorithm which works with a population of solutions and able to find multiple Pareto optimal solutions in a single simulation run. The algorithm incorporates innovative features compared to other genetic algorithms; (a) a fast non-dominated sorting procedure, (b) a fast crowded distance estimation procedure and (c) a simple crowded comparison operator, ensuring preservation of diversity in the produced solutions by monitoring the performance of each design variant, as well as

the distance between the solutions within the design space. A non-dominated solution which is located in a lesser crowded region is generally preferred.

In iteration t of the algorithm the following steps take place (Figure 31):

- An offspring population Q_t of designs is formed, containing N designs, according to the selection, cross-over and mutation operators' properties
- Population Q_t is combined with the parent population P_t, which also contains N designs. Hence, the combined population $R_t=P_t \cup Q_t$ contains $2N$ designs
- Population R_t is sorted according to non-domination and subsets F_i, $i=1,\ldots,n$ of solutions are created based on their level of elitism. Subset F_1 contains the best non-dominated designs; solutions in subset F_2 are dominated only by the designs contained in F_1, and so on
- The solutions of best subsets are passed on to the next parent population P_{t+1}, until the number N is reached. Thus, solutions of subset F_1 are selected first, followed by solutions of subset F_2, and so on
- To choose exactly N population members, solutions of the last subset are sorted using the crowded comparison operator in descending order and the best solutions needed to fill all population slots are chosen

The user is required to specify the number of generations and the population size for each one, along with the mutation and cross-over operator values. The values will affect the total number of design variants to be produced, as well as their variance in the design space to ensure the determination of a global optimum, following the decision making process at the next stage.

In addition, the setup of the algorithm requires the determination of the design variables and their limits, selection of the objective functions and constraints applied to the problem to isolate the invalid designs from the feasible solutions.

4.8 Multi-criteria decision analysis

The solution of a multi-objective optimisation problem requires a post-processing step which is vital for the designer to identify the best design produced by the process described in this Chapter. The results obtained from the operation mentioned in Section 4.7 need to be analysed to determine the Pareto front which includes the best solutions according to the objective functions and constraints defined in the multi-objective optimisation setup. As mentioned in Section 3.4, a solution is properly Pareto optimal if there is at least one pair of objectives for which a finite decrement in one objective is possible only at the expense of some reasonable increment in the other objective. This means that a decision making process has to follow to reveal the single best solution, based on a method determined by the user.

In this methodology, the utility function theory presented in Section 3.6 is employed, providing the best compromise solution to the problem. The objective function values are normalised based on the best and worst performance in each objective according to (29).

$$x_n = \frac{x - x_{worst}}{x_{best} - x_{worst}} \tag{29}$$

where x_n is the normalised response and x_{best}, x_{worst} are the best and worst responses respectively. Case scenarios are defined at this stage, which determine the weights taken into consideration in the decision making process. The user can specify the weights for each objective function, prioritising the significance of the objectives they believe are the most important, depending on the building purpose of the vessel. The weight assignment is directly related to the decision maker's preference. Sen and Yang (1998) outline the various techniques available for that purpose. Three major methods are mentioned, namely the direct assignment, the eigenvector method and the entropy method. In this study, the direct assignment approach is adopted. The user decides the weight values in each examined scenario. The total of these values in each scenario add up to 100%, while each objective can be assigned a weight, ranging between 0% and 100%.

Afterwards, the utility function is calculated for each design for each case scenario. The designs are then ranked according to their utility function values. The maximum score achieved by one design can be 1, whereas the lowest can be 0. The highest ranked design is identified as the best for the specific case scenario.

4.9 Summary

A highly automated, integrated approach to ship design optimisation under uncertainty is presented in this Chapter. The methodology described in previous Sections demonstrate the process followed to optimise a ship design in its early design phase in a holistic manner, incorporating the uncertainty induced by external factors or lack of knowledge during the concept design stage.

A parametric model for a specific ship type is constructed first, allowing a considerable amount of flexibility in the hull form definition. The user is able to select which of the parameters controlling the hull shape become the design variables of the optimisation problem, increasing the versatility of the problem definition and the focus of the problem.

A detailed ship model is defined afterwards, based on the hull form defined in the first step, where all the necessary computations to calculate the values for the selected objective functions and constraints of the problem take place. Various software tools are seamlessly interconnected at this stage, with CAESES® being the main platform, taking advantage of their capabilities in producing the required values in short lead time.

Designs of experiment are conducted once the ship model is properly defined using the Sobol algorithm. The design space is explored, identifying the trends and relations between the design variables and the objective function values. The selection of the design variables' limits is verified and the results allow the user to determine which of the ship model computations are eligible to be substituted by surrogate models, so as to reduce the overall computational time, without

compromising in the accuracy of the results. Factors such as computational time per design variant or variance of the output are considered for that purpose.

Next, the uncertainty quantification of the problem takes place, utilising surrogate models to calculate the standard deviation and mean of selected output, based on the variance of the uncertain parameters of the problem.

Following the definition of all the required calculation components, the solution of the multi-objective optimisation problem takes place, using the NSGA 2. The produced design variants are post-processed to determine the Pareto front.

Finally, in order to identify the best solution to the problem, a decision making process follows, where the utility function theory is employed. Case scenarios defining the significance of each objective are created by the user and the calculation of the utility function for each design variant determines the ranking of the feasible solutions. The highest ranked design variant is identified as the best solution to the specific case scenario.

All in all, a robust solution to a multi-objective ship design optimisation problem is the outcome of the overall procedure. Despite the investigation of the concept design stage, the consideration of the effects of uncertainty allows the identification of a design which performs well regardless of the uncertain parameters of the problem. The objective functions are related to the three main categories defined by Nowacki (2018); economics, safety and environment, with more than a single performance indicator considered for each category. In addition, newly introduced regulations regarding the control and management of water ballast and sediments, EEDI and intact stability of ships are incorporated in the methodology in an attempt to identify their effect in the design of the construction and operation of ships.

5 Case studies

5.1 Introduction

The methodology presented in Chapter 4 is validated through two different case studies, each one involving different ship types, objective functions and constraints. Through this process, results of the solution of the optimisation problem are obtained and analysed to ensure the robustness of the proposed workflow, as well as its ability to provide meaningful results to support the designer's task in producing an optimal ship design in the concept design phase.

In addition, the two case studies prove the versatility of the methodology, examining different hull forms and operational profiles, while focusing on various objectives, specific to the ship type being optimised.

In this Chapter, further information on the setup of the workflow presented in Chapter 4 is provided, elaborating on how each step is implemented and how the optimisation problem is processed and solved.

5.2 Containership case study

5.2.1 Challenges associated with containership design

The first case study examined in this thesis is a containership. This particular ship type involves various challenges in its design phase, which can be resolved through an optimisation procedure. Intact stability is a major issue associated with containerships and their operation. The introduction of the second generation intact stability criteria increases the complexity of this issue, reducing the number of valid

designs obtained through an optimisation process. The consideration of both the current and the newly developed criteria in the design optimisation process helps the designer understand which design elements affect the stability of this particular ship type.

Another issue associated with containerships is the resistance and powering. Until recently, this ship type used to operate in a speed range of 22 ÷ 26 Knots. Changes in the fuel prices in the recent years have induced a decrease in the speed range, with most containerships operating in the region of 18 ÷ 22 Knots (Banks et al., 2013). The practice of reducing the operational speed, adopted by the shipping industry in an attempt to lower the fuel consumption, is known as slow steaming and super slow steaming (Bonney and Leach, 2010).

Considering the strong relation between speed and resistance/powering, the optimisation of a containership hull for lower operational speed can have a huge impact on the efficiency of the design. The majority of research carried out on this subject has either been associated with single-objective design optimisation studies, considering only the resistance as an objective function, or have been focusing on the hull optimisation with regard to a specific operational speed, overlooking the uncertainty related to the changes in the operational profile in the future. On the contrary, in this thesis, a multi-objective optimisation procedure takes place, where resistance is taken into account as part of a number of objective functions, investigating its relation with design constraints applied to the problem. In addition, uncertainties associated with external factors, such as the fuel price or wind speed, are considered in the design process, revealing their effects on various operational profiles associated with different velocities.

Ship strength is another issue which requires attention during a design optimisation process. Containerships' structure arrangement to accommodate as much containers as possible requires careful design, involving high values for the overall ship's length and absence of main deck structure. As mentioned in Paragraph 4.4.7, design of the midship section needs to be validated for compliance with structural rules imposed

by classification societies, taking into account the bending moments and shear forces applied as a result of a loading condition.

Table 9: Examples of containership hull definition parameters in CAESES®

Parameter	Explanation
Acc_Pos	Position of the deckhouse along the ship
Hub_Radius	Bossing radius
CPC_X_Bulb_Tip	X-coordinate of the bossing tip
Fullness_Aft	Fullness of the aft fairing boundary sections
Weight_At_Bottom	Fullness of the bossing area sections
FOB_At_Mid	Y-coordinate of the mid-point of the aft FOB curve
FOS_Fullness	Fullness of the aft FOS curve represented by an F-spline
Bulb_Fairing_Spread_Factor	Fullness of the bulbous bow sections
Fullness	Fullness of the deck curve represented by an F-spline
Entrance_Angle	Entrance angle of the DWL

5.2.2 Optimisation problem setup

The setup of the problem begins with the hull design. As mentioned in Section 4.2, the geometric model is constructed in CAESES® and consists of four parts, the aft body, main frame, fore body and main deck (Figure 32, Figure 33, Figure 34 and Figure 35). The aft part contains the propeller area and the transom, both controlled by a set of parameters. The main frame can also be adjusted to change the midship section coefficient. The fore body includes the bulbous bow whose shape can be manipulated by several parameters. In total, 128 parameters are introduced in the design of the hull within CAESES®. Examples of these parameters are given in Table 9.

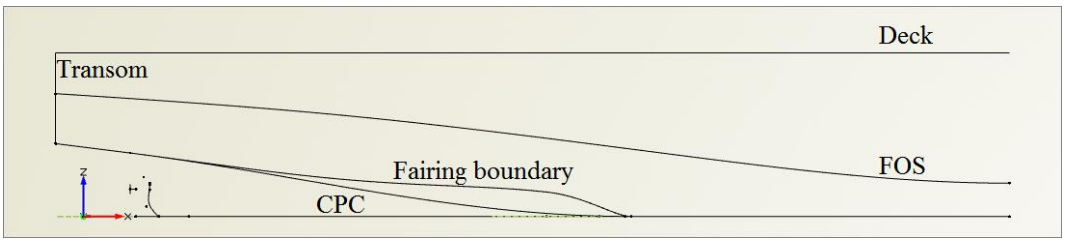

Figure 32: Containership hull aft section curves (profile view)

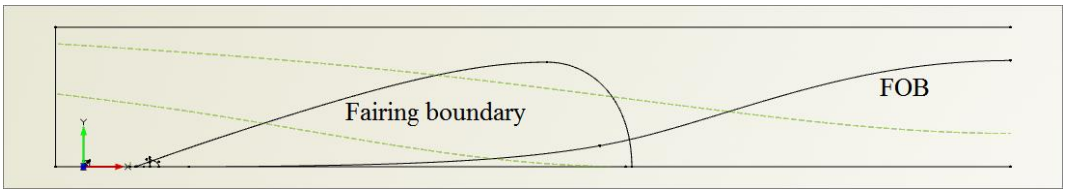

Figure 33: Containership hull aft section curves (top view)

Figure 34: Bulbous bow curves

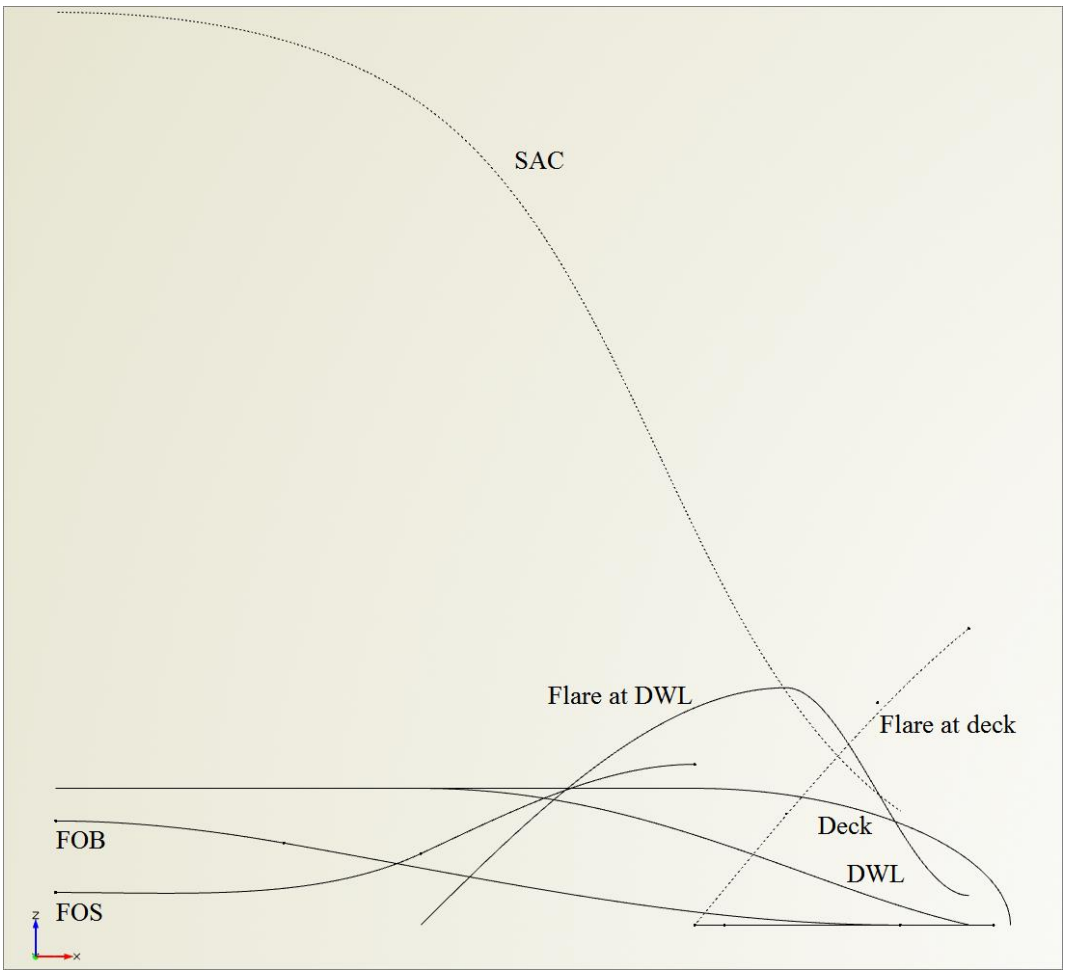

Figure 35: Containership hull fore section curves

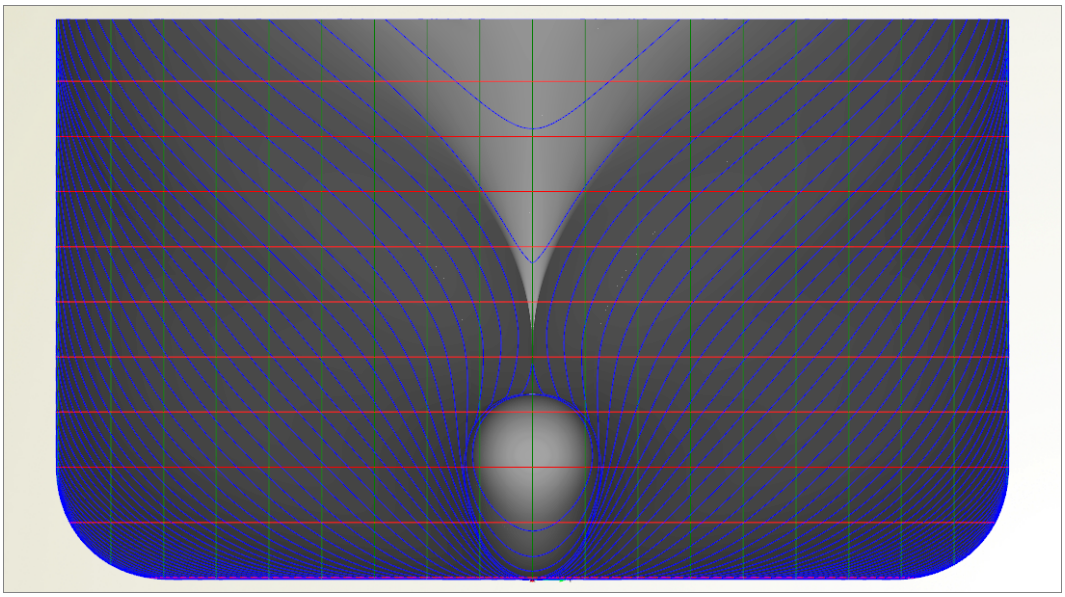

Figure 36: Containership baseline model hull (body plan view)

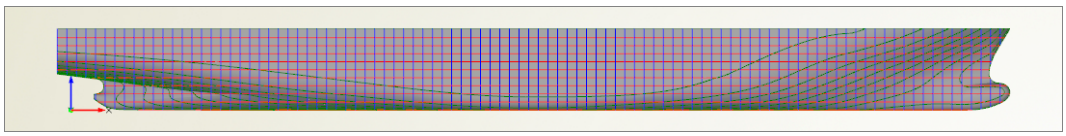

Figure 37: Containership baseline model hull (profile view)

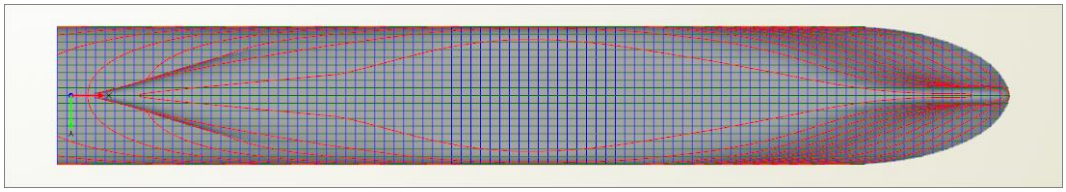

Figure 38: Containership baseline model hull (top view)

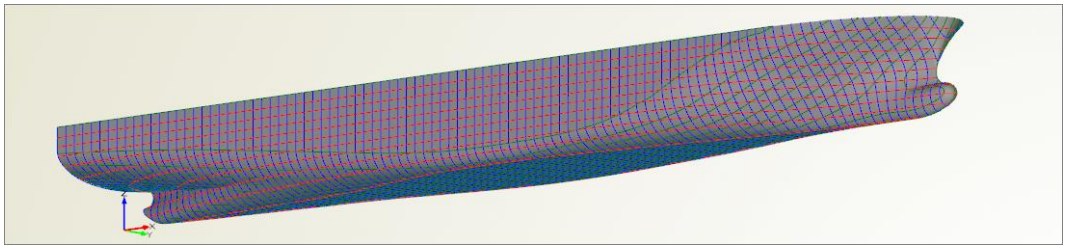

Figure 39: Containership baseline model hull (perspective view)

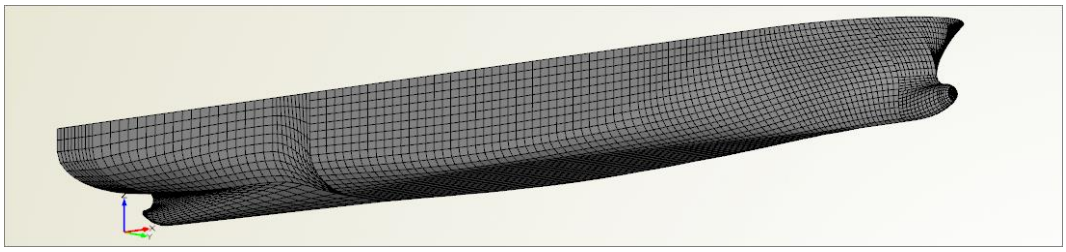

Figure 40: Containership baseline model hull (panel mesh)

The baseline geometric model for the containership case study produced in CAESES® is presented in Figure 36, Figure 37, Figure 38 and Figure 39, while a panel mesh of the hull surface used for some calculations involving the connection with Maxsurf® Stability is illustrated in Figure 40.

At this stage, the design variables of the optimisation problem are selected. An overall hull design optimisation procedure is selected to be performed; hence parameters controlling the main particulars are appointed as design variables. Ten

design variables are defined for that purpose and their values will be varying during the optimisation phase. The explanation of each design variable is given in Table 10.

The amount of the design variables affects the number of the generated design variants required to investigate the design space. Too many design variables result in a complex optimisation problem setup, calling for an extensive number of designs to be evaluated to guarantee the identification of the global optimum solution. In this case study, the number of design variables is kept low, focusing on the ones affecting the main dimensions of the ship.

Table 10: Main set of design variables selected for the containership case study

Design variable	Baseline value	Explanation
Acc_Pos	4	Position of the deckhouse along the ship (expressed as the number of bays located aft of the deckhouse)
Bays	18	Number of bays
Bilge_A	5.5	Y-coordinate of the bilge radius (m)
Bilge_B	5.5	Z-coordinate of the bilge radius (m)
DB	2	Double bottom height (m)
d_C_Prismatic	0	Percentage change of the prismatic coefficient (Lackenby transformation parameter)
d_LCB	0	Percentage change of the LCB (Lackenby transformation parameter)
Rows	18	Number of rows
Tiers_In	9	Number of tiers below the main deck
Tiers_On	6	Number of tiers above the main deck

Apart from the main design variables of the problem, secondary design variables are defined, which are related to the operational profile of the ship. The majority of these

design variables are identified as the uncertain parameters of the problem and play a major role in the uncertainty quantification process (Table 11).

The values selected for the parameters displayed in Table 11 derive from several sources. Taking into account the schedule of similar-sized containerships, a roundtrip of 13567 nm is selected, starting from the Mediterranean Sea, reaching the Gulf of Mexico, before returning to Europe. The corresponding number of port calls, along with an average time of the ship moored at the various ports is used as input in the case study. The average price of diesel (MDO) and fuel (IFO 380) oil are used as input (Bunker Index, 2018). Taking into account the latest trends in the operational speed of containerships, a mean value is used for the case study (Banks et al., 2013). Moreover, historical weather data are used to define the average wind speed in the areas matching the operational profile of the case study (NOAA, 2018).

Table 11: Secondary set of design variables selected for the containership case study

Design variable	Baseline value	Explanation
`Distance`	13567	Round trip distance (nm)
`Port_No`	18	Number of port calls
`Port_Time`	13.17	Average time spent at port (h)
`Price_DO`	721.67	Diesel oil price ($/t)
`Price_FO`	488.81	Fuel oil price ($/t)
`V_S`	20	Ship speed (Knots)
`V_Wind`	11.97	Wind speed (Knots)
`W_Cont`	10	TEU homogeneous weight (t)

A Lackenby transformation takes place to adjust the overall hull form through the design variables `d_C_Prismatic` and `d_LCB` mentioned in Table 10. Following the parametric hull form definition in CAESES®, the construction of the ship model in

NAPA® takes place. Within NAPA®, 24 additional parameters are introduced, all relevant to specific calculations performed by macros. Although the user has access to these parameters, specific values are assigned remaining constant throughout the optimisation phase. Examples of these parameters are given in Table 12.

The definition of the ship model is carried out according to the steps outlined in Section 4.3. The baseline ship model for the containership case study is presented in Figure 41. The various colours represent the purpose of each room. For instance, green stands for the water ballast tanks, while light blue is used for the cargo space.

Table 12: Examples of containership model parameters in NAPA®

Parameter	Explanation
`V.S.Low`	Ship speed during port operation (expressed as a percentage of the ship speed)
`C.AA`	Coefficient related to the calculation of the wind resistance component
`F.Cor.2`	Correction factor for the calculation of the lightship's VCG
`Dens.DO`	Diesel oil density
`F.Broker`	Coefficient related to the calculation of the broker cost

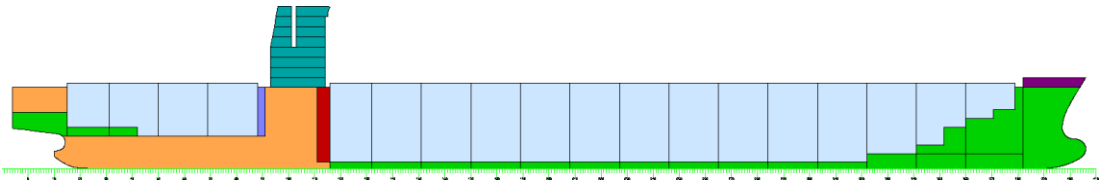

Figure 41: Containership baseline ship model defined in NAPA®

The process continues with the definition of the objective functions. The calculations mentioned in Section 4.4 take place. In general, the setup is irrelevant of the ship type under investigation and computations related to the ship type take place at this stage. For instance, in the containership case study the calculations of the container capacity and stowage ratio take place. As far as the RFR estimation is concerned,

different methods are used, depending on the ship type, as mentioned in Paragraph 4.4.3. In the containership case study, RFR is calculated based on the total cost associated with the ship's lifetime, according to Levander (2012). In particular, the total cost is divided into the capital and operating cost.

The capital cost is divided into the following categories (Levander, 2012):

- General
- Payload related (hatch covers, container cranes, cell guides in holds/on deck)
- Hull structure
- Deckhouse
- Ship outfitting
- Accommodation
- Machinery
- Ship systems
- Reserve
- Design
- Finance

On the other hand, the operating cost involves several categories, mentioned in Figure 42.

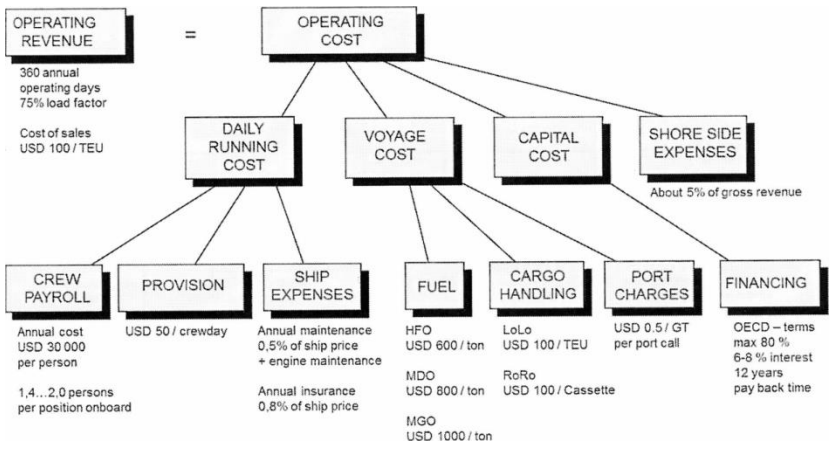

Figure 42: Operating cost model for containerships (Levander, 2012)

As far as the calm water resistance CFD calculation setup is concerned, the CAESES® feature mentioned in Paragraph 4.4.5 is defined accordingly to produce the necessary input for the Star-CCM+® operations. The generated mesh and the wave elevation measurement during the CFD runs of the baseline model of the containership case study are presented in Figure 43 and Figure 44 respectively.

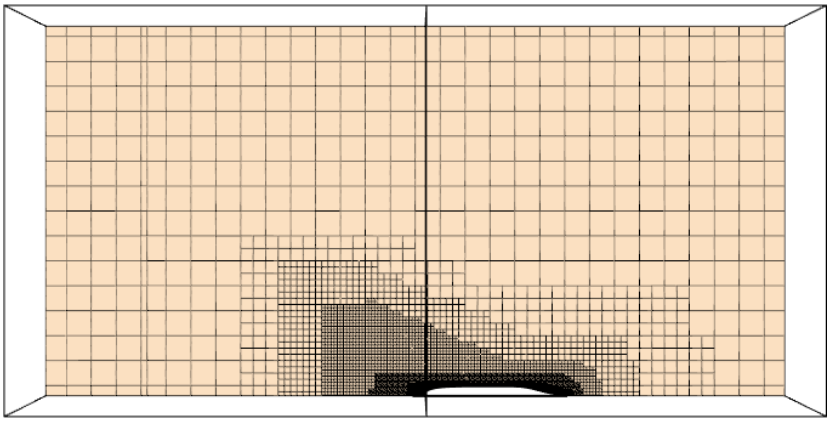

Figure 43: Generated mesh of the containership baseline model in Star-CCM+®

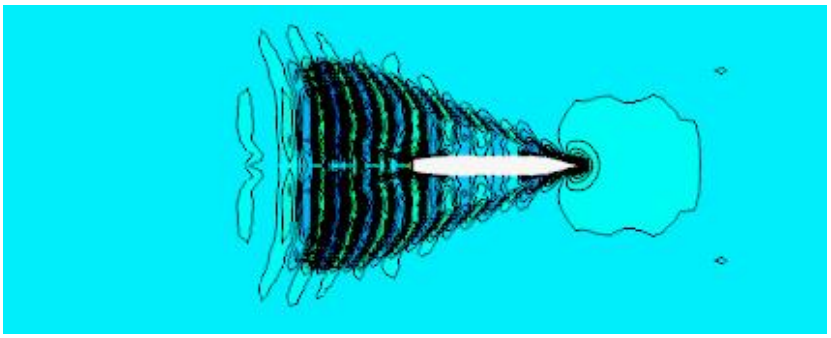

Figure 44: Wave elevation of the containership baseline model in Star-CCM+®

Following the definition of all the necessary computations, several designs of experiment take place for the construction of the surrogate models mentioned in Section 4.6. Following an analysis of the designs of experiment conducted to identify which design variables influence the particular calculations the most, the setups are defined for the construction of the surrogate models for the calm water resistance CFD calculations, IMO second generation intact stability criteria and uncertainty quantification. The design variables, monitored parameters, number of design

variants generated during the preparation and evaluation phases –as described in Section 4.6– are provided in Table 13.

Table 13: Surrogate model setups for the containership case study

Calm water resistance CFD calculations	
Design variables	Bays, Bilge_A, Bilge_B, d_C_Prismatic, d_LCB, Rows, Tiers_In
Investigated parameters	F_Drag_Model, Wetted_Surface_Full_Scale, Wetted_Surface_Model
Setup (preparation phase)	Sobol algorithm (300 design variants)
Setup (evaluation phase)	Sobol algorithm (30 design variants)
IMO second generation intact stability criteria	
Design variables	Acc_Pos, Bays, Bilge_A, Bilge_B, DB, d_C_Prismatic, d_LCB, Rows, Tiers_In, Tiers_On
Investigated parameters	EA_Criteria, PL_Criteria, PR_Criteria
Setup (preparation phase)	Sobol algorithm (300 design variants)
Setup (evaluation phase)	Sobol algorithm (30 design variants)
Uncertainty quantification	
Design variables	Bays, DB, Rows, Tiers_In, Tiers_On, Price_DO, Price_FO, Variance, V_S, V_Wind, W_Cont
Investigated parameters	Capacity_Ratio, EEDI_Ratio_10, R_Total, RFR, Stowage_Ratio
Setup (preparation phase)	Sobol algorithm (1000 design variants)
Setup (evaluation phase)	Sobol algorithm (100 design variants)

F_Drag_Model stands for the calm water resistance of the model scale version of the hull, Wetted_Surface_Full_Scale and Wetted_Surface_Model are the wetted surface values for the full scale and the model scale version of the hull respectively.

EA_Criteria, PL_Criteria and PR_Criteria stand for the examined IMO second generation intact stability criteria (excessive acceleration, pure loss of stability, parametric rolling) values; compliance with the rules provide a value of one for each parameter, whereas zero is provided for the opposite case.

Capacity_Ratio and Stowage_Ratio stand for the container capacity and stowage ratio of the design respectively; EEDI_Ratio_10 is the ratio of the attained to the required EEDI value, when the first implementation phase of the rule is taken into account (Table 8). R_Total stands for the total resistance of the ship (calm water, added wave, wind) and RFR is the required freight rate of the design.

Table 14: Uncertain parameters of the containership case study

Parameter	Probability distribution	Minimum value	Maximum value	Average value	Standard deviation
Price_DO	Normal	308.93	1058.2	721.67	200.52
Price_FO	Normal	188.18	759.61	488.81	149.83
Variance	Uniform	0.95	1.05	N/A	N/A
V_S	Uniform	18	22	N/A	N/A
V_Wind	Normal	0.00	70.95	11.97	4.27
W_Cont	Uniform	10	14	N/A	N/A

With regard to the uncertainty quantification setup, half of the design variables used for the construction of the surrogate model (Price_DO, Price_FO, Variance, V_S, V_Wind, W_Cont) are the identified uncertain parameters of the optimisation problem. They are also a subset of the secondary design variables mentioned in Table 11. During the uncertainty quantification run, taking place in the multi-objective optimisation phase, these design variables vary according to user-defined probability distributions. Details about the definition of these distributions for each uncertain parameter are found in Table 14. Variance is responsible for the variance

factor mentioned in Paragraph 4.6.3, which is used for the variation of uncertain parameters for which data are not available due to the investigated design stage. The number of scenarios examined for each design variant (as described in Paragraph 4.6.3) is set to 25.

The next step involves the multi-objective optimisation run. As mentioned in Section 4.7, NSGA 2 is utilised. Several parameters need to be specified before initiating the algorithm. These include the number of generations and the population size for each one, along with the mutation and cross-over operator values. In addition, the design variables and their limits are determined, while the objective functions and constraints applied to the problem are selected. This information can be found in Table 15, Table 16 and Table 17.

The optimal number of generations and population size depends on the examined optimisation problem. Taking into account the amount of time required to evaluate each design variant, as well as previous studies on a similar optimisation problem setup mentioned in the Research output Section of the thesis, the total number of generated designs is set to 1500. Deb et al. (2002) emphasise the efficiency of the NSGA 2 over other available algorithms, converging to a global optimum solution much faster. In addition, several combinations of number of generations and population size have been tested on a similar optimisation problem setup using the NSGA 2 (Priftis et al., 2018, Priftis et al., 2016). The results obtained from the various optimisation runs indicated that an increase on the number of generated designs does not improve the response of the optimal solution significantly.

The selected objective functions for the containership case study are the following:

- Calm water resistance difference between CFD and approximation methods
- Container capacity ratio
- RFR
- Container stowage ratio
- Total resistance

Table 15: NSGA 2 setup for the containership case study

Number of generations	125
Population size per generation	12
Mutation operator	0.1
Cross-over operator	0.9
Number of design variables	10
Number of objective functions	5
Number of constraints	6

Table 16: Design variables in the NSGA 2 setup for the containership case study

Design variable	Lower limit	Upper limit
Acc_Pos	4	5
Bays	15	20
Bilge_A	4.000	6.000
Bilge_B	4.000	6.000
DB	2.000	3.000
d_C_Prismatic	-0.02000	0.02000
d_LCB	-0.02000	0.02000
Rows	15	20
Tiers_In	8	10
Tiers_On	6	8

Table 17: Constraints in the NSGA 2 setup for the containership case study

Parameter	Constraint
EEDI_Ratio_10	≤ 1
EEDI_Ratio_10_Mean	≤ 1
FLD_Trim	≤ 0.5% L_{BP}
IS_Criteria	= 1 (pass)
IMO_SGIS_Criteria	= 1 (pass)
Structural_Analysis	= 1 (pass)

After the completion of the NSGA 2 run, the results of the optimisation are available to the user for post-processing. The Pareto front can be identified and the decision making process as described in Section 4.8 takes place.

The utility function (31) is formed after normalising the results of the NSGA 2. Normalisation of the data is required to make the comparison of the various objective functions possible (e.g. container capacity ratio, which varies between zero and one, cannot be compared with the total resistance, which can be around 2500 KN). The normalisation transforms all the data to values between zero and one. One represents the best response while zero represents the worst.

Three case scenarios are defined to identify the optimal design. In each scenario different weights are applied to each objective function, selected by the user. The scenarios are described in Table 18.

In the first scenario, all objective functions are considered equally important, while in the second and third scenario, specific objectives are assigned higher weights, acknowledging their significance over the remaining objective functions. In particular, in scenario 2 the objectives related to the resistance are assigned higher weights than the remaining measures of merit. Scenario 3 focuses on the financial

performance of the vessel, with the RFR and container stowage ratio being considered as the most important objectives. Nevertheless, different scenarios can be defined by the user depending on the preferences of the decision maker, using the same NSGA 2 results taken into account in this case study.

Table 18: Scenarios for the containership case study

Objective	Scenario 1	Scenario 2	Scenario 3
Calm water resistance difference between CFD and approximation methods (δ_R)	20%	35%	10%
Container capacity ratio (r_C)	20%	10%	10%
RFR	20%	10%	35%
Container stowage ratio (r_S)	20%	10%	35%
Total resistance (R_{Total})	20%	35%	10%

In the containership case study, instead of applying a linear utility function (as described in Section 3.6), the uncertainty of the problem is incorporated in the decision making process. During the uncertainty quantification computations, several scenarios are investigated for each design variant of the NSGA 2 run and the standard deviation and average value for the container capacity ratio, RFR, container stowage ratio and total resistance are calculated. A new parameter is introduced (30), which is defined as the ratio of the standard deviation over the average value for each of the aforementioned objectives.

$$\sigma_x = \frac{\text{Standard deviation}_x}{\text{Mean}_x} \tag{30}$$

x represents the objective function. Instead of taking the actual standard deviation of each objective into consideration, a "normalised" version is used to eliminate the numerical differences between the objective functions. For instance, the standard deviation for the container capacity ratio is significantly lower than the one for the

total resistance. The lower is the value of the "normalised" standard deviation for each objective function, the higher is the score achieved by the design variant, increasing its performance among the results and its probability of being identified as the optimal design.

$$U = w_{\delta_R} u(\delta_R) + w_{r_C} \sigma_{r_C} u(r_C) + w_{RFR} \sigma_{RFR} u(RFR) + w_{r_S} \sigma_{r_S} u(r_S) + w_{R_{Total}} \sigma_{R_{Total}} u(R_{Total}) \quad (31)$$

After the calculation of the utility function for each design variant, the results are sorted and the optimal design for the specific case scenario is identified.

5.3 Ro-Pax vessel case study

5.3.1 Challenges associated with Ro-Pax vessel design

Similar to the containership case study, a Ro-Pax vessel design is used to validate the proposed methodology. Ro-Pax and containerships share some design elements, however, their operational profile bears little resemblance. Ro-Pax vessels are designed to transport people and vehicles. The lightship-to-deadweight ratio is different to that of containerships'. A reduction in the steel weight can have a significant impact in the financial aspects associated with the production and operation of such a ship type. Reduction of the lightweight value can result in the decrease of the building cost and the RFR. Competitiveness is high in the Ro-Pax vessel industry, with each shipping company trying to achieve as low ticket prices as possible. The steel weight influences the total resistance and therefore the power requirements. Hence, the fuel consumption is closely related to the lightweight and the overall design of the ship.

Ro-Pax vessel design will be influenced in the near future by the introduction of the second generation intact stability criteria. Similar to containerships, Ro-Pax vessels are often associated with slender hull forms, low block and waterplane area

coefficient values, which affect the response of the hull to the newly developed intact stability criteria. This thesis aims to elaborate on how the former affect the design and operation of Ro-Pax vessels through an optimisation study which involves these criteria as part of the design constraints applied to the optimisation problem. Research involving the second generation intact stability criteria has only been carried out for other ship types. This thesis aims to provide an insight on which design elements affect the stability of this particular ship type with regard to the new criteria.

In addition, Ro-Pax vessels, contrary to containerships, have not been significantly affected by the slow steaming practice. Most vessels continue to operate on high speeds in order to remain competent within the market. However, fuel costs have been fluctuating in the recent years and an optimisation focusing on the efficiency of Ro-Pax vessels with regard to the resistance and required power can result in significant savings and fuel consumption reduction. The introduction of the EEDI had not affected the operation of passenger vessels until recently, when the rules were adjusted to incorporate this particular ship type. Power and speed of such vessels may need to be revised under the new regulations and a multi-objective design optimisation study incorporating the EEDI regulation as a design constraint can identify which designs comply with the new regulations, without losing points with regard to their efficiency.

A multi-objective design optimisation methodology incorporating factors such as resistance and the building cost, along with new constraints (such as newly introduced international regulations) and the effects of the uncertainty imposed by external factors becomes a valuable tool to naval architects whose objective is to produce efficient designs.

5.3.2 Optimisation problem setup

As with the containership case study, the setup of the problem begins with the hull design. As mentioned in Section 4.2, the geometric model is constructed in

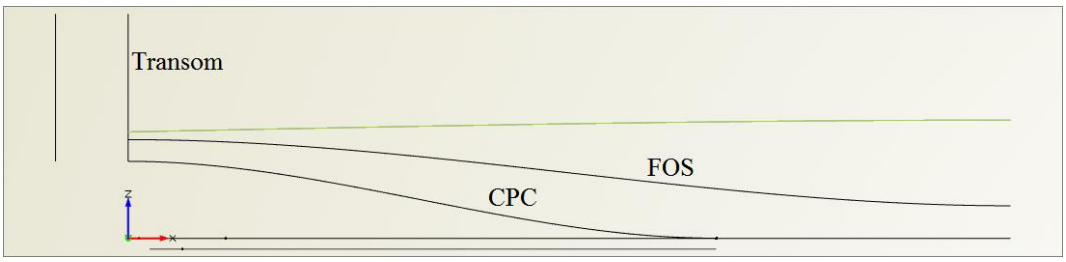

Figure 45: Ro-Pax vessel hull aft section curves (profile view)

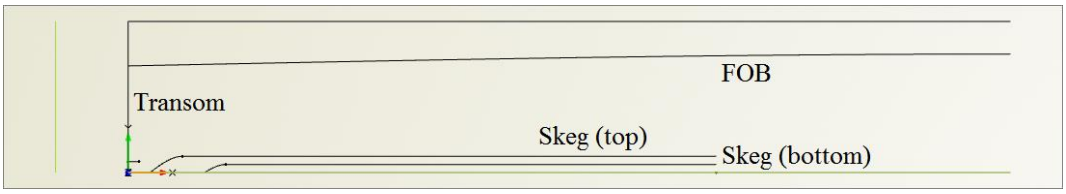

Figure 46: Ro-Pax vessel hull aft section curves (top view)

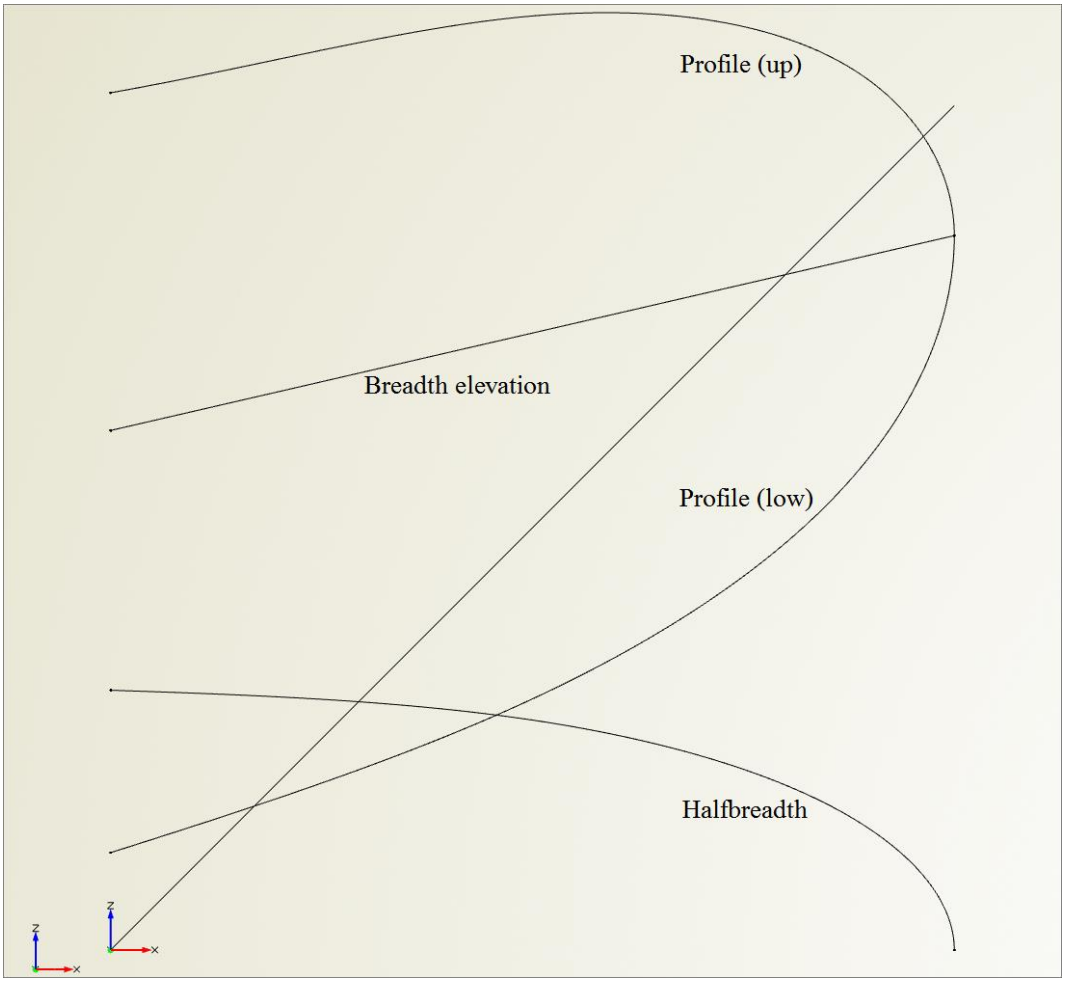

Figure 47: Bulbous bow curves

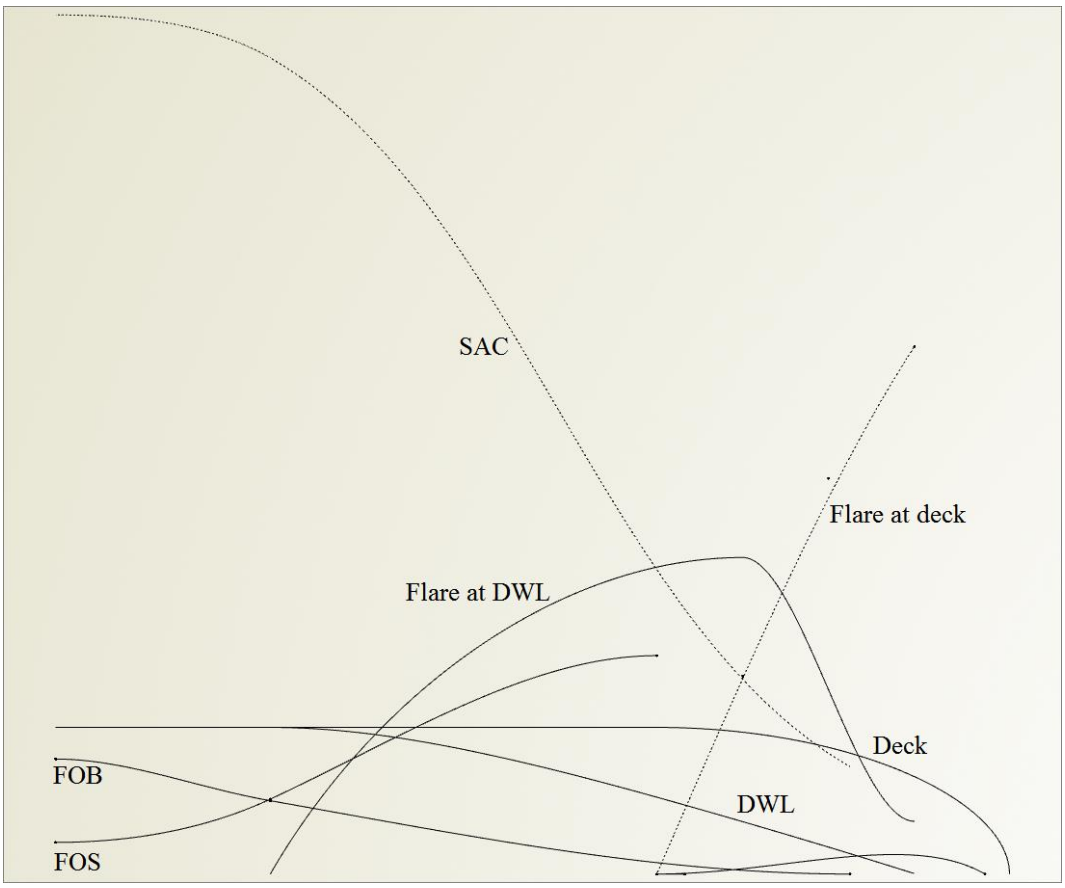

Figure 48: Ro-Pax vessel hull fore section curves

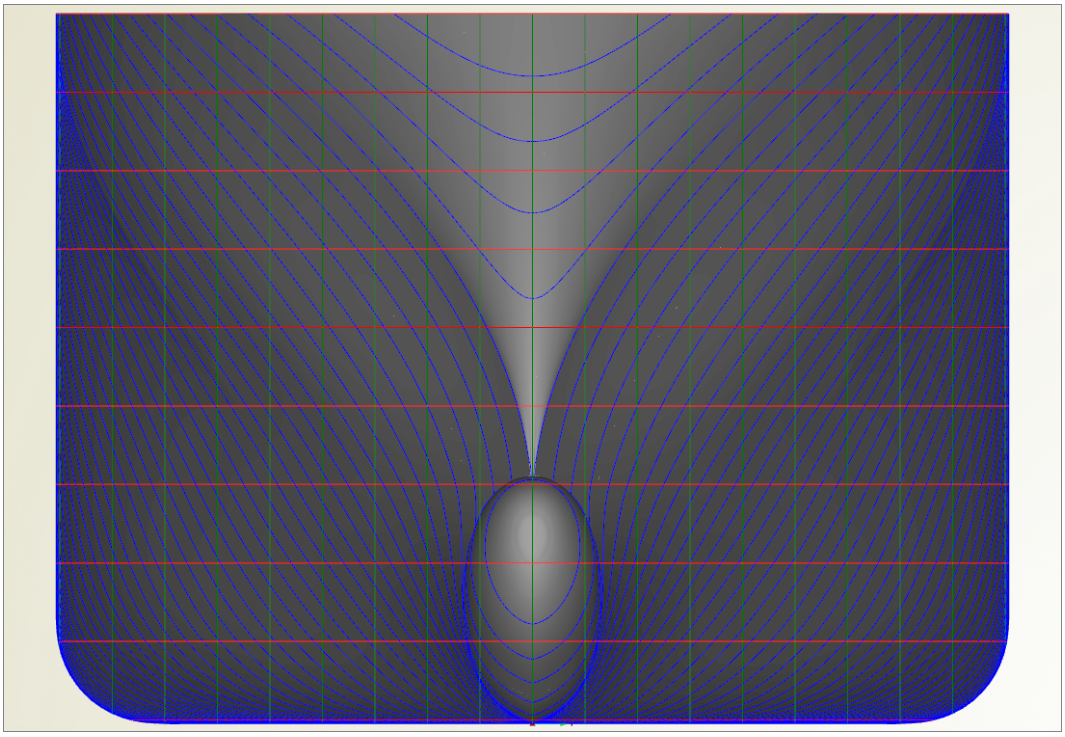

Figure 49: Ro-Pax vessel baseline model hull (body plan view)

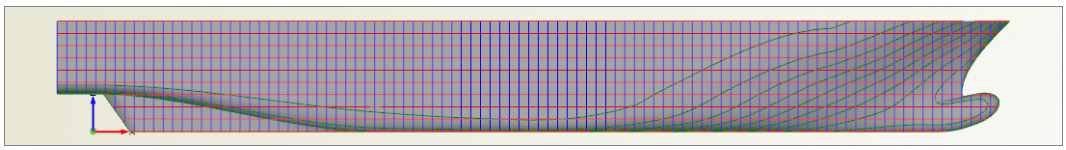

Figure 50: Ro-Pax vessel baseline model hull (profile view)

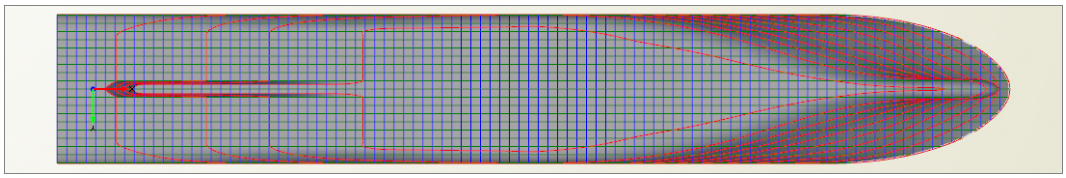

Figure 51: Ro-Pax vessel baseline model hull (top view)

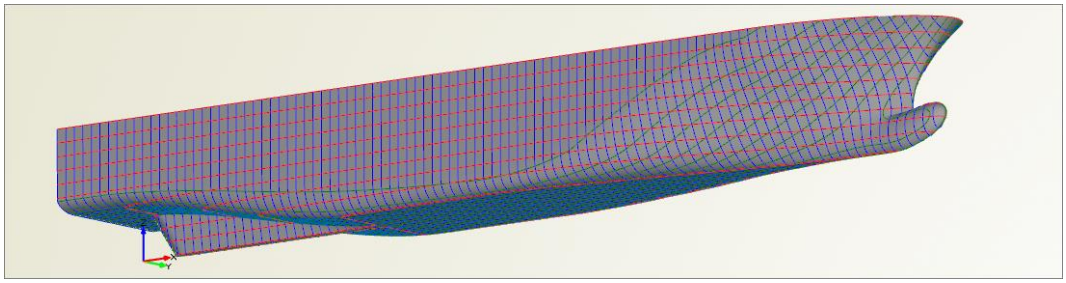

Figure 52: Ro-Pax vessel baseline model hull (perspective view)

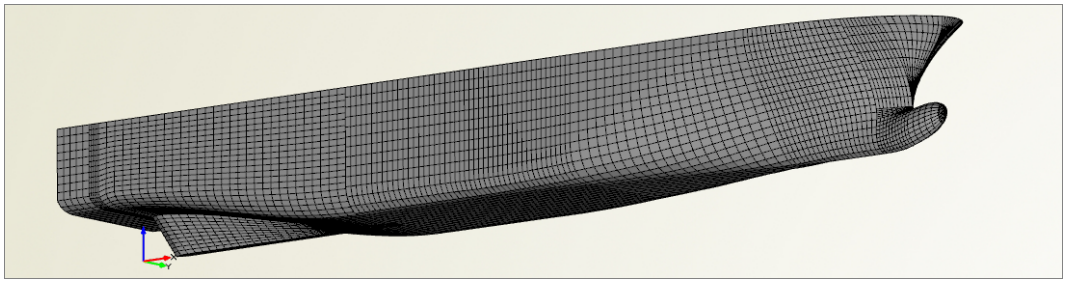

Figure 53: Ro-Pax vessel baseline model hull (panel mesh)

CAESES® and consists of four parts, the aft body, main frame, fore body and main deck (Figure 45, Figure 46, Figure 47 and Figure 48). The aft part contains the skeg and the transom, both controlled by a set of parameters. The main frame can also be adjusted to change the midship section coefficient. The fore body includes the bulbous bow whose shape can be manipulated by several parameters.

Several curve and surface definitions used to create the hull form are shared between the two case studies, underlining the versatility of the setup. It is the values assigned to the different parameters which define the final result, specific to the case study. In total, 98 parameters are introduced in the design of the Ro-Pax vessel hull within CAESES®. Examples of these parameters are given in Table 19.

The baseline geometric model for the Ro-Pax vessel case study produced in CAESES® is presented in Figure 49, Figure 50, Figure 51 and Figure 52, while a panel mesh of the hull surface used for some calculations involving the connection with Maxsurf® Stability is illustrated in Figure 53.

Table 19: Examples of Ro-Pax vessel hull definition parameters in CAESES®

Parameter	Explanation
B	Breadth
Bulb_Fairing_Spread_Factor	Fullness of the bulbous bow sections
Fullness	Fullness of the deck curve represented by an F-spline
Entrance_Angle	Entrance angle of the DWL
At_Bulb_Tip	Flare of the hull surface at the bulb area close to the baseline
At_Peak	Flare of the fore part of the hull surface close to the deck line
At_FP	Flare of the hull surface at the DWL
FOB_Mid	Y-coordinate of the middle point used to define the fore part of the FOB
Rel_X_FOS_Emerge	X-coordinate of the middle point used to define the fore part of the FOS
Coefficient_At_FOS_Emerge	Fullness of the transverse sections of the fore part of the hull

At this stage, the design variables of the optimisation problem are selected. As in the containership case study, an overall hull design optimisation procedure is selected to be performed; hence parameters controlling the main particulars are appointed as

design variables. Ten design variables are defined for that purpose and their values will be varying during the optimisation phase. The explanation of each design variable is given in Table 20. Similar to the containership case study, the amount of design variables selected for the optimisation setup is kept low, focusing on the ones affecting the main dimensions of the vessel to reduce the required amount of design variants during the optimisation run.

Apart from the main design variables of the problem, secondary design variables are defined, which are related to the operational profile of the ship. The majority of these design variables are identified as the uncertain parameters of the problem and play a major role in the uncertainty quantification process (Table 21).

The values selected for the parameters displayed in Table 21 derive from several sources, similar to the containership case study. Based on the schedule of similar sized Ro-Pax vessels in the Mediterranean Sea, a route between the port of Piraeus and the island of Crete is taken into account. Round trip distance is about 366 nm.

The corresponding number of port calls, along with an average time of the ship moored at the various ports is used as input in the case study. The average price of diesel (MDO) and fuel (IFO 380) oil are used as input (Bunker Index, 2018). Based on the operational speed of vessels in that route, a mean value is used for the case study. Moreover, historical weather data are used to define the average wind speed in the areas matching the operational profile of the case study (NOAA, 2018).

A Lackenby transformation takes place to adjust the overall hull form through the design variables `d_C_Prismatic` and `d_LCB` mentioned in Table 20. Following the parametric hull form definition in CAESES®, the construction of the ship model in NAPA® takes place. Within NAPA®, 55 additional parameters are introduced, all relevant to specific calculations performed by macros. Although the user has access to these parameters, specific values are assigned remaining constant throughout the optimisation phase. Examples of these parameters are given in Table 22.

Table 20: Main set of design variables selected for the Ro-Pax vessel case study

Design variable	Baseline value	Explanation
Bilge_A	3	Y-coordinate of the bilge radius (m)
Bilge_B	3	Z-coordinate of the bilge radius (m)
DB	1.5	Double bottom height (m)
Deck_No_Pax	5	Number of superstructure decks
Deck_No_RoRo	2	Number of ro-ro decks
Draught	7.1	Design draught (m)
d_C_Prismatic	0	Percentage change of the prismatic coefficient (Lackenby transformation parameter)
d_LCB	0	Percentage change of the LCB (Lackenby transformation parameter)
Lane_No	8	Number of car lanes
L_BP	162.85	Length between perpendiculars (m)

Table 21: Secondary set of design variables selected for the Ro-Pax vessel case study

Design variable	Baseline value	Explanation
Distance	366	Round trip distance (nm)
Port_No	1	Number of port calls
Port_Time	1.5	Time spent at port (h)
Price_DO	721.67	Diesel oil price ($/t)
Price_FO	488.81	Fuel oil price ($/t)
V_S	27	Ship speed (Knots)
V_Wind	11.08	Wind speed (Knots)

Table 22: Examples of Ro-Pax vessel model parameters in NAPA®

Parameter	Explanation
V.S.Low	Ship speed during port operation (expressed as a percentage of the ship speed)
C.AA	Coefficient related to the calculation of the wind resistance component
N.S	Shaft efficiency
SFOC.AE	Specific fuel oil consumption for the auxiliary engine
F.Com	Complexity index (according to (Guarin, 2007))

The definition of the ship model is carried out according to the steps outlined in Section 4.3. The baseline ship model for the Ro-Pax vessel case study is presented in Figure 54. The various colours represent the purpose of each room. For instance, green stands for the water ballast tanks, while pink is used for the ro-ro decks.

The process continues with the definition of the objective functions. The calculations mentioned in Section 4.4 take place. As far as the RFR estimation is concerned, different methods are used, depending on the ship type, as mentioned in Paragraph 5.2.2. In the Ro-Pax vessel case study, RFR is calculated based on the total cost associated with the ship's lifetime, according to (Guarin, 2007). In particular, the total cost is divided into the initial and running cost. On the other hand, earning is divided into on-board, sale/decommissioning, passenger and vehicle (Figure 55).

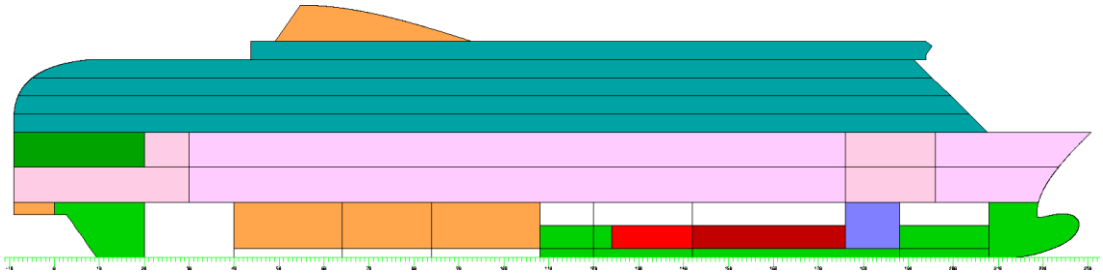

Figure 54: Ro-Pax vessel baseline ship model defined in NAPA®

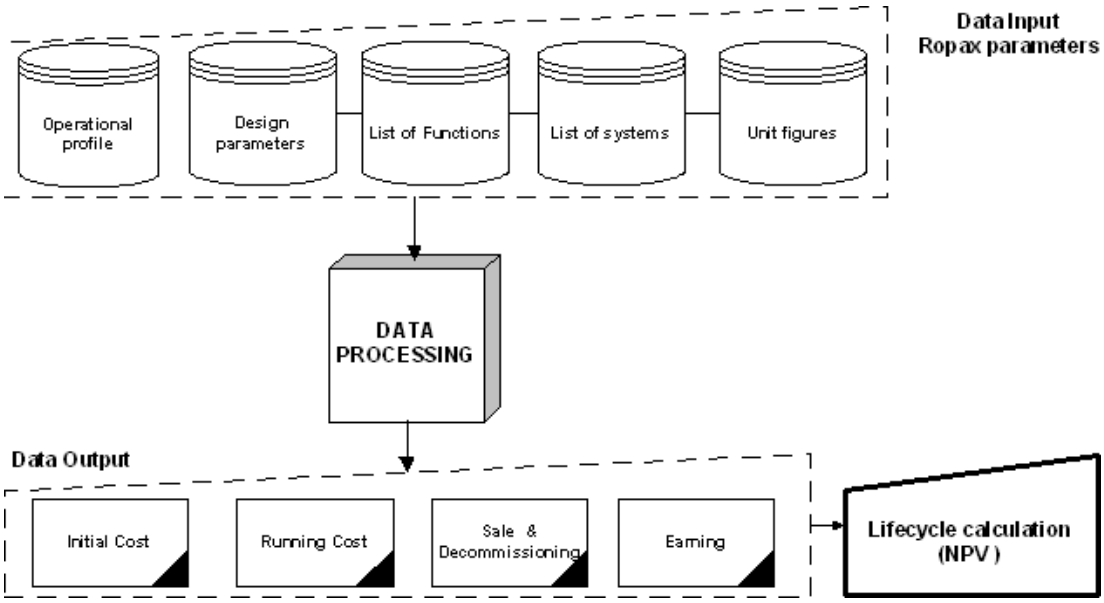

Figure 55: Cost model for Ro-Pax vessels (Guarin, 2007)

As mentioned in Paragraph 4.4.3, relations are defined between the different rates with regard to the passenger and vehicle tickets in form of parameters controlled by the user in order to simplify the computation. The same principle is applied to the different time periods of operation (i.e. high and low season), during which the prices can fluctuate, providing a more accurate value for the RFR. The relations are expressed as percentages of the base fare. In particular, in this case study, the economy passenger ticket for the middle season is considered the base fare. Based on the ticketing policy adopted by shipping companies operating in the selected route, the remaining ticket categories (e.g. passenger cabin, car, lorry) for the low and high seasons are expressed as percentage of the base fare. Therefore, the price of the ticket for a passenger cabin is considered to be 2.32 times the price of the base fare, while the economy passenger ticket price for the high season is considered to be 18% higher than the one for the middle season. As a result, the RFR calculation corresponds to the base fare for that route.

The load factors for each season for both passengers and vehicles, as well as the duration of each season are also controlled by the user through a set of parameters in a similar way.

The approach described above results in a detailed calculation of the RFR for the Ro-Pax vessel case study, keeping the complexity of the process low at the same time.

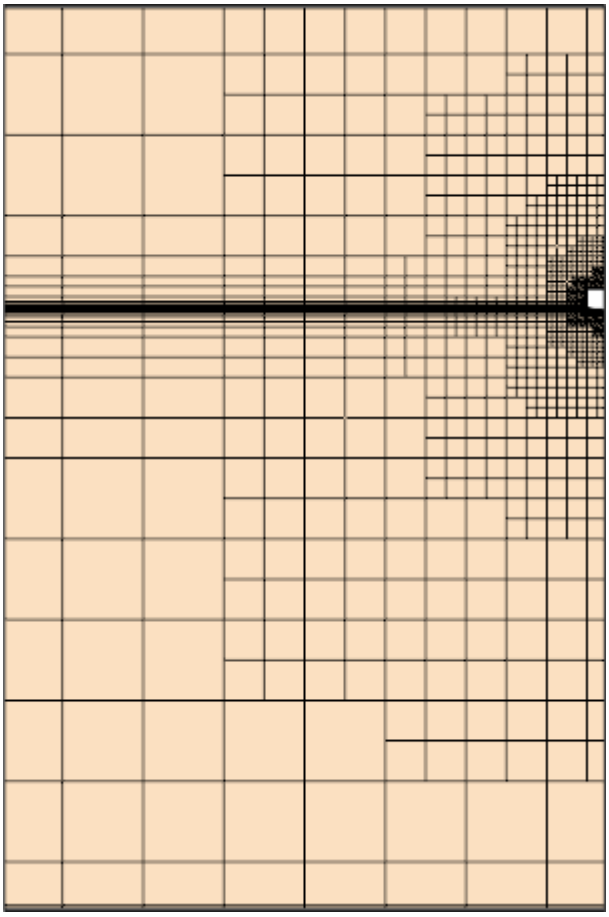

Figure 56: Generated mesh of the Ro-Pax vessel baseline model in Star-CCM+®

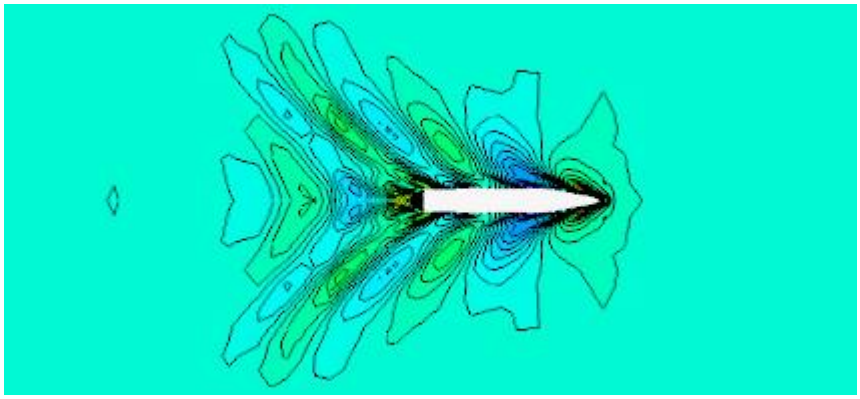

Figure 57: Wave elevation of the Ro-Pax vessel baseline model in Star-CCM+®

As far as the calm water resistance CFD calculation setup is concerned, the CAESES® feature mentioned in Paragraph 4.4.5 is defined accordingly to produce the necessary input for the Star-CCM+® operations. The generated mesh and the wave elevation measurement during the CFD runs of the baseline model of the Ro-Pax vessel case study are presented in Figure 56 and Figure 57 respectively.

Table 23: Surrogate model setups for the Ro-Pax vessel case study

Calm water resistance CFD calculations	
Design variables	Bilge_A, Bilge_B, Draught, d_C_Prismatic, d_LCB, Lane_No, L_BP
Investigated parameters	F_Drag_Model, Wetted_Surface_Full_Scale, Wetted_Surface_Model
Setup (preparation phase)	Sobol algorithm (300 design variants)
Setup (evaluation phase)	Sobol algorithm (30 design variants)
IMO second generation intact stability criteria	
Design variables	Bilge_A, Bilge_B, DB, Deck_No_Pax, Deck_No_RoRo, Draught, d_C_Prismatic, d_LCB, Lane_No, L_BP
Investigated parameters	EA_Criteria, PL_Criteria, PR_Criteria
Setup (preparation phase)	Sobol algorithm (300 design variants)
Setup (evaluation phase)	Sobol algorithm (30 design variants)
Uncertainty quantification	
Design variables	Deck_No_Pax, Deck_No_RoRo, Draught, Lane_No, L_BP, Price_DO, Price_FO, Variance, V_S, V_Wind
Investigated parameters	C_Building, EEDI_Ratio_5, R_Total, RFR
Setup (preparation phase)	Sobol algorithm (1000 design variants)
Setup (evaluation phase)	Sobol algorithm (100 design variants)

Following the definition of all the necessary computations, several designs of experiment take place for the construction of the surrogate models mentioned in Section 4.6. Following an analysis of the designs of experiment conducted to identify which design variables influence the particular calculations the most, the setups are defined for the construction of the surrogate models for the calm water resistance CFD calculations, IMO second generation intact stability criteria and uncertainty quantification. The design variables, monitored parameters, number of design variants generated during the preparation and evaluation phases –as described in Section 4.6– are provided in Table 23.

`F_Drag_Model` stands for the calm water resistance of the model scale version of the hull, `Wetted_Surface_Full_Scale` and `Wetted_Surface_Model` are the wetted surface values for the full scale and the model scale version of the hull respectively.

`EA_Criteria`, `PL_Criteria` and `PR_Criteria` stand for the examined IMO second generation intact stability criteria (excessive acceleration, pure loss of stability, parametric rolling) values; compliance with the rules provide a value of one for each parameter, whereas zero is provided for the opposite case.

`C_Building` stands for the building cost of the vessel, while `EEDI_Ratio_5` is the ratio of the attained to the required EEDI value, when the first implementation phase of the rule is taken into account (Table 8). `R_Total` stands for the total resistance of the ship (calm water, added wave, wind) and `RFR` is the required freight rate of the design.

With regard to the uncertainty quantification setup, half of the design variables used for the construction of the surrogate model (`Price_DO`, `Price_FO`, `Variance`, `V_S`, `V_Wind`) are the identified uncertain parameters of the optimisation problem. They are also a subset of the secondary design variables mentioned in Table 21. During the uncertainty quantification run, taking place in the multi-objective optimisation phase, these design variables vary according to user-defined probability

distributions. Details about the definition of these distributions for each uncertain parameter are found in Table 24. `Variance` is responsible for the variance factor mentioned in Paragraph 4.6.3, which is used for the variation of uncertain parameters for which data are not available due to the investigated design stage. The number of scenarios examined for each design variant (as described in Paragraph 4.6.3) is set to 25, same with the containership case study.

Table 24: Uncertain parameters of the Ro-Pax vessel case study

Parameter	Probability distribution	Minimum value	Maximum value	Average value	Standard deviation
`Price_DO`	Normal	308.93	1058.2	721.67	200.52
`Price_FO`	Normal	188.18	759.61	488.81	149.83
`Variance`	Uniform	0.95	1.05	N/A	N/A
`V_S`	Uniform	25	29	N/A	N/A
`V_Wind`	Normal	0.00	34.50	11.08	4.79

Table 25: NSGA 2 setup for the Ro-Pax vessel case study

Number of generations	125
Population size per generation	12
Mutation operator	0.1
Cross-over operator	0.9
Number of design variables	10
Number of objective functions	5
Number of constraints	5

The next step involves the multi-objective optimisation run. As mentioned in Section 4.7, NSGA 2 is utilised. Several parameters need to be specified before initiating the

algorithm. These include the number of generations and the population size for each one, along with the mutation and cross-over operator values. In addition, the design variables and their limits are determined, while the objective functions and constraints applied to the problem are selected. This information can be found in Table 25, Table 26 and Table 27.

Table 26: Design variables in the NSGA 2 setup for the Ro-Pax vessel case study

Design variable	Lower limit	Upper limit
Bilge_A	2.000	4.000
Bilge_B	2.000	4.000
DB	0.760	2.000
Deck_No_Pax	4	6
Deck_No_RoRo	2	3
Draught	5.000	9.000
d_C_Prismatic	-0.02000	0.02000
d_LCB	-0.02000	0.02000
Lane_No	6	10
L_BP	150.000	180.000

Similar to the containership case study, the amount of generations and population size is selected, taking the time required to evaluate each design variant and the high efficiency of NSGA 2 into consideration. 1500 designs are generated in total for the Ro-Pax vessel case study.

The selected objective functions for the Ro-Pax vessel case study are the following:

- Building cost

- Calm water resistance difference between CFD and approximation methods
- RFR
- Total Resistance
- Uncertainty indicator for the investigated objective functions (building cost, RFR, total resistance)

The last objective in the aforementioned list is defined in a similar way uncertainty is addressed in the decision making phase in the containership case study. Here, uncertainty is treated as a measure of merit, taken into consideration in the optimisation process.

Table 27: Constraints in the NSGA 2 setup for the Ro-Pax vessel case study

Parameter	Constraint
`EEDI_Ratio_5`	≤ 1
`EEDI_Ratio_5_Mean`	≤ 1
`FLD_Trim`	$\leq 0.5\%\ L_{BP}$
`IS_Criteria`	= 1 (pass)
`IMO_SGIS_Criteria`	= 1 (pass)

During the uncertainty quantification computations, several scenarios are investigated for each design variant of the NSGA 2 run and the standard deviation and average value for the building cost, RFR and total resistance of the vessel are calculated. A parameter similar to the one presented in (30) is introduced, which is defined as the ratio of the standard deviation over the average value for each of the aforementioned objectives. An approach similar to the one followed in the containership case study is adopted; instead of taking the actual standard deviation of each objective into consideration, a "normalised" version is used to eliminate the numerical differences between the objective functions.

The sum of the "normalised" standard deviations forms the uncertainty-related performance indicator for the Ro-Pax vessel case study. The minimisation of this indicator is desired, since this leads to the production of a robust design which is not affected by the uncertain external parameters of the problem and its performance with regard to the investigated objective functions does not deviate in the 25 scenarios examined during the NSGA 2 run.

After the completion of the NSGA 2 run, the results of the optimisation are available to the user for post-processing. The Pareto front can be identified and the decision making process as described in Section 4.8 takes place.

The utility function (32) is formed after normalising the results of the NSGA 2. Normalisation of the data is required to make the comparison of the various objective functions possible, as in the containership case study. The normalisation transforms all the data to values between zero and one. One represents the best response while zero represents the worst.

Three case scenarios are defined to identify the optimal design. In each scenario different weights are applied to each objective function, selected by the user. The scenarios are described in Table 28.

Table 28: Scenarios for the Ro-Pax vessel case study

Objective	Scenario 1	Scenario 2	Scenario 3
Building cost (C_B)	20%	10%	25%
Calm water resistance difference between CFD and approximation methods (δ_R)	20%	35%	12.5%
RFR	20%	10%	25%
Total resistance (R_{Total})	20%	10%	25%
Uncertainty indicator for the investigated objective functions (C_B, RFR, R_{Total}) (i_U)	20%	35%	12.5%

In the first scenario, all objective functions are considered equally important, while in the second and third scenario, specific objectives are assigned higher weights, acknowledging their significance over the remaining objective functions. In particular, in scenario 2 the objectives related to the uncertainty of the problem are assigned higher weights than the remaining measures of merit. On the other hand, scenario 3 focuses on the financial performance of the vessel, assigning lower weight to the uncertainty indicators. Nevertheless, different scenarios can be defined by the user depending on the preferences of the decision maker, using the same NSGA 2 results taken into account in this case study.

$$U = w_{C_B} u(C_B) + w_{\delta_R} u(\delta_R) + + w_{RFR} u(RFR) + w_{R_{Total}} u(R_{Total}) + w_{i_U} u(i_U) \quad (32)$$

In the Ro-Pax vessel case study, a linear utility function is applied (as described in Section 3.6), with each weight mentioned in Table 28 being applied to each objective function. After the calculation of the utility function for each design variant, the results are sorted and the optimal design for the specific case scenario is identified.

5.4 Summary

The verification of the proposed methodology through its implementation on two different case studies –involving a containership and a Ro-Pax vessel, respectively– is presented in this Chapter. The input and output data, design variables, parameters, measure of merit functions and constraints as described with regard to their general definition in Section 3.3 are set for each case study.

The methodology described in detail in Chapter 4 is flexible and can be applied to different ship types. Each of the two demonstrations deals with a different ship type, as well as different design variables and objective functions. In addition, the concept of uncertainty quantification is treated differently in both cases. In the containership case study, uncertainty plays a major role in the decision making phase, affecting the identification and selection of the optimal design. The optimisation process is based on a deterministic model and the objective functions are calculated omitting the

effects of the uncertain parameters. However, the same performance indicators are calculated for several scenarios, during which a probabilistic model is evaluated by varying the identified uncertain parameters of the problem. The standard deviation and mean value of the results for each performance indicator are calculated and incorporated in the utility function formed during the decision making phase. Along with the weighting factors defined by the user, a non-linear utility function is utilised, sorting the optimisation results to identify the optimal design. This process takes into account the level of robustness of each design variant and promotes designs characterised by low standard deviation of the examined performance indicators. In other words, the decision making process favours robust designs, whose performance does not deviate from the mean value during the evaluation of the probabilistic model.

On the contrary, uncertainty in the Ro-Pax vessel case study is treated as an objective function. In particular, the indicators used to quantify the uncertainty level of each design are defined as in the containership case study; however, their sum becomes an objective function which is minimised during the optimisation phase. The lower is the attained value for the uncertainty indicator, the lower the deviation of the performance of the design from the mean response during the evaluation of the probabilistic model. Therefore, through its elitist nature, the genetic algorithm utilised during the optimisation process promotes the most robust designs in each generation, resulting in an optimal set of design variants (Pareto front), for which the highest robustness levels are ensured.

The setup presented in this Chapter allows the implementation of the simulation runs which provide the optimisation results presented in Chapter 6.

6 Results

6.1 Introduction

The results of the implementation of the methodology described in Chapter 4 for the case studies presented in Chapter 5 are illustrated in this Chapter. An extensive set of graphs and tables are provided for each case study, demonstrating the outcome of the multi-objective optimisation of a ship design at its concept stage involving the utilisation of surrogate models. Information about the baseline model response is provided, while the results of the multi-criteria decision analysis are discussed.

The effects of the utilisation of surrogate models throughout the optimisation process are demonstrated in this Chapter. The required time for the optimisation run and the accuracy of the results associated with the surrogate models are discussed in the relevant Paragraphs. Furthermore, the consideration of uncertainty in the overall process is evaluated. The effects of uncertainty are presented, while the two utilised methods for the incorporation in the methodology are demonstrated in this Chapter. Finally, the results regarding the examined objective functions and design constraints are evaluated for each case study. The consideration of new regulations and their impact on the identification of the optimal design are demonstrated through the obtained results.

6.2 Containership case study

6.2.1 Baseline model

The baseline model for the containership case study is presented in Paragraph 5.2.2. Table 10 and Table 11 present the design variables' values used to define the model.

Its performance with regard to the examined objective functions is presented in Table 29.

Table 29: Baseline containership model response to objective functions

Objective	Baseline
Calm water resistance difference between CFD and approximation methods (δ_R) (KN)	123
Container capacity ratio (r_C)	1.0000
RFR ($/TEU)	935.29
Container stowage ratio (r_S)	0.9423
Total resistance (R_{Total}) (KN)	2233

6.2.2 Surrogate models

As mentioned in Paragraph 5.2.2, three surrogate models are created for the containership case study. In this Paragraph, the analysis of the results related to the preparation and the evaluation of these surrogate models is presented.

The design of experiment run using the Sobol algorithm to define the surrogate model allows the designer to identify how each of the design variables influences the evaluated parameters. The Pearson correlation coefficient (33) is used to determine the strength of the relationship between two selected variables (Doyle, 2011). The coefficient ranges from -1 to 1, where -1 is total negative linear correlation, 0 is no linear correlation and 1 is total positive linear correlation.

$$\rho_{X,Y} = \frac{\mathrm{cov}(X,Y)}{\sigma_X \sigma_Y} \tag{33}$$

where ρ is the Pearson correlation coefficient, X, Y are the examined variables, $cov(X,Y)$ is the covariance and σ_X, σ_Y is the standard deviation of X and Y respectively.

- Calm water resistance CFD calculations:

For the generation of the calm water resistance CFD calculations surrogate model, a subset of the main design variables of the optimisation problem –presented in Table 10– is used. As expected, the design variables affecting the main particulars of the ship influence calm water resistance results the most. Number of rows (associated with the breadth of the hull), number of tiers below the main deck (associated with the depth and draught of the vessel) and number of bays (associated with the length of the ship) have a correlation coefficient of 0.81, 0.45 and 0.22 respectively. Therefore, all three design variables result in calm water resistance increase. Resistance is directly related to the wetted surface of the hull; increase of the latter results in higher values for the former. An increase in either of the aforementioned design variables leads to higher values for the wetted surface. Hence, the proportional relation between calm water resistance and the main particulars of the vessel is expected.

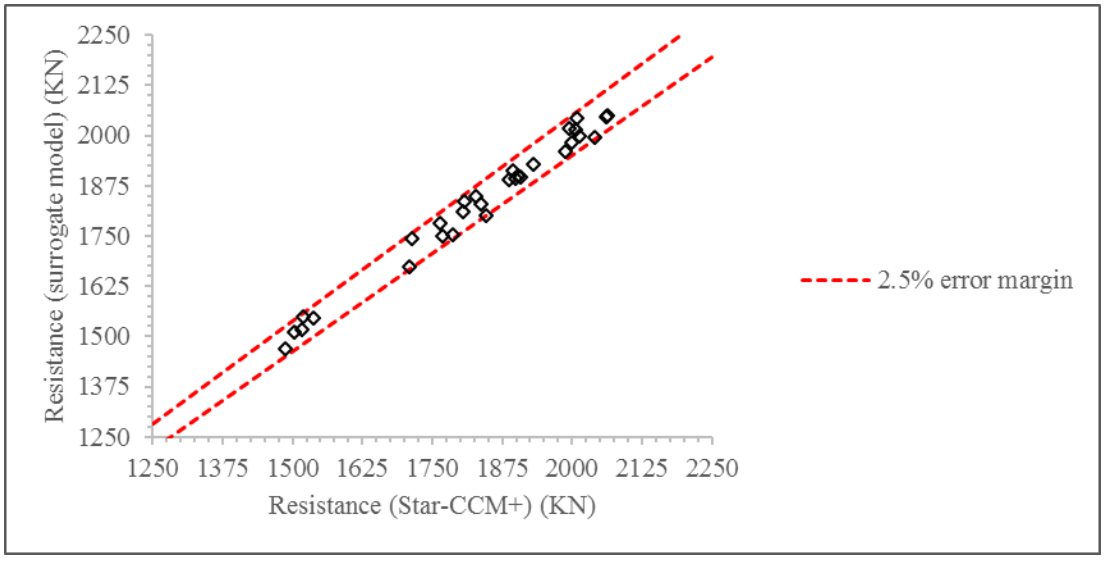

Figure 58: Evaluation of the calm water resistance CFD calculations surrogate model for the containership case study

The evaluation phase of the surrogate model following its generation is crucial to identify its accuracy. A new design of experiment is run, generating a new set of design variants to compare the response of the surrogate model with the actual CFD simulations. Figure 58 shows the comparison results; the red dashed line shows an error margin of 2.5%. All in all, the surrogate model performs adequately for the generated design variants.

As far as the computational time savings are concerned, a considerable decrease in the evaluation of the calm water resistance is achieved through this approach which is greatly reflected in the overall optimisation process. As mentioned in Paragraph 4.6.1, around thirty minutes are required for a CFD simulation of a single design variant. On the other hand, the evaluation of the surrogate model lasts one second per design variant, making the surrogate model 1800 times faster than the CFD simulations. This proves the advantage of surrogate model utilisation over the actual use of high-fidelity tools, considering the achieved accuracy levels. The overall time required for the completion of all three phases (preparation, generation, evaluation) related to the surrogate model definition is 165 hours.

- IMO second generation intact stability criteria:

As far as the IMO second generation intact stability criteria surrogate model is concerned, the main design variables of the optimisation problem –presented in Table 10– are used for its generation. All ten parameters influence the success rate of the generated design variants with regard to meeting the criteria or not to some extent. An increase in the number of rows has a positive impact to the compliance with the criteria, as the correlation coefficient for this design variable is found to be 0.16.

On the other hand, the increase in the number of tiers below and above the main deck, as well as the shifting of the deckhouse towards the bow have a negative impact; the correlation coefficient for these design variables are -0.29, -0.11 and -0.12 respectively. An increase in the value of these design variables results in rule

violation. Even small variations in these parameters can cause significant changes in the loading condition and the centre of gravity of transported cargo. Therefore the stability of the ship is affected

The evaluation phase of the surrogate model following its generation is crucial to identify its accuracy. A new design of experiment is run, generating new design variants to compare the response of the surrogate model with the actual computation regarding the evaluation of the IMO second generation intact stability criteria. Figure 59 presents the results of this comparison. The surrogate model performs adequately well, matching the results of the actual computation in each examined case. The attained value of one denotes compliance with the examined criteria, whereas zero denotes the opposite.

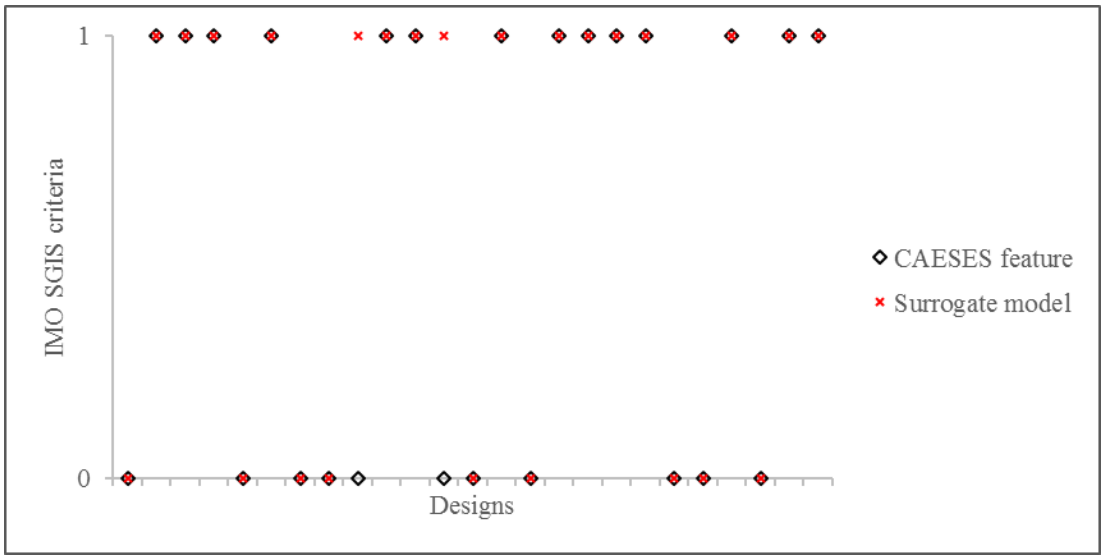

Figure 59: Evaluation of the IMO second generation intact stability criteria surrogate model for the containership case study

Similar to the calm water resistance CFD calculations surrogate model, the decrease in the time required to obtain results for a single design variant is significant; a simulation using the defined CAESES® feature to identify the compliance with the examined IMO second generation intact stability criteria requires fifteen minutes, whereas the evaluation of the surrogate model requires a couple of seconds, making it 450 times faster than the actual simulation. This difference is greatly amplified in

the main optimisation run, during which 1500 designs are evaluated. The overall time required for the completion of all three phases (preparation, generation, evaluation) related to the surrogate model definition is 82.5 hours.

- Uncertainty quantification:

The third surrogate model defined for the containership case study is the one related to the uncertainty quantification. For its generation, eleven design variables are used; five main design variables of the optimisation problem and six uncertain design variables (Table 10 and Table 14). As mentioned in Table 13, five uncertain parameters are evaluated, namely the capacity ratio, $EEDI_{10}$ ratio, RFR, total resistance and stowage ratio.

The correlation coefficient is calculated for each evaluated parameter to identify which design variables influence these parameters the most. The most important design variables are shown in Table 30.

Table 30: Correlation coefficients for the uncertainty quantification surrogate model for the containership case study

Evaluated parameter	Design variables
Capacity ratio	`Bays` (-0.44), `Variance` (-0.15), `W_Cont` (-0.53)
$EEDI_{10}$ ratio	`Rows` (0.17), `Tiers_In` (-0.52), `Variance` (0.67)
RFR	`Price_FO` (0.46), `Variance` (0.68), `W_Cont` (0.31)
Total resistance	`Rows` (0.16), `Tiers_In` (0.76), `Variance` (0.57)
Stowage ratio	`Tiers_In` (-0.67), `Tiers_On` (0.71)

The uncertain design variables affect all the objective functions except for the stowage ratio. `W_Cont` influences particularly the capacity ratio. The higher is the homogeneous weight of each TEU; the lower is the achieved capacity ratio. This

trend is expected as increased TEU weight values inhibit the stowage of many containers above the main deck due to stability reasons. RFR is affected mainly by the uncertain parameters. In particular, `Price_FO`, `Variance` and `W_Cont` are all proportionally relative to RFR; increase in the value of any of these design variables leads to increased RFR values. Higher oil price results in higher operating cost; increased homogeneous weight of each TEU results in smaller amount of containers transported. Both lead to an increase of the RFR. Finally, stowage ratio is mainly influenced by the number of tiers below and above the main deck, since its definition is directly related to the amount of containers stored on deck and in holds.

The accuracy of the generated surrogate models for each evaluated parameter is presented in Figure 60, Figure 61, Figure 62, Figure 63 and Figure 64. In general, the results fall within the 2.5% error margin lines illustrated in the graphs. No major discrepancies are identified in the evaluation process which proves the suitability of the Kriging method for the generation of the uncertainty quantification surrogate model. Despite the low error margin values obtained through this setup, the uncertainty associated with the use of some models and methods in NAPA® (e.g. Holtrop and Mennen method) is not analysed.

The evaluation of the surrogate model responsible for the uncertainty quantification takes about a second for each evaluated parameter –five seconds for the evaluation of all five uncertain parameters. The same process takes around a minute to be completed when the NAPA® macros are run. Although the time difference in this case, compared to the aforementioned surrogate models for the containership case study, is considerably smaller for a single evaluation round, it becomes more significant when the uncertainty quantification process takes place in the main optimisation phase. 25 evaluations need to take place for the setup presented in Paragraph 5.2.2. Therefore, the utilisation of a surrogate model results in a time saving of around twenty minutes per design variant, being twelve times faster than the full NAPA® computations. The overall time required for the completion of all three phases (preparation, generation, evaluation) related to the surrogate model definition is 18 hours.

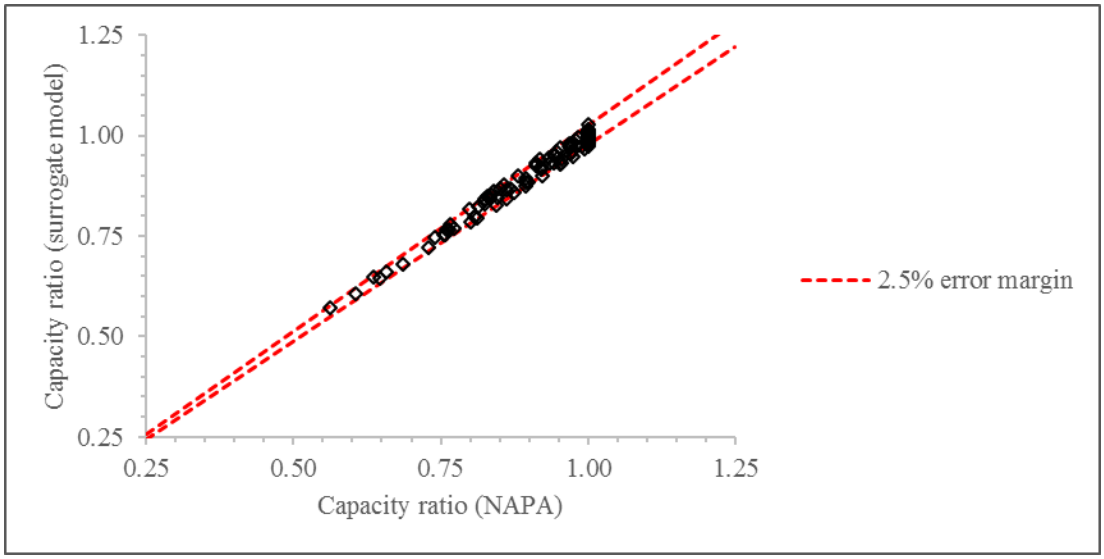

Figure 60: Evaluation of the uncertainty quantification (capacity ratio) surrogate model for the containership case study

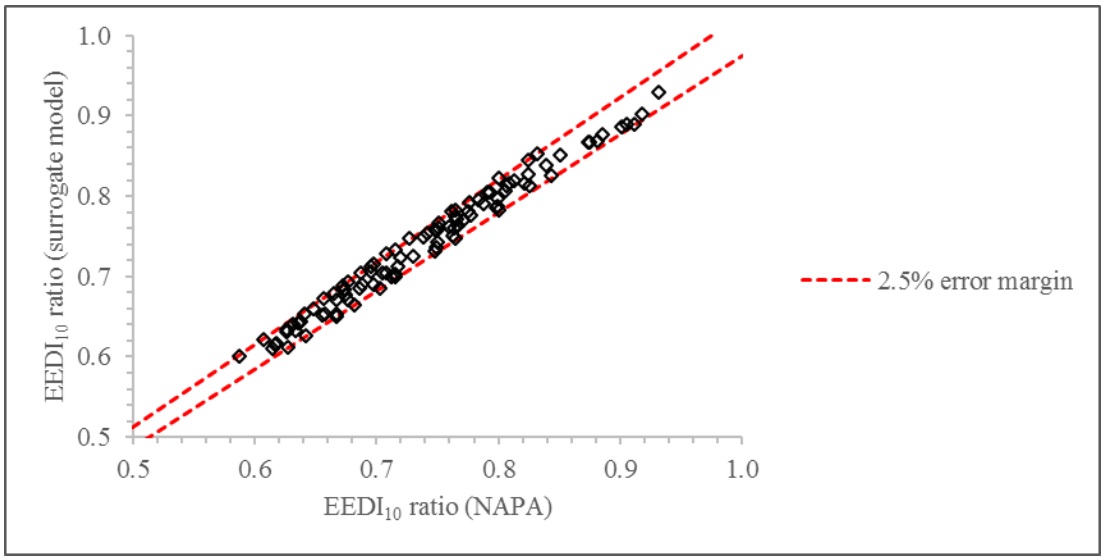

Figure 61: Evaluation of the uncertainty quantification ($EEDI_{10}$ ratio) surrogate model for the containership case study

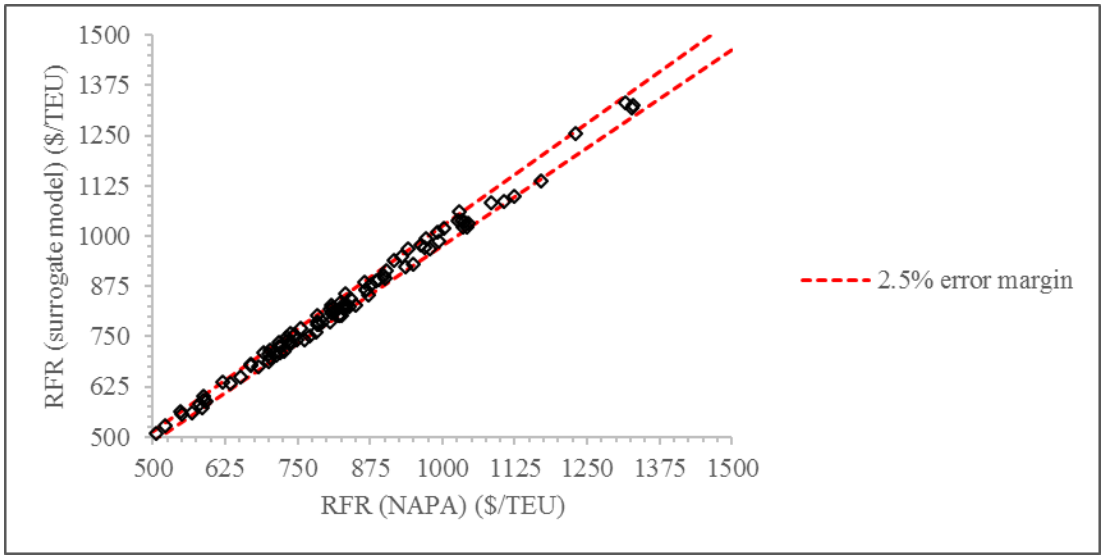

Figure 62: Evaluation of the uncertainty quantification (RFR) surrogate model for the containership case study

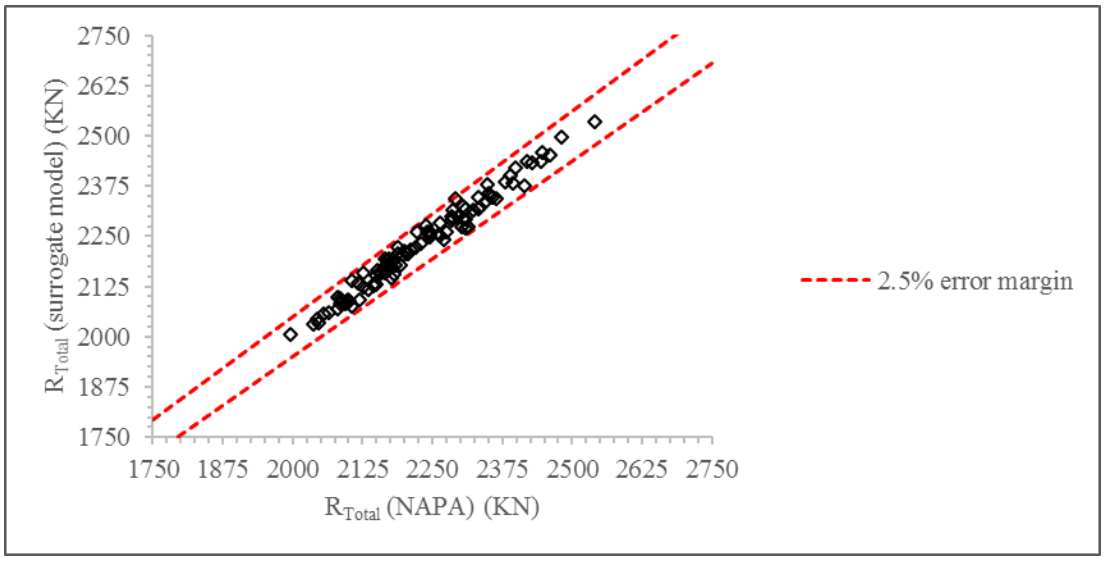

Figure 63: Evaluation of the uncertainty quantification (total resistance) surrogate model for the containership case study

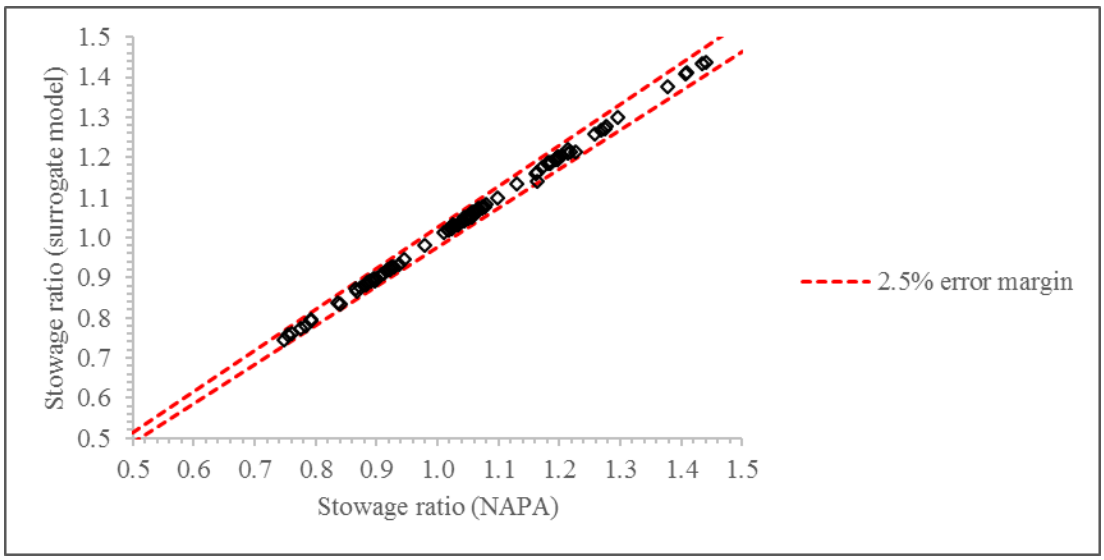

Figure 64: Evaluation of the uncertainty quantification (stowage ratio) surrogate model for the containership case study

6.2.3 Multi-objective optimisation

The NSGA 2 is run for the main optimisation phase of the containership case study, according to the setup mentioned in Table 15. 1500 designs are created in total; 1039 valid and 461 invalid, due to the specified design constraints of the problem. Figure 65 shows this distribution, while the number of designs violating each design constraint is presented in Figure 66.

The most sensitive design constraint is the IMO second generation intact stability criteria, which is violated by 272 out of the 461 invalid design variants. As mentioned in Paragraph 4.4.6, the development of the IMO second generation intact stability criteria aims at the reinforcement of the current intact stability regulations. Therefore, the new rules are more stringent, affecting the number of designs which comply with these regulations. The trim at the examined loading condition follows with 169 invalid designs. The existing intact stability criteria are violated by 116 designs, while for 19 designs no valid midship section can be defined to comply with the rules.

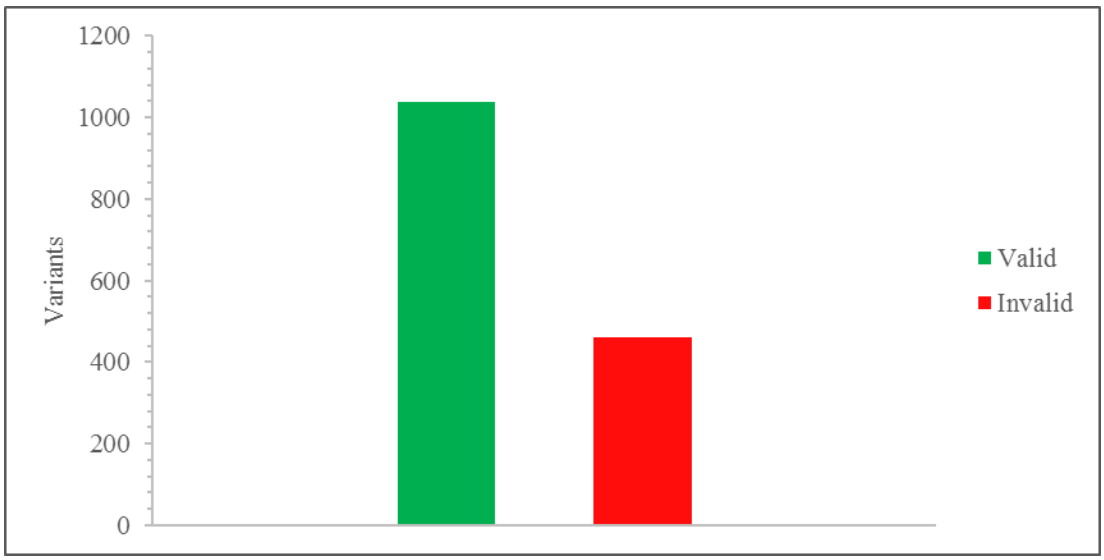

Figure 65: Generated design variants for the containership case study

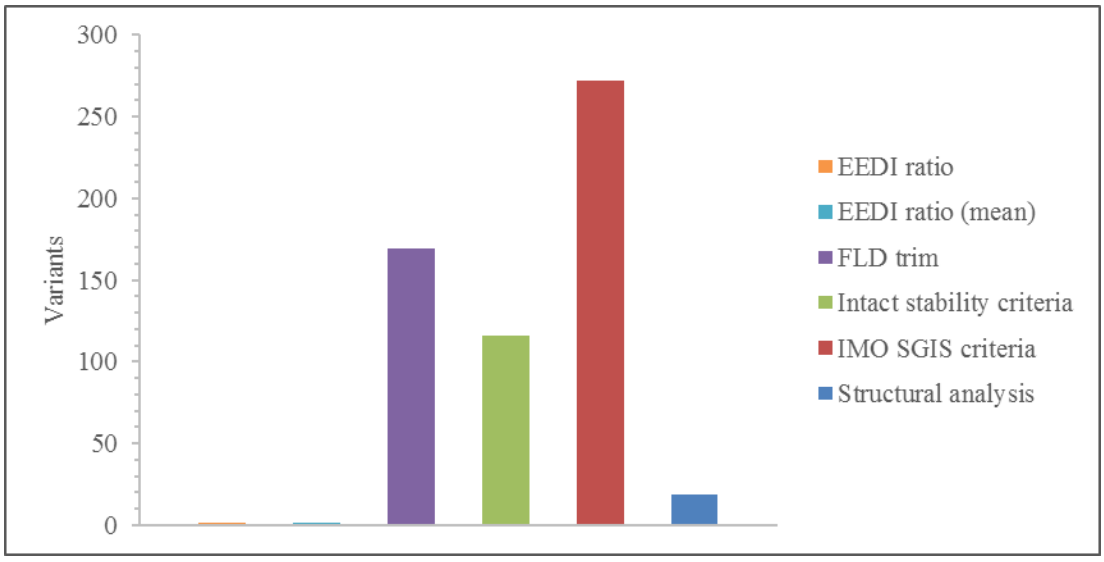

Figure 66: Analysis of design constraints' violation for the containership case study

Interestingly, no violations are spotted with regard to the $EEDI_{10}$ and mean $EEDI_{10}$ ratio constraints. Current EEDI regulations do not seem to be an encumbrance for the particular optimisation problem, mostly due to the relatively low service speed selected for the examined operational profile. Although one would expect EEDI to be a serious problem for containerships, this particular case study examines vessels designed for a service speed much lower than the one most containerships currently in service have been designed for. Therefore, the installed power associated with the design variants is adequately low to result in compliance with the first phase of the

regulation. Nevertheless, the EEDI ratio for the upcoming rule phases is also calculated during the optimisation run and violations are observed in both valid and invalid designs. In particular, 235 out of the 1500 generated designs fail phase 2 of the EEDI regulations, while 676 out of the 1500 generated designs fail phase 3 using the operational profile defined in Table 11.

These results underline the importance of incorporating newly enforced or developed regulations to the ship design optimisation problem. The number of invalid designs violating IMO second generation intact stability criteria implies that the new rules will most likely affect optimal containership design when they come into force. EEDI rule is already applied to containerships; however, as regulations become more stringent, changes in containership design will be introduced.

The Pearson correlation coefficient is calculated to identify the relation between the design variables and the objective functions. The design variables associated with the main dimensions of the hull –`Bays`, `Tiers_In` and `Tiers_On`– are strongly related to all five objective functions (Table 31).

Table 31: Correlation coefficients for the NSGA 2 run for the containership case study

Objective	`Bays`	`Tiers_In`	`Tiers_On`
Capacity ratio	-0.51	0.68	-0.62
Calm water resistance difference between CFD and approximation methods (δR)	-0.18	0.40	-0.17
RFR	0.46	-0.82	0.27
Total resistance (R_{Total})	-0.27	0.66	0.05
Stowage ratio	0.29	-0.71	0.81

Capacity ratio is mainly affected by the number of tiers below and above the main deck (Figure 67). In particular, a direct relation is observed between the `Tiers_In` design variable. On the other hand, design variables `Bays` and `Tiers_On` are inversely proportional to the capacity ratio values. As the number of tiers above the main deck rises, the possibility of having empty slots in the examined loading condition gets higher. The minimal amount of water ballast carried on-board does not allow container stacking at higher tiers above the main deck. Therefore, the ratio is decreased, since the increase of the `Tiers_On` value leads to an increase of the total TEU capacity. On the contrary, higher `Tiers_In` values allow the increase of the capacity ratio since container loading under the main deck does not have a significant impact on the vessel's stability.

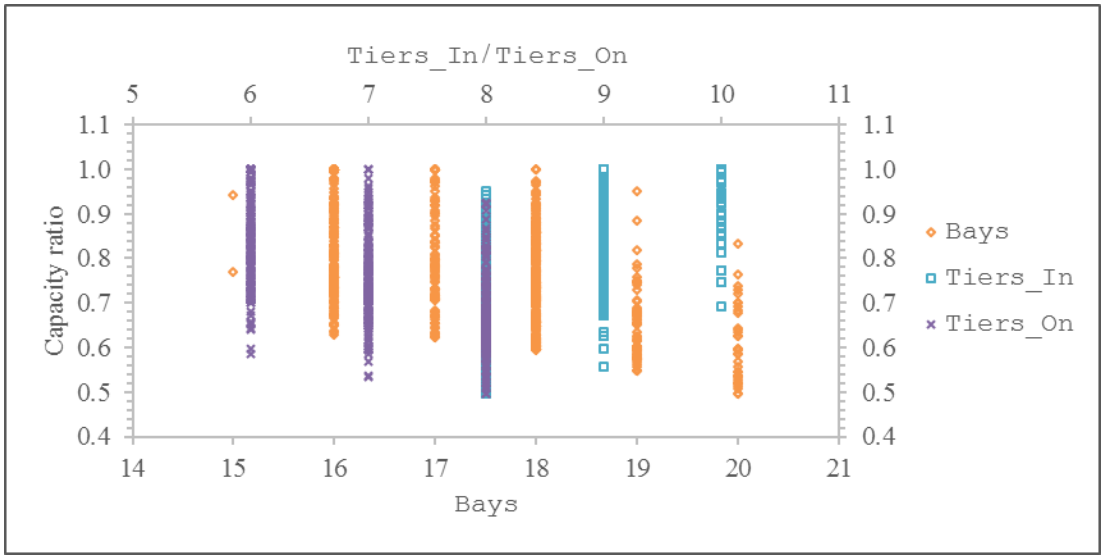

Figure 67: Comparison of capacity ratio with `Bays`, `Tiers_In` and `Tiers_On`

Objective function δR is closely related to the same design variables (`Bays`, `Tiers_In`, `Tiers_On`). As with the capacity ratio, `Bays` and `Tiers_On` are inversely proportional to δR, while increase of `Tiers_In` causes increase of δR (Figure 68). In addition, the latter design variable has a stronger relation to δR than the other two, since it is directly related to the vessel's draught which heavily influences wetted surface and resistance.

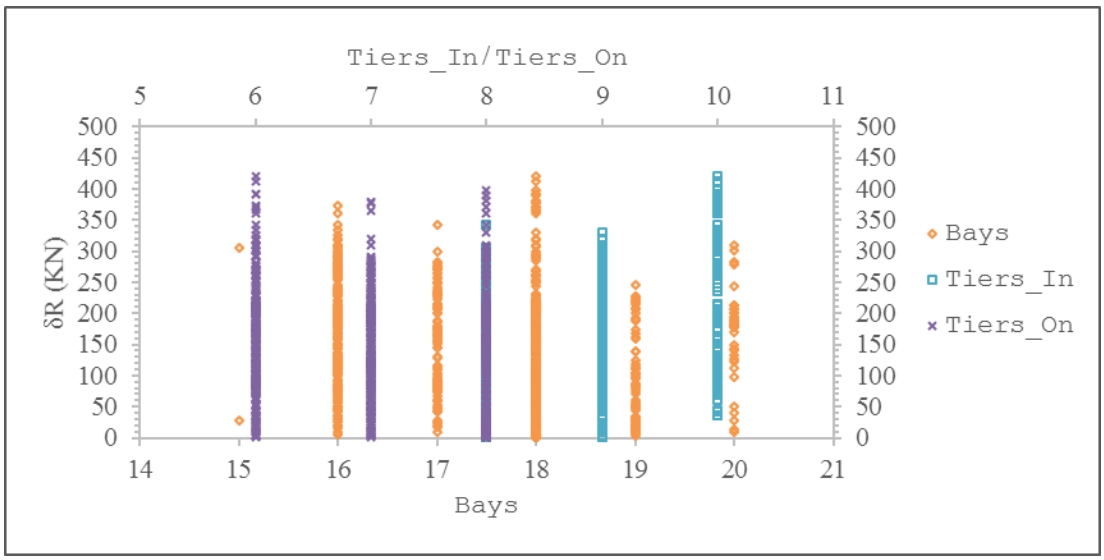

Figure 68: Comparison of δR with `Bays`, `Tiers_In` and `Tiers_On`

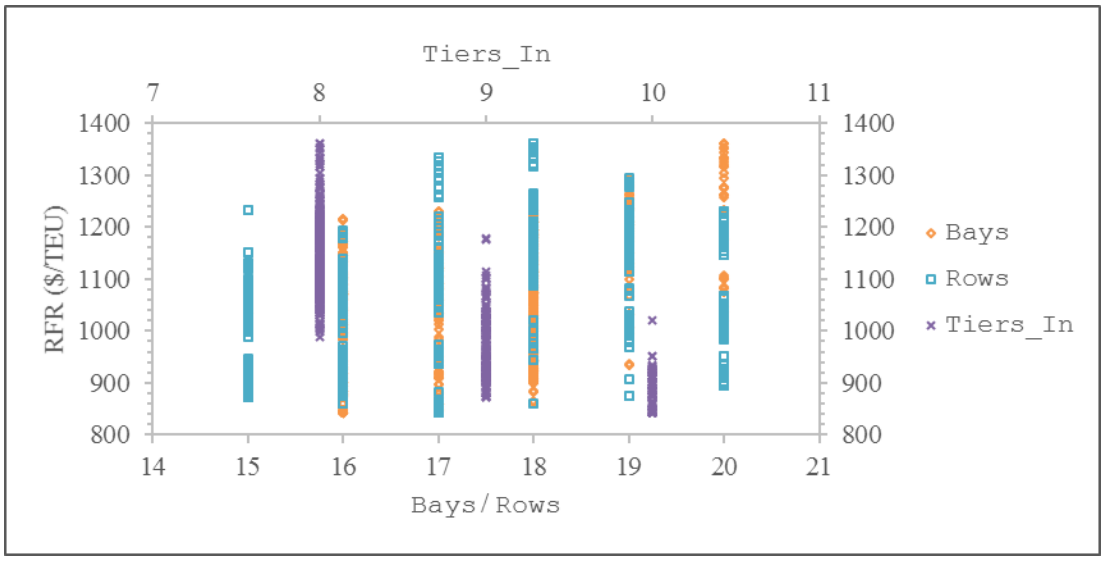

Figure 69: Comparison of RFR with `Bays`, `Rows` and `Tiers_In`

Figure 69 shows the relation between the RFR and three design variables; `Bays`, `Rows` and `Tiers_In`. RFR increases gradually as the number of bays and rows gets higher, while decreases drastically as the number of tiers below the main deck gets higher. This trend is expected due to the increase in the building cost of the vessel when the length and breadth values rise. On the other hand, increase of the tiers below the main deck results in higher values for the ship's depth. Larger depth offers larger cargo capacity without causing significant increase in the ship's structural

weight and consequently building cost (Papanikolaou, 2014). Hence, increase of Tiers_In is beneficial to RFR objective function.

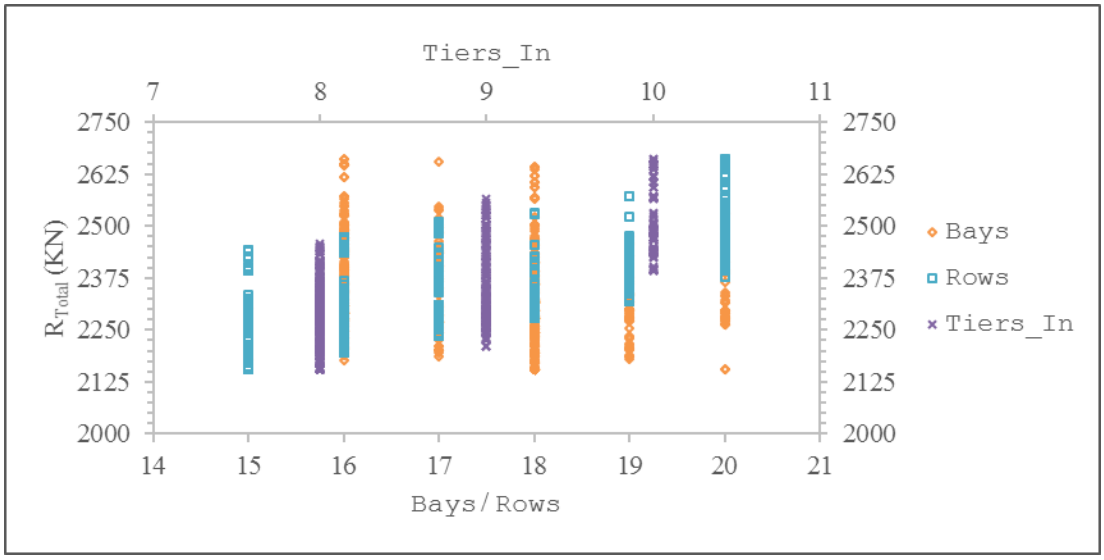

Figure 70: Comparison of total resistance with Bays, Rows and Tiers_In

Bays and Tiers_In relation with total resistance is opposite to the one with RFR described above. Increase in length (associated with Bays) results in lower resistance values, while higher Tiers_In values increase the ship's draught which has a negative impact on resistance. In addition, Rows, connected to the ship's breadth, is directly proportional to the total resistance objective function; the higher is the number of rows, the higher are the resistance values (Figure 70).

Finally, the relation between the stowage ratio and the position of the deckhouse and the number of tiers above and below the main deck is presented in Figure 71. A clear trend is observed with regard to all three design variables. Positioning the deckhouse towards the bow increases the number of containers stacked above the main deck aft of the superstructure which can extend to the highest possible tier, while at the same time the angle of the visibility line defined by regulations changes, allowing a higher number of containers to be stacked above the main deck forward of the deckhouse. Moreover, as expected, higher Tiers_On values and lower Tiers_In values lead to an increased stowage ratio.

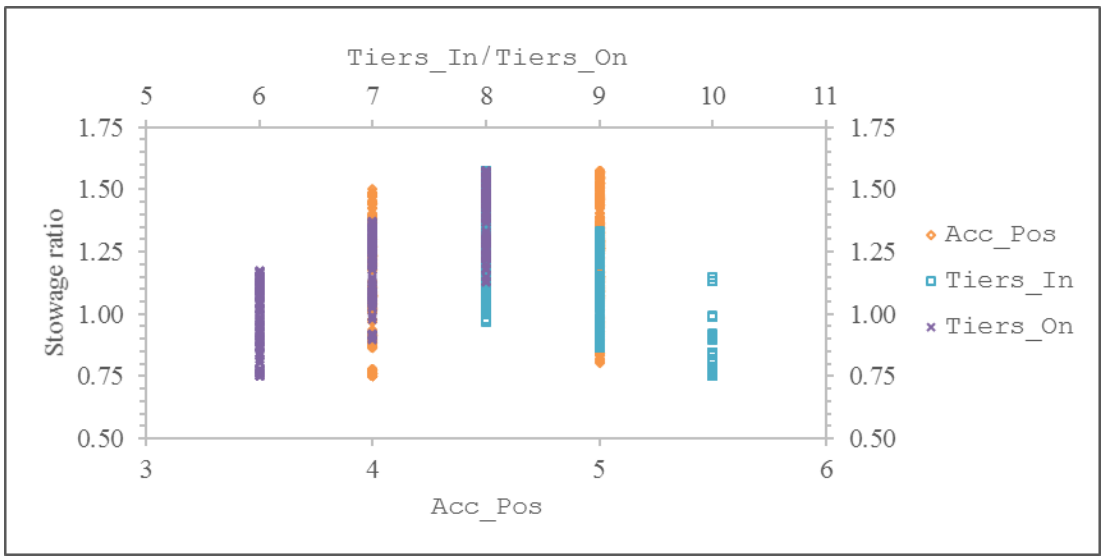

Figure 71: Comparison of stowage ratio with `Acc_Pos`, `Tiers_In` and `Tiers_On`

6.2.4 Multi-criteria decision analysis

The decision making process described in Paragraph 5.2.2 is applied to the NSGA 2 results and the optimal solution is identified. Three scenarios are defined (Table 18), each one considering the significance of each objective function differently. A utility function is defined taking as input the results of the NSGA 2 run and the weighting factors of each scenario (31). Instead of applying a linear utility function, design uncertainty is incorporated as described in Paragraph 5.2.2. The utility function provides the final score for each design variant and the optimal design is found.

The first scenario considers all five objectives to be equally important. Hence, each objective is assigned a weight of 20%. Scenario 2 prioritises the objectives related to resistance –δR and total resistance– assigning a weighting factor of 35% to each of them. The remaining objectives are assigned a weighting factor of 10%. In scenario 3 the objective functions of RFR and stowage ratio are assigned a weighting factor of 35%, with the remaining objectives having a weighting factor of 10%. A normalised standard deviation σ_x (30) is taken into account for the objective functions having their uncertainty levels measured during the optimisation run.

The ranking of the best designs for each scenario is presented in Figure 72, Figure 73 and Figure 74. In all cases, a score of one denotes the best design, while a score of zero denotes the worst performing variant.

The decision making analysis identifies three optimal designs, namely Des0303, Des0657 and Des0949. The former dominates scenario 3, Des0657 dominates scenario 1, while Des949 is identified as the dominant design in scenario 2.

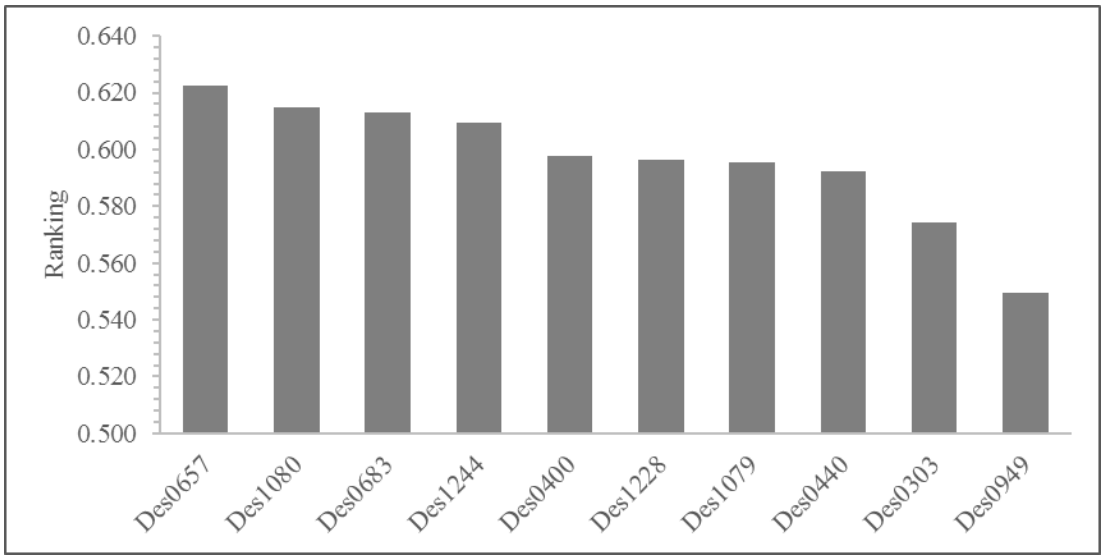

Figure 72: Scenario 1 results for the containership case study

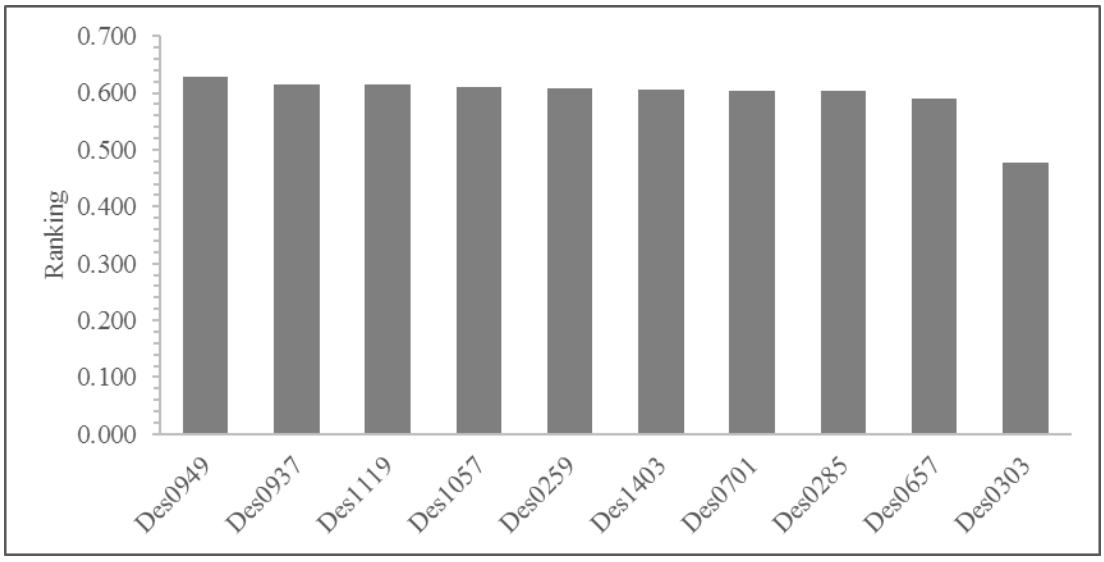

Figure 73: Scenario 2 results for the containership case study

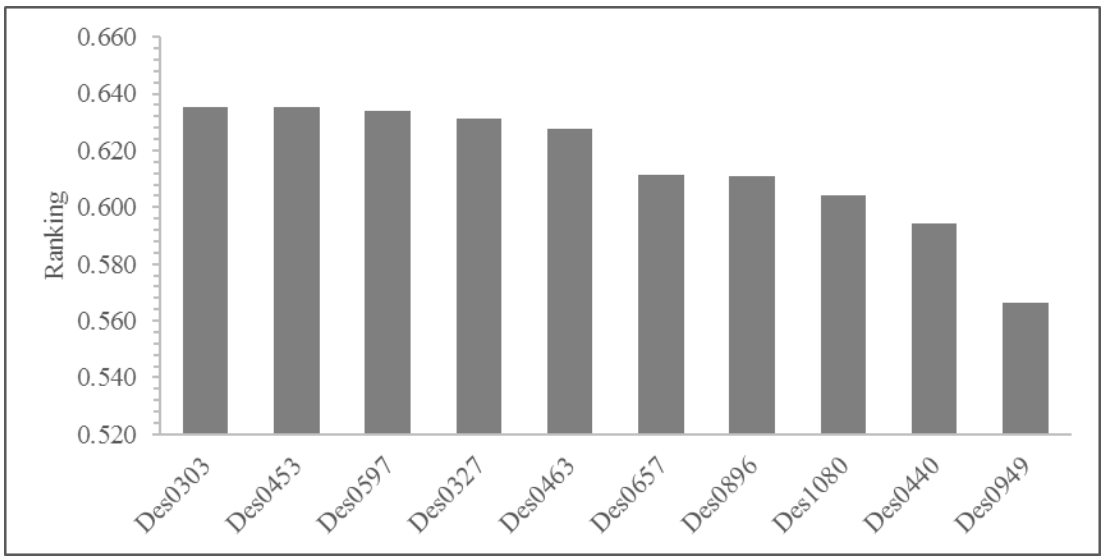

Figure 74: Scenario 3 results for the containership case study

In addition, the difference in the results between the three designs in each scenario is evident. In the first scenario, Des0303 and Des0949 are found away from the top ranked designs in the list, having both a difference of 7.8% and 11.8% from the score achieved by the top ranked Des0657, respectively. Same pattern is observed in the second scenario, however there is a bigger difference between the performance of Des0303 and Des0949 which ranks first (24%). Finally, in the third scenario, Des0657 manages to achieve a score close to the top ranked designs, having a difference of only 3.8% from Des0303 which dominates the specific scenario. The design variable values for the two designs are presented in Table 32, while their performance is presented in Table 33. The CAESES® and NAPA® models for the two optimal designs are presented in Figure 75, Figure 76, Figure 77, Figure 78, Figure 79 and Figure 80.

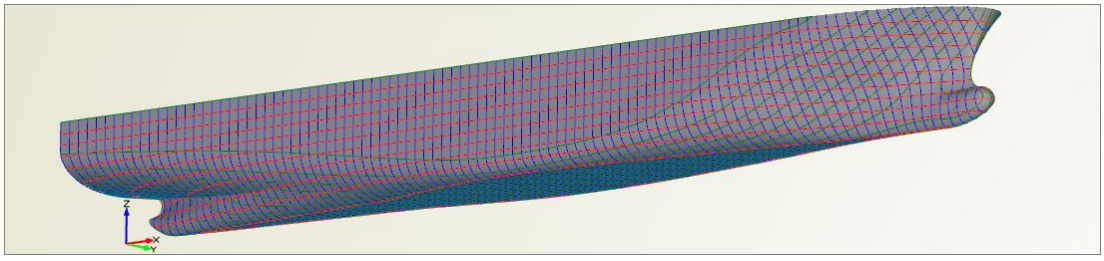

Figure 75: Des0303 CAESES® model

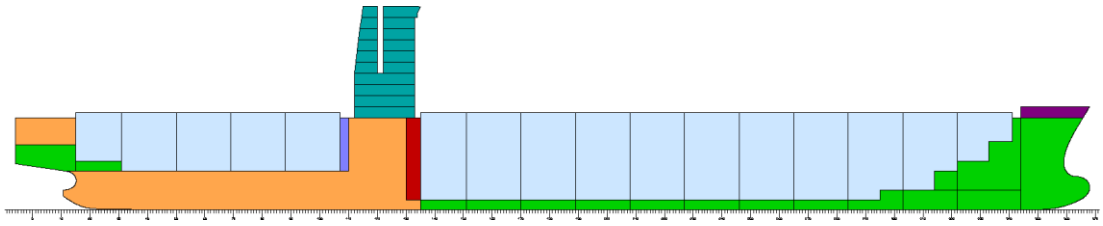

Figure 76: Des0303 NAPA® model

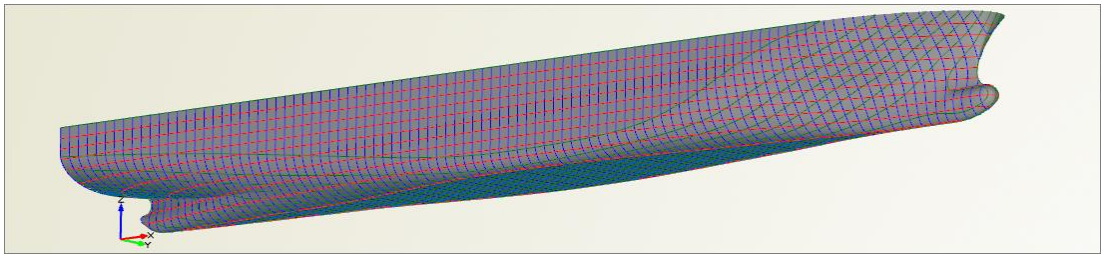

Figure 77: Des0657 CAESES® model

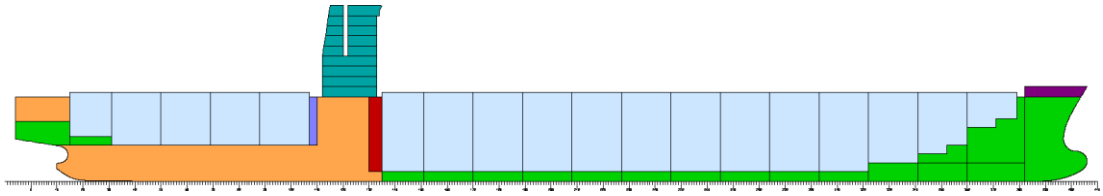

Figure 78: Des0657 NAPA® model

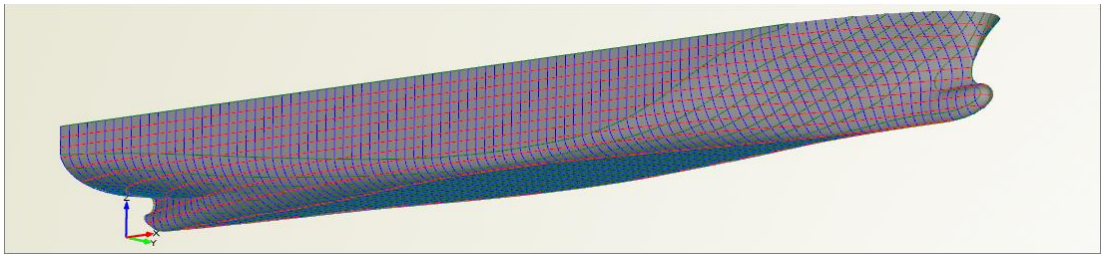

Figure 79: Des0949 CAESES® model

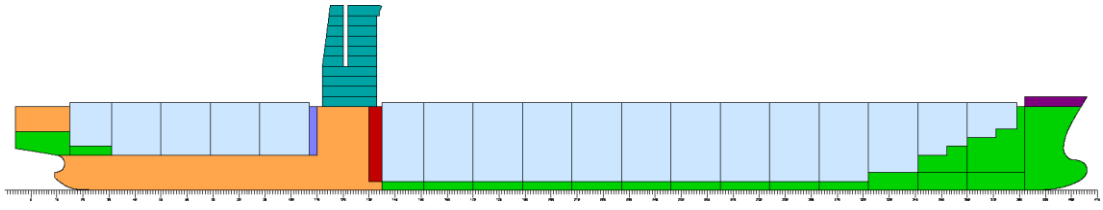

Figure 80: Des0949 NAPA® model

Table 32: Main set of design variables for Des0303, Des0657 and Des0949

Design variable	Des0303	Des0657	Des0949
Acc_Pos	5	5	5
Bays	16	18	18
Bilge_A	5.285	4.598	5.297
Bilge_B	5.232	5.980	5.224
DB	2.693	2.896	2.657
d_C_Prismatic	-0.00747	0.00765	-0.00100
d_LCB	0.00748	0.00205	-0.01439
Rows	15	15	17
Tiers_In	9	9	9
Tiers_On	8	7	8

Table 33: Des0303, Des0657 and Des0949 response to objective functions

Objective	Des0303	Des0657	Des0949
Calm water resistance difference between CFD and approximation methods (δR) (KN)	306	185	16
Container capacity ratio (r_C)	0.9253	0.9493	0.7509
RFR ($/TEU)	879.12	885.47	955.67
Container stowage ratio (r_S)	1.2292	1.1102	1.2955
Total resistance (R_{Total}) (KN)	2326	2273	2366

The results of the decision making process clearly illustrate the effect uncertainty has in the selection of the optimal design. A ranking of the produced design variants is performed, excluding the effects of uncertainty and in all three scenarios the best designs are different from the results presented above. This becomes obvious in the graphs presented below, where the location of the optimal designs is compared with the Pareto front, for which generation uncertainty is not taken into account. In most cases the identified designs do not lie on the Pareto front, hence as far as their performance with regard to the examined objective functions is concerned, design variants with better performance exist among the NSGA 2 results. This observation underlines the fact that robustness is not always linked with best performance. The designer needs to choose between optimal and robust performance. On the one hand, a design performs ideally for the very specific scenario it is tested on, while on the other hand another design achieves a uniform and consistent performance when tested on various scenarios during which uncertain parameters are assigned different values. The latter proves to be more robust, unaffected by external factors which could have a severe impact on the former design, degrading its overall performance.

In addition, the identification of three optimal designs shows the importance of the incorporation of decision making process in a multi-objective optimisation problem. The different scenarios generate different ranking of the same pool of design variants, depending on the significance of each objective function. The difference in the weighting factors applied to the investigated measures of merit results in promotion of designs which perform best in the respective objective functions in each scenario. However, the optimal design of scenario 1, in which all objectives are considered equally important, achieves a performance which is not significantly different from the top ranked designs in the other two scenarios. This behaviour is expected as the top ranked design of scenario 1 is considered an all-around solution.

Some indicative graphs showing the results of the optimisation are presented and analysed below.

Figure 81 presents the relation between RFR and capacity ratio. Minimisation of RFR is desired while at the same time maximisation of the capacity ratio is pursued. Des0303 and Des0657 perform adequately well, located close to the Pareto front, contrary to Des0949 which lies far away from both the remaining two optimal and the baseline designs. This result is anticipated due to the low impact capacity ratio and RFR have on the selection of Des0949.

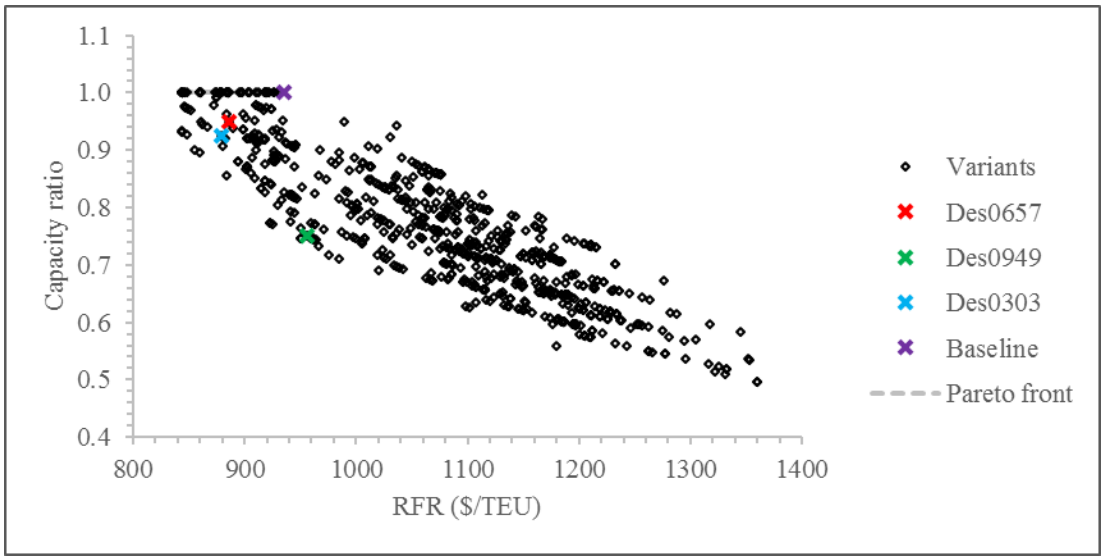

Figure 81: RFR vs. capacity ratio

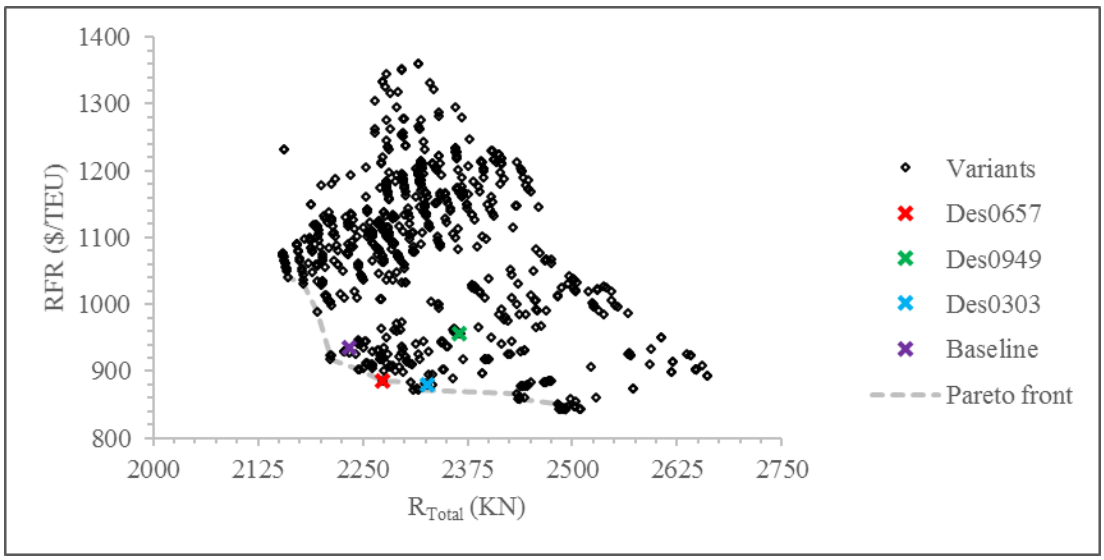

Figure 82: Total resistance vs. RFR

Figure 82 illustrates the relation between the total resistance and the RFR. The same pattern described above is observed in this graph. `Bays` and `Tiers_In` have opposite impact on these objectives. Increase of the number of bays leads to an increase in the RFR due to higher building cost; on the other hand, more slender designs –defined by higher number of bays– are associated with lower resistance values, hence the decrease in the total resistance. Similarly, higher `Tiers_In` values result in higher draught values which are associated with increased total resistance, yet the RFR is decreased due to higher cargo capacity. It is worth mentioning that Des0303 and Des0657 lie on the Pareto front, contrary to Des0949 which performs worse than the other two optimal designs with regard to the RFR.

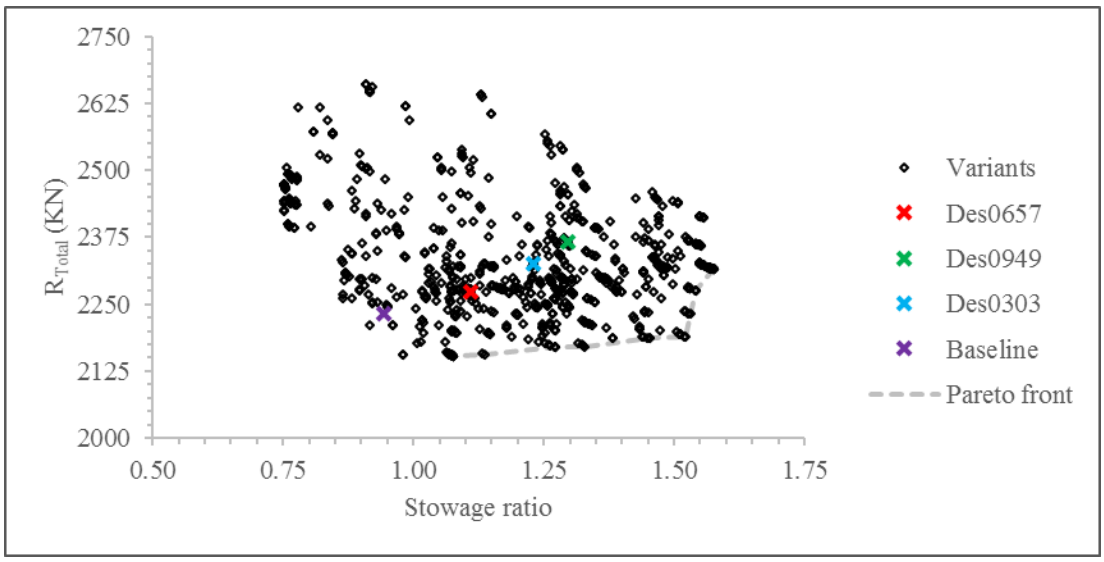

Figure 83: Stowage ratio vs. total resistance

The relation between stowage ratio and total resistance is presented in Figure 83. Maximisation of the stowage ratio is desired, whereas minimisation of total resistance is pursued. The identified optimal designs are located far from the Pareto front. However, a trend between their responses is identified; as the performance with regard to one objective is improved among the three designs, the performance with regard to the other objective becomes poorer, thus forming a local Pareto front themselves.

Finally, Figure 84 shows the relation between the two examined ratios; the stowage and capacity ratio. A clear Pareto front is identified in the comparison of these objective functions. Similarly to previous graphs, the two objectives are quite contradictive; increase of one results in decrease of the other. Specific design variables (`Tiers_In` and `Tiers_On` in this case) are responsible for this relation.

This illustrates how complex the solution of the specific optimisation problem proves to be, since improvement in one objective does not necessarily lead to an overall improved performance. Hence, it is very important to perform a decision making process following the optimisation run to set priorities for the optimal design selection. As far as the identified best designs are concerned, Des0303 and Des0657 lie on the Pareto front, while Des0949 is located far away, despite achieving the best stowage ratio among the selected designs.

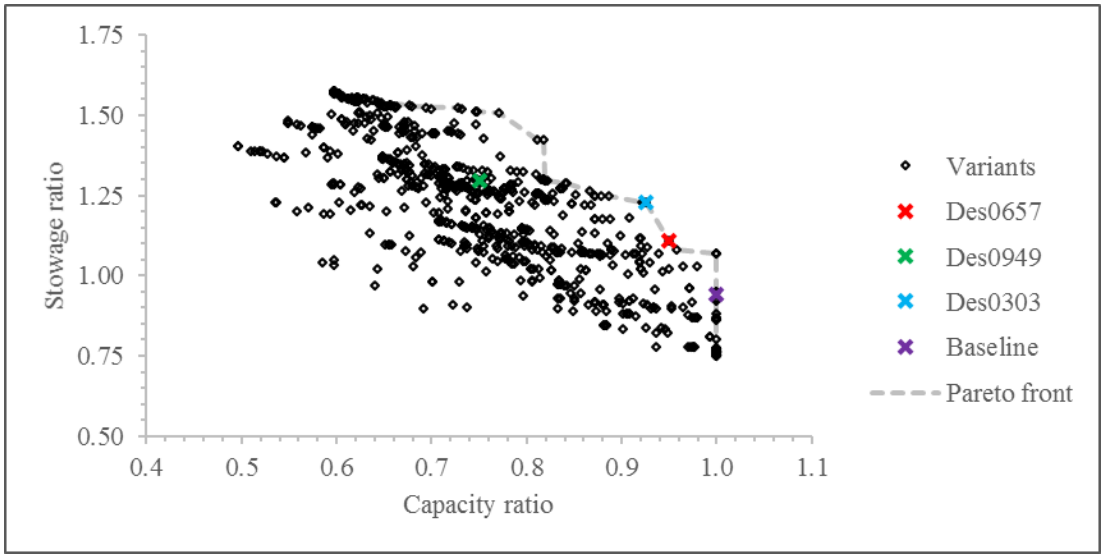

Figure 84: Capacity ratio vs. stowage ratio

A comparison between the identified optimal designs and the baseline model is presented in Table 34, showing the differences in their performance.

The optimal designs generally perform better with regard to objective functions of δR, RFR and stowage ratio, while their performance on capacity ratio and total resistance is slightly worse than the baseline model. As far as δR is concerned,

Des0949 achieves the lowest value, creating a difference of from the baseline model value. Des0303 scores the lower RFR value among the designs and the two best stowage ratio values, along with Des0949. Des0657 is an all-around solution performing better than the baseline model in most of the objective functions.

Nevertheless, all three identified improved designs are selected taking uncertainty into account, assuring the decision maker that their performance reaches high levels of robustness. Their response to the investigated objective functions is more likely to remain constant in different situations, compared to other variants generated during the NSGA 2 run which respond better to one examined scenario.

The investigation of uncertainty in the decision making phase shows its impact on ship design, producing results which would otherwise seem suboptimal.

Table 34: Optimal designs and baseline model response to objective functions for the containership case study

Objective	Baseline	Des0303	% Diff.	Des0657	% Diff.	Des0949	% Diff.
Calm water resistance difference between CFD and approximation methods (δR) (KN)	123	306	149.2	185	50.2	16	-87.0
Container capacity ratio (r_C)	1.0000	0.9253	-7.5	0.9493	-5.1	0.7509	-24.9
RFR ($/TEU)	935.29	879.12	-6.0	885.47	-5.3	955.67	2.2
Container stowage ratio (r_S)	0.9423	1.2292	30.4	1.1102	17.8	1.2955	37.5
Total resistance (R_{Total}) (KN)	2233	2326	4.2	2273	1.8	2366	5.9

6.3 Ro-Pax vessel case study

6.3.1 Baseline model

The baseline model for the Ro-Pax vessel case study is presented in Paragraph 5.3.2. Table 20 and Table 21 present the design variables' values used to define the model. Its performance with regard to the examined objective functions is presented in Table 35.

6.3.2 Surrogate models

As mentioned in Paragraph 5.3.2, three surrogate models are created for the Ro-Pax vessel case study. In this Paragraph, the analysis of the results related to the preparation and the evaluation of these surrogate models is presented.

Table 35: Baseline Ro-Pax vessel model response to objective functions

Objective	Baseline
Building cost (C_B) (M \$)	62.5
Calm water resistance difference between CFD and approximation methods (δ_R) (KN)	548
RFR (\$)	41.86
Total resistance (R_{Total}) (KN)	1999
Uncertainty indicator for the investigated objective functions (C_B, RFR, R_{Total}) (i_U)	0.3756

As in containership case study, the design of experiment run using the Sobol algorithm to define the surrogate model allows the designer to identify how each of the design variables influences the evaluated parameters. The Pearson correlation coefficient is used to determine the strength of the relationship between two selected variables (Doyle, 2011).

- Calm water resistance CFD calculations:

For the generation of the calm water resistance CFD calculations surrogate model, a subset of the main design variables of the optimisation problem –presented in Table 20– is used. The number of car lanes, draught and L_{BP} influence the calm water resistance CFD result the most, followed by the percentage change in the LCB and c_P. The number of car lanes is directly related to the breadth of the vessel. The correlation coefficient for the number of car lanes and draught is 0.70 and 0.56 respectively, which denotes a proportional relation; an increase in either of these design variables results in a higher calm water resistance value. On the other hand, the correlation coefficient for the L_{BP} is found to be -0.24, which affirm the inversely proportional relation between length and resistance.

The positive correlation coefficient values of 0.15 and 0.24 for the design variables `d_C_Prismatic` and `d_LCB` respectively reveal the positive change in the resistance value as the two design variables are assigned higher values. On the other hand, the same analysis shows that a small, yet noticeable, decrease is achieved in the calm water resistance by increasing the bilge radius. This trend is expected, as an increased bilge radius results in a lower wetted surface area which affects the frictional resistance.

The evaluation phase of the surrogate model following its generation is crucial to identify its accuracy. A new design of experiment is run, generating a new set of design variants to compare the response of the surrogate model with the actual CFD simulations. Figure 85 shows the comparison results; the red dashed line shows an error margin of 2.5%. All in all, the surrogate model performs adequately for the generated design variants.

As far as the computational time savings are concerned, the same conclusions as in the containership case study can be drawn. A considerable decrease in the evaluation of the calm water resistance is achieved. Instead of spending thirty minutes for the CFD computation per design variant, a second is needed to evaluate the relevant

surrogate model, making the latter 1800 times faster than the CFD simulations, thus reducing the overall computation time of the optimisation run significantly. The overall time required for the completion of all three phases (preparation, generation, evaluation) related to the surrogate model definition is 165 hours.

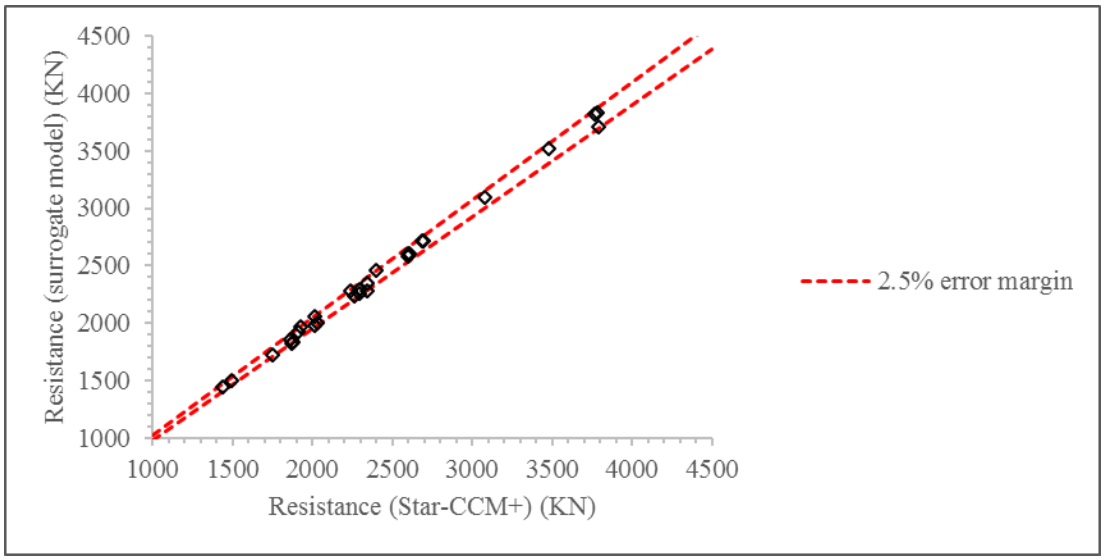

Figure 85: Evaluation of the calm water resistance CFD calculations surrogate model for the Ro-Pax vessel case study

- IMO second generation intact stability criteria:

As far as the IMO second generation intact stability criteria surrogate model is concerned, the main design variables of the optimisation problem –presented in Table 20– are used for its generation. All ten parameters influence the success rate of the generated design variants with regard to meeting the criteria or not to some extent.

The number of ro-ro decks, the number of car lanes and the L_{BP} are found to affect the success rate the most. The first two design variables are directly related to the depth and the breadth of the vessel. In particular, the correlation coefficient for the number of ro-ro decks is found to be -0.78, while the correlation coefficients for the number of car lanes and the L_{BP} are 0.34 and 0.13 respectively.

The evaluation phase of the surrogate model following its generation is crucial to identify its accuracy. A new design of experiment is run, generating new design variants to compare the response of the surrogate model with the actual computation regarding the evaluation of the IMO second generation intact stability criteria. Figure 86 presents the results of this comparison. The surrogate model performs adequately well, matching the results of the actual computation in each examined case. The attained value of one denotes compliance with the examined criteria, whereas zero denotes the opposite.

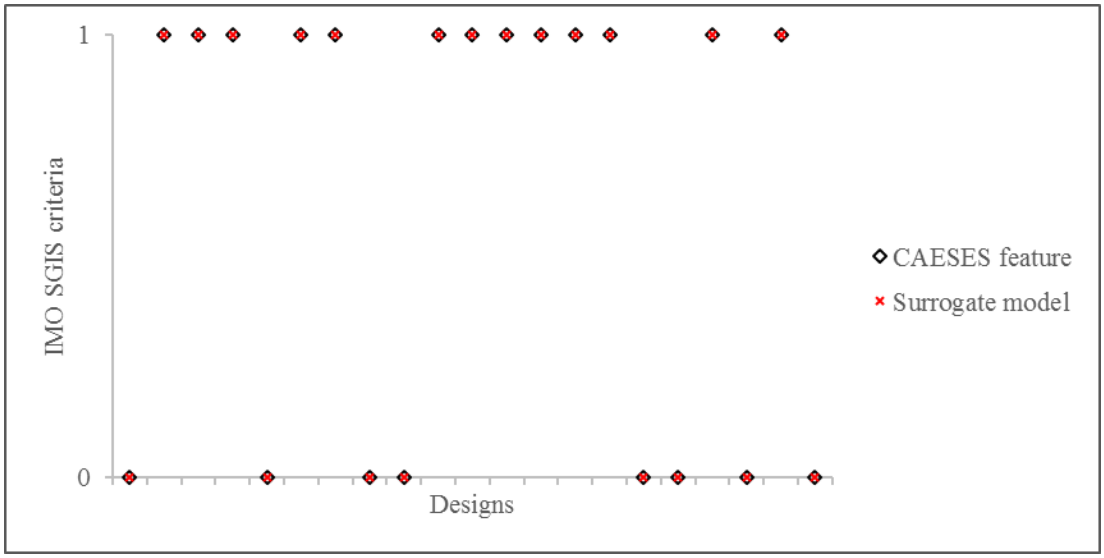

Figure 86: Evaluation of the IMO second generation intact stability criteria surrogate model for the Ro-Pax vessel case study

Similar to the containership case study, the decrease in the time required to obtain results for a single design variant is significant; a couple of seconds are required for the evaluation of the surrogate models, whereas about fifteen minutes are needed for a direct simulation in CAESES® for the evaluation of the IMO second generation intact stability criteria. This makes the surrogate model 450 times faster than the actual simulation. The difference is greatly amplified in the main optimisation run, during which 1500 designs are evaluated. The overall time required for the completion of all three phases (preparation, generation, evaluation) related to the surrogate model definition is 82.5 hours.

- Uncertainty quantification:

The third surrogate model defined for the Ro-Pax vessel case study is the one related to the uncertainty quantification. For its generation, ten design variables are used; five main design variables of the optimisation problem and five uncertain design variables (Table 20 and Table 24). As mentioned in Table 23, four uncertain parameters are evaluated, namely the building cost, $EEDI_5$ ratio, RFR and total resistance. The correlation coefficient is calculated for each evaluated parameter to identify which design variables influence these parameters the most. The most important design variables are shown in Table 36.

Table 36: Correlation coefficients for the uncertainty quantification surrogate model for the Ro-Pax vessel case study

Evaluated parameter	Design variables
Building cost	`Draught` (0.51), `Lane_No` (0.28), `Variance` (0.50)
$EEDI_5$ ratio	`Deck_No_RoRo` (-0.23), `Draught` (0.81), `Lane_No` (-0.35),
RFR	`Lane_No` (-0.66), `Price_FO` (0.44), `V_S` (0.13)
Total resistance	`Draught` (0.90)

As far as the uncertain design variables are concerned, they mostly affect the objective functions of the building cost and RFR. The $EEDI_5$ ratio is calculated based on international regulations which require as input nominal values which are normally not affected by parameters affecting the operational profile of the ship (e.g. oil price, operational speed, wind speed).

However, parameters such as the added wave and the wind resistance which are monitored throughout the optimisation process are closely related to the uncertain design variables, especially the operational and wind speed. In particular, the correlation coefficient calculated for the identification of the relation between the

wind speed and the wind resistance is found to be 0.94, a value which is expected when (17) is taken into account.

Total resistance is calculated based on the design speed and an average wind speed to correctly identify the required propulsion power, which is used as input in several calculations during the concept design stage (e.g. estimation of the machinery weight).

The accuracy of the generated surrogate models for each evaluated parameter is presented in Figure 87, Figure 88, Figure 89 and Figure 90. In general, the results fall within the 2.5% error margin lines illustrated in the graphs. No major discrepancies are identified in the evaluation process which proves the suitability of the Kriging method for the generation of the uncertainty quantification surrogate model.

Despite the low error margin values obtained through this setup, the uncertainty associated with the use of some models and methods in NAPA® (e.g. Holtrop and Mennen method) is not analysed.

The evaluation of the surrogate model responsible for the uncertainty quantification takes about a second for each evaluated parameter –four seconds for the evaluation of all four uncertain parameters. The same process takes around a minute to be completed when the NAPA® macros are run. Although the time difference in this case, compared to the aforementioned surrogate models for the Ro-Pax vessel case study, is considerably smaller for a single evaluation round, it becomes more significant when the uncertainty quantification process takes place in the main optimisation phase. 25 evaluations need to take place for the setup presented in Paragraph 5.3.2. Therefore, the utilisation of a surrogate model results in a time saving of around twenty minutes per design variant, being fifteen times faster than the full NAPA® computations.

The overall time required for the completion of all three phases (preparation, generation, evaluation) related to the surrogate model definition is 18 hours.

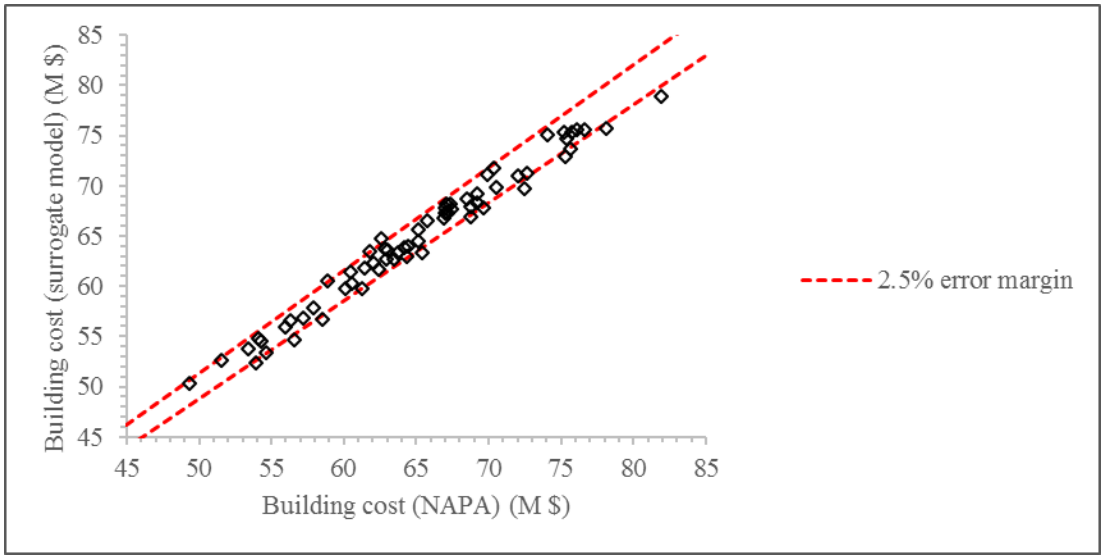

Figure 87: Evaluation of the uncertainty quantification (building cost) surrogate model for the Ro-Pax vessel case study

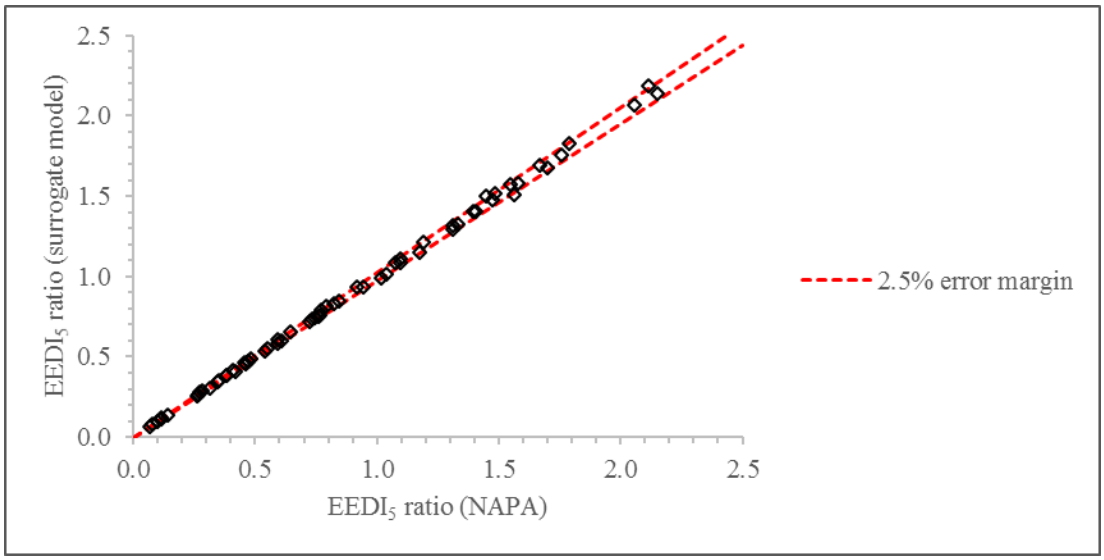

Figure 88: Evaluation of the uncertainty quantification ($EEDI_5$ ratio) surrogate model for the Ro-Pax vessel case study

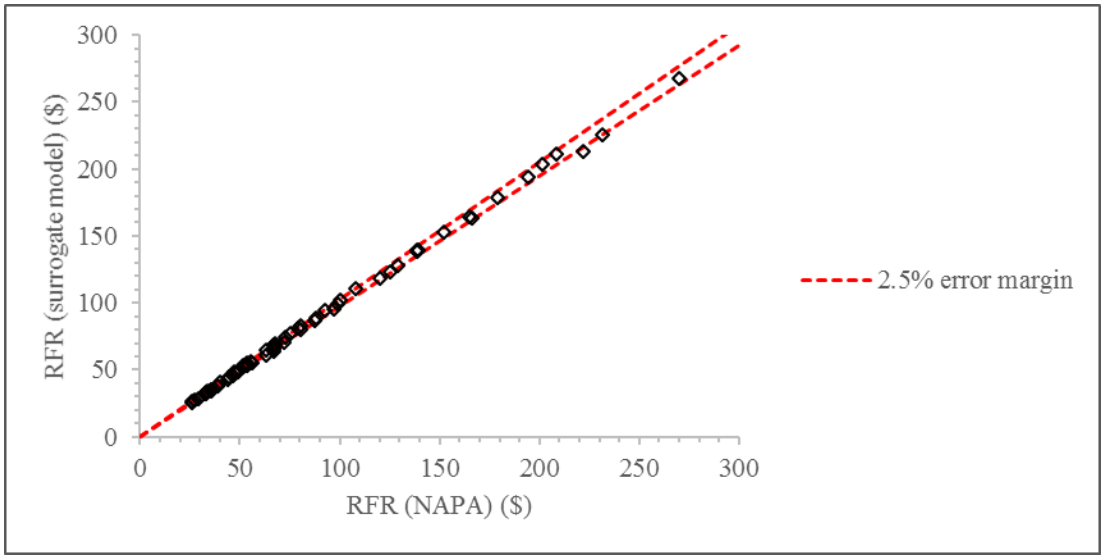

Figure 89: Evaluation of the uncertainty quantification (RFR) surrogate model for the Ro-Pax vessel case study

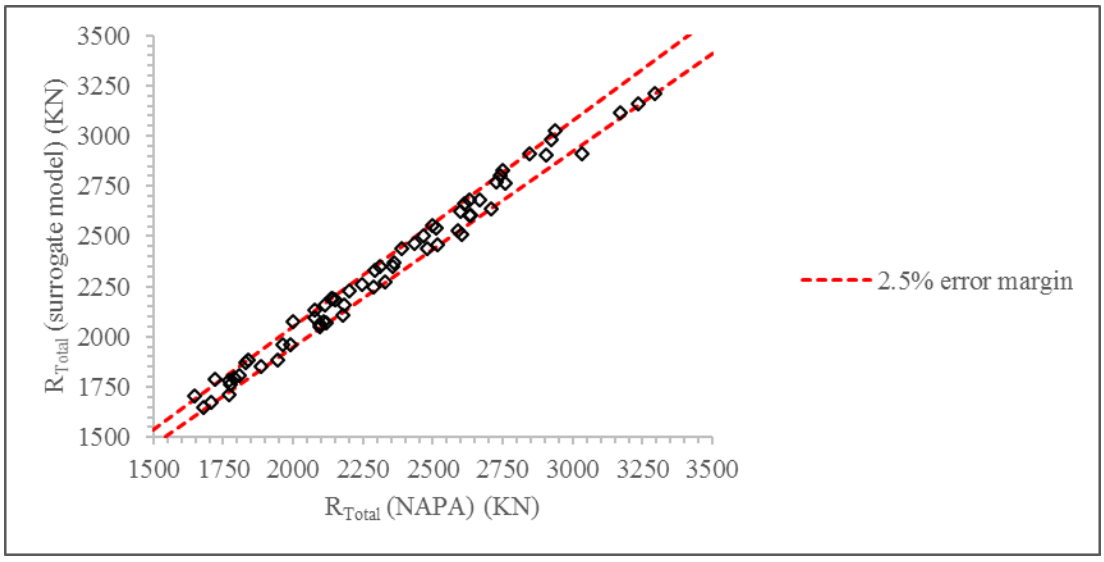

Figure 90: Evaluation of the uncertainty quantification (total resistance) surrogate model for the Ro-Pax vessel case study

6.3.3 Multi-objective optimisation

The NSGA 2 is run for the main optimisation phase of the Ro-Pax vessel case study, according to the setup mentioned in Table 25. 1500 designs are created in total; 1099 valid and 401 invalid, due to the specified design constraints of the problem. Figure 91 shows this distribution, while the number of designs violating each design constraint is presented in Figure 92.

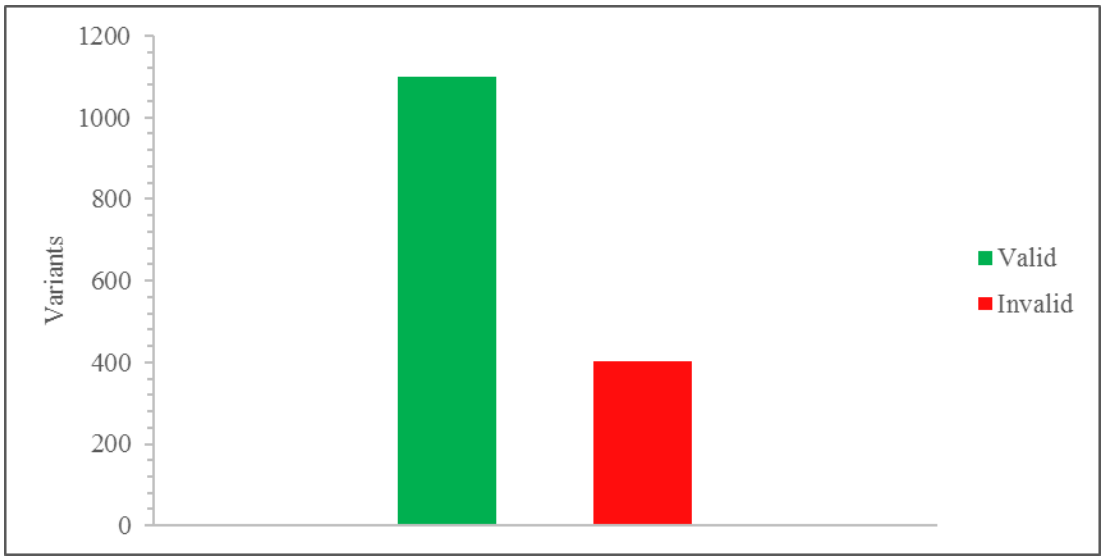

Figure 91: Generated design variants for the Ro-Pax vessel case study

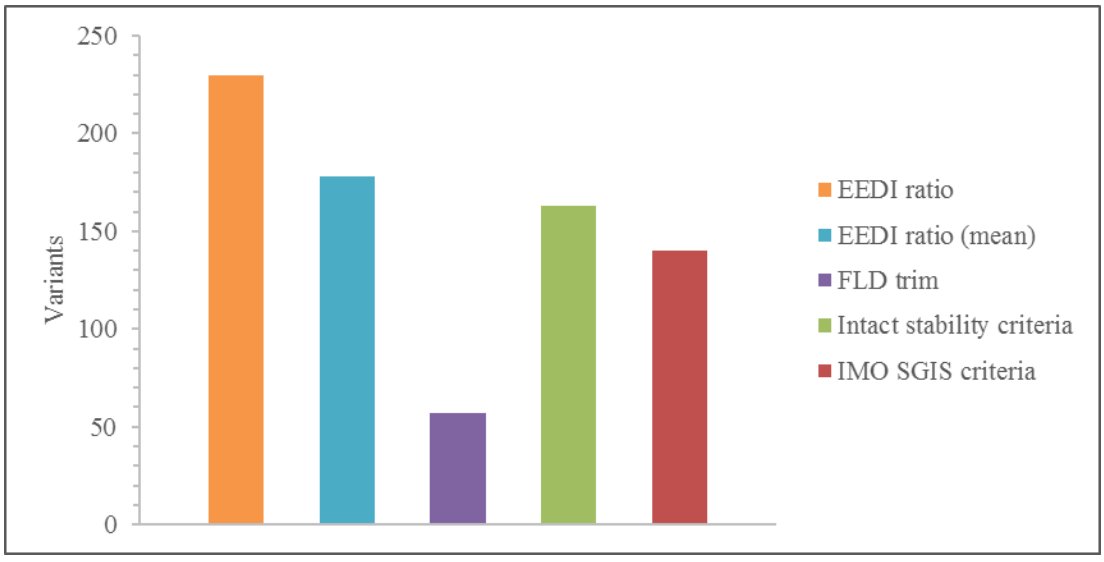

Figure 92: Analysis of design constraints' violation for the Ro-Pax vessel case study

The most sensitive design constraint is the $EEDI_5$ ratio, which is violated by 230 out of the 401 invalid design variants. The mean $EEDI_5$ ratio follows, which derives from the uncertainty quantification process, with 178 invalid designs violating the specific constraint. The existing and the second generation intact stability criteria are violated by 163 and 140 invalid designs respectively, while the trim at the examined loading condition seems to be the least sensitive constraint, with only 57 invalid designs having a trim of more than 0.5% of the L_{BP}.

As with the containership case study, the results presented above emphasise the importance of including new regulations in the ship design optimisation problem. The number of invalid designs violating the EEDI rule indicates that the application of the EEDI rule to Ro-Pax vessels might induce changes in their design. The same conclusions can be drawn for the stability criteria. Although the invalid designs violating the second generation intact stability criteria are slightly less than those violating the existing ones, their overlap is 53%. Hence, the relation between the two criteria sets is not very significant and advocates the consideration of the second generation intact stability criteria in the design optimisation problem.

Table 37: Correlation coefficients for the NSGA 2 run for the Ro-Pax vessel case study

Objective	Draught	Lane_No	L_BP
Building cost (C_B)	0.65	0.65	0.41
Calm water resistance difference between CFD and approximation methods (δR)	-0.33	0.34	-0.61
RFR	-0.01	-0.60	-0.10
Total resistance (R_{Total})	0.89	0.31	0.47
Uncertainty indicator for the investigated objective functions (C_B, RFR, R_{Total}) (i_U)	-0.36	-0.01	-0.42

The Pearson correlation coefficient is calculated to identify the relation between the design variables and the objective functions. The design variables associated with the main dimensions of the hull –draught, number of car lanes and L_{BP}– are strongly related to all five objective functions (Table 37).

As far as the building cost is concerned, all three design variables are proportional to the building cost. A stronger relation is identified between the draught and breadth (directly relevant to the number of car lanes), followed by the L_{BP} (Figure 93). This trend falls in line with the analysis found in Papanikolaou (2014). Larger draught values are associated with higher hydrostatic pressures at the bottom and higher bending moments due to larger displacement values, which affect the required strengthening and consequently the steel weight. An increase in the breadth of the hull results in a greater surface area and higher required plate thickness values to withstand the increased weight and hydrostatic forces. Therefore, the steel weight is increased, leading to a higher building cost. The same applies to the relation between the length and the building cost of the vessel.

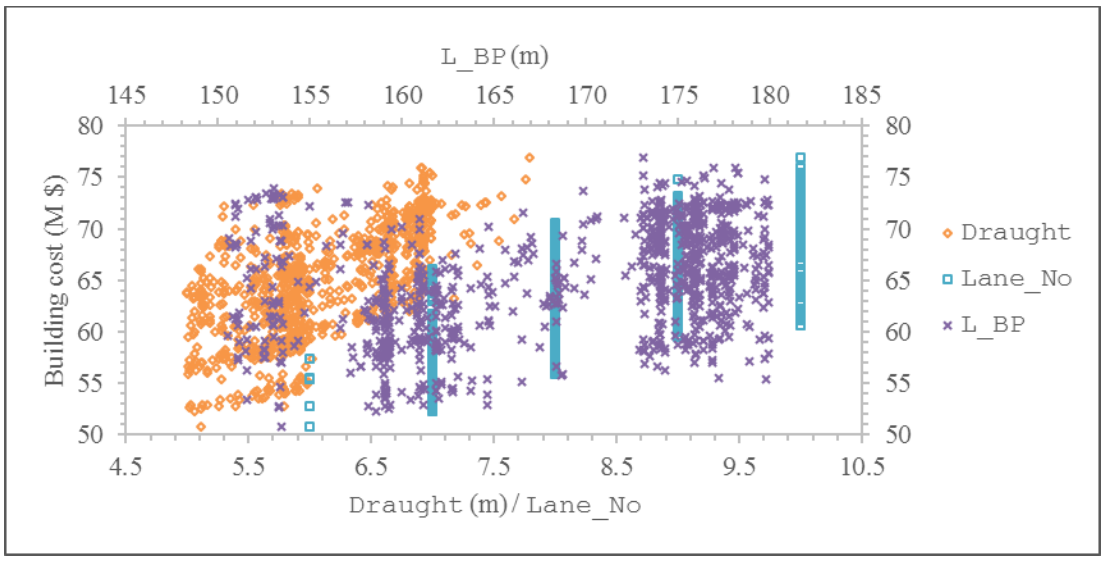

Figure 93: Comparison of building cost with `Draught`, `Lane_No` and `L_BP`

RFR is greatly affected by the number of car lanes. In particular, the relation is inversely proportional; the RFR decreases as the number of car lanes gets higher. This is expected due to the increased transport capacity achieved by the addition of

car lanes in the car decks. Similar relation is observed between the RFR and the number of passenger decks (correlation coefficient is found to be -0.14). However, the revenue from transporting vehicles (cars or lorries) is much higher per nominal value, compared to passengers due to the ticket price structure. In addition, hull length influences slightly the RFR value, as longer designs are associated with a lower RFR (Figure 94).

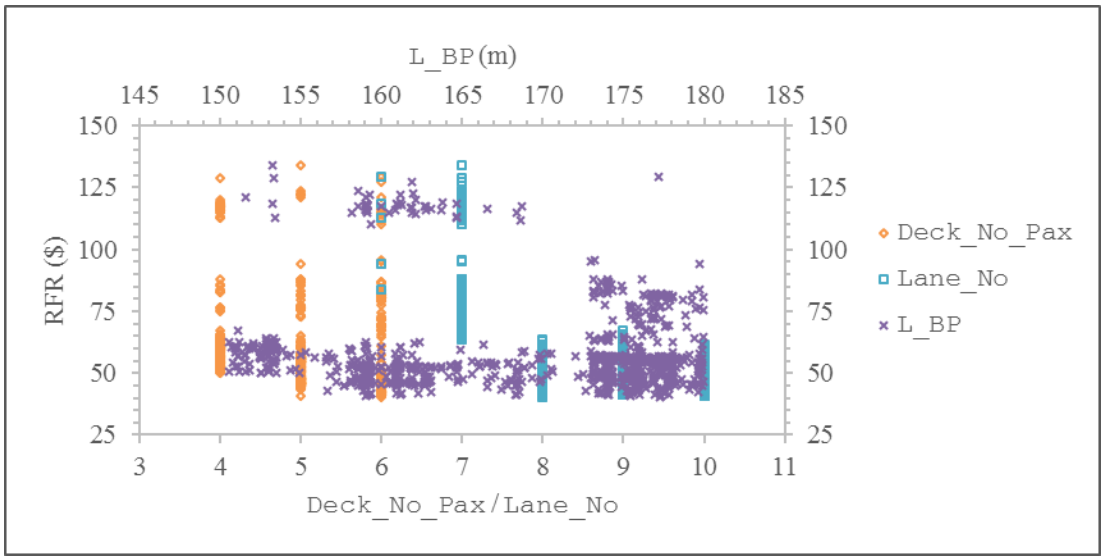

Figure 94: Comparison of RFR with `Deck_No_Pax`, `Lane_No` and `L_BP`

Total resistance, which includes the calm water, added wave and wind components, is directly related to the draught of the vessel. L_{BP} also affects the total resistance value, being proportional to the latter but to a lesser extent than the draught. The two design variables associated with the Lackenby transformation –`d_C_Prismatic` and `d_LCB`– influence the resistance due to the impact they have on the hull wetted surface which affects the calm water resistance component. Their correlation coefficient with regard to the total resistance value is -0.38 and -0.30 respectively (Figure 95).

Finally, an interesting observation with regard to the examined uncertainty indicators is worth mentioning. Both the draught and the L_{BP} are closely related to the δR and the i_U objectives. In particular, both design variables are inversely proportional to these objective functions. Higher draught and L_{BP} values result in more robust

designs for which high- and low fidelity methods for the calm water resistance calculation converge to a single value and the variation of the uncertain parameters of the problem does not result in high variation of the building cost, RFR and total resistance. This observation is supported by the results of the multi-criteria decision analysis which follows the optimisation run. The scenario which prioritises the significance of the objective functions related to the uncertainty ranks longer designs to the top.

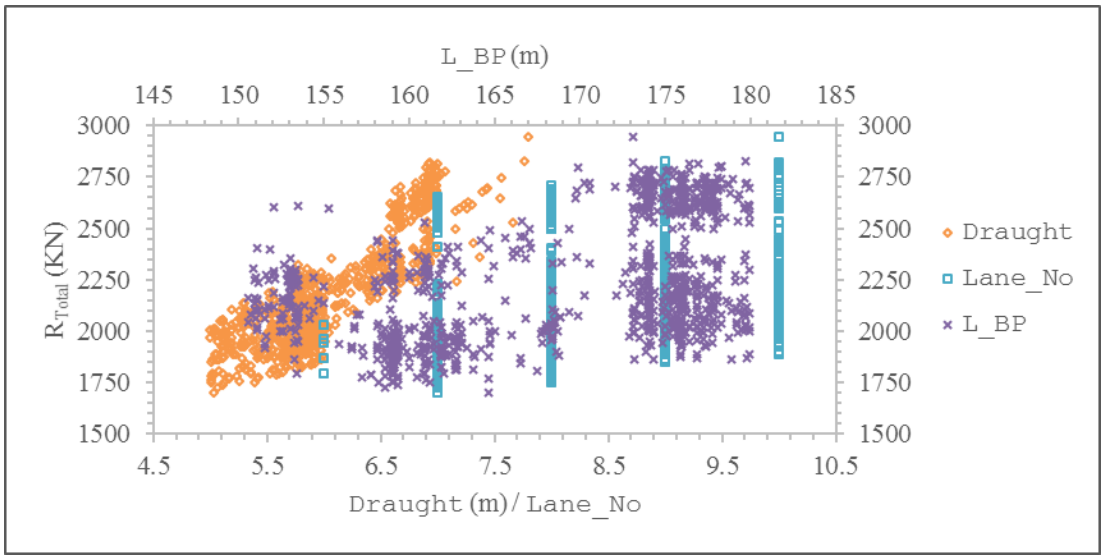

Figure 95: Comparison of total resistance with `Draught`, `Lane_No` and `L_BP`

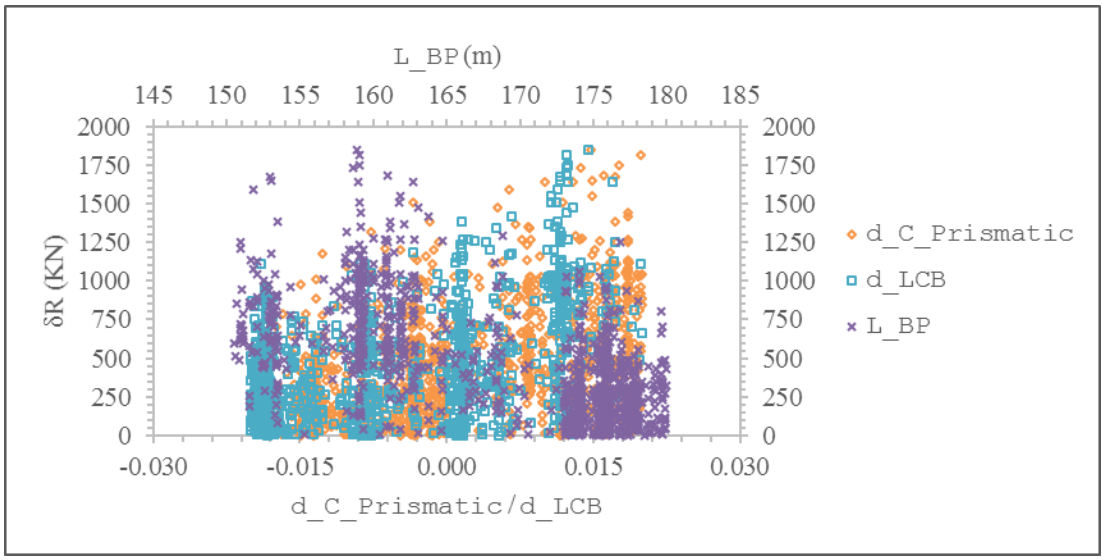

Figure 96: Comparison of δR with `d_C_Prismatic`, `d_LCB` and `L_BP`

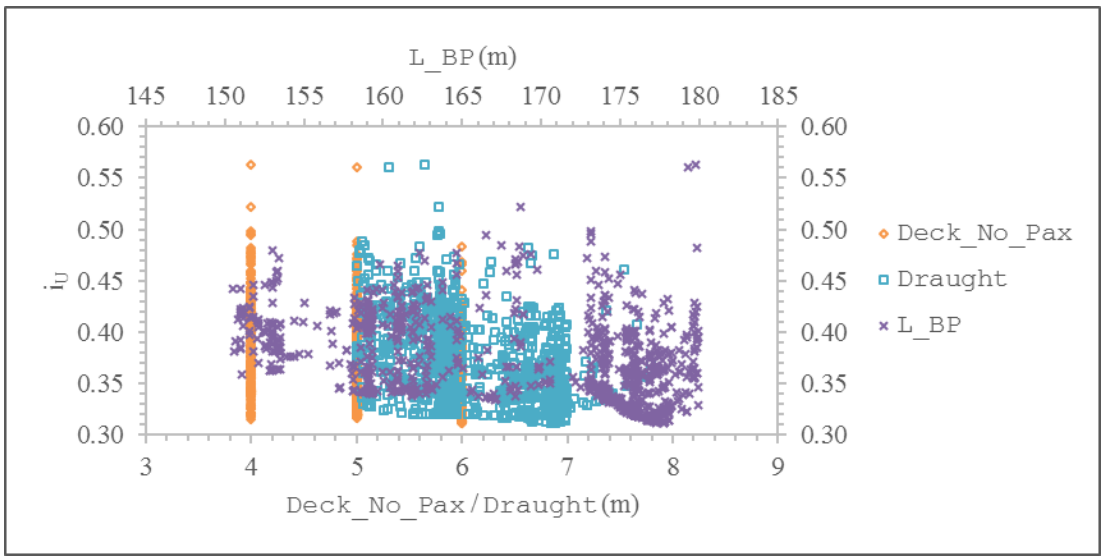

Figure 97: Comparison of i_U with `Deck_No_Pax`, `Draught` and `L_BP`

The number of passenger decks have a similar impact to the uncertainty indicator i_U, albeit to a lesser extent (correlation coefficient is found to be -0.22). On the other hand, `d_C_Prismatic` and `d_LCB` design variables have the opposite effect on δR objective function. Their correlation coefficient values of 0.44 and 0.47 respectively lead to the conclusion that convergence between the CFD and approximation method results is achieved as their value decreases (Figure 96 and Figure 97).

6.3.4 Multi-criteria decision analysis

The decision making process described in Paragraph 5.3.2 is applied to the NSGA 2 results and the optimal solution is identified. Three scenarios are defined (Table 28), each one considering the significance of each objective function differently. A utility function is defined taking as input the results of the NSGA 2 run and the weighting factors of each scenario (32). The sum of all five normalised and weighted objective values provides the final score for each design variant.

The first scenario considers all five objectives to be equally important. Hence, each objective is assigned a weight of 20%. Scenario 2 prioritises the objectives related to design robustness –δR and i_U– assigning a weighting factor of 35% to each of them. The remaining objectives are assigned a weighting factor of 10%. Scenario 3 is the

opposite of scenario 2, i.e. priority is given to building cost, RFR and total resistance, with each one being assigned a weighting factor of 25%, while δR and i_U are considered less important, appointed a weighting factor of 12.5% each.

The ranking of the best designs for each scenario is presented in Figure 98, Figure 99 and Figure 100. In all cases, a score of one denotes the best design, while a score of zero denotes the worst performing variant.

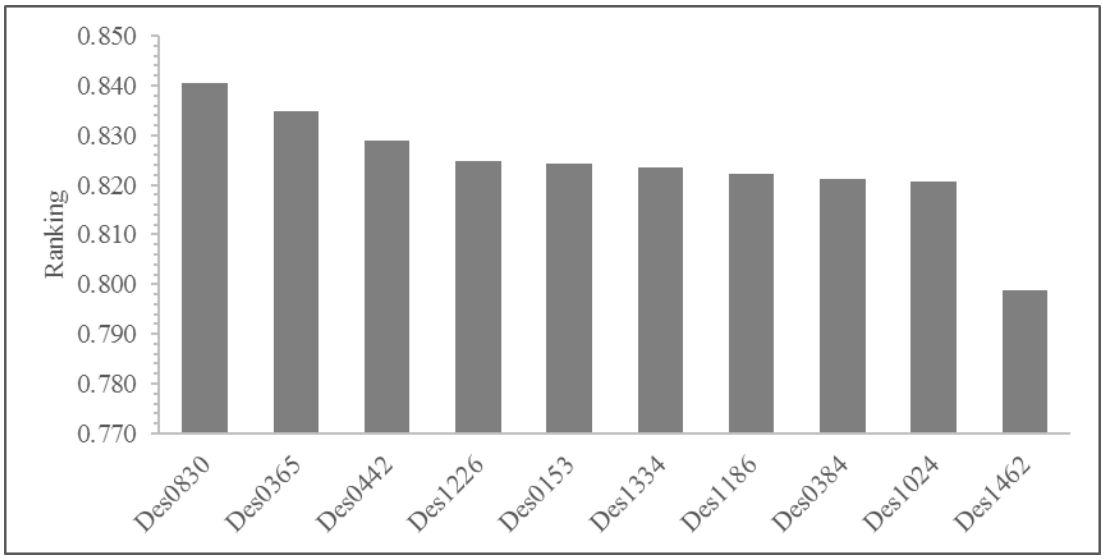

Figure 98: Scenario 1 results for the Ro-Pax vessel case study

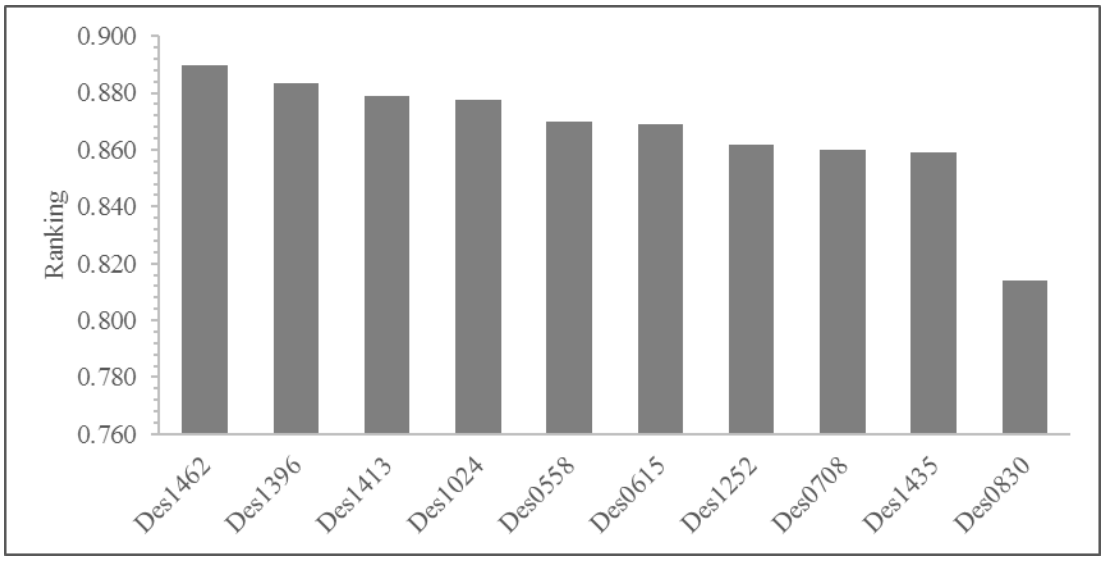

Figure 99: Scenario 2 results for the Ro-Pax vessel case study

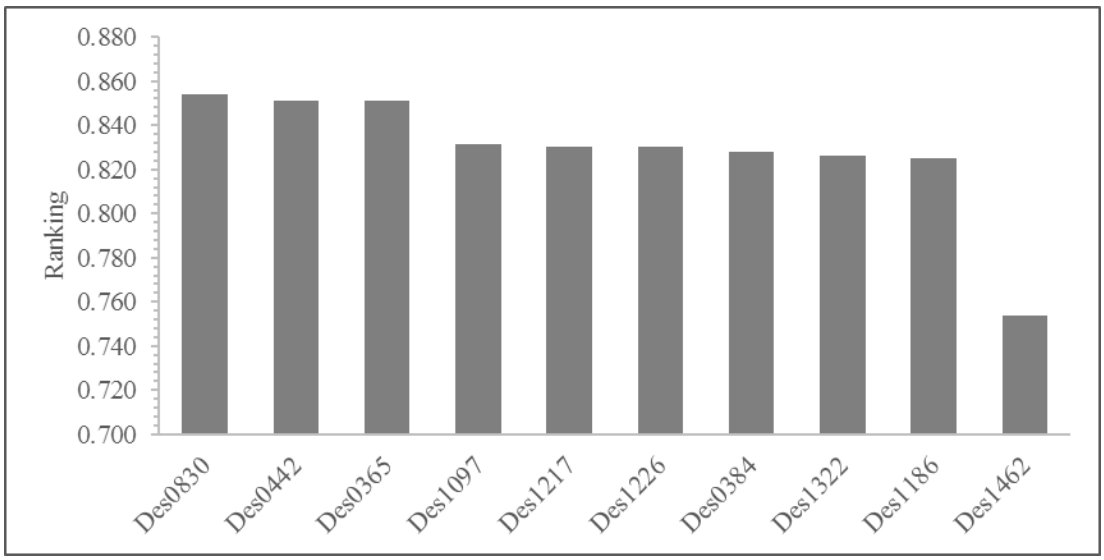

Figure 100: Scenario 3 results for the Ro-Pax vessel case study

The decision making analysis identifies two optimal designs, namely Des0830 and Des1462. The former dominates scenarios 1 and 3, while the latter is identified as the dominant robust design, ranking first in the second scenario. In addition, the difference in the results between the two designs in each scenario is evident, with Des0830's score in scenario 2 being 8.5% lower than Des1462. Likewise, Des1462's score is 5% and 11.8% lower than Des0830 in scenario 1 and 3 respectively. The design variable values for the two designs are presented in Table 38, while their performance is presented in Table 39. The CAESES® and NAPA® models for the two optimal designs are presented in Figure 101, Figure 102, Figure 103 and Figure 104.

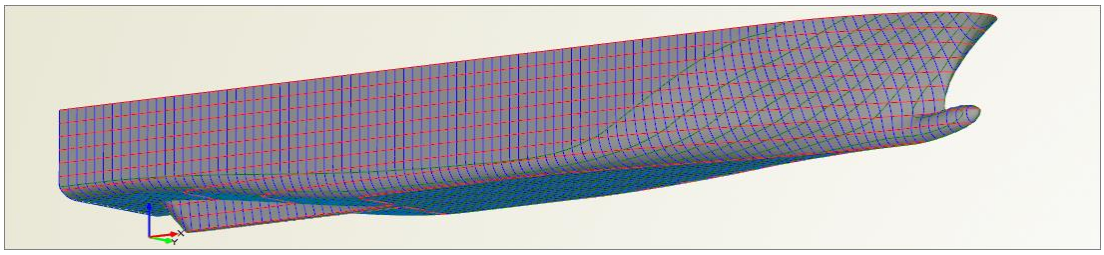

Figure 101: Des0830 CAESES® model

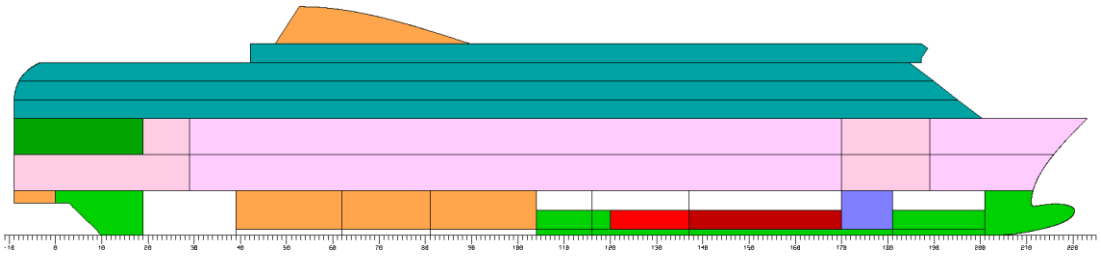

Figure 102: Des0830 NAPA® model

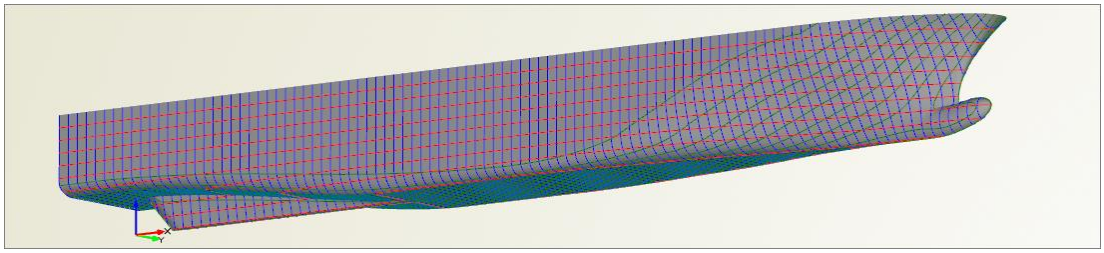

Figure 103: Des1462 CAESES® model

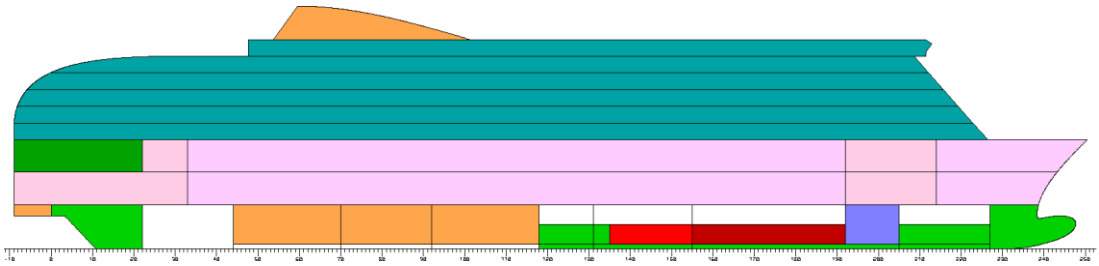

Figure 104: Des1462 NAPA® model

Two conclusions can be drawn from the decision making analysis. Firstly, the effect of uncertainty in ship design optimisation becomes evident, as the scenario which promotes robustness ranks first a design whose performance is inferior to other variants otherwise. A safer decision is always related to a more conservative solution and this is the case in this optimisation problem. However, the enhanced robustness of Des1462 ensures that the performance levels are less likely to vary should uncertain external parameters change. For instance, Des1462's lower uncertainty indicator i_U value indicates that its building cost is less likely to deviate from the identified value of 60.1 million $. Likewise the RFR value of 68.54 $ (economy passenger ticket for middle season for the investigated operational profile) is more likely to compensate for changes in fuel price throughout the vessel's lifetime.

Table 38: Main set of design variables for Des0830 and Des1462

Design variable	Des0830	Des1462
Bilge_A	3.260	2.651
Bilge_B	3.166	2.246
DB	0.932	0.797
Deck_No_Pax	4	6
Deck_No_RoRo	2	2
Draught	5.165	5.945
d_C_Prismatic	-0.01891	-0.01491
d_LCB	0.00162	0.01292
Lane_No	8	7
L_BP	157.196	177.550

Table 39: Des0830 and Des1462 response to objective functions

Objective	Des0830	Des1462
Building cost (C_B) (M $)	56.0	60.1
Calm water resistance difference between CFD and approximation methods (δ_R) (KN)	364	7
RFR ($)	50.85	68.54
Total resistance (R_{Total}) (KN)	1777	2084
Uncertainty indicator for the investigated objective functions (C_B, RFR, R_{Total}) (i_U)	0.3697	0.3213

Secondly, the top ranking of Des0830 in the two remaining scenarios shows the robustness of the optimisation setup and methodology. NSGA 2, given the optimisation setup presented in Paragraph 5.3.2, managed to detect a design which

performs well irrelevant of the weighting factors of scenarios 1 and 3. Des0830 is identified as an all-around solution with regard to the building cost, RFR and total resistance and assures the user that is superior to the remaining design variants produced during the optimisation run.

In the following graphs, some indicative results of the NSGA 2 run are presented, identifying the identified optimal designs, the baseline design and the Pareto front.

Figure 105 presents the relation between i_U and building cost. Minimisation of both values is desired and an aggregation of design variants is spotted in the region of 0.34-0.35 for the i_U and 57-60 million $ for the building cost. Both identified optimal designs are lying on the Pareto front while the baseline design is located far away which illustrates the benefits of the optimisation process.

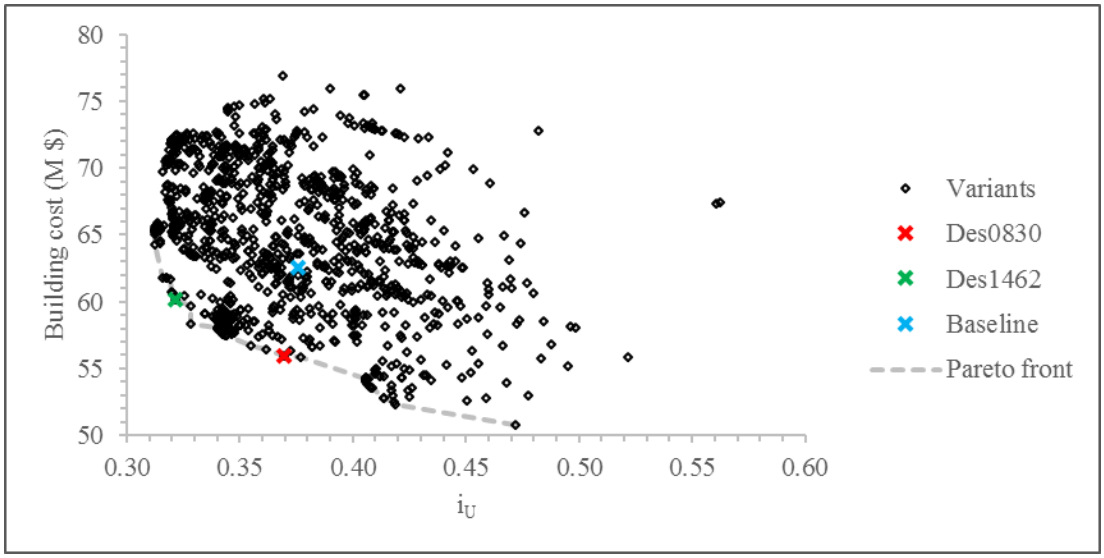

Figure 105: i_U vs. building cost

The relation between RFR and δR is demonstrated in Figure 106. The majority of the generated designs lie in the region of 40-65 $ for the RFR. A small group of design variants performed poorly with regard to this objective, achieving values of around 120 $ which is considerably higher than the optimal or baseline designs. Following the analysis on the relation between the design variables and the objectives, presented in Paragraph 6.3.3, the strong connection between RFR and the number of

car lanes justifies this trend; the majority of designs achieving high RFR values are associated with low `Lane_No` values (Figure 94). The latter leads to decreased transportation capacity which has an impact on the ticket price in order to even out the vessel's expenses. Des0830 does not lie on the Pareto front regarding the two objective functions as one of them is a robustness indicator (δR), which is not acknowledged significant in scenarios 1 and 3, where Des0830 ranks first. On the other hand, Des1462 is part of the Pareto front, since its selection among the design variants is mainly based on its performance with regard to δR.

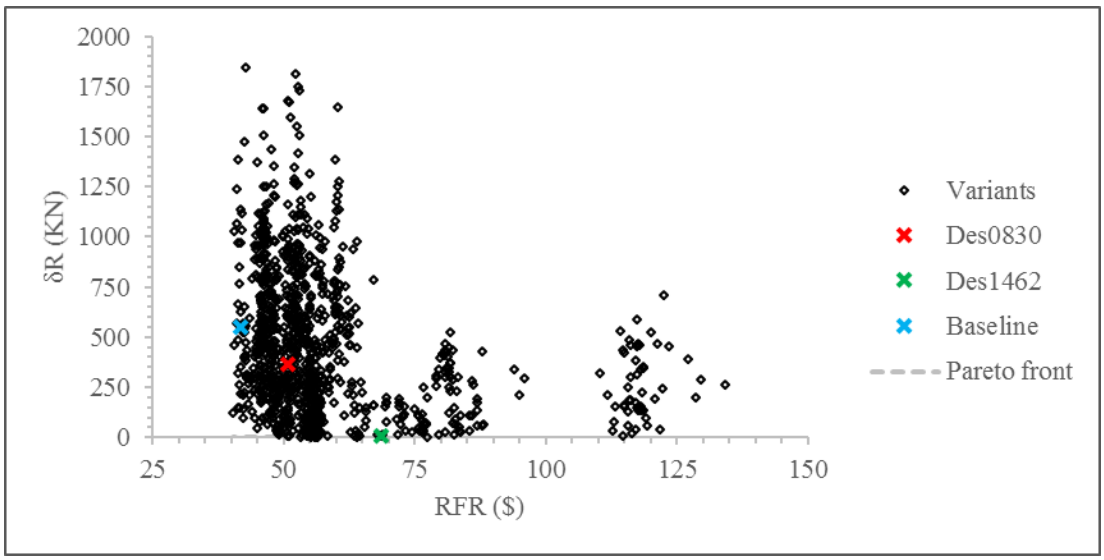

Figure 106: RFR vs. δR

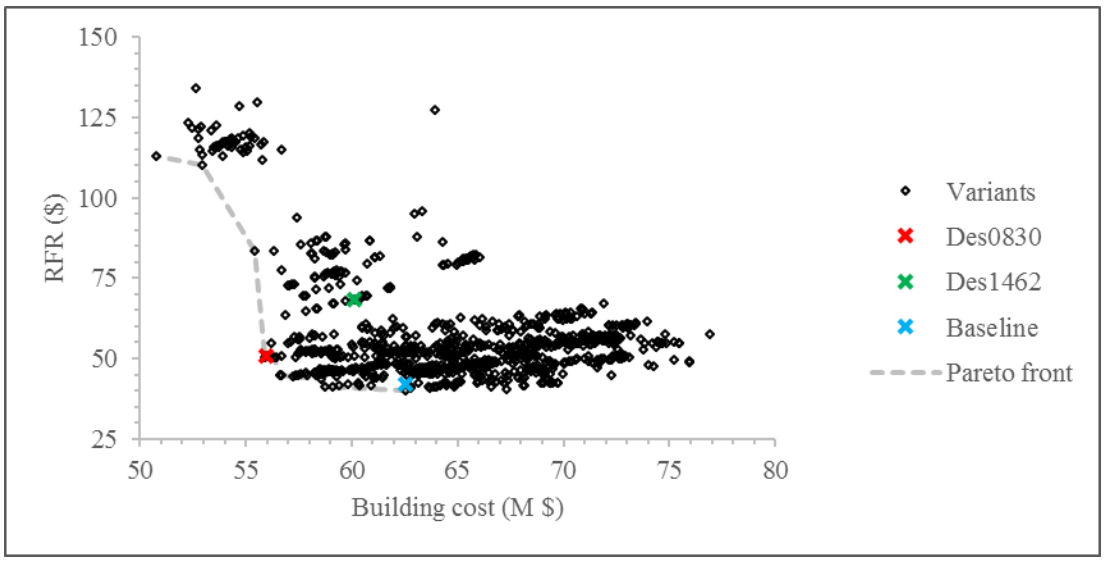

Figure 107: Building cost vs. RFR

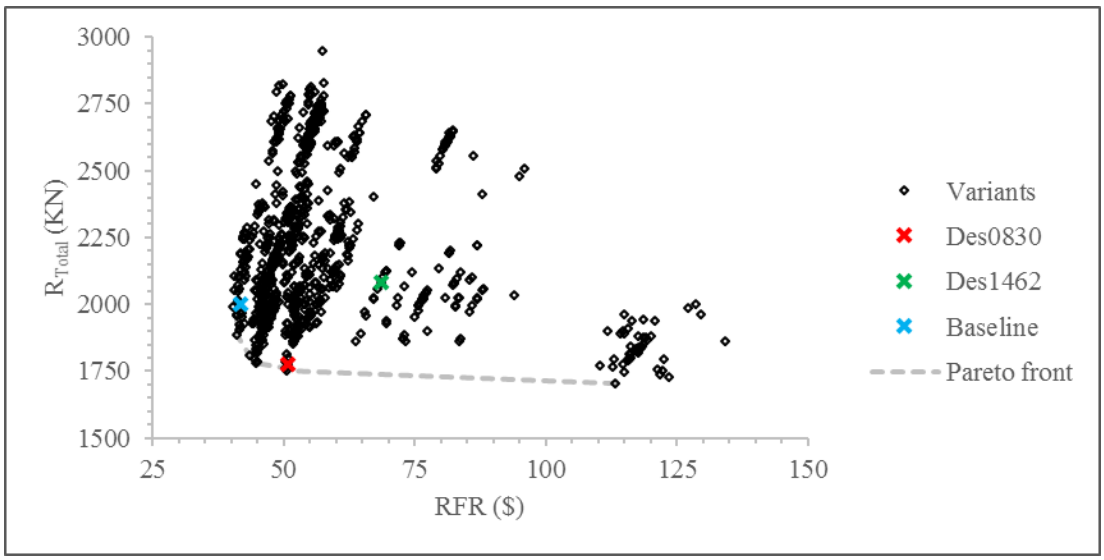

Figure 108: RFR vs. total resistance

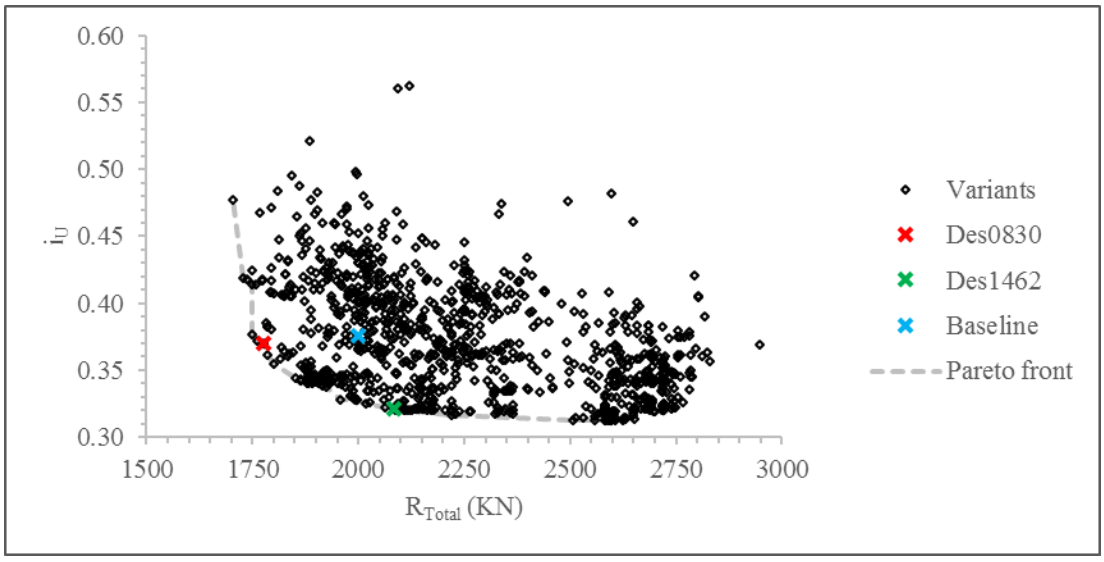

Figure 109: Total resistance vs. i_U

Figure 107 illustrates the relation between the building cost and the RFR. The same pattern described above is observed regarding the RFR in this graph. For each design group –based on the RFR value– a slight increase in the building cost can be noticed. This is interpreted by the fact that both objectives are closely related, as the RFR is calculated based on the building cost; the higher is the value of the latter, the greater is the former to compensate for the higher initial costs. As far as the two identified optimal designs are concerned, Des0830 is part of the Pareto front, contrary to

Des1462, for which the selection in scenario 2 is not heavily influenced by the two examined objectives.

The relation between RFR and total resistance is presented in Figure 108. An increase in the RFR is observed as the total resistance value rises. This trend is expected due to the increased power requirements associated with higher resistance values. This leads to increased fuel consumption which affects the running costs, used to calculate the RFR.

Finally, Figure 109 shows the relation between the total resistance and i_U. Although minimisation of both objective values is desired, a decrease in the uncertainty is achieved as the total resistance increases. This remark is connected to the correlation analysis performed in Paragraph 6.2.3 (Figure 97). Increase of draught results in lower i_U values, while at the same time, resistance is increased.

A comparison between the identified optimal designs and the baseline model is presented in Table 40, showing the differences in their performance.

Table 40: Optimal designs and baseline model response to objective functions for the Ro-Pax vessel case study

Objective	Baseline	Des0830	% Diff.	Des1462	% Diff.
Building cost (C_B) (M $)	62.5	56.0	-10.5	60.1	-3.8
Calm water resistance difference between CFD and approximation methods (δ_R) (KN)	548	364	-33.7	7	-98.7
RFR ($)	41.86	50.85	21.5	68.54	63.7
Total resistance (R_{Total}) (KN)	1999	1777	-11.1	2084	4.3
Uncertainty indicator for the investigated objective functions (C_B, RFR, R_{Total}) (i_U)	0.3756	0.3697	-1.6	0.3213	-14.4

Overall, both improved designs perform better than the baseline model except for the RFR, which is higher in both selected designs. Des1462 is a more conservative solution to the problem, hence the slighter improvements compared to Des0830. Nevertheless, the former achieves the best responses with regard to the robustness indicators (δR and i_U). It becomes clear that uncertainty influences the selection of optimal solutions in the ship design problem. By prioritising its significance in the decision making process, a more conservative –yet robust– design is identified for which the user feels more confident that its performance remains unchanged when uncertain parameters vary.

6.4 Summary

The results of the optimisation for the two case studies are presented in this Chapter, illustrating the effect of the design variables, problem setup, surrogate models and uncertainty on the optimal design selection. Two different ship types are being optimised focusing on different objectives. Uncertainty quantification is taken into account in both cases, however, its incorporation into the setup is different; in the containership case study uncertainty is considered during the decision making phase, while in the Ro-Pax vessel case study it is minimised during the main optimisation run.

As far as the utilisation of surrogate models is concerned, significant time savings are achieved in both case studies in all three stages of the problem where surrogate models substitute the actual simulations. The interconnection of specialised software and the use of high-fidelity time-consuming software tools call for a solution to the encumbrances they induce in the setup of the optimisation problem. In total, more than an hour would be needed to complete all calculations avoiding the use of surrogate models. On the contrary, utilisation of the latter in key stages of the problem reduces the computation time to less than five minutes pre design variant. It becomes clear that a multi-objective optimisation problem incorporating the holistic approach to ship design requires clever utilisation of available tools and techniques to produce accurate results and benefit from modern technology. Yet, this does not

come without any drawbacks, as surrogate models cannot match the accuracy of the proper simulations. The results presented in Paragraphs 6.2.2 and 6.3.2 illustrate this disadvantage; values produced by the surrogate models varied up to 2.5% from the original simulations. This difference should be considered during the analysis of the results and not ignored when the final decision is taken. Nevertheless, the advantages they offer cannot be overlooked, as they certainly offer a comprehensive view on the ship design optimisation problem.

The investigation of the relation between design variables and objectives shows not only how the former affect the latter, but also the impact of the latter on the optimisation problem. Several objectives contradict with each other, rendering the convergence of the optimisation algorithm in a clear solution a real challenge. Often, improvement in one objective results in poor performance with regard to another one. This is the case in most real-life problems and proves that ship design optimisation is not a trivial task. The decision making phase in multi-objective optimisation problems is a key stage which requires careful selection of methods and approaches to distil the raw results produced by an optimisation algorithm and identify the optimal solution.

Through the application of the holistic model in the optimisation process, the designer is able to identify which objectives are the most critical in the design process. The holistic approach incorporates various aspects of the ship's nature, such as stability, structural integrity, logistics and efficiency, all expressed as objectives and constraints. The variety of the objectives inspected throughout the optimisation process produces valuable results, available to the end user, who can identify not only the correlation between the design variables and the optimisation objectives, as mentioned earlier, but also can have a clear view of which measures of merit have the strongest impact in the overall procedure and understand their significance in the design process.

The analysis of the results of the optimisation run demonstrates the effect of constraints on the feasibility of the design variants. In both case studies, newly

introduced and developed regulations are applied and the percentage of invalid designs violating the constraints related to these regulations prove that their effect on ship design is considerable. The IMO second generation intact stability criteria will most probably have a considerable impact on containership design, while the introduction of the EEDI rule to the Ro-Pax vessel category may induce changes on the operational profile of passenger vessels. The results of the optimisation study provides indications on how ship design changes along the time, when design, operational and regulatory constraints are constantly introduced and become part of the problem.

In both case studies, the selected NSGA 2 setup generates clear Pareto fronts, indicating the fast convergence of the algorithm to an optimal solution. As mentioned in Paragraph 5.2.2, similar optimal solutions have been identified on a similar optimisation problem setup, regardless of the total number of design variants. Nevertheless, a different combination of number of generations and population size can be tested in the future to verify the results of the present study.

The results related to uncertainty quantification provide a new insight on how ship design methodology should be structured. Uncertainty has been incorporated in ship design studies; however the extent to which it is applied varies. Two different approaches are presented in this thesis, leading to different trends among the results.
In one case, uncertainty is incorporated in the decision making phase, defining a non-linear utility function which ranks the produced design variants according to their robustness levels. On the one hand there are designs which perform significantly better than other but they lack in robustness. On the other hand, designs which are highly robust compared to other produced design variants are generated by NSGA 2. The decision making phase aims at finding the right combination of these two elements among the design variants and identify a design with an improved overall performance, while ensuring this performance does not deviate when uncertain parameters vary. The results show that the ideal, perfect combination of superior performance and remarkable robustness is not feasible and the decision maker needs to compromise between the two aspects.

In the second case study, uncertainty is incorporated in the main optimisation phase, where it becomes an objective the genetic algorithm aims to minimise. This approach leads to production of design variants which essentially are improved in terms of robustness compared to the baseline model. Since uncertainty becomes part of the objective functions, the overall results are more conservative than in the first case where NSGA 2 does not take uncertainty into account. Presumably, a new round of calculations for the Ro-Pax vessel case study ignoring the objective related to uncertainty would produce different results. However, the decision maker is ensured that the optimal design identified during the decision making phase is more robust than the baseline model. This is proved by the results presented in Paragraph 6.3.4. Two optimal designs are found, both achieving lower values with regard to objective i_U. A higher weighting factor assigned to this objective results in a much more robust design than in any other case and this is reflected by its more conservative response to the non-related to uncertainty objective functions.

7 Discussion and conclusions

7.1 Introduction

The thesis ends with some conclusions and final remarks presented in this Chapter. The work performed for this PhD topic is reviewed, summarising its key parts and findings. The novelty elements of the thesis are analysed and evaluated, while based on the detailed presentation of the workflow and the results of this study in Chapters 4, 5 and 6, the thesis objectives outlined in Chapter 1 are reviewed. Finally, recommendations for future work on this subject are presented.

7.2 Thesis review

Shipping industry has become very competitive, with a lot of research being carried out to investigate possible ways to improve ship design and create efficient and economical ships. Technological improvements allow the detailed exploration of design space and assist the theory of optimisation in becoming a vital part of ship design.

The topic of ship design optimisation has been investigated by numerous researchers, resulting in establishment of techniques and structured methodologies which can be applied to real case studies and produce efficient solutions to the ship design problem. Starting from the fundamentals (Evans, 1958), which set the base for this particular research field, and moving on to the more recent developments (HOLISHIP, 2016-2020), it becomes clear that the definition of the ship design problem constantly changes; researchers integrate new design aspects in existing methodologies, concentrate on specific areas of naval architecture to improve the

precision levels of the obtained results, or investigate the effect of new constraints to the problem, resulting from new developments in the industry.

This thesis contributes to the aforementioned developments with regard to the ship design optimisation problem. The mission is to develop a methodology for a multi-objective robust early stage ship design optimisation under uncertainty. Adhering to the most recent model developed for the multi-objective design optimisation – namely the holistic model– the enhancement and further development of previously proposed methodologies is achieved, while several aspects of ship design are incorporated, taking into account the three main categories associated with the operation of a ship; economics, safety and environment. Various performance indicators are used as measures of merit to evaluate the response of possible solutions to the problem.

A parametric ship model is defined, controlling both the hull form and the internal compartmentation through a variety of parameters. The performance indicators are defined receiving as input various aspects of the defined ship model and become the objective functions of the problem. Recent developments in the shipping industry are taken into consideration for the definition of the latter. Regulations affecting the operation and design of ships, such as the EEDI and the IMO second generation intact stability criteria, are incorporated to the problem definition to investigate their effect on the optimal design selection.

Advancements in computing allow not only the utilisation of powerful software tools to perform complex calculations, such as CFD, but also the integration of such tools in an optimisation problem. High-fidelity techniques are incorporated in the design methodology through use of surrogate models –approximation models imitating the behaviour of the original tools producing results based on data deriving from the original calculations. Utilisation of surrogate models in an optimisation study offers a level of accuracy in results which is similar to the one obtained by running the original simulations, yet at a fraction of the computational time required by the latter.

In this work, surrogate models are used in key areas of the methodology, taking into account eligibility issues, such as the computational setup or the computational time per design variant. In particular, CFD calculations for the estimation of the calm water resistance, calculations for the evaluation of the IMO second generation intact stability criteria and calculations relative to the uncertainty quantification of the problem are substituted by surrogate models. The result is a remarkable reduction of the time needed to evaluate a single design during the optimisation phase. The definition of the surrogate models starts with the preparation phase which involves several designs of experiment to obtain the training data set, continues with the generation phase, during which the approximation model is constructed and ends with the evaluation phase when their accuracy is tested and verified.

Genetic algorithms are utilised for the solution of the optimisation problem. The user is able to select the design variables of the problem, choosing to perform a global or a local design optimisation. In addition, the user decides which are the objective functions and constraints of the problem. The solution of the multi-objective optimisation problem concludes with the multi-criteria decision analysis. The optimisation algorithm produces a Pareto front of designs with regard to the investigated objective functions; however the designer needs to set up a decision making model to identify the optimal design. The utility function approach is employed in this thesis, which suggests which the best solution is according to the user's priorities through the utilisation of weighting factors, which quantify the significance of each objective.

Design uncertainty is monitored throughout the optimisation process. As mentioned in Paragraph 2.3.3, research has been undertaken with regard to capturing the uncertainty in ship design. Various approaches have been introduced. In this work a novel way of capturing the uncertainty in design is tested through two different case studies. Apart from incorporating uncertainty in the constraints of the optimisation, the former becomes a vital part of the decision making process or the optimisation phase. The stages at which uncertainty effects on ship design are taken into account influence the optimisation results.

The proposed methodology is validated through two case studies involving different ship types and optimisation setups. The application of uncertainty quantification is implemented in different ways to investigate its impact on the results.

The results of the multi-objective optimisation study of both cases provide an insight on the robustness of the methodology. The effect of surrogate models on the computational time is evaluated. The consideration of recent developments in the shipping industry (e.g. IMO second generation intact stability criteria) is investigated by applying newly introduced and recently developed regulations to ship types for the first time. The results indicate how the former affect the current ship design trends and show indications of possible changes in the latter in the near future.

The impact of different design variables on contradictive objective functions underline the complexities associated with holistic ship design optimisation; it becomes clear that the ideal solution is not always available.

Finally, the stage of the proposed methodology at which uncertainty quantification is applied influences the optimisation results. More conservative solutions are promoted either during the optimisation phase or the decision making process. The robustness of the results becomes an important factor during the optimal design selection and the application of the methodology shows the contradiction between optimal performance and enhanced robustness of the produced designs.

7.3 Novelty elements

This study proposes a ship design optimisation methodology incorporating novel elements concerning design uncertainty and recent developments in the shipping industry. Through this study, an expansion and improvement of current ship design methodologies is achieved. A robust approach to ship design optimisation is essentially introduced, emphasising on the effects of uncertainty in ship design and benefiting from the utilisation of state-of-the-art tools. In particular, proper use of software tools allows the establishment of a core platform, such as CAESES®,

which supports the integration of all the necessary tools to perform the required simulations in a fast and efficient manner.

The study explores the ways uncertainty quantification can be applied to an optimisation methodology. The effects of each approach is analysed and compared with a deterministic solution of the same problem where uncertainty is disregarded. The analysis leads to some general conclusions regarding the effects of uncertainty in optimisation, but also reveals specific trends related to each approach. Uncertainty influences the optimal solution. A deterministic approach produces more radical solutions with improved performance which often does not correspond to real-life application. On the other hand, optimisation under uncertainty takes into account the effect of uncertain parameters and evaluates the response of a potential optimal solution comprehensively, emphasising on its robustness.

Integration of uncertainty in various stages of the optimisation has a different impact on the results. Measurement of the uncertainty of the applied constraints results in a stricter evaluation of the validity of the design variants, thus altering the feasible design space and the availability of improved designs. Consideration of uncertainty as a measure of merit does not limit the feasible design space; however it affects the way the employed algorithm works towards the identification of the optimal solution. The minimisation of uncertainty is desired and becomes priority during the search for improved designs. This results in production of a more robust and conservative pool of design variants the user is able to choose from. Finally, incorporating uncertainty in the decision making phase of a multi-objective optimisation problem influences the selection of the optimal solution. The pool of available designs is produced regardless of their robustness levels; however the latter becomes an important factor in the optimal design selection. The decision making analysis leads to the selection of robust, yet conservative solutions, which do not necessarily lie on the Pareto front defined by a deterministic solution of the problem.

As far as the ongoing developments in the shipping industry are concerned, this study takes into consideration two major regulations which are either recently

enforced or towards their finalisation. Their effect on the design of specific ship types is investigated for the first time and conclusions are drawn. EEDI rules are now applied to passenger vessels and the proposed methodology incorporates them as one of the optimisation constraints. The number of invalid designs due to the application of this constraint indicates the impact of the latter to the current design trends and operational profiles structure. The evaluation of the IMO second generation intact stability criteria becomes part of the optimisation constraints and influences the feasible design space of two different ship types. International regulations become stricter and the results of this study demonstrate their significance in ship design.

7.4 Accomplishment of thesis objectives

In Chapter 1, the objectives for this thesis are outlined. Following the detailed description of the work undertaken for this study, it is possible to evaluate their accomplishment.

- A detailed parametric ship model is defined for this study, including both the exterior (hull shape) and the interior (internal compartmentation), as well as all the required functions to evaluate the model's performance. The strategic introduction of parameters in the parametric model allows the user to select which act as the design variables of the optimisation problem, depending on the nature of the problem.
- The proposed methodology is based on existing models for the multi-objective optimisation of ship design, benefiting from high-fidelity software tools' computational capabilities, as well as efficient engineering methods (e.g. surrogate models) which reduce computational time while retaining accuracy and reliability in the obtained results.
- Elements deriving from the holistic design concept are integrated in the proposed methodology, defining performance indicators which are related to the three main aspects of ships' operation; economics, safety and environment.

Each of these aspects is evaluated by various objective functions and constraints, providing a broader view of the design performance.

- Three failure modes of stability introduced in the IMO second generation intact stability criteria are included in the proposed methodology. Each design variant in the optimisation process is evaluated to check their compliance to the newly developed rules. The optimisation results indicate that the proposed criteria are violated by a number of generated designs and suggest that the former will affect ship design in the near future.
- A key aspect of this study, design under uncertainty, is taken into account in different levels of the proposed methodology. One of the aims of this study is to develop a design optimisation method which promotes robustness in the results by using probabilistic models to perform the required calculations and capture the uncertainty in the design process. The results indicate that consideration of uncertainty influences the outcome of an optimisation study.
- This study incorporates a variety of power- and time-demanding software tools for the calculation of the required parameters used throughout the optimisation process. To make the overall process less time-consuming, surrogate models are utilised, increasing the speed of the optimisation runs without compromising in accuracy.
- The proposed methodology is evaluated by two case studies involving different ship types and optimisation setups. Application of some of the key elements of this study (e.g. capture of uncertainty) varies among the cases to explore their effects in the overall process.

7.5 Future work

Through the work carried out for this study, potential future research areas are identified, which can extend the research scope and thesis impact.

Firstly, the proposed methodology is applied on two ship types for demonstration purposes of this study. It would be interesting to expand this research to more case

studies, involving different types of merchant ships, such as oil tankers, bulk carriers or cruise ships. Each of the aforementioned ship types involve various operational profiles and used in different markets. Therefore, new objective functions can be introduced, specific to the purpose of each vessel.

This study focuses on a global optimisation of the main particulars of two different ship types. However, the formulation of the problem and the parametrisation process followed in the proposed methodology allows the selection of different parameters to become the design variables set of the optimisation problem. Depending on the measures of merit, a local hull form optimisation can be carried out to investigate further the results of a global optimisation process.

Implementing the holistic ship design optimisation approach in a literal way is a rather challenging task. One of the definitions of "holistic" in ship design is to examine every aspect related to a ship's life cycle and evaluate its response holistically. This study incorporates elements of this approach; yet there are opportunities to expand the focus areas beyond the scope of this thesis. For instance, a detailed investigation of the propulsion systems could be integrated to the proposed methodology, manoeuvring and detailed seakeeping behaviour of the ship could be investigated, while damage stability of the ship could be examined to enhance the safety aspect of the ship's life. The design uncertainty quantification of the ship design problem could be expanded through the addition of the aforementioned focus areas of naval architecture and improve further the robustness of the results.

As far as the surrogate models methods are concerned, in this thesis a global approximation method is utilised, which accepts as input known data and creates a surrogate model that can estimate a response for a new set of data. The accuracy of this method is evaluated in this work; however, a further investigation could be carried out on other available techniques and compare the outcome. Similarly, different optimisation algorithms could be tested and analyse the difference in the quality of the results, convergence to optimal solution and overall computational time.

7.6 Summary

In this Chapter the thesis is reviewed, summarising its key features, while identifying the novelty elements of this work. A description of the accomplishment of the research aim and objectives is provided. Through the research outcome, future work recommendations are presented.

References

Abt, C. & Harries, S. 2007. Hull Variation and Improvement Using the Generalised Lackenby Method of the Friendship-Framework. *The Naval Architect***,** 166-167.

Agarwal, H. 2004. *Reliability Based Design Optimization: Formulations and Methodologies.* Doctor of Philosophy, University of Notre Dame.

Agarwal, H. & Renaud, J. 2004. Reliability Based Design Optimization Using Response Surfaces in Application to Multidisciplinary Systems. *Engineering Optimization,* 36.

Aistleitner, C., Hofer, M. & Tichy, R. 2012. A Central Limit Theorem for Latin Hypercube Sampling with Dependence and Application to Exotic Basket Option Pricing. *International Journal of Theoretical and Applied Finance,* 15.

Andrews, D. & Erikstad, S. O. 2015. State of the Art Report on Design Methodology. *12th International Marine Design Conference.* Japan.

Andrews, D., Kana, A. A., Hopman, J. J. & Romanoff, J. 2018. State of the Art Report on Design Methodology. *13th International Marine Design Conference.* Finland.

Azmin, F. M. & Stobart, R. 2015. Benefiting from Sobol Sequences Experiment Design Type for Model-Based Calibration. *SAE Technical Papers,* 1.

Baird, N. 2017. Global Ferry Market Surges. Available: www.bairdmaritime.com/work-boat-world/passenger-vessel-world?979-feature-global-ferry-market-surges.

Banks, C., Turan, O., Incecik, A., Theotokatos, G., Izkan, S., Shewell, C. & Tian, X. 2013. Understanding Ship Operating Profiles with an Aim to Improve Energy Efficient Ship Operations. *3rd Low Carbon Shipping Conference.* United Kingdom.

Barrico, C. & Antunes, C. H. 2006. Robustness Analysis in Multi-Objective Optimization Using a Degree of Robustness Concept. *IEEE International Conference on Evolutionary Computation.* Canada.

Bentley Systems 2014. Maxsurf. 20 V8i ed.

Bertram, V. 1998. Knowledge-Based Systems for Maritime Applications. *27th WEGEMT School on Expert Systems for Marine Applications.* Germany.

Bertram, V. 2003. Optimization in Ship Design. *Optimistic.* Germany: Mensch & Buch.

Bertram, V. & Isensee, J. 1998. Ship Design Applications of an Optimization Shell. *Workshop on Artificial Intelligence and Optimization for Marine Applications.*

Birk, L. 2003. Introduction to Nonlinear Programming. *Optimistic.* Germany: Mensch und Buch.

Bonney, J. & Leach, P. T. 2010. Slow Boat from China. Available: http://www.joc.com/maritime/slow-boat-china.

Boom, H., van den Huisman, H. & Mennen, F. 2013. New Guidelines for Speed/Power Trials. *SWZ/Maritime*.

Boulougouris, E. & Papanikolaou, A. 2009. Energy Efficiency Parametric Design Tool in the Frame of Holistic Ship Design Optimization. *10th International Marine Design Conference.* Norway.

Boulougouris, E. & Papanikolaou, A. 2013. Risk-Based Design of Naval Combatants. *Ocean Engineering,* 65**,** 61.

Boulougouris, E., Papanikolaou, A. & Pavlou, A. 2011. Energy Efficiency Parametric Design Tool in the Framework of Holistic Ship Design Optimization. *Proceedings of the Institution of Mechanical Engineers, Part M: Journal of Engineering for the Maritime Environment,* 225**,** 242-260.

Boulougouris, E., Papanikolaou, A. & Zaraphonitis, G. 2004. Optimization of Arrangements of Ro-Ro Passenger Ships with Genetic Algorithms. *Journal of Ship Technology Research,* 51**,** 99.

Branke, J., Deb, K., Miettinen, K. & Slowinski, R. 2008. *Multi-Objective Optimization: Interactive and Evolutionary Approaches,* Germany, Springer.

Brefort, D. & Singer, D. 2018. Managing Epistemic Uncertainty in Multi-Disciplinary Optimization of a Planing Craft. *13th International Marine Design Conference.* Finland.

Breinholt, C., Ehrke, K. C., Papanikolaou, A., Sames, P., Skjong, R., Strang, T., Vassalos, D. & Witolla, T. 2012. Safedor - the Implementation of Risk-Based Ship Design and Approval. *Procedia - Social and Behavioral Sciences,* 48**,** 753-764.

Bunker Index. 2018. *Bunker Index* [Online]. Available: https://www.bunkerindex.com [Accessed 2018].

Buxton, L. I. 1966. The Design of Tanker Hull Structures by Computer with Particular Reference to One Midship Cargo Tank. *Trans. RINA,* 108.

Buxton, L. I. 1976. *Engineering Economics and Ship Design,* United Kingdom, British Ship Research Association.

Choi, M., Erikstad, S. O. & Ehlers, S. 2015. Mission Based Ship Design under Uncertain Arctic Sea Ice Conditions. *34th International Conference on Ocean, Offshore and Arctic Engineering.* Canada.

CONTIOPT 2012-2013. Formal Safety Assessment and Optimization of Containerships. Germanischer Lloyd.

Cressie, N. 1990. The Origins of Kriging. *Mathematical Geology,* 22**,** 239-252.

Dai, C. & Hambric, S. 1995. Propeller Design Optimization Technique for the Minimization of Propeller Induced Vibration Using Artificial Intelligence and Numerical Optimization. *6th Practical Design of Ships and Mobile Units.* South Korea.

Dai, C., Hambric, S., Mulvihill, L., Tong, S. & Powell, D. 1995. A Prototype Marine Propulsor Design Tool Using Artificial Intelligence and Numerical Optimization Techniques. *Trans. SNAME,* 102.

De Groot, M. H. 1970. *Optimal Statistical Decisions,* USA, McGraw Hill.

De Jongh, M., Olsen, K. E., Berg, B., Jansen, J. E., Torben, S., Abt, C., Dimopoulos, G., Zymaris, A. & Hassani, V. 2018. High-Level Demonstration of Holistic Design and Optimisation Process of Offshore Support Vessel. *13th International Marine Design Conference.* Finland.

Deb, K. & Gupta, H. 2006. Introducing Robustness in Multi-Objective Optimization. *Evol Comput,* 14**,** 463-94.

Deb, K., Pratap, A., Agarwal, S. & Meyarivan, T. 2002. A Fast and Elitist Multiobjective Genetic Algorithm: Nsga-Ii. *IEEE Transactions on Evolutionary Computation,* 6**,** 182-197.

Diez, M. & Peri, D. 2010. Robust Optimization for Ship Conceptual Design. *Ocean Engineering,* 37**,** 966-977.

Dixit, A. 1989. Entry and Exit Decisions under Uncertainty. *Journal of Political Economy,* 97**,** 620-638.

Doyle, C. 2011. *A Dictionary of Marketing,* United Kingdom, Oxford University Press.

Du, X. & Chen, W. 2000. Towards a Better Understanding of Modeling Feasibility Robustness in Engineering Design. *Journal of Mechanical Design,* 122.

Duy, N. T. & Hino, T. 2015. Hydrodynamic Shape Optimization of a Container Ship Transom Using Navier-Stokes Analysis. *12th International Marine Design Conference.* Japan.

Eames, M. & Drummond, T. 1977. Concept Exploration - an Approach to Small Warship Design. *Trans. RINA,* 119.

Ehlers, S., Remes, H., Klanac, A. & Naar, H. 2015. A Multi-Objective Optimisation-Based Structural Design Procedure for the Concept Stage - a Chemical Product Tanker Case Study. *Ship Technology Research,* 57**,** 182-196.

Erfani, T. & Utyuzhnikov, S. V. 2011. Control of Robust Design in Multiobjective Optimization under Uncertainties. *Structural and Multidisciplinary Optimization,* 45**,** 247-256.

Erikstad, S. O. 1994. Improving Concept Exploration in the Early Stages of the Ship Design Process. *5th International Marine Design Conference.* The Netherlands.

Erikstad, S. O. & Rehn, C. F. 2015. Handling Uncertainty in Marine Systems Design - State-of-the-Art and Need for Research. *12th International Marine Design Conference.* Japan.

Eurostat 2018. Energy, Transport and Environment Indicators.

Evans, J. 1958. A Structural Analysis and Design Integration with Application to the Midship Section Characteristics of Transversely Framed Ships. *Trans. SNAME,* 66.

Evans, J. & Khoushy, D. 1963. Optimized Design of Midship Section Structure. *Trans. SNAME,* 71.

Fagerholt, K., Hvattum, L. M., Esbensen, E. F. & Nygreen, B. 2010. Using Decision Trees for a Stochastic Maritime Routing Problem. *24th European Conference on Operational Research.* Portugal.

Fisher, K. 1972. Economic Optimization Procedures in Preliminary Ship Design (Applied to the Australian Ore Trade). *Trans. RINA,* 114.

Friendship Systems 2018. Caeses. 4.4.1 ed.

Gale, P. A. 2003. The Ship Design Process. *Ship Design and Construction.* USA: SNAME.

Geoffrion, A. M. 1968. Proper Efficiency and the Theory of Vector Maximization. *Journal of Mathematical Analysis and Applications,* 22**,** 618-630.

Georgescu, C. & Verbaasm, F. B. H. 1990. Concept Exploration Models for Merchant Ships. *CFD and CAD in Ship Design.* The Netherlands.

Gilfillan, A. 1969. The Economic Design of Bulk Cargo Carriers. *Trans. RINA,* 111.

Goldberg, D. 1989. *Genetic Algorithms in Search, Optimization and Machine Learning,* USA, Addison-Wesley Longman Publishing Co.

Gregor, J. A. 2003. *Real Options for Naval Ship Design and Acquisition: A Method for Valuing Flexibility under Uncertainty.* Master of Science, Massachusetts Institute of Technology.

Gualeni, P. & Maggioncalda, M. 2018. Life Cycle Ship Performance Assessment (Lcpa): A blended Formulation between Costs and Environmental Aspects for Early Design Stage. *International Shipbuilding Progress,* 65**,** 127-147.

Guarin, L. 2007. Ro-Pax Vessel Specific Cost-Earning Model.

Gudenschwager, H. 1988. Optimierungscompiler Und Formberechnungsverfahren : Entwicklung Und Anwendung Im Vorentwurf Von Ro/Ro-Schiffen. *Schriftenreihe Schiffbau,* 482.

Guegan, A., Le Nena, R., Rafine, B., Descombes, L., Fadiaw, H., Marty, P. & Corrignan, P. 2018. Compliance Matrix Model Based on Ship Owners' Operational Needs. *7th Transport Research Arena.* Austria.

Han, S., Lee, Y. S. & Choi, Y. B. 2012. Hydrodynamic Hull Form Optimization Using Parametric Models. *Journal of Marine Science and Technology,* 17**,** 1-17.

Harries, S., Abt, C. & Brenner, M. 2015. Upfront Cad - Parametric Modeling Techniques for Shape Optimization. *11th International Conference on Evolutionary and Deterministic Methods for Design, Optimization and Control with Applications to Industrial and Societal Problems.* United Kingdom.

Hassan, G. & Clack, C. D. 2008. Multiobjective Robustness for Portfolio Optimization in Volatile Environments. *10th Annual Conference on Genetic and Evolutionary Computation.* USA.

Hoegh, M. W. 1998. *Options in Shipbuilding Contracts.* Master of Science, Massachusetts Institute of Technology.

HOLISHIP 2016-2020. Holistic Optimisation of Ship Design and Operation for Life Cycle. European Union.

Holland, J. 1975. *Adaptations in Natural and Artificial Systems,* USA, University of Michigan Press.

Holtrop, J. & Mennen, G. G. J. 1978. An Approximate Power Prediction Method. *International Shipbuilding Progress,* 25**,** 166-170.

Hughes, O. 1983. *Ship Structural Design - a Rationally Based, Computer-Aided, Optimization Approach,* United Kingdom, John Wiley & Sons.

Hurst, R. 1971. Advanced Techniques in Ship Design and Construction. *Lloyd's List*.

IMO 2004. International Convention for the Control and Management of Ships' Ballast Water and Sediments. *In:* IMO (ed.). United Kingdom.

IMO 2012a. Consideration of the Energy Efficiency Design Index for New Ships - Minimum Propulsion Power to Maintain the Maneuverability in Adverse Conditions. *In:* IMO (ed.). United Kingdom.

IMO 2012b. Guidelines for Calculation of Reference Lines for Use with the Energy Efficiency Design Index (Eedi). *In:* IMO (ed.). United Kingdom.

IMO 2012c. Guidelines on the Method of Calculation of the Attained Energy Efficiency Design Index (Eedi) for New Ships. *In:* IMO (ed.). United Kingdom.

IMO 2016. Finalization of Second Generation Intact Stability Criteria. *In:* IMO (ed.). United Kingdom.

IMO 2018. Finalization of Second Generation Intact Stability Criteria. *In:* IMO (ed.). United Kingdom.

Jensen, G. 1994. *Moderne Schiffslinien. Handbuch Der Werften,* Hansa.

Jones, W. P. & Launder, B. E. 1972. The Prediction of Laminarization with a Two-Equation Model of Turbulence. *International Journal of Heat Mass Transfer,* 15**,** 301-314.

Kanerva, M. 2002. Simulation Based Ship Design with Parametrized 3d Modelling. *6th Annual European CATIA Forum.* France.

Kiss, R. K. 1980. Mission Analysis and Basic Design. *Ship Design and Construction.* USA: SNAME.

Köpke, M., Papanikolaou, A., Harries, S., Nikolopoulos, L. & Sames, P. 2014. Contiopt - Holistic Optimisation of a High Efficiency and Low Emission Containership. *Transport Research Arena 2014.* France.

Kuniyasu, T. 1968. Application of Computer to Optimization of Principal Dimensions of Ships by Parametric Study. *Jpn Shipbuild Mar Eng*.

Kupras, L. 1976. Optimization Method and Parametric Study in Precontracted Ship Design. *International Shipbuilding Progress,* 23.

Lackenby, H. 1950. On the Systematic Geometrical Variation of Ship Forms. *Transactions of RINA,* 92**,** 289-316.

Levander, K. 2012. *System Based Ship Design,* Norway, Norwegian University of Science and Technology.

Liu, D., Hughes, O. & Mahowald, J. 1981. Applications of Computer-Aided, Optimal Preliminary Structural Design Method. *Trans. SNAME,* 89.

Lloyd's Register 2014. Rules and Regulations for the Classification of Ships. *In:* Lloyd's Register (ed.).

Mandel, P. & Leopold, R. 1966. Optimization Methods Applied to Ship Design. *Trans. SNAME,* 74.

Marzi, J., Papanikolaou, A., Corrignan, P., Zaraphonitis, G. & Harries, S. 2018. Holistic Ship Design for Future Waterborne Transport. *13th International Marine Design Conference.* Finland.

Mathworks 2014. Matlab. R2014a ed.

Michell, J. 1898. The Wave Resistance of a Ship. *Phil. Mag.*

Mistree, F., Smith, W. F., Bras, B. A., Allen, J. K. & Muster, D. 1990. Decision-Based Design: A Contemporary Paradigm for Ship Design. *SNAME Transactions,* 98**,** 565-597.

Murphy, R. D., Sabat, D. J. & Taylor, R. J. 1963. Least Cost Ship Characteristics by Computer Techniques. *Marine Technology,* 2.

NAPA 2018. Napa. 2018.3 ed.

Nehrling, B. 1976. Recognizing and Using Patterns in Preliminary Ship Compartmentation. *2nd International Conference on Computer Applications in Shipbuilding.* Sweden.

Nethercote, W., Eng, P. & Schmidtke, R. 1981. A Concept Exploration Model for Swath Ships. *The Naval Architect***,** 113.

Nikolopoulos, L. & Boulougouris, E. 2018. A Methodology for the Holistic, Simulation Driven Ship Design Optimization under Uncertainty. *13th International Marine Design Conference.* Finland.

NOAA. 2018. *National Oceanic and Atmospheric Administration* [Online]. Available: https://www7.ncdc.noaa.gov/CDO/cdoselect.cmd?datasetabbv=GSOD&countryabbv=&georegionabbv=&resolution=40 [Accessed 2018].

Nowacki, H. 2003. Design Synthesis and Optimization - an Historical Perspective. *Optimistic*. Germany: Mensch & Buch.

Nowacki, H. 2018. On the History of Ship Design for the Life Cycle. *A Holistic Approach to Ship Design.* Switzerland: Springer.

Nowacki, H., Brusis, F. & Swift, P. M. 1970. Tanker Preliminary Design - an Optimization Problem with Constraints. *SNAME Transactions*.

Nowacki, H., Papanikolaou, A., Holbach, G. & Zaraphonitis, G. 1990. Concept and Hydrodynamic Design of a Fast Swath Ferry for the Mediterranean Sea. *Jahrbuch der STG*, 84.

OECD 2018. Shipbuilding Market Developments.

Okumoto, Y., Takeda, Y., Mano, M. & Okada, T. 2009. *Design of Ship Hull Structures*, Germany, Springer.

Papanikolaou, A. 2008. Holistic Ship Design Optimization: Risk-Based Optimization of Tanker Design. *Kolloquium Schiffsentwurf: Vergangenheit und Zukunft, to the honor of the 75th birthday of Professor Horst Nowacki.* Germany.

Papanikolaou, A. 2009. *Risk-Based Ship Design: Methods, Tools and Applications*, Germany, Springer.

Papanikolaou, A. 2010a. Holistic Ship Design Optimization. *Computer-Aided Design*, 42**,** 1028-1044.

Papanikolaou, A. 2010b. Risk-Based Tanker Design. *Annual Conference of the Society of Naval Architects and Ocean Engineers of Japan.* Japan.

Papanikolaou, A. 2011. Holistic Design and Optimization of High-Speed Marine Vehicles. *9th Symposium on High Speed Marine Vehicles.* Italy.

Papanikolaou, A. 2014. *Ship Design: Methodologies of Preliminary Design*, The Netherlands, Springer.

Papanikolaou, A. 2018. *A Holistic Approach to Ship Design*, Switzerland, Springer.

Papanikolaou, A., Andersen, P., Kristensen, H. O., Levander, K., Riska, K., Singer, D. & Vassalos, D. 2009. State of the Art Design for X. *10th International Marine Design Conference.* Norway.

Papanikolaou, A., Harries, S., Wilken, M. & Zaraphonitis, G. 2011. Integrated Design and Multiobjective Optimization Approach to Ship Design. *15th International Conference on Computer Applications in Shipbuilding.* Italy.

Parsons, M. & Singer, D. 1999. A Hybrid Agent Approach for Set-Based Conceptual Ship Design. *10th International Conference on Computer Applications in Shipbuilding.* USA.

Peri, D., Rossetti, M. & Campana, E. F. 2001. Design Optimization of Ship Hulls Via Cfd Techniques. *Journal of Ship Research,* 45**,** 140-149.

Peters, W., Belenky, V., Bassler, C., Spyrou, K. J., Umeda, N., Bulian, G. & Altmayer, B. 2011. The Second Generation Intact Stability Criteria: An Overview of Development. *Annual Meeting of the Society of Naval Architects and Marine Engineers.* USA.

Plessas, T., Papanikolaou, A., Liu, S. & Adamopoulos, N. 2018. Optimization of Ship Design for Life Cycle Operation with Uncertainties. *13th International Marine Design Conference.* Finland.

Priftis, A., Boulougouris, E., Turan, O. & Papanikolaou, A. 2018. Parametric Design and Multi-Objective Optimisation of Containerships. *Ocean Engineering,* 156**,** 347-357.

Priftis, A., Papanikolaou, A. & Plessas, T. 2016. Parametric Design and Multiobjective Optimization of Containerships. *Journal of Ship Production and Design*, 32**,** 1-14.

Puchstein, K. 1969. Automatic Project Design of Optimal Ships. *Seewirtschaft*, 1.

Riska, K. 2009. Design for Arctic Operation. *10th International Marine Design Conference.* Norway.

SAFEDOR 2005-2009. Design, Operation and Regulation for Safety. European Union.

Sandia 2018. Dakota. 6.9 ed.

Schneekluth, H. & Bertram, V. 1998. *Ship Design for Efficiency and Economy,* United Kingdom, Butterworth-Heinemann.

Sen, P. & Yang, J. B. 1998. *Multiple Criteria Decision Support in Engineering Design,* United Kingdom, Springer.

Siemens 2017. Star-Ccm+.

Simpson, T. W., Jiao, J., Siddique, Z. & Hölttä-Otto, K. 2014. *Advances in Product Family and Product Platform Design,* USA, Springer.

Singer, D., Doerry, N. & Buckley, M. E. 2009. What Is Set-Based Design? *Naval Engineers Journal,* 121**,** 31-43.

Söding, H. 1977. Ship Design and Construction Programs. *New Ships,* 22**,** 272.

Söding, H. & Poulsen, I. 1974. Methods of Programming for Tasks of Ship Design. *Jahrbuch der STG,* 68.

Steponavice, I. & Miettinen, K. 2012. Survey on Multi-Objective Robustness for Simulation-Based Optimization.

Sues, R. H., Cesare, M. A., Pageau, S. & Wu, J. Y. T. 2001. Reliability-Based Optimization Considering Manufacturing and Operational Uncertainties. *Journal of Aerospace Engineering,* 14.

Taguchi, G. & Phadke, M. S. 1989. *Quality Engineering through Design Optimization,* USA, Springer.

Trosset, M. W., Alexandrov, N. M. & Watson, L. T. 2003. New Methods for Robust Design Using Computer Simulations. *Proceedings of the Section on Physical and Engineering Sciences, American Statistical Association*.

Tu, J., Choi, K. K. & Park, Y. H. 1999. A New Study on Reliability-Based Design Optimization. *Journal of Mechanical Design,* 121.

UNCTAD 2018. Review of Maritime Transport.

Vassalos, D. 2007. Risk-Based Design: Passenger Ships. *SAFEDOR midterm conference.* Belgium.

Weinblum, G. 1932. Hull Form and Wave Resistance. *Jahrbuch der STG,* 33.

Wigley, C. 1935. Ship Wave Resistance, Progress since 1930. *Trans. RINA,* 77.

Winjnolst, N. & Waals, F. A. J. 1995. *Design Innovation in Shipping: The Only Constant Is Change,* The Netherlands, Delft University Press.

Yang, C. X., Tham, L. G., Feng, X. T., Wang, Y. J. & Lee, P. K. K. 2004. Two-Stepped Evolutionary Algorithm and Its Application to Stability Analysis of Slopes. *Journal of Computing in Civil Engineering,* 18**,** 145-153.

Zakerdoost, H., Ghassemi, H. & Ghiasi, M. 2013. Ship Hull Form Optimization by Evolutionary Algorithm in Order to Diminish the Drag. *Journal of Marine Science and Application,* 12**,** 170-179.

Zaraphonitis, G., Boulougouris, E. & Papanikolaou, A. 2013. Multi-Objective Optimization of Cruise Ships Considering the Solas 2009 and Goalds Damage Stability. *5th International Maritime Conference on Design for Safety.* China.

Zaraphonitis, G., Papanikolaou, A. & Mourkoyannis, D. 2003. Hull-Form Optimization of High Speed Vessels with Respect to Wash and Powering. *8th International Marine Design Conference.* Greece.

Zhao, Y., Zong, Z. & Zou, L. 2015. Ship Hull Optimization Based on Wave Resistance Using Wavelet Method. *Journal of Hydrodynamics, Ser. B,* 27**,** 216-222.

A Calculation of excessive acceleration stability criterion

Large angles of rolling lead to extreme lateral accelerations, which result in objects in higher locations (such as the top decks of the superstructure) to travel longer distances. The period of roll motions is the same in each location on the ship. Hence, the linear velocity increases to cover the longer distance at the same time. Velocity changes its direction every half a period, therefore, this phenomenon affects the linear accelerations, which get larger in higher locations on the ship (Figure 110).

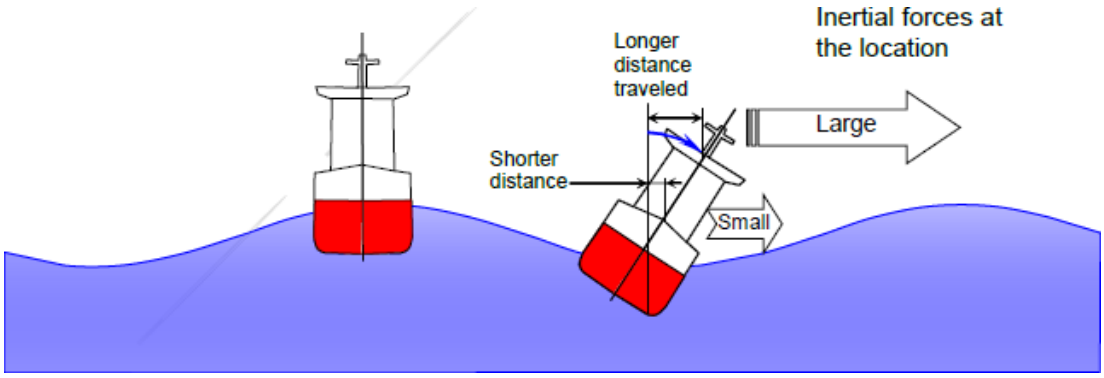

Figure 110: Scenario of stability failure related to excessive accelerations (IMO, 2016)

The period of roll motion decreases as the GM value gets higher. Hence, for the same roll amplitude, the linear velocity changes faster, resulting in larger accelerations.

One of the reasons causing excessive accelerations is the synchronous resonance, a phenomenon of amplification of the motion response when the natural frequency of the ship motion is close to the frequency of the wave excitation. The wave excitation frequency depends on the wave frequency, ship heading relative to waves and ship speed. The frequency of encounter becomes higher than the frequency of the waves in head waves when the ship sails against them, while the opposite is observed in

following seas when the ship sails in the same direction as them. Higher speeds increase this effect (IMO, 2016).

According to IMO (2018), the first level of the vulnerability criteria for excessive acceleration is based on the calculation of the lateral acceleration for each condition of loading and location along the length of the ship where passengers or crew may be present. The value is compared with an upper limit to identify whether the ship is vulnerable or not (34).

$$\varphi k_L \left(g + \frac{4\pi^2 h}{T_\varphi^2} \right) < R_{EA1} \tag{34}$$

where φ is the characteristic roll amplitude, k_L is a factor taking into account the simultaneous action of roll, yaw and pitch motions, h is the height above the roll axis of the location where passengers or crew may be present, T_φ is the rolling period and R_{EA1} is the upper limit value.

Level 1 check is relatively straightforward and is implemented in a custom CAESES® feature, which reads input data originating from the NAPA® macros run in advance. The feature indicates compliance with or violation of the level 1 check. Should the former be the case, the process is terminated to avoid the implementation of the level 2 check and reduce the computational time.

Level 2 goes into more detail, calculating a long term probability index C that measures the vulnerability of the ship to a stability failure in the excessive acceleration mode for the loading condition and location under consideration, based on the probability of occurrence of short term environmental conditions affecting the wave frequency and amplitude. C is compared with the upper limit value R_{EA2} to check the vulnerability of the ship to the specific criterion (35).

$$C < R_{EA2} \tag{35}$$

where

$$C = \sum_{i=1}^{N} W_i C_i$$

where N is the number of short term environmental conditions, W_i a weighing factor for the short term environmental conditions and C_i the short term excessive acceleration stability failure index for the loading condition and location under consideration and for the short term environmental condition under consideration calculated as shown in (36).

$$C_i = e^{-R_2^2/2\sigma_{LAi}^2} \tag{36}$$

where R_2 is the gravitational acceleration and σ_{LAi} the standard deviation of the lateral acceleration at zero speed and in a beam seaway.

Level 2 check is more complex than level 1 and requires the connection of CAESES® with Maxsurf® Stability, in which the necessary calculations for the determination of the C_i value shown in (36) for each wave case take place. To achieve that, the hull is exported from CAESES® in panelised form and imported to Maxsurf® Stability, while data originating from the NAPA® macros run in advance are read by Maxsurf® Stability.

The results are then imported to CAESES® where a custom feature calculates the C value shown in (35). A comparison of the latter with the limit value R_{EA2} takes place to determine compliance with or violation of the criterion.

B Calculation of parametric roll stability criterion

Parametric roll is the amplification of roll motions caused by the periodic variation of transverse stability in waves. This phenomenon is primarily observed in head, following, bow and stern-quartering seas when the ship's encounter frequency is approximately twice of the ship roll natural frequency and the roll damping of the ship is insufficient to dissipate the additional energy.

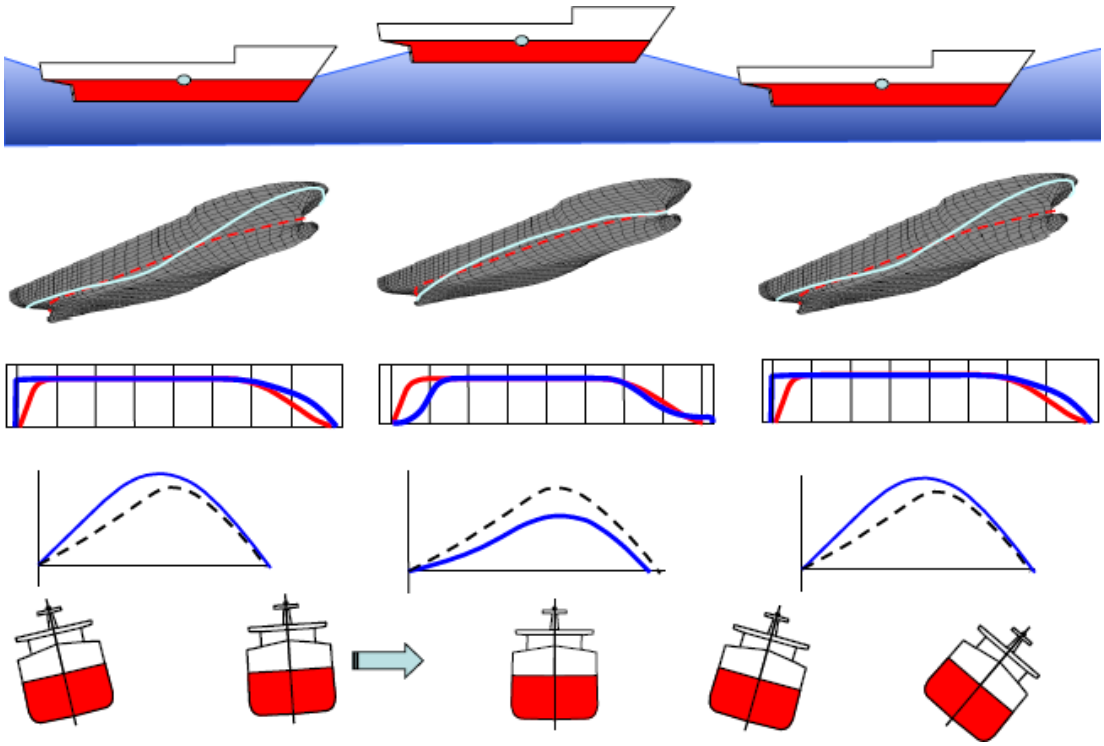

Figure 111: Development of parametric roll (IMO, 2016)

When the ship is rolled while positioned on the wave trough, increased stability provides stronger pushback (restoring moment). As the ship returns to the upright position, its roll rate is greater, since there was an additional pushback from the increased stability. If at that time, the ship has the wave crest at midship, the stability

is decreased and the ship will roll further to the opposite side because of the greater speed of rolling and less resistance to heeling. Then, if the wave trough reaches the midship section when the ship reaches its maximum amplitude roll, stability increases again and the cycle starts again. This phenomenon is shown in Figure 111.

Roll damping influences parametric roll. When a ship rolls in calm water the roll amplitude decreases successively due to roll damping. The rolling motion creates waves and eddies, and the ship experiences viscous drag. All of these processes contribute to roll damping. Roll damping may play a critical role in the development of parametric roll. If the "loss" of energy per cycle caused by damping is more than the energy "gain" caused by the changing stability in longitudinal seas, the roll angles will not increase and the parametric roll will not develop. Once the energy "gain" per cycle is more than the energy "loss" due to damping, the amplitude of the parametric roll starts to grow.

In addition, there is a roll damping threshold for parametric roll. If the roll damping moment is higher than the threshold, then the parametric roll is impossible to develop. On the other hand, if the roll damping moment is below the threshold, parametric roll may take place.

The development of parametric roll depends on the speed and wave direction. The frequency of encounter with waves changes when the ship is in motion. In following or stern-quartering seas, the direction of waves and the ship heading are similar. Hence, the relative speed is low and a ship encounters fewer waves during the same time period. On the contrary, in head or bow-quartering seas, the direction of waves and the ship heading are opposite, resulting in higher relative speed. Therefore, the ship encounters more waves during the same time period (IMO, 2016).

According to IMO (2018), the first level of the vulnerability criteria for parametric roll is based on the comparison of the amplitude of the variation of GM in specific conditions δGM_1 over the GM of the loading condition in calm water GM_C with an upper limit value R_{PR} (37).

$$\frac{\delta GM_1}{GM_C} \leq R_{PR} \tag{37}$$

δGM_1 and GM_C are calculated in Maxsurf® Stability for the loading condition under consideration. To achieve that, the hull is exported from CAESES® in panelised form and imported to Maxsurf® Stability, while data originating from the NAPA® macros run in advance are read by Maxsurf® Stability. The hydrostatic values required for the computations are also calculated in Maxsurf® Stability.

The results are then imported to CAESES® where a custom feature performs the check shown in (37). If the condition is met, the process is terminated to avoid the implementation of the level 2 check and reduce the computational time.

Level 2 consists of two separate checks which examine different combinations of wave amplitudes and periods, as well as various ship speeds and headings. Two values –*C1* (38) and *C2* (41)– are calculated and compared with two lower limit values, R_{PR0} and R_{PR1}.

$$C1 = \sum_{i=1}^{N} W_i C_i \tag{38}$$

where N is the number of the examined wave cases, W_i is a weighting factor for the respective wave case and C_i is assigned a value of either zero or one, depending on the satisfaction of the requirements related to GM and the ship speed presented in (39) and (40).

$$\begin{aligned} &GM(H_i, \lambda_i) > 0 \\ &\text{and} \\ &\frac{\delta GM(H_i, \lambda_i)}{GM(H_i, \lambda_i)} < R_{PR} \end{aligned} \tag{39}$$

In (39), $\delta GM(H_i,\lambda_i)$ is half the difference between the maximum and minimum values of GM calculated for the ship, corresponding to the loading condition under

consideration, considering the ship to be balanced in sinkage and trim on a series of waves characterised by a wave height of H_i and a wave length of λ_i. $GM(H_i,\lambda_i)$ is the average value of GM calculated for the ship, corresponding to the loading condition under consideration, considering the ship to be balanced in sinkage and trim on a series of waves characterised by a wave height of H_i and a wave length of λ_i.

$$V_{PRi} > V_S \tag{40}$$

In (40), V_{PRi} is the reference ship speed corresponding to parametric roll conditions when $GM(H_i,\lambda_i)>0$, while V_S is the service speed.

GM, δGM and V_{PR} are calculated in Maxsurf® Stability for each wave case, taking as input the panelised hull form and the NAPA® macros' output data, as described in the level 1 check. The weighting factor is set by the IMO regulation and depends on the wave case.

The results are then imported to CAESES® where a custom feature calculates the value of *C1* shown in (38). A comparison of the latter with the limit value R_{PR0} takes place to determine compliance with or violation of the criterion.

C2 is calculated in more detail, based on the values of the maximum roll angle in head and following waves calculated for various ship speed and heading combinations (41).

$$C2 = \frac{\left[\sum_{i=1}^{12} C2(Fn_i, \beta_h) + \frac{1}{2}\left(C2(0, \beta_h) + C2(0, \beta_f)\right) + \sum_{i=1}^{12} C2(Fn_i, \beta_f)\right]}{25} \tag{41}$$

where $C2(Fn_i,\beta)$ is calculated as a weighted average from a specified set of waves according to (42), *h* stands for head waves and *f* stands for following waves.

$$C2(Fn_i, \beta) = \sum_{i=1}^{N} W_i C_i \tag{42}$$

In (42), N is the total number of wave cases for which maximum roll angle is evaluated for a combination of speed and ship heading, W_i is a weighting factor for the respective examined wave case and C_i is assigned a value of either one or zero, depending on whether the maximum roll angle exceeds 25 degrees or not.

Calculation of *C2* is more complex than the one of *C1*, due to the high number of evaluations involved in the process, which depend on the heading and speed of the ship. The cases are set by the IMO regulation and for each one the maximum roll angle is calculated based on Ikeda's method defined in the proposed regulation.

The required input data for the implementation of Ikeda's method are calculated in a custom feature within CAESES®. They are exported to a text file, which is read by Matlab®. The latter is responsible for the solution of a complex equation which provides the maximum roll angle.

Matlab® output is exported to a text file, which is read by CAESES®. The process continues within a custom feature which is responsible for the calculation of the C_i value shown in (42). This process is carried out for each examined case in order to calculate the value of *C2* shown in (41).

Finally, *C2* is compared with the limit value R_{PR1} and the compliance with or violation of the criterion is determined.

C Calculation of pure loss of stability criterion

Stability varies in different wave conditions. As a ship sails through waves, the submerged part of the hull changes. For most ships, the upper part of the bow section is usually wide, due to bow flare. The latter makes the waterplane area larger when the upper part of the bow section becomes partially submerged. The upper part of the aft section of the hull is typically even larger. Hence, the aft part of the waterplane area also increases, when the upper part of the aft section becomes submerged. On the other hand, unlike the bow and aft sections, the midship section of most ships remains the same along its depth. Therefore, the waterplane area remains mostly unchanged with the variation of draught. When the wave trough is amidships, the draught at the midship section is low, but as the hull is wall-sided in this region, there is little waterplane area change. As a result, when the wave trough is located around the midship section, the overall waterplane area is increased (Figure 112).

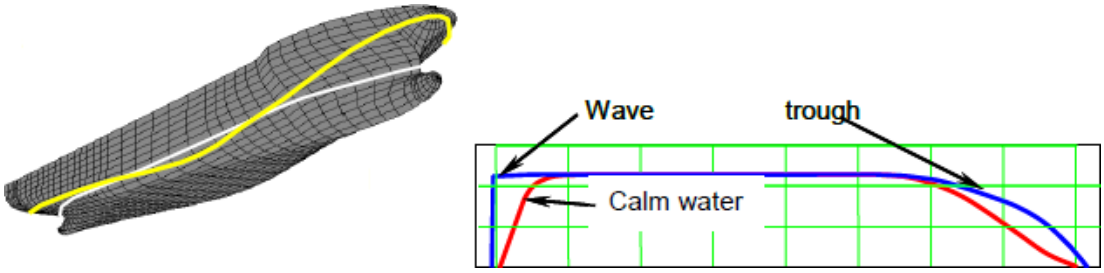

Figure 112: Changes in hull geometry (wave trough) (IMO, 2016)

The opposite happens when the wave crest is located near the midship section. The underwater part of the bow section is usually quite narrow, especially around the waterline for hydrodynamic reasons. The faster the ship is, the narrower its underwater bow section should be. If the wave crest is located amidships and the wave length is comparable to the ship's length, the wave trough is located around the bow section. The low draught at the bow area results in a very narrow waterplane area around the bow section. Similarly, the lower part of the stern is usually narrow and the location of the wave trough near the stern results to a decreased waterplane

area in the aft section. As mentioned previously, the midship section usually has a uniform shape along the depth, so it does not affect the waterplane area significantly. Therefore, the overall waterplane area is decreased in this case (Figure 113).

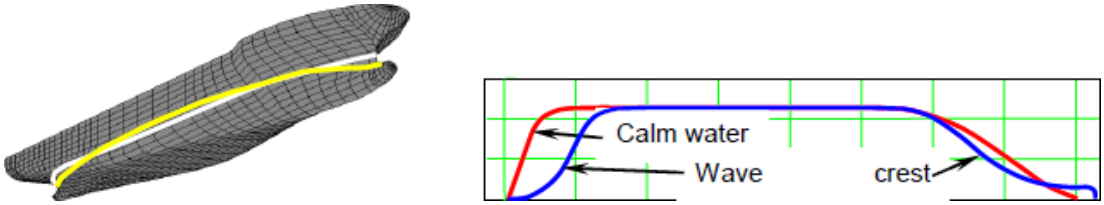

Figure 113: Changes in hull geometry (wave crest) (IMO, 2016)

The waterplane area influences significantly the ship's stability. Reduction of the waterplane area leads to the reduction of the GZ curve. Hence the stability of the ship declines (Figure 114) (IMO, 2016).

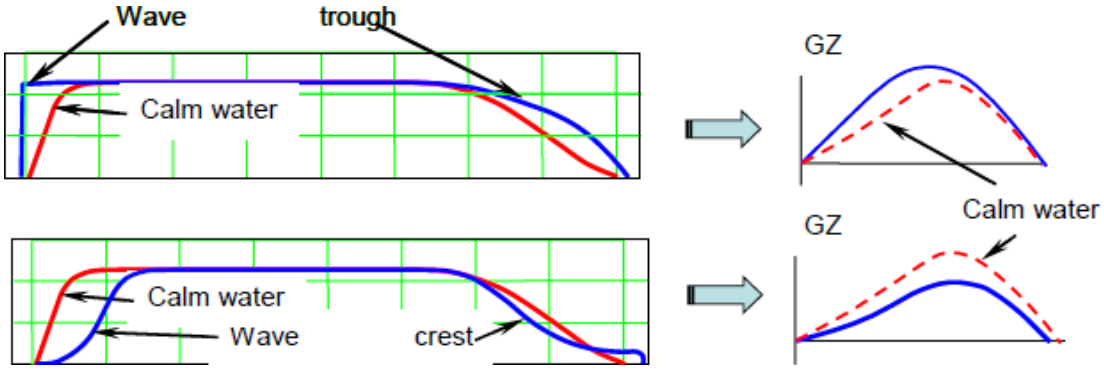

Figure 114: Stability corresponding to waterplane area changes (IMO, 2016)

According to IMO (2018), the first level of the vulnerability checks for pure loss of stability failure mode compares the minimum value of GM among various conditions, GM_{min}, with a lower limit value R_{PLA}, as seen in (43).

$$\mathrm{GM_{min}} > \mathrm{R_{PLA}} \tag{43}$$

GM_{min} is calculated in Maxsurf® Stability for the loading condition under consideration. To achieve that, the hull is exported from CAESES® in panelised form and imported to Maxsurf® Stability, while data originating from the NAPA®

macros run in advance are read by Maxsurf® Stability. The hydrostatic values required for the computations are also calculated in Maxsurf® Stability.

The results are then imported to CAESES® where a custom feature performs the check shown in (43). If the condition is met, the process is terminated to avoid the implementation of the level 2 check and reduce the computational time.

Level 2 consists of two separate checks, comparing two criteria representing a weighted average of certain stability parameters for a ship considered to be statically position in waves of specific height and length –CR_1 (44) and CR_2 (45)– with an upper limit value R_{PL0}. In particular, the larger of the two values –CR_1 and CR_2– should be less than R_{PL0}.

$$\mathrm{CR}_1 = \sum_{\mathrm{i}=1}^{\mathrm{N}} \mathrm{W_i C1_i} \tag{44}$$

$$\mathrm{CR}_2 = \sum_{\mathrm{i}=1}^{\mathrm{N}} \mathrm{W_i C2_i} \tag{45}$$

where N is the number of wave cases for which $C1$ and $C2$ are evaluated, W_i is a weighting factor and $C1$ and $C2$ the two examined criteria. $C1$ is based on the calculation of the angle of vanishing stability φ_v as seen in (46). $C2$ is based on the calculation of the angle of heel φ_s as seen in (47), under the action of the heeling lever R_{PL3} (48).

$$\mathrm{C1_i} = \begin{cases} 1, & \varphi_\mathrm{v} < \mathrm{R_{PL1}} \\ 0, & \text{otherwise} \end{cases} \tag{46}$$

where R_{PL1} is 30 degrees.

$$\mathrm{C2_i} = \begin{cases} 1, & \varphi_\mathrm{s} > \mathrm{R_{PL2}} \\ 0, & \text{otherwise} \end{cases} \tag{47}$$

where R_{PL2} is 15 degrees for passenger ships and 25 degrees for any other ship type.

$$R_{PL3} = 8\left(\frac{H_i}{\lambda}\right) dFn^2 \quad (48)$$

Where H_i is the wave height for the respective examined wave case, λ is the wave length, d is the draught amidships corresponding to the loading condition under consideration and Fn is the Froude number.

Calculation of CR_1 and CR_2 takes place in Maxsurf® Stability, taking as input the panelised hull form and the NAPA® macros' output data, as described in the level 1 check. The calculation of the angle of vanishing stability and angle of heel takes place. The results are imported to CAESES® where a custom feature is responsible for the comparison of the two angle values with the limit values R_{PL1} and R_{PL2}. The value of $C1_i$ and $C2_i$ are then determined. This process is repeated for each wave case.

Finally, the values of CR_1 and CR_2 are calculated and compared with R_{PL0} to determine the compliance with or violation of the criterion.